SPATIAL VARIATION OF WOOD COMPOSITES

By

ALEJANDRO M. BOZO

A dissertation submitted in partial fulfillment of
the requirements for the degree of

DOCTOR OF PHILOSOPHY

WASHINGTON STATE UNIVERSITY
Department of Civil Engineering

August 2002

To the Faculty of Washington State University:

The members of the Committee appointed to examine the dissertation of ALEJANDRO M. BOZO find it satisfactory and recommend that it be accepted.

_____
Chair

_____

_____

_____

_____

Acknowledgement

The author would like to thank his major professor, Dr. Michael Wolcott, and his committee members, Dr. John Hermanson, Dr. Donald Bender, Dr. Jay Johnson, and Dr. Stanley Miller, for their advice and the time they spent reviewing this dissertation.

The author is appreciative of the financial support provided by the Louisiana-Pacific Research Endowment, the Wood Materials and Engineering Laboratory at Washington State University, and his Family. This funding made the project possible. A special thanks is extended to Alberta Research Council for providing the non-destructive measurements of the horizontal density distribution used in this study.

The author expresses sincere thanks to the staff of the Wood Materials and Engineering Laboratory for their help to resolve technical and administrative problems. The fellow graduate students: Karl Englund, David Harper, Heming Alwin. A special thank is offered to my friend and officemate Vikram Yadama for his friendship and support, to Suzanne and John for their friendship and support, and to Linda Miklosko for her friendship and time to edit this work.

A very important and special thank to Sally Burkhard and Paola Madariaga to help the author to solve the innumerable problems arise during all this time between him and University of Chile, also thank both of you for your friendship and support.

The author also would like to thank the visit of his parents, Ricardo and Oriana, and his sister-in-law, Amelia, their time in Pullman help him to continue his program.

Most important, the author would like to thank Isabel, Francisca, Karina, and Fabiana, for their love, patience, and understanding as he has continued his studies. Without their support and understanding this would not have been possible.

SPATIAL VARIATION IN WOOD COMPOSITES

Abstract

by Alejandro M. Bozo, Ph.D.
Washington State University
August 2002

Chair: Michael P. Wolcott

The variability in wood composites is a recognized problem that is crucial to better understand to facilitate it role as a quality control indicator. Density can be used to interpret of spatial variability; moreover, current sensor technology can be employed to monitor localized horizontal density in composite wood panel manufacture. Also recognized is a direct correlation between density and mechanical properties of wood composites. The objectives of this research were to: 1) analyze the horizontal density distribution (HDD) of oriented strandboard (OSB) using available statistical methods; 2) develop regression models between density and mechanical properties; and 3) model the influence of spatial distribution in localized mechanical properties on OSB performance criteria.

To conduct spatial characterization, several graphical and analytical methods were applied, and a practical application example was conducted using the concentrated static load (CSL) test. Statistical input models were developed to generate mechanical properties from known values of density for use in Monte Carlo simulation models of panel performance. To model the influence of spatial distribution in localized mechanical properties on OSB

performance criteria, the CSL test was performed and maximum deflection and ultimate load were obtained experimentally and employing finite element models.

The results of this research garnered several methods for assessing variability, all of which prove useful for the panels studied. The results obtained from the correlogram and variogram showed that there was an indication of spatial dependence for density, both along and across machine directions. Results of the spatial characterization indicate that using local density variation in mechanical analysis for CSL behavior is more appropriate than considering an average global density. Test results revealed a clear relationship exists between OSB properties and density. All property values examined increase with density. The regression model developed in this research can be used to simulate mechanical properties based on density at specific locations using conditional Monte Carlo simulation. The finite element results for the CSL test using local properties produced more accurate results than those values obtained using global properties.

Table Of Contents

List of Tables

List of Figures

Chapter 1

Project Introduction

Introduction

The performance of oriented strandboard (OSB) is affected by several production parameters that include strand geometry, strand lay up, adhesive type and distribution mechanism, pressing process, and species (Lu and Lam 2001). The variability in OSB properties is a problem that has drawn the attention of many researchers (Suchland and Xu 1989, 1991; Xu and Steiner 1995; Dai and Steiner 1993, 1994; Lang and Wolcott 1996; Lu, Steiner, and Lam 1998; Wang and Lam 1998). This variability is due to the properties of the wood elements themselves and the manner in which they were arranged during the mat formation process. Each press run of OSB can be taken as a production sample, and variability can be determined with spatial and temporal characteristics. The spatial variability refers to the variability between individual sheets from different locations in the mat. However, this variation can also be viewed from a temporal standpoint, which is correlated with the time of production.

Based on the conceptual model elaborated by Suchland (1959,1962), Suchland and Xu (1989,1991) developed a model that allows the analysis of the effect of horizontal density variation in flakeboard. The results show that the wood composites are affected by the horizontal density distribution, which is a direct consequence of the forming process. Xu and Steiner (1995) showed that the specimen size has a large impact on the variability of the density (e.g., The smaller the specimen size, larger the variability). They also state that the standard deviation of density could be used to quantify horizontal density distribution based on the approximation of the normal distribution of density data.

Dai and Steiner (1993, 1994) and Lang and Wolcott (1996) mathematically describe the mat consolidation process for flake and strand composites. They concluded that the final properties of the wood composite products are directly influenced by mat structure originating in the forming process.

Lang and Wolcott (1996) used Monte Carlo simulation to make a characterization of the spatial structure of a randomly formed, wood strand mat. They concluded that the distribution of mat spatial characteristics could be reproduced by Monte Carlo simulation. Lu, Steiner, and Lam (1998) also studied the internal mat structures and the related properties based on Monte Carlo simulation. They developed a two-dimensional mathematical model to describe the structural characteristics of flakeboards, assuming uniform flake size and random process. The conclusion of their work was that the simulation program could be used as a tool to improve the understanding of internal mat structures and the related properties. Wang and Lam (1998) investigated the organization of wood elements in a composite mat using a combination of the robot system with experimental design, and the concept of a three-layer oriented mat. They concluded that this tool could be applied in future studies because the potential to repeat the structure and performance of the patterns exists.

With the exception of Xu and Steiner (1995), all of the previously cited research was conducted using non-commercial panels, and most of these had been directed to randomly formed mats. Additionally, none of previous works used the spatial or time dependence between data to characterize the horizontal density distribution.

The purpose of this further research was to address the variability in OSB properties and characteristics. Specifically, this work is intended to provide a means to characterize variability

of panel properties and relate this variation to performance requirements of OSB products, as well as promote effective decisions to optimize the production process.

Variability in Wood Composites

A composite structure can be defined by a three-dimensional density distribution, which can be subdivided into vertical and horizontal components. The density variation between layers or vertical variation is well known and studied by many researchers. However, the horizontal density distribution, which is the distribution of the density in the plane of the board, has not been well understood.

Suchland and Xu (1989,1993) explain the horizontal density distribution through two mat structures: one mat with airspace uniformly distributed into the layers; the other mat with no airspace, thus an ideal mat. Both mats have the same amount of wood elements, but are of different thicknesses before the pressing process. After pressing, both mats must have the same thickness, which results in a reasonable uniformity of the density in the ideal mat, but a high-density distribution in the mat with air space. The ideal mat does not need densification, its behavior is that of plywood, and develops no density variation. The other mat requires densification to develop glue-bonds and with the reduction of airspace, certain elements will have higher density than wood, and other elements will have lower density. The amount of void or airspace, is directly related to the horizontal density distribution: the higher the void space, the more severe the horizontal density distribution. An important property that is highly affected by the horizontal density distribution is the thickness swelling (TS) of the board. The element with lower density imposes restraint on the elements that have higher density and greater swelling potential. The result is the development of compression stress in the higher density elements and

tension stresses in the lower density elements. The TS is dominated by the higher density elements, and the tensile stresses developed in the lower density elements can result in failure in the elements or in the glue-bonds. These are in agreement with the finding of Linville (2000). This research indicates that density is linearly related to swelling strain. Linville developed an empirical model to describe the swelling strain was developed.

Suchland's model for mat structure was followed by Dai and Steiner (1994). They applied the concept of two-dimensional random field theory to describe mat formation from a theoretical viewpoint. The mat structure was described using a Poisson distribution of overlapping flake numbers. The void volume could then be calculated based on average mat thickness

Xu and Steiner (1995) worked with commercial flakeboard panels to characterize the horizontal density distribution. Xu and Steiner concluded that the horizontal density variation could be viewed as a stationary Gaussian random field with the magnitude of the density variation decreasing as the specimen size increases.

Lang and Wolcott (1995) included in their model flake columns of finite size, void of varying heights, and the connectivity of adjacent columns. They divided the mat into 152.4-mm square blocks, which were divided again into 19.05-mm squares for columns. Random orientation was used to form the wood strand mats. They sectioned a block from the center of the mat. A video image of the mat perimeter was digitized and divided into columns. The variables that characterized each visible column were the number of overlapping strands, the individual void heights, and the location of the column centroid relative to the strand length. Lang and Wolcott used Monte Carlo simulation to simulate the mat structure.

Dai and Steiner (1993) summarized the importance of mat compression behavior of flake mats related to wood composites as follows: (1) heat and mass transfer processes during hot pressing are affected by changes in the internal structure during mat compression; (2) a nonuniform densification through the thickness of board (vertical density distribution) can be explained by the physical, chemical, and mechanical interaction between mat compression; (3) the mat compression result in highly localized wood compression stresses and densification because of random variation in mat structure; (4) and after press opening, because of varying moisture condition, the compressed wood composite can spring back and exhibit irreversible excessive dimensional change.

The structure of the mat depends on the number of elements in each location. To analyze this fact, the mat is divided into columns of infinite small cross sectional areas. The result shows a high variability in the number of elements in each column, which follows a Poisson distribution. The Poisson distribution is suitable for probabilistic characterization of a large number of events randomly occurring with a very slight possibility of success. In the case of the element packing process, an event is the deposition of an element onto the mat area. Success can be defined as when a specific column or point in the mat is covered by a given element. The compression force applied to a random mat produces a diminution of the thickness to T. Due to the random distribution of element numbers in columns, the force (F) can only be supported by element columns that have **i** greater than T/ τ, where τ is the average element thickness.

Lu et al. (1998) wrote a windows-based simulation program to evaluate density and overlap distribution of wood-flake composite mat structures. They also developed a robotic control system where the position of flakes could be controlled for experimental study. The joint utilization of both a simulation program and robotic system allows for verification of the theory

and the generation of a new database. The constant mass in a given volume was used to obtain the relationship between the overlaps and the local density. Their assumptions were that the flake thickness, flake density, and panel thickness are fixed for a given mat; and as such, they found that the overlap distribution is linearly proportional to the panel local density.

Wang and Lam (1998) continued the work of Lu et al. (1998). They too used a simulation program to calculate density variation along the horizontal plane and a robot mat formation system to manufacture small composite mats with a different structure predefined by the simulation program. A different core structure and face to core ratio were used to generate four kinds of three-layer oriented flake boards. X-ray densitometry was used to analyze the horizontal density distribution with a resolution of 2- by 1.5-mm. The panels were also tested to determine the static bending modulus of elasticity (MOE), internal bond, and thickness swelling. Wang and Lam concluded that the robot system could be a very effective tool to link a simulation program with an experimental mat. Additionally, they found that the bending modulus of elasticity (MOE) along the face alignment is strongly influenced by core structure and face to core ratio.

The works, previously described, evidence the spatial variability in wood composite material. However, any of these researches provide a statistical methodology to address the spatial variability. The study presented in this dissertation also involves the spatial variation with performance and standard requirement.

Objectives

The performance requirements of structural use panels are covered by Voluntary Product Standards PS 2-92 and APA PRP-108. Panel producers need periodic quality control of their products to meet performance requirements. The spatial variability of properties is not considered in the quality control process due to a lack of clear understanding of this variability.

The objective of this research is to develop a statistical methodology to evaluate the spatial variation in wood composites, and to relate that variation to product performance. The specific objectives within this research are to:

1. Analyze the horizontal density distribution (HDD) of OSB using available statistical methods such as exploratory data analysis, time series analysis, and geostatistics; and to define a statistical methodology to characterize variability of wood composite properties.

2. Develop regression models between density and modulus of elasticity, tensile and compression strength, shear modulus, and shear strength using different specimen sizes.

3. Model the influence of spatial distribution in localized modulus of elasticity, tensile and compression strength, shear modulus, and shear strength on OSB performance criteria (concentrated static load test) according to Voluntary Product Standard PS 2-92 and APA PRP-108.

Rationale and Significance

Variability in properties of OSB is observed both within and between individual panels. Although this variability should logically link to both panel performance and production variables, neither has yet been realized. Much of the difficulty in considering decreasing production variability can be attributed to the lack of an effective method to consistently assess the amount and type of variability and its influence on panel performance.

This research focused on developing methods that can be applied to panel performance in real production processes. The work was significant for two reasons. First, as OSB markets diversify to value-added and specialty products, meeting new and different performance requirements will became necessary. These requirements may tolerate different levels of variability based on the specific product needs. Much of this depends on the size of the scale on which the panel is to perform. Secondly, production variables influencing variability also influence profitability. Therefore, any research directed at variability must have the potential to address both product performance requirements and production methods.

Structure of the Dissertation

This dissertation contains six chapters. Chapter 1 is an introduction to the investigation and a brief literature review and objectives are presented. Chapters 2, 3, 4, and 5 are considered stand-alone sections each consisting of an introduction, objectives, methodology, results, and a conclusion. Chapter 2 explains the statistical methodology developed to characterize the variability of wood composite properties. Chapter 3 covers modeling variation in wood composite properties. Chapter 4 refers in depth to the influence of spatial variation in localized properties on OSB performance criteria. Chapter 5 shows a theoretical approach to an inverse

methodology using finite elements for determining the elastic constants of wood. Lastly, Chapter 6 provides a summary of conclusions.

References

Dai, C. and P.R. Steiner. 1993. Compression Behavior of Randomly Formed Wood Flake Mats. Wood and Fiber 25(4): 349-358.

Dai, C. and P.R. Steiner. 1994. Spatial structure of wood composites in relation to processing and performance characteristic. Part 1. Rationale for model development. Wood Science and Technology 28: 45-51.

Lang, E. and M.P. Wolcott. 1996. A model for viscoelastic consolidation of wood-strand mats Part I: Structural characterization of the mat via Monte Carlo simulation. Wood and Fiber Science. 28(1): 100-109.

Linville, J.D. 2000. The influence of a horizontal density distribution on moister-related mechanical degradation of oriented strand composites. Master's Thesis. Washington State University, Pullman, Washington.

Lu, C., P.R. Steiner, and F. Lam. 1998. Simulation Study of Wood-Flake Composite Mat Structures. Forest Product Journal 48(5): 89-93.

Lu, C.,and F. Lam. 2001. Random Field Representation of Horizontal Density Distribution in Partially Oriented Strandboard Mat. Wood and Fiber Science, 33(3), 2001, pp. 437-449.

Suchsland, O. 1959. An analysis of the particleboard process. Michigan Quarterly Bulletin, Agricultural Experiment Station, Michigan State University, East Lansing Michigan. 42(2): 350-372.

Suchsland, O. 1962. The density distribution in flakeboard. Michigan Quarterly Bulletin, Agricultural Experiment Station, Michigan State University, East Lansing Michigan. 45(1): 104-121.

Suchsland, O. and H. Xu. 1989. A simulation of the horizontal density distribution in a flakeboard. Forest Product Journal 39(5): 29-33.

Suchsland, O. and H. Xu. 1991. Model analysis of flake board variables. Forest Product Journal 41(11/12): 55-60.

Wang, K. and F. Lam. 1998. Robot-Based Research on Three-Layer Oriented Flakeboards. Wood and Fiber Science 30(4): 339-347.

Xu, W. and P.R. Steiner. 1995. A Statistical Characterization of the Horizontal Density Distribution in Flakeboards. Wood and Fiber Science 27(2): 160-167.

Xu, W. and O. Suchsland. 1998. Modulus of elasticity of wood composite panels with a uniform vertical density profile: a model. Wood and Fiber Science. 30(3): 293-300.

Chapter 2

Statistical Methodology to Characterize Variability of Wood Composite Properties

Introduction

The variability in oriented strandboard (OSB) properties is an issue that has drawn the attention of several researchers (Suchsland and Xu 1989, 1991; Xu and Steiner 1995; Dai and Steiner 1993; Steiner and Dai 1994; Lang and Wolcott 1996; Lu et al. 1998; Wang and Lam 1998). The variability can be seen as two distinct levels. The first level is the differences seen in individual panels from either the same or different press runs. The second level is the variation within a panel, which is shown by both the horizontal and vertical density distributions. The origin of this variability is explained by Lang and Wolcott (1996), these authors say "For material produced with discontinuous wood elements such as fibers, particles, and strands, the final material structure is governed by not only the wood elements themselves, but also the forming methods and pressing operation."

The OSB process starts with the mat formation that is a continuous operation to form large mats (2.44- by 21.96-m). These mats are pressed and divided into smaller individual panels (1.22- by 2.44-m) (Lowood 1997 and Smulski 1997). Each press run of OSB can be taken as a production sample, and variability can be determined with spatial and temporal characteristics. The spatial variation is a three-dimensional issue; however, for most panel uses, a two-dimensional description is sufficient. From a two-dimensional viewpoint, the spatial variability refers to the variability between individual sheets at different locations in the mat. However, this variation can also be viewed from a temporal standpoint, which is correlated with the time of production (Wolcott et al. 1998).

Based on the conceptual model elaborated by Suchland (1959, 1962), Suchland and Xu (1989, 1991) developed a model that facilitates an analysis for horizontal density variation in flake board and related that variation with some physical properties. Their results showed that the flake board properties are affected by the horizontal density distribution. Specifically, they found that the thickness swelling of the board was highly affected by horizontal density variation. Xu and Steiner (1995) used the standard deviation as a measurement of variability, they showed that the specimen size has a large impact on the standard deviation of density; e.g., the smaller the specimen, the larger the standard deviation. They also found that the standard deviation of density could be used to quantify horizontal density distribution based on the approximation of the normal distribution of density data. The horizontal density variation is originated by three factors: wood element density, the forming process, and presence of voids (Xu and Steiner 1995; Suchsland and Xu 1989). These three factors each play a different role at different specimen sizes. At large specimen size the forming process is the preponderant factor, and the voids and element density are secondary. Unlikely, at specimen sizes smaller than the less sensitive range, all three factors play an equivalent role (Xu and Steiner 1995).

Density in wood composites is considered an indicator of board properties (Strickler 1959; Plath and Schnitzler 1974; Steiner et al. 1978). There are several examples of mechanical properties which are influenced by density such as: modulus of elasticity (MOE) (Rice and Carey 1978; Xu and Suchsland 1998), modulus of rupture (MOR) (Rice and Carey 1978, Hse 1975; Wong et al. 1998; Kwon and Geimer 1998), tension strength perpendicular to panel surfaces (Heebink et al. 1972; Plath and Schnitzler 1974; Steiner et al., 1978 Wong et al. 1998), shear strength (Shen and Carroll 1969, 1970). Since many panel properties are related to density, it is imperative to understand density variability in wood composites.

With the exception of Xu and Steiner (1995), all of the works previously cited were conducted on laboratory-scale panels, and most of the panels were constructed with random particle alignment. Additionally, the researchers have not applied the spatial or time dependence of data to characterize the horizontal density distribution. Therefore, this investigation characterizes commercially produced OSB panels, while considering the spatial location of the density data values.

Objectives

The research presented here is directed toward providing a means to characterize the variability of panel properties. Additionally, a practical application of the spatial variation effects on the concentrated static load test is given. Specifically, the objectives are to:

1. Characterize the horizontal density distribution (HDD) of OSB using available statistical methods such as exploratory data analysis, time series analysis, and geostatistics.
2. Define the area size, around the loading zone in the concentrated static load (CSL) test, to optimize the relationship between density and the CSL test results.

Materials and Methods

Material Sampling

The material population for this study consisted of 18 commercially produced three-layer OSB panels each1.22- by 2.44-m by 19-mm. The panels were sampled from a single commercial press run comprising of 22-m continuous mat divided into three master panels. After pressing, each master panel was subdivided into six panels as shown in Figure 2.1.

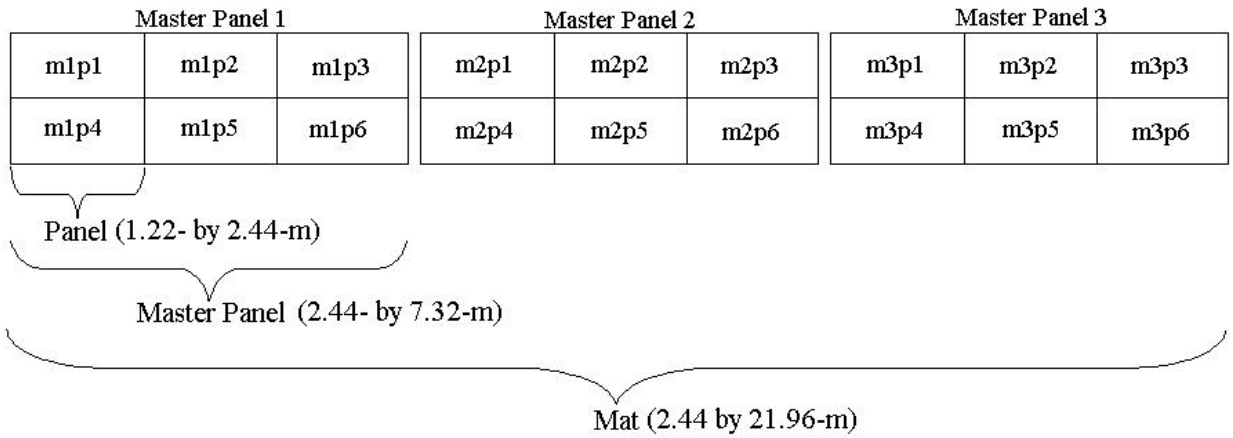

Figure 2.1. *Mat, master panel, and panel.*

Density Data

Density data was acquired from the Alberta Research Council (ARC) through scanning x-ray densitometry (Alberta Research Council). The spatial resolution to scan the complete panel was 12.7- by 12.7- mm (18,432 density values in a 1.22- by 2.44-m panel), and from these data, various sub-element sizes were averaged to obtain the density variation at different scales. Density determination by scanning densitometers is based on the relationship of x-ray attenuation and density, as expressed in the following equation:

$$\frac{I}{I_0} = e^{-m_m \cdot r \cdot t} \qquad \text{Equation 2.1}$$

where: I = intensity of radiation beam after passing through the sample
I_o = intensity of radiation beam without passing through the sample
μ_m = material mass attenuation coefficient
ρ = material density
t = material thickness
e = natural logarithm base

Each single density value of a small area of OSB can be associated with the coordinates of a position vector within the panel, master panel, and mat.

Spatial Characterization (Density)

One aspect not typically considered in the property analysis of OSB is the spatial relationships that form patterns within the panel. The basis of such treatment is that the data belong to a specific location in space. Spatial features of the data set that could have potential influence on overall panel performance include the location of extreme values, weak areas, the degree of continuity, and the overall trend. To conduct a spatial characterization, several tools were used including graphical methods (e.g., data plots or contour plots) and analytical methods (e.g., basic statistic or moving window statistics). In this work, graphical methods are used to visualize the data and time series analysis and geostatistics were used to study spatial continuity of the data set.

Graphical Methods

The purpose of graphical methods is to visualize variability and patterns (Armstrong 1998; Governs 1997; and Isaaks 1989). To facilitate this process, the data is plotted various ways to detect any trends or patterns. The least complex display of spatial data is a post plot or data map, on which, each data location is plotted with its corresponding data value.

A data map indicating all of the data values may not be feasible for very large, regularly gridded data sets. In these instances, an alternative would be to use gray-scale maps on which the data values are transformed according to an appropriate color scale. Another appropriate method is to visualize variability and patterns with three-dimensional surface plots where the data values are plotted against the location coordinates (Goovaerts 1997). Additionally, the overall trend can be easily revealed by contour plots, which represent linear interpolation of the data values, to produce approximate spatial location of the contour lines (Armstrong 1998; Goovaerts 1997; and Isaaks 1989).

Analytical Methods

Random Statistical Characterization

Traditional measures of statistical variation and position can be used to characterize the data, however, these measures do not consider spatial correlation present in the data. The characteristics addressed by basic statistics include a measure of central tendency (mean), a measure of dispersion (standard deviation), a measure of asymmetry (coefficient of skewness), and a measure of peakedness (coefficient of kurtosis). In addition, the maximum and minimum data values are obtained to determine the range.

Histograms were created and probability density functions (PDF) were applied to the data sets. The information provided by the histogram and PDF is used to simulate data values from the regression models.

Moving Window Statistics

In the spatial characterization of a data set, anomalies are often of the most interest, i.e., areas of lower properties or weak areas (Goovaert 1997). Anomalies in the average values can be identified using a contour map, but they are not the only items of interest. Not surprisingly, in some areas, the data values present a higher variability than in others. In statistical terminology, this observation is called nonstationarity. In addition, to investigate the anomalies of both average values and variability, computations of some statistics within moving windows are frequently used. Several local neighborhoods of equal size are used to divide the complete area. The statistics are then calculated within each local area. The mean and standard deviation are the statistics commonly used since mean provides a measurement of average values and standard deviation provides a measurement of variability. The relationship between local mean and local

standard deviation is easily observed in a scatterplot; a relationship often referred to as proportional effect. For normally distributed values, there is usually no proportional effect.

Three different window sizes were used to conduct this segment of the investigation: 1) 50- by 50- mm; 2) 100- by 100- mm; and 3) 200- by 200- mm. Mean and standard deviation within each window were calculated, and the contour map was created to identify zones with anomalies. Finally, a simple linear regression model of local mean and local standard deviation was generated to evaluate the proportional effect.

Spatial Continuity

Spatial continuity is based on the presumption that data closely positioned are more apt to have similar values than data positioned apart (Goovaerts 1997; Isaaks 1989; and Miller 1999). The methods used to detect the spatial continuity of the data set are similar as those used to determine the relationship between two variables. However, in the case of spatial continuity, the methods are used to describe the relationship between the values of one variable and the values of the same variable at nearby locations. The methods used to describe spatial continuity are part of time series analysis (e.g., autocorrelation function and spectral density function) and geostatistics (e.g., covariance function and variogram).

Spectral Analysis

Spectral analysis was applied to individual arrays both parallel and perpendicular to the machine direction, respectively. The purpose of applying this analysis is to describe the behavior of the data set. The basic steps of conducting the spectral analysis are to 1) plot the data series; 2) perform the autocorrelation function calculation; 3) plot correlogram; and 4) compute and plot the spectral density. Plotting the raw data helps to better understand the behavior of the data set;

specifically, the plot of the time series indicates what type of variation they present, cyclic changes, temporal effect, trend, and/or any other irregular fluctuation.

The autocorrelation function is a measure of correlation between observations at different distances apart (Bloomfield 1976; Chatfield 1996; and Fuller 1996), and is defined as:

$$r_h = \frac{\sum_{i=1}^{N-h} (x_i - m) \cdot (x_{i+h} - m)}{\sum_{i=1}^{N} (x_i - m)^2} \qquad \text{Equation 2.2}$$

where: $r_h =$ autocorrelation function
$x_i =$ the ith observation of X
$m =$ the sample mean
$h =$ separation distance (or lag), measured in number of steps
$N =$ number of observation

The correlogram is a graphic on which the autocorrelation function, r_h is plotted against the lag, $\boldsymbol{h}$. Interpreting the correlogram helps determine the type and amount of correlation in the data set (Chatfield 1996) (e.g., random series, short-term correlation, or seasonal fluctuation). From this information, range of influence or spatial dependence of the data set may be defined.

The spectral density analysis is another method of finding the range of influence and the spatial dependence of the data set. The spectral density function is obtained through the fast Fourier transform (FFT) of the autocorrelation function where the time domain is transformed to the frequency domain. Using the covariance method, the spectral density function is defined by:

$$\boldsymbol{S_m} = \Delta \boldsymbol{h} \cdot \sum_{\boldsymbol{n}=0}^{N-1} \boldsymbol{C_n} \cdot \boldsymbol{e}^{\frac{-\boldsymbol{i}\, 2p\boldsymbol{mn}}{N}} \qquad \text{Equation 2.3}$$

where: $S_m =$ spectral density (or spectrum)
$C_n =$ covariance (base on regular spaced data)
$m =$ frequency separation lag, measured in number of steps
$\Delta h =$ step increment

and as the following using the direct FFT method:

$$\boldsymbol{S_m} = \frac{1}{\boldsymbol{T}} \cdot \left|\boldsymbol{A_m}\right|^2 \qquad \text{Equation 2.4}$$

where: A_m = amplitude
T = period

Geostatistics

The geostatistics method was performed on individual panels using the commercial software VARIOWIN 2.2, which is a public domain application. Differently, geostatistics works with two-dimensional arrays, permitting a better interpretation of the spatial dependence of the data set. The variogram and correlogram are used to perform the analysis of spatial dependence (Isaaks 1989).

A variogram is a measure of spatial dependence, which is defined as:

$$I_m = g(h) = \frac{1}{2 \cdot n_h} \cdot \sum_{i=1}^{n_h} (x_i - x_{i+h})^2 \qquad \text{Equation 2.5}$$

where: $g(h)$ = variogram
h = separation distance (or lag)
n_h = number of pairs
x_i = the ith observation of X

Concentrated Static Load (CSL) Test

The concentrated static load testing values for maximum deflection and ultimate load were obtained from Bozo 2002. The concentrated static load was applied at the center-span between supports at 63.5 mm from the edge of the panel. The test was applied using a 76.2-mm diameter-loading disk for deflection and a 25.4-mm diameter-loading disk for ultimate load. First the panel was loaded with a constant deflection rate of 2.5 mm/minute, and recording the maximum deflection under the point load when at a load of 890 N was attained. Then the load

was removed and the loading disk replaced by the 25.4-mm diameter. The panel is subsequently loaded at the rate of 5 mm/minute until failure, recording the ultimate load.

Density-CSL Correlations

Because density is so highly correlated to many mechanical properties, it is often used as a key material design or quality assurance parameter. This segment of the investigation was developed to determine the size of density region necessary for optimal prediction of CSL behavior. The mean density was determined for 12 different areas surrounding the load region (Fig. 2.2 and 2.3 and Tab. 2.1). These density values are then correlated to maximum deflection and ultimate load values using linear regression.

Area	Dimensions	
	Maximum deflection	Ultimate load
d1	76.2-mm	25.4-mm
d2	76.2- by 76.2-mm	25.4- by 25.4-mm
d3	101.6- by 101.6-mm	50.8- by 50.8-mm
d4	127.0- by 127.0-mm	76.2- by 76.2-mm
d5	152.4- by 139.7-mm	101.6- by 101.6-mm
d6	177.8- by 152.4-mm	127.0- by 127.0-mm
d7	203.2- by 165.1-mm	152.4- by 139.7-mm
d8	228.6- by 177.8-mm	177.8- by 152.4-mm
d9	254.0- by 190.5-mm	203.2- by 165.1-mm
d10	279.4- by 203.2-mm	228.6- by 177.8-mm
d11	304.8- by 215.9-mm	254.0- by 190.5-mm
Global	609.6- by 1176.0-mm	609.6- by 1176.0-mm

Table 2.1. *Dimension of the defined areas for maximum deflection and ultimate load.*

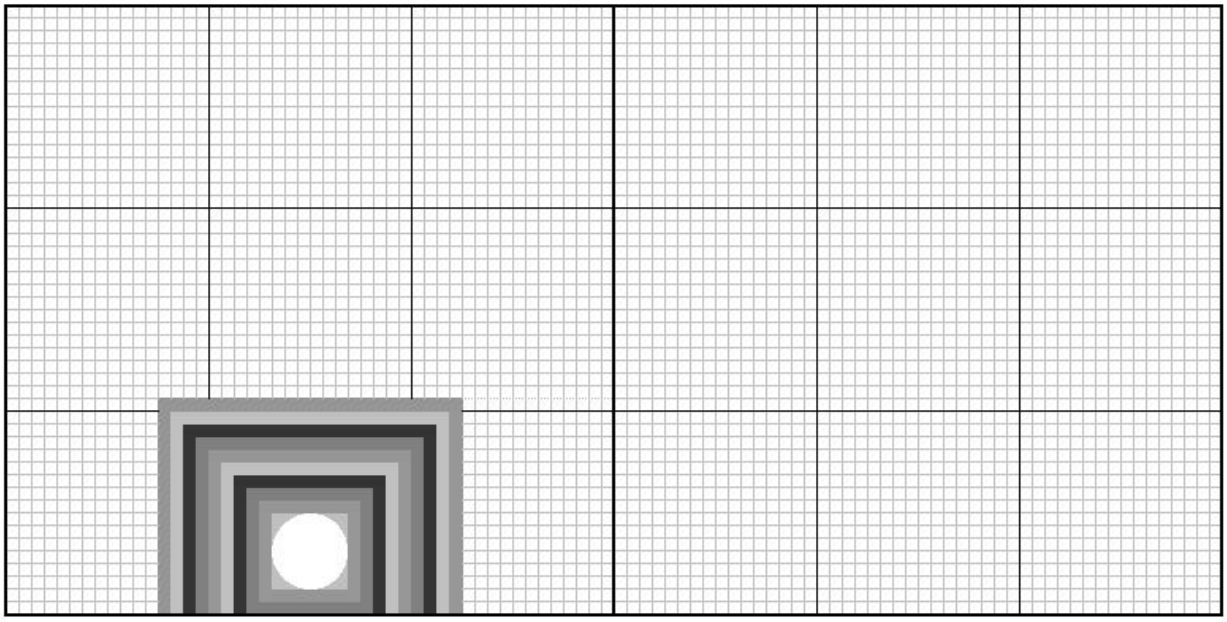

Figure 2.2. *Area definition to relate local density and maximum deflection.*

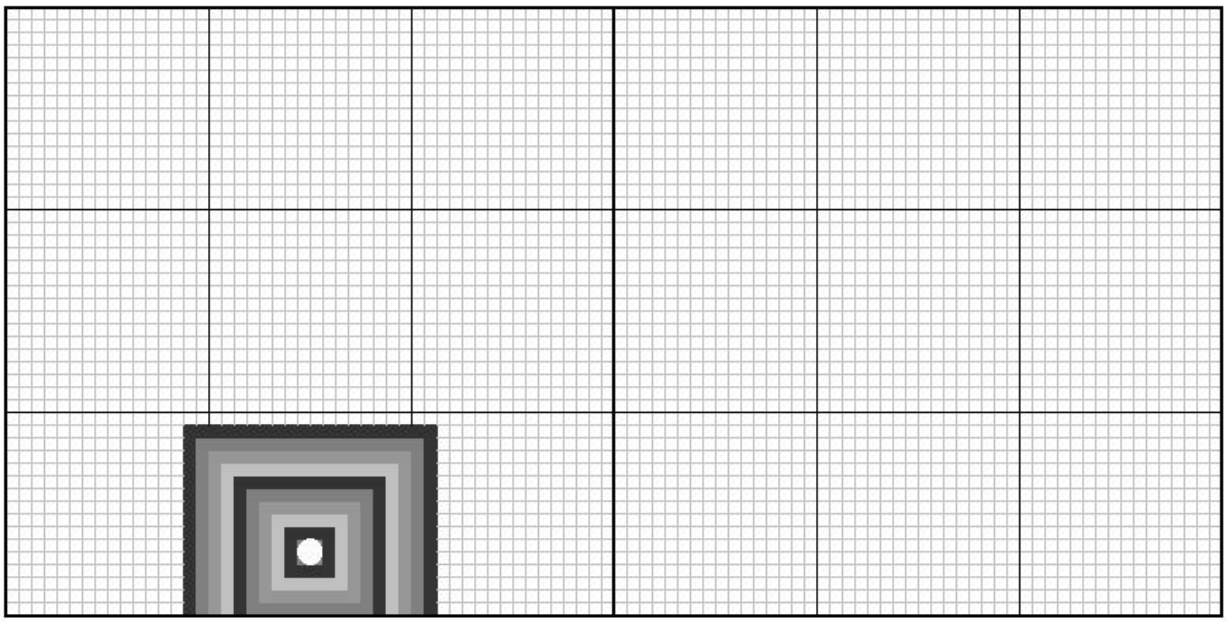

Figure 2.3. *Area definition to relate local density and ultimate load.*

Results and Discussion

Variability exists at many levels within OSB panels (Xu and Steiner 1995; Lang and Wolcott 1996; Wolcott et al. 1998). From a population standpoint, traditional statistical sampling and distribution techniques can be effective at quantifying production variability. However, different methods must be employed to visualize and describe variability of properties within panels. Contour and three-dimensional graphing techniques can be used to visualize the local density and patterns formed in a panel. While these techniques can be extremely effective in conveying qualitative patterns through visualization, they are lacking in quantitative measurement for comparison. Differences in localized panel properties can vary in random or systematic manners. Techniques exist to describe and model random variation; however, the random nature of the data implies that any patterns that form in a panel are purely by chance. Therefore, property patterns that contribute to material structure are not very reproducible on many levels. In contrast, systematic aspects of variation can often be found in data that appears random. With systematic variation, characterizing and describing the patterns can often lead to recognizing and controlling the source of variability. Time series analysis techniques can be used to examine the correlation of adjacent and distant units of data. Systematic components of correlation can be exhibited and described in step-changes, trends, and periodicity.

Windows Size

The density values at different specimen sizes were taken as the average of several 12.7- by 12.7- mm density values. Using the global mean and corresponding standard deviation of density, the coefficient of variation (COV) was determined for different window sizes. The numerical results are shown in Figure 2.4.

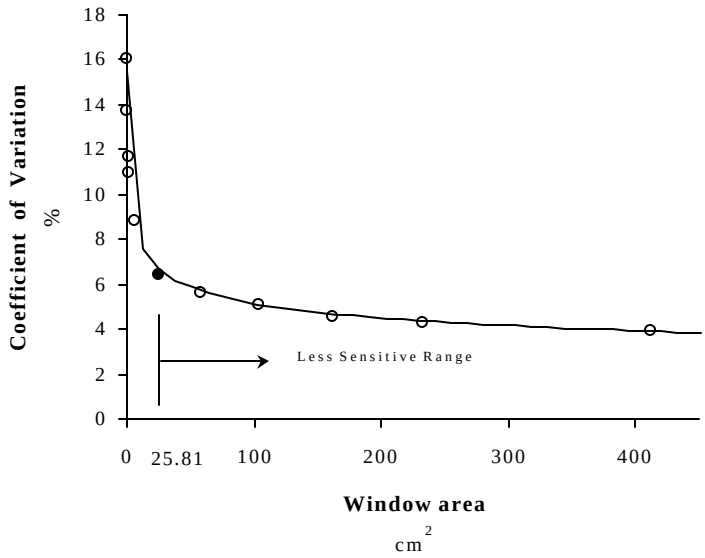

Figure 2.4. *Coefficient of variation vs. window size.*

The coefficient of variation of density decreases as window size increases. Similar results were found by others researchers (Suchsland and Xu 1991b; Xu and Steiner 1995). The less sensitive range, defined by Xu and Steiner (1995), was found to be beyond 25-cm^2, which corresponds to a windows size of 5- by 5-cm (Fig. 2.4). Windows sizes smaller than 5- by 5-cm result in high variability due to the effect of void spaces, and window sizes larger than 5- by 5-cm results in a dramatic drop of variability. Consequently, a 5- by 5-cm window area was used in this research.

Graphical Methods

When properties are determined over an entire panel, it is useful to visualize them with respect to the panel location. Four graphical methods were used: 1) data plot; 2) color-scale plot; 3) three-dimensional surface plot; and 4) contour plots. An example of a data plot is shown in Figure 2.5 and corresponds to panel named m1p3, which was selected because it was a typical panel.

The visualization of data values through the data plot is an efficient means of recognizing the level of variation. Moreover, this plot could be most useful for identifying outliers or data values that may be erroneous (Isaaks and Srivastava 1989). The 10 highest and 10 lowest values from Figure 2.5 were highlighted by white and gray boxes, respectively. The seven highest values: 664, 643, 640, 671, 641, 697, and 686 were located in the longitudinal central part of the panel. The nine lowest values: 454, 464, 467, 471, 463, 459, 418, 458, and 461, were located in the lowest third part of the panel.

density	25	76	127	178	229	279	330	381	432	483	533	584	635	686	737	787	838	889	940	991	1041	1092	1143	1194 mm
25	491	551	569	543	547	499	523	528	541	556	551	577	625	560	591	569	599	539	573	556	542	529	524	625
76	501	524	501	532	552	506	518	524	539	578	577	534	576	577	589	549	565	614	544	548	530	551	522	530
127	487	479	499	541	561	522	524	525	582	586	571	511	533	557	615	621	588	573	572	524	541	591	587	533
178	524	486	505	524	544	555	570	588	559	547	514	579	574	595	575	608	521	550	536	569	536	492	565	616
229	545	561	512	552	543	528	541	556	573	592	579	590	602	551	545	589	595	543	584	550	538	558	572	540
279	575	546	547	596	586	569	554	475	536	506	544	586	577	571	575	595	587	535	517	513	518	583	565	584
330	560	572	565	579	560	621	523	516	556	535	579	555	522	553	570	581	573	624	577	591	553	552	532	563
381	554	481	560	552	517	595	513	523	536	509	590	588	510	542	498	558	579	553	572	600	583	521	549	583
432	539	577	544	632	544	566	551	533	482	519	532	524	572	538	565	555	563	567	565	534	597	592	577	579
483	556	555	500	563	543	551	563	522	574	545	539	509	535	549	560	594	577	582	585	545	577	543	550	559
533	564	573	571	524	515	505	574	516	556	512	532	563	538	589	538	551	575	627	592	550	576	505	497	572
584	571	605	556	524	500	508	549	529	551	462	548	579	512	611	601	664	621	566	591	554	553	562	506	504
635	556	578	569	543	489	504	541	544	514	481	571	609	571	608	572	615	561	587	503	567	508	506	562	626
686	517	525	534	540	572	551	528	537	514	546	537	520	555	586	604	557	552	578	511	546	531	502	546	620
737	568	527	502	525	563	517	569	565	554	584	533	551	522	553	565	547	578	610	506	573	535	522	591	554
787	494	517	525	540	615	564	517	537	576	573	533	527	535	526	616	559	556	532	565	542	519	500	511	516
838	490	489	545	555	617	600	534	523	568	621	561	596	643	576	640	598	582	565	547	614	544	511	572	542
889	562	517	502	570	566	558	575	546	545	634	621	530	598	491	575	594	580	543	548	579	568	575	604	543
940	537	473	504	506	548	562	606	558	556	550	564	554	593	564	586	547	521	541	577	582	563	549	553	577
991	536	478	564	558	545	569	550	561	506	530	554	587	598	574	553	552	543	551	623	631	592	583	563	545
1041	514	477	559	546	534	557	596	570	526	576	597	564	582	553	607	585	555	583	585	594	588	542	567	612
1092	554	535	587	526	550	503	533	547	529	566	607	546	534	558	554	531	544	555	529	584	562	579	560	563
1143	573	588	584	556	503	490	543	507	549	560	612	609	553	591	554	523	559	511	555	521	581	533	600	521
1194	491	534	557	527	514	582	576	549	530	505	521	503	528	528	513	516	541	557	569	576	583	592	571	565
1245	563	551	554	527	544	573	608	580	531	524	530	505	545	539	606	528	596	520	501	527	538	571	570	553
1295	543	641	524	535	544	552	549	552	574	568	532	508	556	554	579	551	588	572	548	497	572	581	552	500
1346	532	565	547	538	519	558	609	605	588	566	525	518	535	529	542	569	560	518	517	511	576	560	560	475
1397	544	522	535	570	542	576	580	592	516	546	544	504	508	536	552	580	532	561	521	524	520	529	547	541
1448	564	548	576	536	500	549	604	516	494	498	569	539	561	525	562	616	576	565	524	547	568	543	589	621
1499	518	544	586	577	556	541	602	603	526	577	615	571	545	565	617	615	578	579	581	525	541	577	564	591
1549	567	539	590	552	525	550	589	598	542	596	575	552	523	548	563	577	671	629	612	566	609	567	583	570
1600	602	531	516	572	534	557	559	524	533	533	572	561	545	556	576	546	523	636	579	619	566	566	555	545
1651	524	477	499	580	595	555	590	541	581	588	579	622	556	531	536	481	517	572	553	536	564	573	527	454
1702	546	555	575	589	523	540	548	524	588	549	541	564	568	537	511	538	573	615	562	583	538	528	604	519
1753	577	560	609	596	562	590	561	529	524	542	553	501	567	527	534	548	557	592	527	542	525	489	591	554
1803	562	599	576	568	554	555	533	553	520	550	523	505	555	518	535	582	547	514	569	561	518	504	560	587
1854	634	588	543	596	629	601	537	524	579	516	538	547	553	519	577	616	535	548	547	543	500	481	514	605
1905	592	592	500	516	597	490	464	517	628	545	505	564	549	563	571	586	572	591	574	560	515	549	484	574
1956	540	513	467	498	566	575	507	500	592	603	524	531	541	558	539	573	577	524	552	471	545	504	508	536
2007	546	523	463	526	601	498	554	571	538	459	509	510	534	539	602	562	540	520	533	525	545	508	529	418
2057	549	579	573	541	538	560	553	511	529	525	587	529	523	561	584	571	569	574	555	514	558	561	520	458
2108	549	524	549	547	558	582	520	553	517	550	546	539	569	559	518	584	608	573	574	539	565	578	583	556
2159	580	540	600	522	507	581	535	558	570	538	551	542	587	587	563	574	597	544	557	594	558	534	697	614
2210	574	559	579	490	505	546	566	572	525	586	528	583	580	585	641	617	628	566	550	560	550	551	557	547
2261	583	631	555	461	524	554	572	489	494	506	500	571	566	620	601	566	599	568	545	580	562	569	551	555
2311	566	603	604	554	543	561	633	561	543	564	554	538	516	585	697	551	539	609	547	582	570	581	593	634
2362	594	523	616	559	562	538	524	519	549	604	574	513	562	586	686	633	581	595	612	533	511	581	631	626
2413	583	559	529	554	641	571	542	531	559	567	599	550	594	599	617	590	608	592	600	541	577	598	579	548
mm																								

Figure 2.5. *Data plot of density (kg/m^3) of panel m1p3 (window size 50- by 50-mm)*

The data plot was an important first step to analyzing spatial data sets, and provided a quick visual reference for the amount of variability that exists within a panel; however it did not facilitate recognizing patterns of data that might form from this variation. When viewing the same data in a gray-scale plot, the variability was more easily seen (Fig. 2.6). This treatment provides a clear picture of the variability level of the data set. Similar to the gray-scale plot was the three-dimensional plot shown in Figure 2.7, where the three-dimensional effect was incorporated to indicate variability. The contour plot of the density data of panel m1p3 is shown in Figure 2.8. This contour plot clearly shows the zones with high and low densities, which are highly dominated by the high and low local densities values presented in the data plot in Figure 2.5. The data values are interpolated to generate the contour plot, making the contoured surfaces appear smoother.

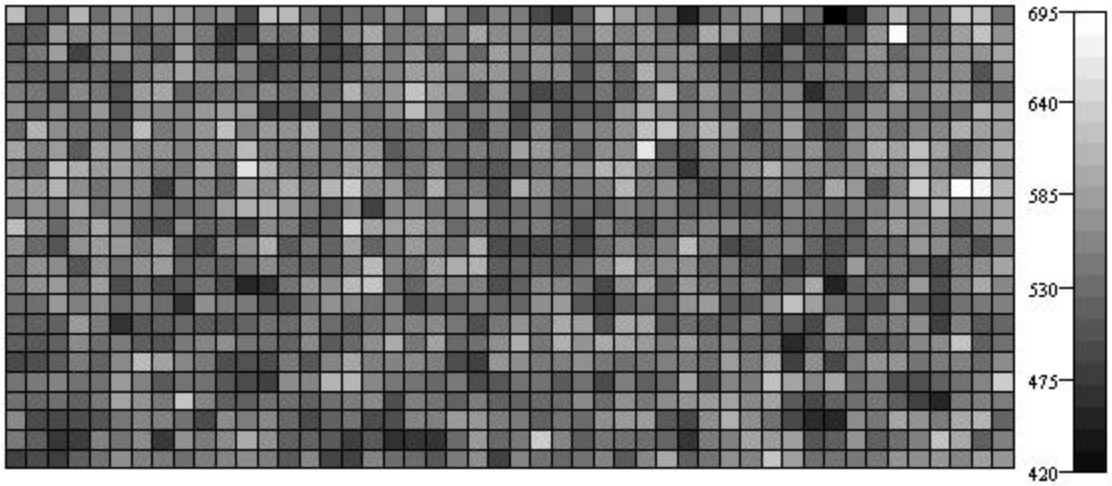

Figure 2.6. *Gray-scale plot of density (kg/m^3) of panel m1p3 (window size 50- by 50- mm).*

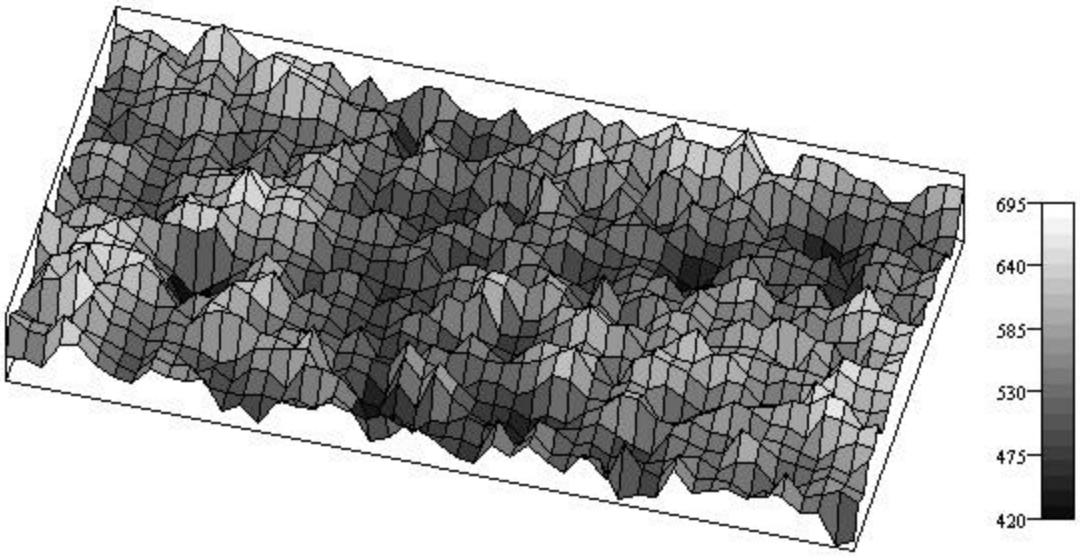

Figure 2.7. *Three-dimensional plot of density (kg/m^3) of panel m1p3 (window size 50- by 50- mm).*

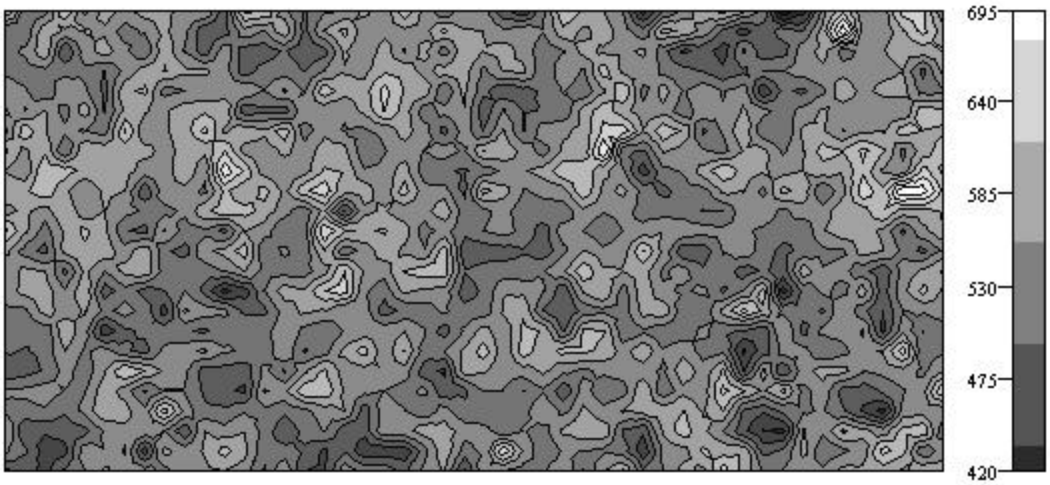

Figure 2.8. *Contour plot of density (kg/m^3) of panel m1p3 (window size 50- by 50- mm).*

The graphical results of the remaining 17 panels are shown in Appendix A. The contour plot corresponding to master panel 1, master panel 2, and master panel 3 are shown in Figures 2.9, 2.10, and 2.11, respectively.

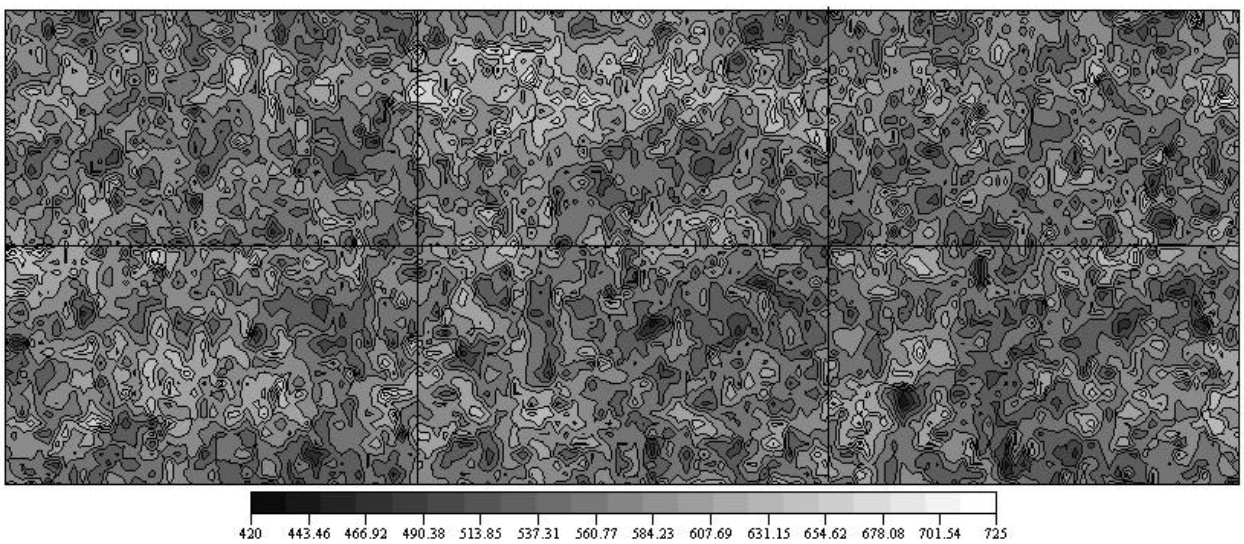

Figure 2.9. *Contour plot of density values (kg/m^3) for master panel 1.*

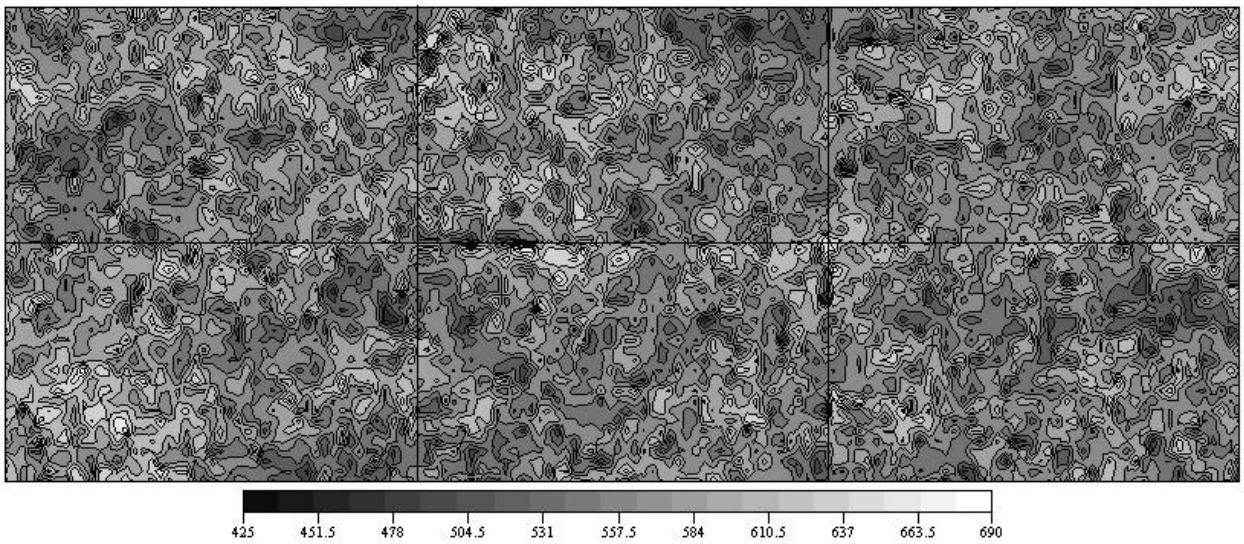

Figure 2.10. *Contour plot of density values (kg/m^3) for master panel 2*

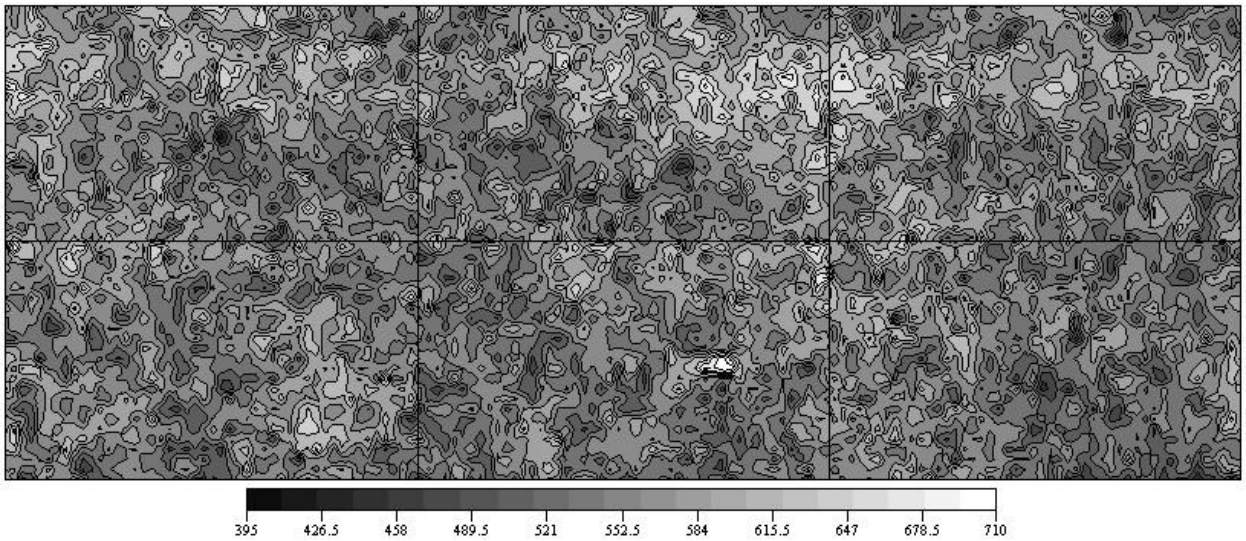

Figure 2.11. *Contour plot of density values (kg/m^3) for master panel 3).*

The regions of high and low density as well the continuity from panel to panel can be seen through Figures 2.9, 2.10, and 2.11. For example, regions with high density are presented in the top-left part of panel *m1p2*, the left part of panel *m2p4*, the top-right of panel *m3p2*, and top-left part of panel *m3p3*. Regions with low density are presented in the central part of panel *m1p6*, the right part of panel *m2p4*, and bottom-left part of panel *m3p6*. The continuity between panels and master is seen in all panels with a common boundary. A clear example of panel continuity is the corner formed by panels *m2p2*, *m2p3*, *m2p5*, and *m2p6*. Continuity between the master panels can be seen between panels *m1p3* and *m2p1*, as well as between panels *m2p3* and *m3p1*.

Analytical Methods

Basic Statistics

The basic statistical results are presented in Table 2.2, and correspond to mean, standard deviation, coefficient of skewness, coefficient of kurtosis, maximum, minimum, and range.

Density kg/m^3	Mean kg/m^3	Coefficient of variation %	Coefficient of skewness (kg/m^3)^2	Coefficient of kurtosis (kg/m^3)^3	Maximum kg/m^3	Minimum kg/m^3	Range kg/m^3
m1p1	557.1	5.98	0.0256	-0.0575	663.8	455.1	208.6
m1p2	573.4	6.96	0.0915	-0.1865	715.6	457.4	258.1
m1p3	554.8	6.19	0.1352	0.6598	697.3	417.9	279.4
m1p4	560.7	6.68	0.1825	0.3862	723.6	445.9	277.7
m1p5	552.4	6.26	-0.0093	-0.1543	654.1	422.8	231.3
m1p6	551.2	6.89	0.0370	-0.0733	676.1	423.6	252.6
m2p1	563.2	6.08	-0.0472	0.1007	668.3	443.2	225.1
m2p2	561.4	6.55	0.0257	-0.0555	676.1	424.3	251.8
m2p3	564.9	5.84	0.0754	0.2715	688.4	460.6	227.8
m2p4	568.7	6.55	0.0161	-0.0815	692.3	453.6	238.6
m2p5	560.8	6.04	0.2261	0.2076	690.6	452.4	238.2
m2p6	557.6	6.12	0.0095	-0.0001	676.1	459.3	216.8
m3p1	561.6	6.90	0.0681	0.1502	692.0	395.5	296.5
m3p2	565.7	7.34	0.1043	-0.1958	688.9	431.1	257.9
m3p3	559.8	6.87	0.0658	-0.0362	686.9	413.3	273.6
m3p4	551.0	6.51	0.0839	0.0032	678.5	450.1	228.4
m3p5	545.4	6.90	0.5487	0.9305	708.4	455.1	253.4
m3p6	541.8	6.57	0.0166	-0.0691	647.4	425.9	221.5
Master 1	558.3	6.64	0.1336	0.1706	724.0	418.0	306.0
Master 2	562.8	6.23	0.0578	0.0697	692.0	424.0	268.0
Master 3	554.3	7.04	0.1935	0.0894	708.0	396.0	312.0
Mat	558.5	6.67	0.1100	0.1046	724.0	396.0	328.0

Table 2.2. *Basic Statistics*

These results show that all panels are similar for all statistics analyzed, as well as for master panels, and also that they are comparable to the mat result. The coefficient of skewness and kurtosis suggests that the data sets be of normal behavior.

Histogram and PDF

The histogram of the entire data set or mat is presented in Figure 2.12 along with the normal distribution curve, which was fitted by Pearson Chi-squared statistics, χ^2, and Kolmogorov-Smirnov (KS) test. The calculated χ^2 was less than the corresponding critical value at a significance level of 0.05, consequently, the normal fitting is justified. The same general behavior was observed in the master panels and in all individual panels. Similar distribution results were found by Lang and Wolcott (1996); and Xu and Steiner (1995). The histogram and PDF for *m1p3* is presented in Figure 2.13. The Chi-squared, χ^2 and Kolmogorov-Smirnov, KS results for all panels, master panels, and mat are presented in Table 2.3. The histogram and PDF for all other panels and master panels are presented in Appendix B.

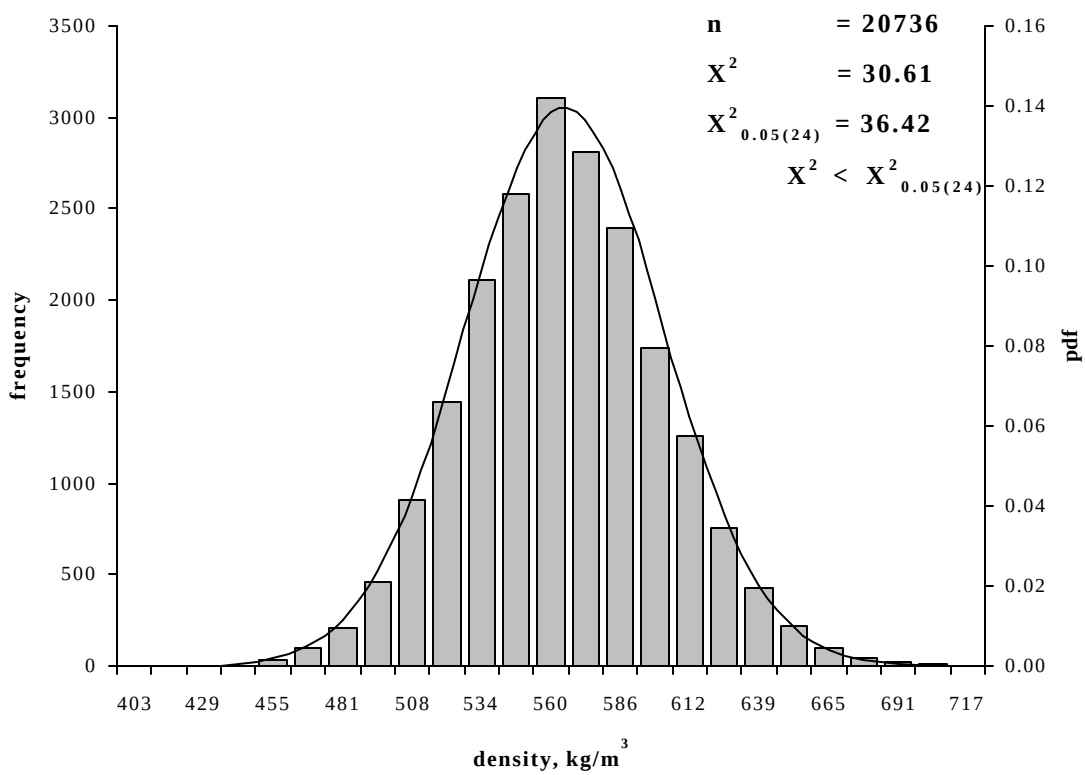

Figure 2.12. *Histogram and PDF for density data values of the complete mat.*

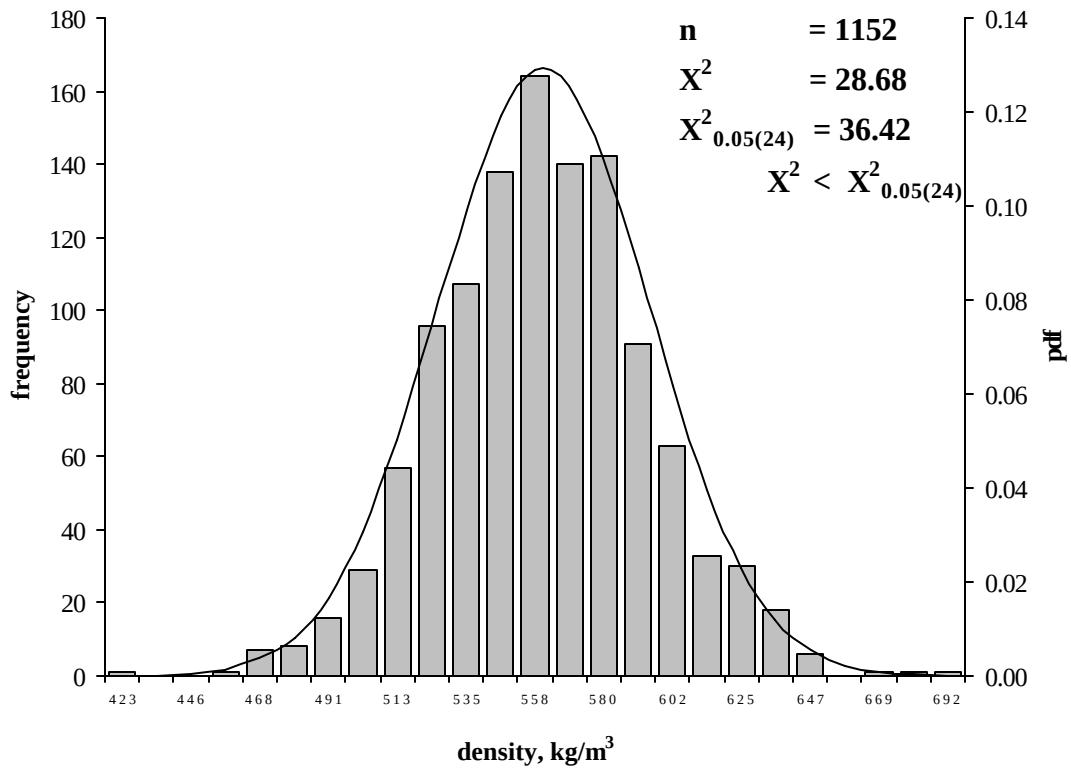

Figure 2.13. *Histogram and PDF for density data values of m1p3.*

Data set	n	d.o.f.	X^2_{cal}	$X^2_{0.05}$	KS	C_a	H_0
m1p1	1152	24	12.44	36.42	0.0167	0.0401	not rejection
m1p2	1152	24	17.15	36.42	0.0172	0.0401	not rejection
m1p3	1152	24	28.69	36.42	0.0317	0.0401	not rejection
m1p4	1152	24	28.56	36.42	0.0235	0.0401	not rejection
m1p5	1152	24	30.46	36.42	0.0219	0.0401	not rejection
m1p6	1152	24	18.06	36.42	0.0275	0.0401	not rejection
m2p1	1152	24	14.69	36.42	0.0195	0.0401	not rejection
m2p2	1152	24	24.96	36.42	0.0180	0.0401	not rejection
m2p3	1152	24	17.20	36.42	0.0196	0.0401	not rejection
m2p4	1152	24	17.33	36.42	0.0233	0.0401	not rejection
m2p5	1152	24	21.40	36.42	0.0366	0.0401	not rejection
m2p6	1152	24	21.38	36.42	0.0291	0.0401	not rejection
m3p1	1152	24	15.45	36.42	0.0236	0.0401	not rejection
m3p2	1152	24	15.33	36.42	0.0283	0.0401	not rejection
m3p3	1152	24	21.60	36.42	0.0232	0.0401	not rejection
m3p4	1152	24	21.20	36.42	0.0204	0.0401	not rejection
m3p5	1152	24	32.68	36.42	0.0399	0.0401	not rejection
m3p6	1152	24	21.54	36.42	0.0169	0.0401	not rejection
master 1	6912	24	34.07	36.42	0.0107	0.0160	not rejection
master 2	6912	24	24.11	36.42	0.0071	0.0160	not rejection
master 3	6912	24	31.14	36.42	0.0089	0.0160	not rejection
mat	20736	24	30.61	36.42	0.0098	0.0157	not rejection

Table 2.3. *Results of the χ^2 test of goodness of fit for normal distribution*

Moving Window Statistics

To complete this segment of the research, three specimen sizes were used: 50- by 50-mm, 100- by 100- mm, and 200- by 200-mm. Mean and standard deviation were computed for all of the windows. These measures were then used to construct contour maps used to identify zones with anomalies at different sizes. The proportional effect was evaluated using a linear regression model between the local mean and local standard deviation. The contour plot of mean and standard deviation at different window sizes for *m1p3* is shown in Figure 2.14, and corresponding scatterplots with respective regression models are presented in Figure 2.15. The contour plots show the variability level of density. More details are visible from the plot made using the smallest window size; however, the patterns are reproduced at different scales. The contour plots of standard deviation show that at the smallest window size, the variability of standard deviation is the largest; and, that variability decreases as the window size increases.

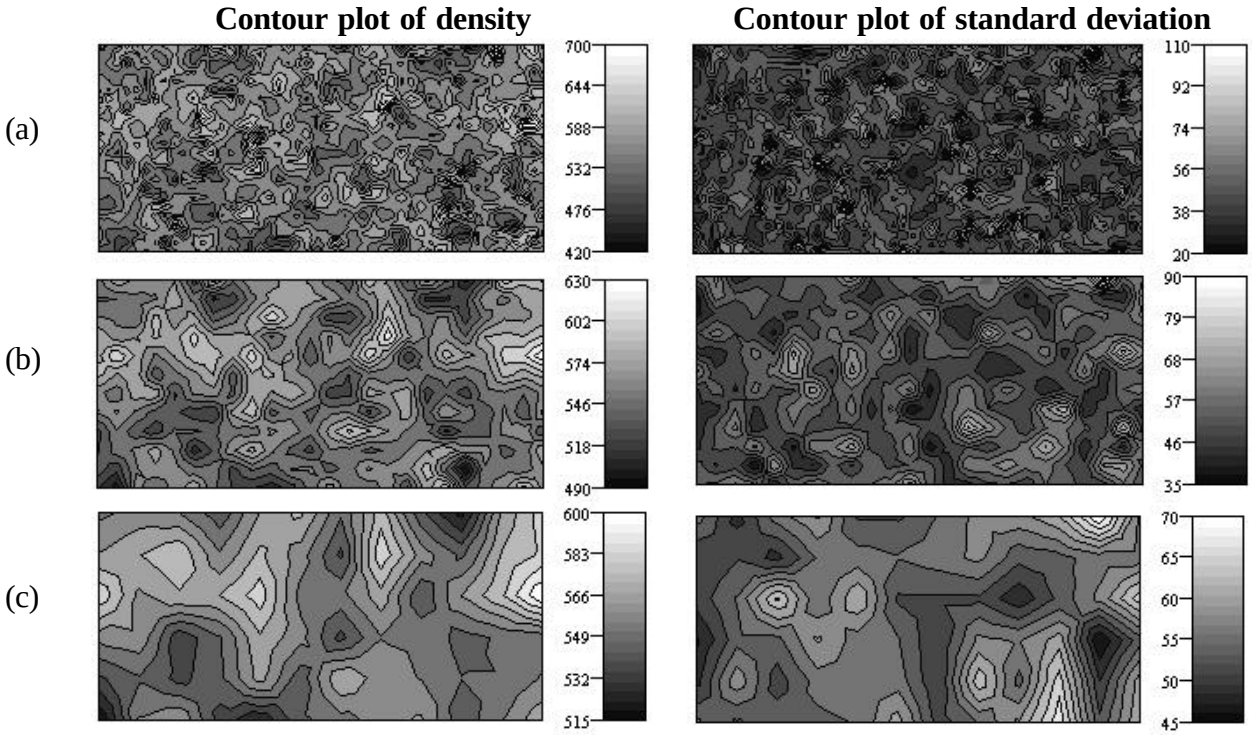

Figure 2.14. *Contour plot of proportional effect for panel m1p3: (a) windows size 50- by 50-mm, (b) windows size 100- by 100-mm, and (c) windows size 200- by 200-mm.*

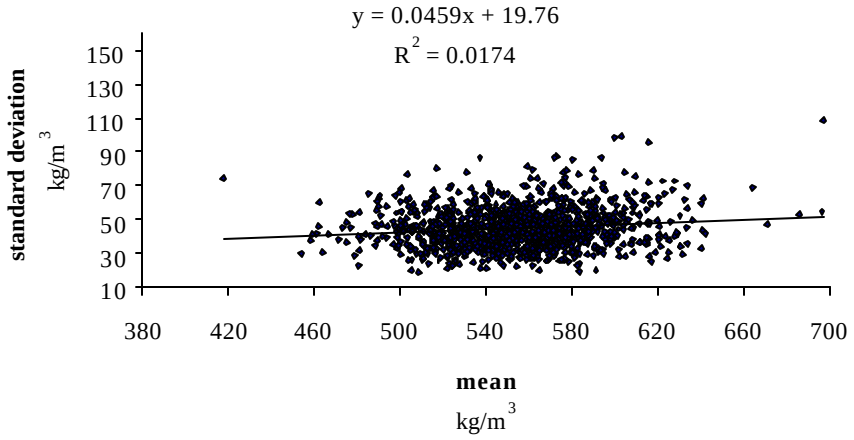

(a)

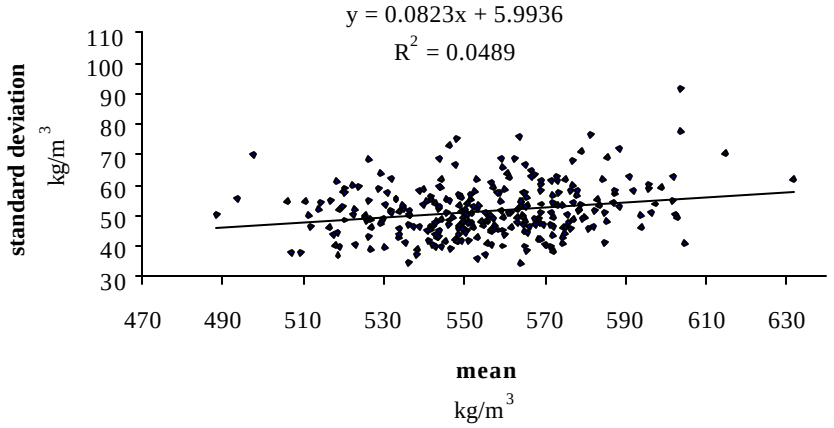

(b)

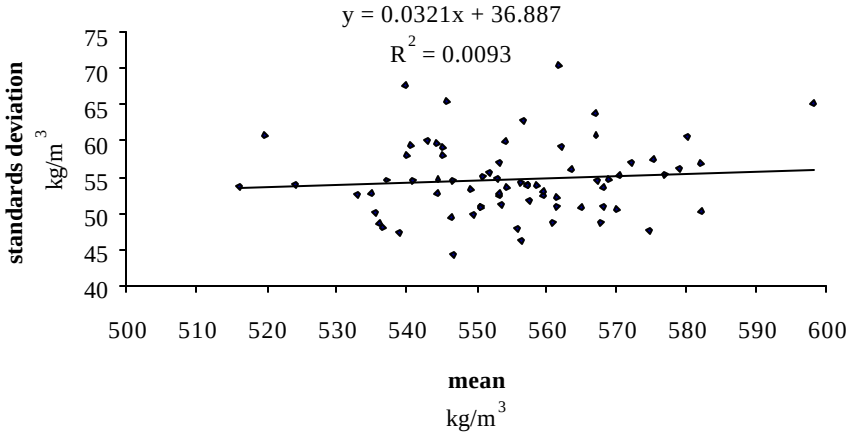

(c)

Figure 2.15. *Regression plot of proportional effect m1p3: (a) window size 50- by 50-mm, (b) window size 100- by 100-mm, and (c) window size 200- by 200-mm.*

The scatterplots and their corresponding regression models shown in Figure 2.15, indicate no proportional effect. Interpretation of this result indicates that there is no relationship between the local mean and local standard deviation for density data as reflected by the very low values of the coefficient of determination. The regression results at different window sizes for all panels are presented in Table 2.4. For a normally distributed data set, these results are to be expected and indicate that any reasonable estimation method will be positively influenced by this low proportional effect. Analogous results are obtained for all other panels and are included in Appendix C.

Panel	R^2_{50}	R^2_{100}	R^2_{200}
m1p1	0.0194	0.0421	0.1111
m1p2	0.0151	0.0281	0.0789
m1p3	0.0174	0.0489	0.0093
m1p4	0.0362	0.0620	0.1186
m1p5	0.0203	0.0057	0.0159
m1p6	0.0130	0.0011	0.0040
m2p1	0.0137	0.0083	0.0038
m2p2	0.0008	0.0054	0.0453
m2p3	0.0248	0.0480	0.0216
m2p4	0.0207	0.0426	0.0111
m2p5	0.0152	0.0222	0.1417
m2p6	0.0290	0.0633	0.1737
m3p1	0.0146	0.0198	0.0448
m3p2	0.0111	0.0027	0.0028
m3p3	0.0072	0.0006	0.0061
m3p4	0.0143	0.0285	0.0463
m3p5	0.0294	0.1233	0.0937
m3p6	0.0172	0.0163	0.0626

Table2.4. *Coefficient of determination results for proportional effect at different window sizes.*

Spatial Continuity

When the data or contour plots are carefully observed, the density data values do not appear randomly located. Low density values are commonly found near other low density values, and vise versa. Determining the zone or area of influence is highly important to describe the spatial continuity of the data set and also essential for certain estimation methods. The

methods used to describe spatial continuity are the autocorrelation function, variogram, and spectral density analysis applying Equations 2.2, 2.4, and 2.5. The plot of uniformly spaced density data for one randomly selected column is shown in Figure 2.16 (a), the corresponding correlogram in Figure 2.16 (b), and the spectral density applied to the autocorrelation function in Figure 2.16 (c). Analogous results for a randomly selected row are shown in Figure 2.17 (a), (b), and (c), respectively. The digitizing increment for the row data was 50.8 mm. Thus, for N=48 increments, the corresponding frequency increment for the spectrum is 1/(48*50.8)=0.00041 cycles/mm. The purpose here is to find the range of influence of the linear array in both directions, transverse and longitudinal, with respect to the machine direction of the panel.

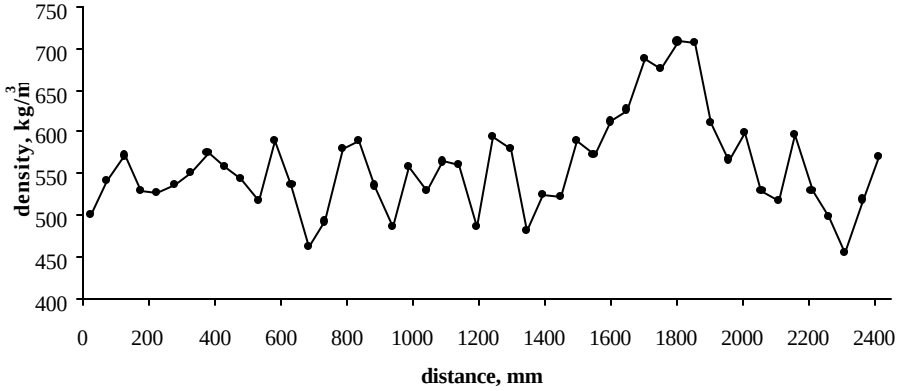

(a)

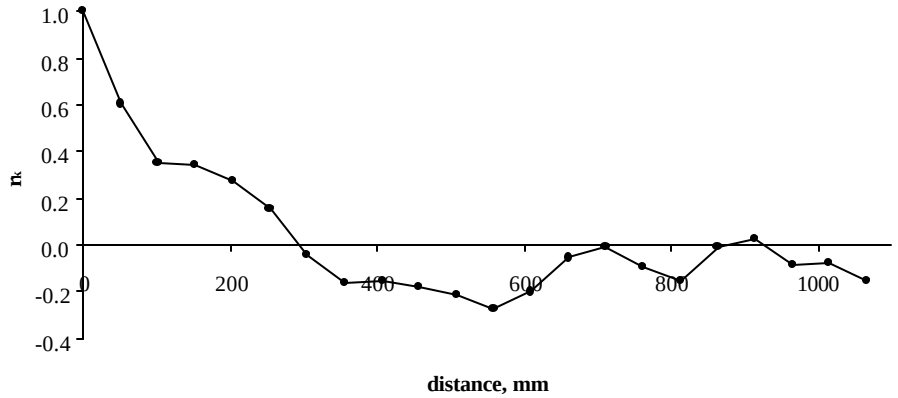

(b)

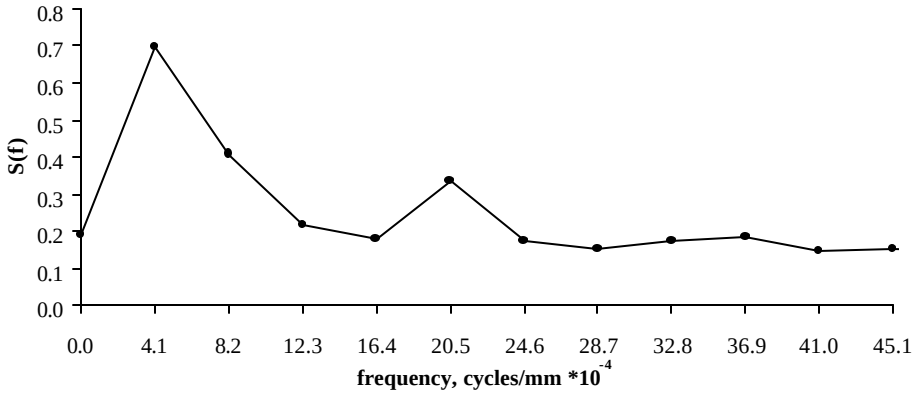

(c)

Figure 2.16. *Density data array of m3p5, Column 12 (longitudinal direction). (a) raw data, spacing Dx=50.8 mm N=48, (b) correlogram, and (c) spectrum, Df=1/(Dx*N)=0.00041.*

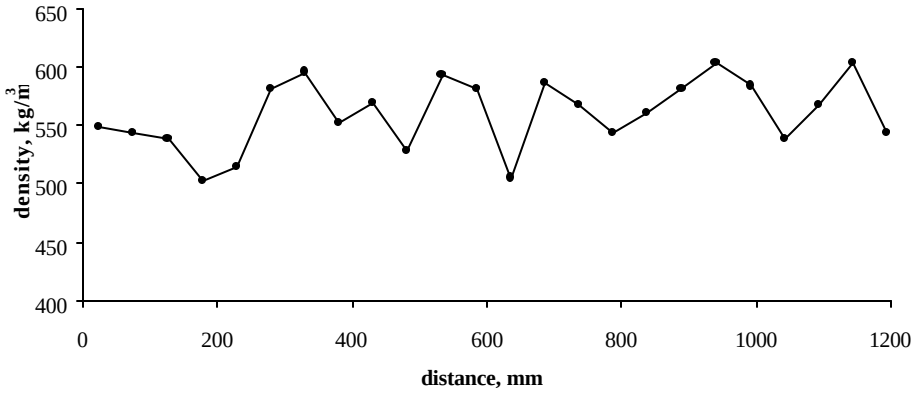

(a)

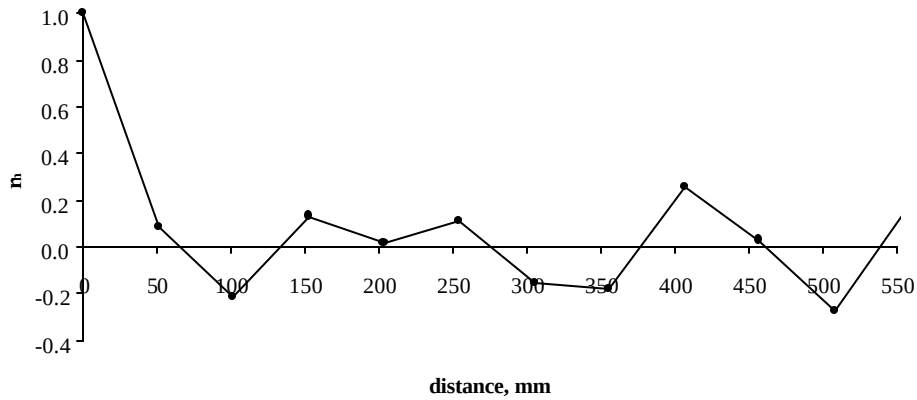

(b)

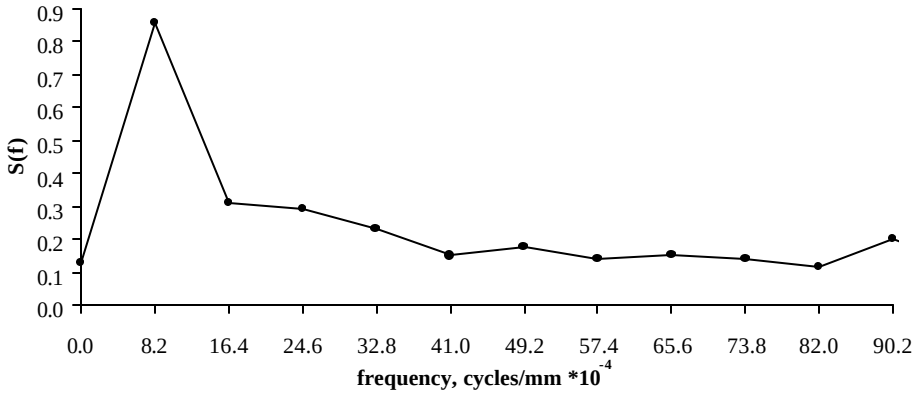

(c)

Figure 2.17. *Density data array of m1p6, Row 5 (transversal direction). (a) raw data, spacing* Δx*=50.8 mm N=24 , (b) correlogram, and (c) spectrum,* Δf*=1/(*Δx**N)=0.00082*.

The particular examples presented in Figures 2.16 and 2.17 show an indication of spatial dependence in both transverse and longitudinal directions, respectively. In the longitudinal direction the indication of spatial dependence is between 250 mm and 400 mm according to the correlogram (Fig. 2.16 b). The previous result agrees with Figure 2.16 c where the spatial dependence is at a frequency of 28.7 x 10^{-4} cycles/mm that corresponds to a distance of 348 mm. In the transverse direction, the correlogram in Figure 2.17a suggests that the spatial dependence of density data is between 100 and 200 mm. However, the spectral density indicates that the spatial dependence is a value of frequency between 41 and 49.2 x 10^{-4} cycles/mm that corresponds to 203.2 and 243 mm, respectively. These results are for column 12 of panel *m3p5*, and row 5 of panel *m1p6*. All of the correlograms begin at 1.0 and decrease to nearly 0.0 with increasing lag. Most of the curves display some degree of periodicity with oscillations about the zero line; however, this periodicity is relatively weak in many cases. In general, the indication of spatial dependence in the longitudinal direction is between 250 and 400 mm, and in the transverse direction it is between 100 and 200 mm.

Perhaps more interesting to analyze is the spatial dependence in two dimensions if considering the panel as a two-dimensional array as opposed to individual columns and rows. To conduct the two-dimensional analysis, the first step was to obtain the variogram and correlogram of density data for each panel in different orientations (0°, 45°, 90°, and 135°). The next step was to perform the FFT on the correlogram results to obtain the spectral density. And finally, the results were compared to identify the range of influence of the density data values. Figures 2.18, 2.19, and 2.20 correspond to the variograms and correlograms of *m1p3* at omnidirectional, transverse, and longitudinal directions, respectively. Figure 2.21 represents the spectral density of the correlogram results at the same directions.

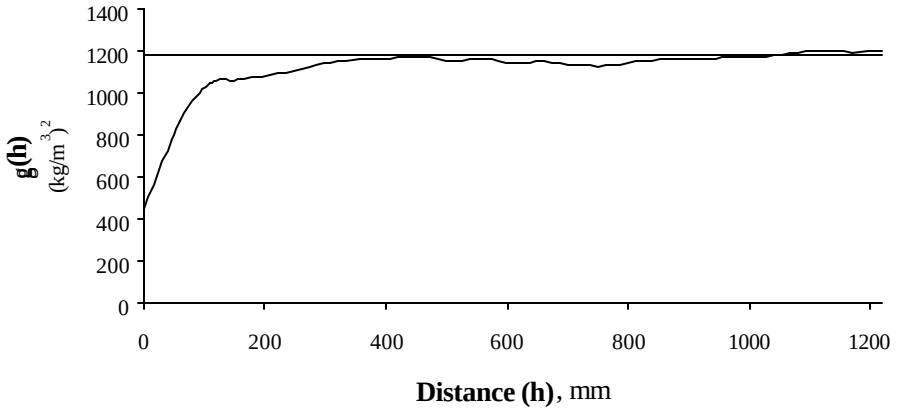

(a)

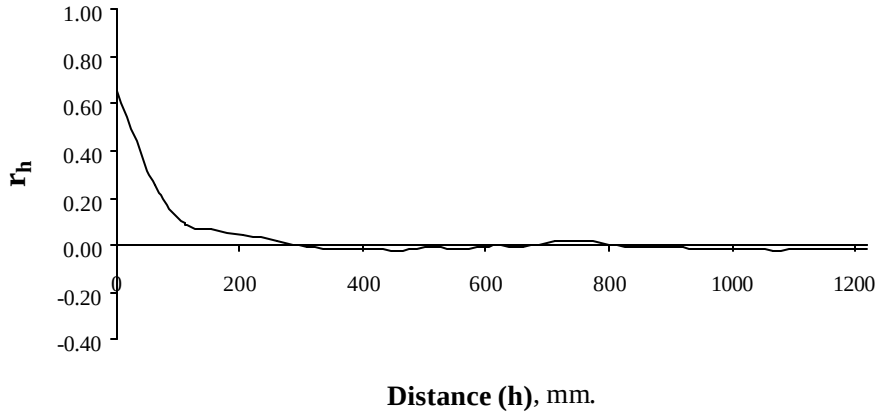

(b)

Figure 2.18. *Panel m1p3: (a) omnidirectional variogram and (b) omnidirectional correlogram.*

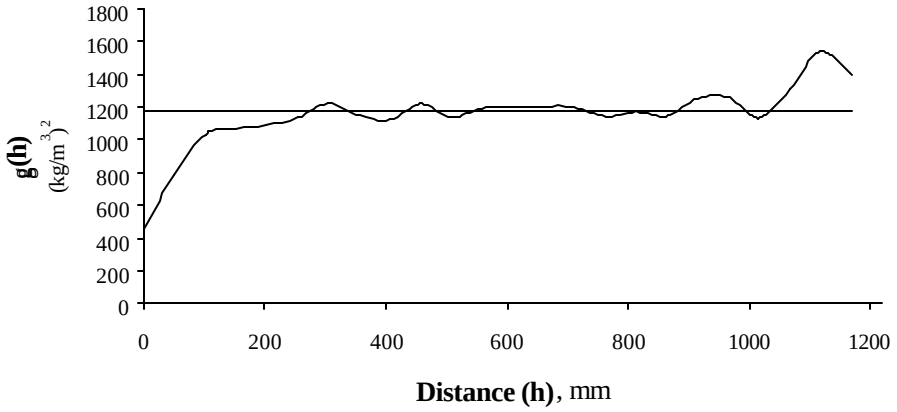

(a)

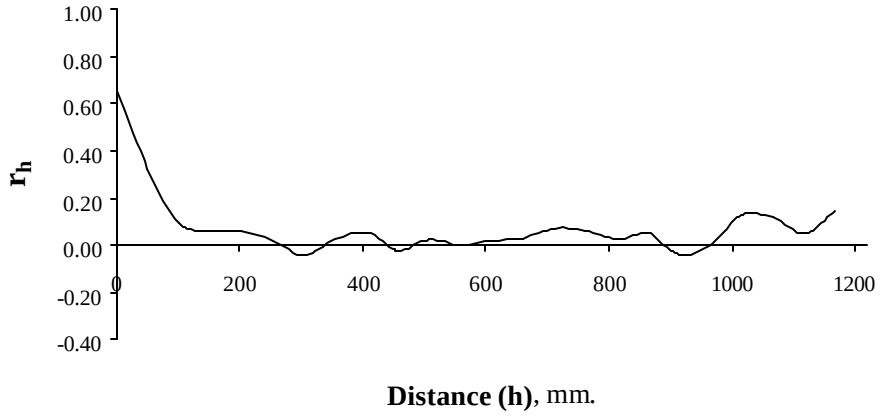

(b)

Figure 2.19. *Panel m1p3: (a) transverse variogram and (b) transverse correlogram.*

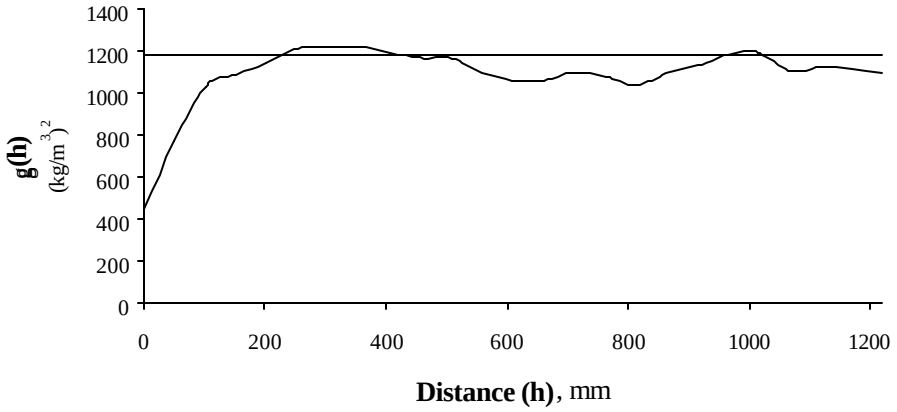

(a)

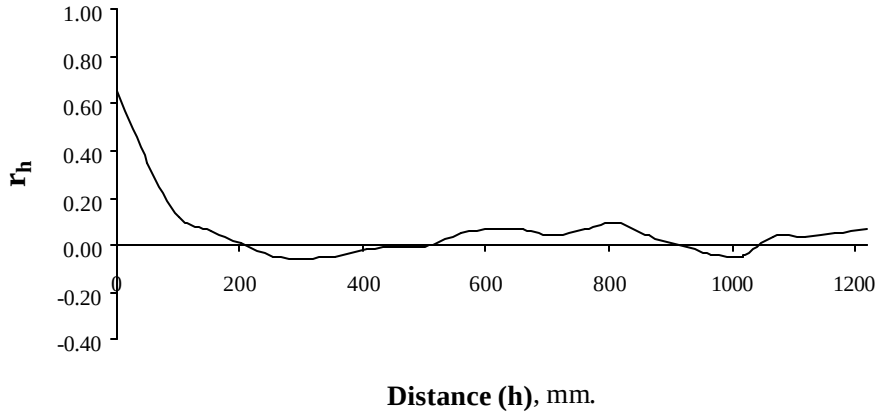

(b)

Figure 2.20. *Panel m1p3: (a) longitudinal variogram and (b) longitudinal correlogram.*

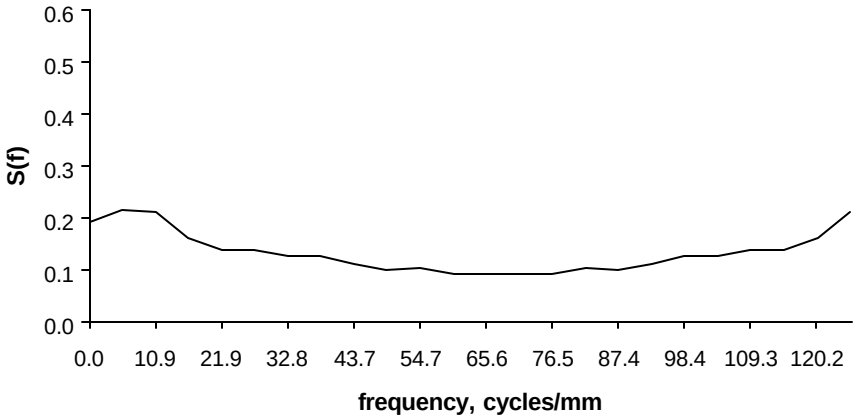

(a)

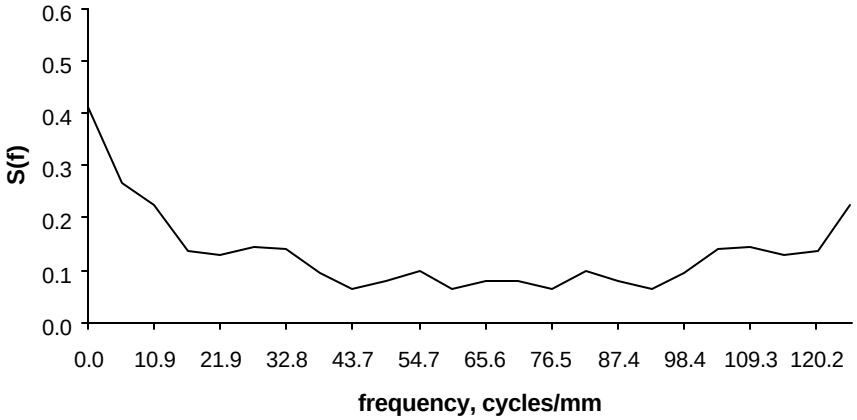

(b)

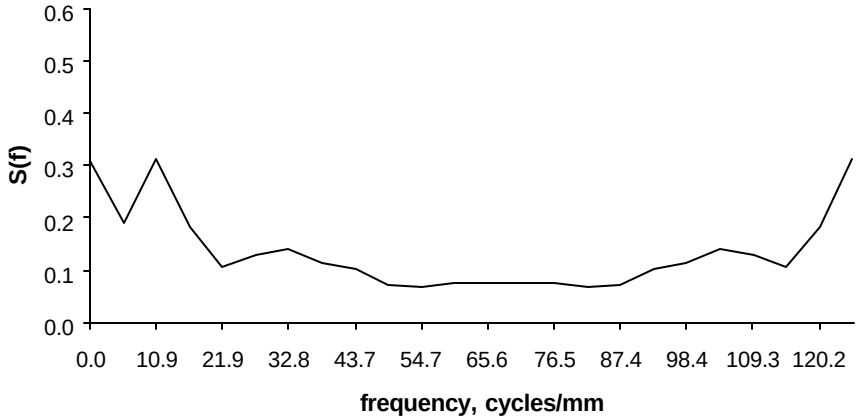

(c)

Figure 2.21. *Spectral density of panel m1p3: (a) omnicorrelogram, (b) transverse correlogram, and (c) longitudinal correlogram.*

The results shown by each pair of variogram and correlogram are similar, and each plot appears to mirror the other (Figs. 2.18, 2.19, and 2.20). Interpretation of these plots indicates spatial dependence of the density data. In the omnidirectional plots, the spatial dependence is between 350 to 450 mm (Fig. 2.18). This result contrasts to the transverse direction, where the variogram and correlogram plots indicate the spatial dependence of density is between 150 and 300 mm (Fig. 2.19). Similarly, in the longitudinal direction, the plots show that the spatial dependence is between 200 to 400 mm (Fig. 2.20). The results in different directions are very close, suggesting that the best indicators for spatial dependence of density data of OSB are the omnivariogram and omnicorrelogram. The reason why the results of omnidirectional are greater is because in this case the spatial dependence is calculated considering all possible directions in the plane. The term $(x_i - x_{i+h})$,from Equation 2.5, became smaller in the transversal and longitudinal direction than any other direction. The results of the spectral density compared to the correlogram results are shown in Figure 2.21. These plots also show that there is an indication of spatial dependence of density data. This spatial dependence has values for the omnicorrelogram, transverse correlogram, and longitudinal correlogram spectral density of 457.2; 355.6; and 406.4 mm, respectively. These results agree with those obtained in the variogram and correlogram plots. The variogram and correlogram results for all panels are included in Appendix D and the spectral density results for all panels in Appendix E.

Density-CSL Correlation results

The CSL test results were obtained from Bozo 2002. Table 2.5 presented the results for maximum deflection and ultimate load for 18 panel tested with the corresponding statistic summary. The coefficients of determination between density areas and CSL test results are presented in Table 2.6.

Specimen Label	**Maximum Deflection mm**	**Ultimate Load kN**
m1p1	2.15	2.80
m1p2	2.00	3.56
m1p3	2.29	2.80
m1p4	2.20	3.11
m1p5	2.51	2.62
m1p6	2.43	2.48
m2p1	2.13	3.30
m2p2	1.84	3.94
m2p3	2.18	3.17
m2p4	2.22	2.91
m2p5	2.42	2.51
m2p6	2.27	3.49
m3p1	2.03	3.23
m3p2	2.46	2.70
m3p3	1.87	3.48
m3p4	2.46	3.02
m3p5	2.40	2.93
m3p6	2.13	3.32
mean	2.22	3.08
COV	9.12	12.90
minimum	1.84	2.48
maximum	2.51	3.94

Table 2.5. *Maximum deflection and ultimate load values for the CSL tests conducted.*

Density Zone	R^2	
	Max. Deflection	Ultimate Load
d1	0.722	0.373
d2	0.720	0.373
d3	0.750	0.620
d4	0.753	0.662
d5	0.817	0.677
d6	0.866	0.653
d7	0.883	0.662
d8	0.884	0.664
d9	**0.887**	**0.679**
d10	0.884	0.665
d11	0.881	0.641
Global	0.473	0.283

Table 2.6. *Coefficient of determination between density areas and test results*

For the density areas studied, d1 coincides with the loading area and d2 corresponds to the square where the circular loading area is circumscribed. Areas d3 and d4 are defined increasing the corresponding earlier area by 12.7 mm in both directions, then areas d5 through d11 increase by 25.4 and 12.7mm in the longitudinal and transversal direction, respectively. The global area corresponds to the area of the entire specimen. The density results for all different areas, as well as the results of maximum deflection and ultimate load are presented in Appendix F.

The coefficient of determinations (r^2) indicate that global panel density represents the poorest correlation with CSL for any of the panel areas studied (Tab. 2.6). The r^2 increases for the density directly under the load region (d1) and continues to increase until reaching density zone d9, which represents the highest r^2 for both maximum deflection and ultimate load scenarios. The density zone d9 corresponds to a rectangular area of 254.0- by 190.5-mm and 203.2- by 165.1-mm for maximum deflection and ultimate load, respectively. These rectangular areas indicate that the average dimensions were 228.6 mm and 177.8 mm longitudinal and transverse, respectively. These results agree with the values of 200 to 400 and 150 to 300 mm (longitudinal and transversal, respectively) for the range of influence for density found on the same panels. The distance from the periphery of the circular loading zone and the outer side of

the rectangular area in the machine direction were equivalent in both maximum deflection and ultimate load cases (88.9 mm).

Conclusions

Two complementary methods to assess variability in the localized density of oriented strandboard (OSB) panels were presented using graphical and analytical methods. Graphical methods provided a means of visualizing the data and their variability. Density patterns were evident in the contour plots and represented large-scale panel structure. Correlation and periodicity among neighboring specimens can be quantified using analytical methods such as spectral analysis and geostatistics. Spectral analysis and geostatistics indicated correlation between neighboring density specimens, and were used to identify spatial dependence within the density data. The spatial dependence results obtained by variogram, correlogram, and spectral density were consistently equivalent.

Non-destructive methods (X-ray) were needed to determine density for accurate analysis at high frequency or small periods. This research resulted in several methods for assessing variability, all of which proved useful for the panels studied. Because variability results from production processes that occur on a much larger scale than a 1220- by 2440-mm panel, full production panels were studied to assess the absolute value of these methods.

The results observed in this research suggest that the use of local density rather than global density as a predictor of physical or mechanical properties would be more effective because the local density involves the neighborhood effect. The horizontal density distribution itself has no value if the spatial effect is not considered. Moreover, it is highly recommended for

simultaneously describing the horizontal density variation, its distribution, and the range of influence at different directions for any specific property.

The results presented in this investigation revealed that the global panel density was the poorest predictor of CSL behavior. In contrast, the mean density for an area of 254.0- by 190.5-mm and 203.2- by 165.1-mm around the load point, represented the highest correlation for maximum deflection and ultimate load, respectively. In both cases, the distance from the periphery of the circular loading area and the outer edge of the rectangular area was 88.9 mm. These results agree with the statistical range of influence for density in the longitudinal and transverse directions, which was between 200 and 400 mm and between 150 and 300 mm, respectively.

References

Armstrong, M.1998. Basic Linear geostatistics. Springler-Verlag Berlin Heidelberg New York.

Bloomfield, P. 1976. Fourier Analysis of Time Series: An Introduction. John Wiley & Sons.

Chatfield, C. 1996. The Analysis of Time Series an Introduction. Chapman & Hall.

Dai, C. and P.R Steiner. 1993. Compression Behavior of Randomly Formed Wood Flake Mats. Wood and Fiber 25(4): 349-358.

Fuller, W. 1996. Introduction to Statistical Time Series. John Wiley & Sons, INC. New York.

Goovaerts, P. 1997. Geostatistics for Natural Resources Evaluation. New York Oxford. Oxford University press.

Heebink, B. G., W. F. Lehmann, and F. V. Hefty. 1972. Reducing particleboard pressing time: exploratory study. Research paper FPL-180. USDA Forest Service, Forest Products Laboratory. Madison, Wisconsin.

Isaaks, E. and R. Mohan Stivastava. 1989. An Introduction to Applied Geostatistics. New York Oxford. Oxford University press.

Hse, C. 1975. Properties of flakeboards from hardwoods growing on southern pine sites. Forest Products Journal. 25(3): 48-53.

Kwon, J. H. and R. L. Geimer. 1998. Impact of Steam pressing variables on the dimensional stabilization of flakeboard. Forest Products Journal. 48(4): 55-61.

Lang, E. and M.P. Wolcott. 1996. A model for viscoelastic consolidation of wood-strand mats Part I: Structural characterization of the mat via Monte Carlo simulation. Wood and Fiber Science. 28(1): 100-109.

Lowood, J.1997. Oriented Strand Board and Waferboard. Chapter 5 of Engineered Wood Products. FPS Research Foundation. PP 123-146.

Lu, C., P.R. Steiner, and F. Lam. 1998. Simulation Study of Wood-Flake Composite Mat Structures. Forest Product Journal 48(5): 89-93.

Plath, E. and E. Schnitzler. 1974. The density profile, a criterion for evaluating particleboard. Holz asl Roh-und Werkstoff. 32:443-449.

Rice, J. T. and R. H. Carey. 1978. Wood density and board composition effects on phenolic resin-bonded flakeboard. Forest Products Journal. 28(4): 21-28.

Snedecor, G.W. and W.G. Cochran. 1980. Statistical Methods. The Iowa State University Press. Ames, Iowa, U.S.A. 507 P.

Shen, K. C. and M.N. Carroll. 1969. A new method for evaluation of internal strength of particleboard. Forest Products Journal. 19(8): 17-22.

Shen, K. C. and M.N. Carroll. 1970. Measurement of layer-strength distribution in particleboard. Forest Products Journal. 20(6): 53-55.

Smulski, S. 1997. Engineered Wood Products. FPS Research Foundation, Madison, WI.

Steiner, P. R., S. Chow, and D. Nguyen. 1978. Improving mill waferboard properties by x-ray-densitometry evaluation methods. Forest Products Journal. 28(12): 33-34.

Steiner, P. R., L. A. Jozsa, M. L. Parker, and S. Chow. 1978. Application of x-ray densitometry to determine density profile in waferboard: relationship of density to thickness expansion and internal bond strength under various cycles. Wood Science. 11(1): 48-55.

Steiner, P.R. and C. Dai. 1994. Spatial structure of wood composites in relation to processing and performance characteristic. Part 1. Rationale for model development. Wood Science and Technology 28: 45-51.

Steiner, P. R. and W. Xu. 1995. Influence of flake characteristics on horizontal density distribution of flakeboard. Forest Products Journal. 45(4): 61-66.

Strickler, M. D. 1959. Properties of Douglas-fir flakeboard. Forest Products Journal. 9(7): 203-215.

Suchsland, O. 1959. An analysis of the particleboard process. Michigan Quarterly Bulletin, Agricultural Experiment Station, Michigan State University, East Lansing Michigan. 42(2): 350-121372.

Suchsland, O. 1962. The density distribution in flakeboard. Michigan Quarterly Bulletin, Agricultural Experiment Station, Michigan State University, East Lansing Michigan. 45(1): 104-121.

Suchsland, O. and H. Xu. 1989. A simulation of the horizontal density distribution in a flakeboard. Forest Product Journal 39(5): 29-33.

Suchsland, O. and H. Xu. 1991. Model analysis of flake board variables. Forest Product Journal 41(11/12): 55-60.

Wang, K. and F. Lam. 1998. Robot-Based Research on Three-Layer Oriented Flakeboards. Wood and Fiber Science 30(4): 339-347.

Wong, E. D., M. Zhang, Q. Wang, and S. Kawai. 1998. Effects of mat moisture content and press closing speed on the formation of density profile and properties of particleboard. Journal of Wood Science. 44:287-295

Xu, W. and P.R. Steiner. 1995. A Statistical Characterization of the Horizontal Density Distribution in Flakeboards. Wood and Fiber Science 27(2): 160-167.

Xu, W. and O. Suchsland. 1998. Modulus of elasticity of wood composite panels with a uniform vertical density profile: a model. Wood and Fiber Science. 30(3): 293-300.

Chapter 3

Modeling Variation in Wood Composites Properties

Introduction

Sensor technology exists today for real-time monitoring of localized horizontal density in composites wood panel manufacturing. The most common of these sensor technologies involve the use of γ-ray, infrared, ultrasound, and X-ray (Chen et al. 2000). Using any one of these sensor technologies the horizontal density distribution (HDD) can be obtained for each panel coming out from the press.

Manufacturers must produce panels that conform to product performance specifications. Oriented strandboard (OSB) performance specifications are defined by *the Voluntary Product Standard PS2-92* as defined in the *Performance Standards and Polices for Structural-use Panels PRP-108*. A specific example defined by PS2-92 and PRP-108 is the concentrated static load (CSL) test, which on the application of a standardized point load to an OSB specimen supported by a metal frame. Both, maximum deflection and ultimate load in a CSL test are induced by local density variation.

It is well documented that panel density is correlated to mechanical properties. Many researchers have established positive correlations between density and a variety of mechanical properties for wood composites (Strickler 1959; Plath and Schnitzler 1974; Steiner et al. 1978). Some of the mechanical properties that are directly related to density include: modulus of elasticity (MOE) (Rice and Carey 1978; Xu and Suchsland 1998), modulus of rupture (MOR) (Rice and Carey 1978; Hse 1975; Wong et al. 1998; Kwon and Geimer 1998), tension strength perpendicular to panel surfaces (Heebink et al. 1972; Plath and Schnitzler 1974; Steiner et al.

1978; Wong et al. 1998), and shear strength (Shen and Carroll 1969, 1970). Based on the works cited previously there is no doubt that density is correlated to mechanical properties for most all materials. However, the relationship between localized density and panel performance under a concentrated load is not well understood.

Bozo (2002) explored the spatial statistics of horizontal density distribution and examined the empirical correlation between density and localized concentrated load. He studied the HDD and found the range of influence of density at different orientations using different methods. This research revealed that the poorest correlation was between the global panel density and ultimate load. This discovery has practical value in statistical quality control, but the empirical correlation is limited to the scope of the experimental sampling.

Research is needed to develop a mechanics-based approach for understanding panel performance under a variety of loading and boundary conditions. Key to this modeling approach is capturing relevant statistical variation in input and output parameters. This research evaluates mechanical properties of commercially produced OSB to determine the relationship between these mechanical properties and density. The model should be used to simulate mechanical properties at specific locations in the panel, based on density values at those specific locations.

Objectives

The general purpose of this work was to provide information on mechanical properties of commercially produced oriented strandboard and to find relationships between density and mechanical properties. The specific objectives of this research include to:

1. Characterize mechanical properties (modulus and ultimate stress for tension and compression parallel to surface in the machine direction as well as shear) for a range of element sizes to identify the size needed for subsequent modeling.

2. Develop statistical input models to generate the relevant mechanical properties from known values of localized horizontal density for use in Monte Carlo simulation models of panel performance.

3. Validate the statistical input models with respect to preserving correlation structure between properties.

Material and Methods

Material Sampling

The sample population for this research consisted of 18 commercially produced OSB panels (1.22- by 2.44-m by 19-mm). The panels were removed from three consecutive master panels, which comprised 22 m of continuous production. Each panel was scanned using x-ray densitometry with a spatial resolution of 12.7- by 12.7-mm. A thorough discussion of the procedures and resulting density distributions is presented elsewhere (Bozo 2002).

Specimen Sampling

Seven different types of tension, compression, and shear specimens were sampled from the panels (Fig. 3.1, 3.2, and 3.3). Specimens were sampled for loading along the machine direction of the panel and across the represented density range. The x-ray density data was used to locate specimens for the density groupings. Three different density levels were selected for sampling the specimens, 450 kg/m^3, 550 kg/m^3, and 650 kg/m^3; with tolerance limit of ± 25 kg/m^3. The specimen region selected to meet the target was the central gage length of the specimen, 12.7- by 12.7-mm, 25.4- by 25.4-mm, and 50.8- by 50.8-mm for three different specimens sizes, respectively.

Mechanical Testing

The mechanical properties studied were modulus and ultimate stress for tension (E_{1t}, σ_{1t}) and compression (E_{1c}, σ_{1c}) parallel to surface in the machine direction as well as shear (G_{12}, τ_{12}). Those properties were selected because they are required input in finite element analysis to model the concentrated static load test. Tension and compression tests were performed according to ASTM D1037, with the exception of specimen size. Shear tests were conducted according to ASTM D5379/D5379M-93. A 2-kip screw-driven universal testing machine used for all mechanical tests was equipped with electronic load cells, extensometers, and computer data acquisition. The tension specimens were loaded at a uniform crosshead speed rate of 4.0 mm/minute. The compression and shear specimens were loaded at a uniform crosshead rate of 0.36 mm/minute, with the exception of the 12.7- by 63.5-mm compression specimens that were loaded at 0.3 mm/minute. All together, 25 specimens were tested at each nominal density level and test configuration, i.e., loading mode and size.

The tension fixtures consisted of self-aligning mechanical grips with a constant length separating the grips for each of the three specimen sizes. The compression fixture consisted of a fixed bottom plate and the top plate supported by a ball joint with 3 degrees of freedom. The V-notch shear fixture is shown in Figure 3.4. A 12.7-mm clip extensometer was used to measure displacement for all of the seven test configurations. An additional 25.4-mm clip extensometer was used to simultaneously measure displacements for two of the largest size tension and compression specimens.

(a) (b) (c)

Figure 3.1. *Specimen sizes for tension test: (a) 63.5- by 254.0-mm, (b) 38.1- by 228.6-mm, and (c) 25.4- by 215.9-mm.*

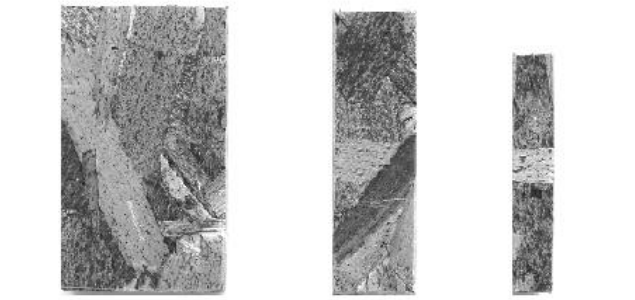

(a) (b) (c)

Figure 3.2. *Specimen sizes for compression test: (a) 50.8- by 76.2-mm, (b) 25.4- by 76.2-mm, and (c) 12.7- by 63.5-mm.*

Figure 3.3. *Specimen for shear test 19.05- by 76.2-mm*

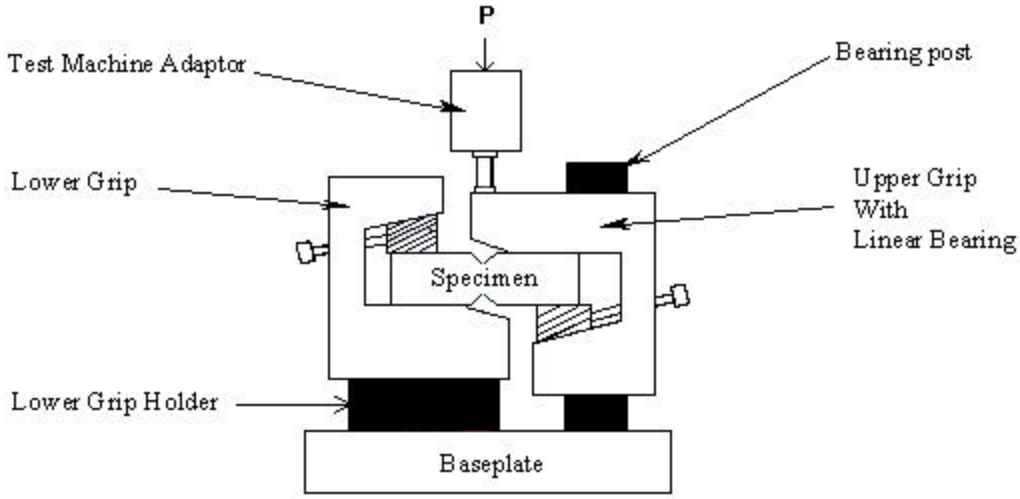

Figure 3.4. *V-notches beam test fixture schematic*

Determining Tensile, Compression, and Shear Modulus

The elastic modulus is usually defined as the tangent to the linear elastic region of the stress-strain curve. However, no consistently definable linear region existed with the OSB specimens in this study. With specimens exhibiting such consistent curvatures, the more appropriate method is the one described by Meyers (2001). Here the elastic modulus is obtained as the tangent at the inflection point of the slope of the stress-strain curve. This point can be consistently selected as the local minima of the 2nd derivative for the stress-strain relation.

Input Modeling Using Regression Approach

Regression models were developed between density and each mechanical property of interest. The basic steps to model were to first fit the density data (independent variable) with an appropriate probability distribution. Secondly, a scatterplot is produced between density and the dependent variable. Least-squares regression test is then conducted and the regression line plotted on the scatterplot. This procedure was repeated (if necessary) with natural log transformation.

Validating Input Model

Because the regression models were to be used for stochastic modeling, 10 batches of values were simulated from each equation to analyze the preservation of the correlation structure between properties. The coefficient of determination (r^2) for each batch was computed. Then a confident interval was determined for r^2 for each regression model. Finally, determine if the actual r^2 for each regression model fall between the confident interval or not.

Results and Discussion

Mechanical Properties

OSB is a structural panel where mechanical properties play an important role in different applications. In this study, tension and compression parallel to the machine direction were determined as well the shear properties. Three different density levels were used to determine the mechanical properties, and three different specimen sizes were utilized for tension and compression tests. The minimum and maximum values for tensile modulus were 3,373 and 4,054 MPa respectively. Analogous, the extreme values for compression and shear modulus were 2250, 4094, 1014, and 1376 MPa, respectively. A summary of the test result of elastic modulus and strength are shown in Tables 3.1 and 3.2.

This research found differences in compression and tension properties of OSB panels. In general, compression strength and stiffness properties were lower than tension properties. Similarly, for solid wood the compression properties are lower than tension properties (Kollman and Cote 1968). However, only minimal information is available in the literature regarding

tension, compression, and shear properties for OSB; most studies have investigated flexure behavior. Two studies have examined the tension and compression of single-layer laboratory manufactured oriented strand lumber (OSL). Both Dong (1979) and Carll (1994) found compression properties were larger than tension, for both elastic modulus and strength. The values found by Dong (1979) were 25.1 MPa and 31.75 MPa for tensile and compression strength, respectively, and 5957 MPa for compression modulus. Carll (1994) found values of 11.1 MPa and 15.8 MPa for tensile and compression strength, and 4750 MPa and 5233 MPa for tensile and compression modulus, respectively. Both authors used the methodology and specimens size described on ASTM D1037. The values found in the current research, for comparable specimen size (25.4-mm width at the central part), were 10.3 MPa and 10.7 MPa for tensile and compression strength, and 3331 MPa and 3298 MPa for tensile and compression modulus, respectively. The values found for OSB are smaller compared to the values for OSL. This difference was expected because in OSL, all wood elements are oriented parallel to machine direction, which is the opposite of OSB where faces are parallel and core is perpendicular to the machine direction. The larger values found by Dong are explained because he adjusted all mechanical properties to a theoretical density of 700 kg/m^3. Carll determined the properties of specimens with average density of 547 kg/m^3 similar to the used in this investigation (550 kg/m^3).

	Density (kg/m^3)	**Characteristic Size**							
		12.7- by 12.7-mm		**25.4- by 25.4-mm**			**50.8- by 50.8-mm**		
		s_{1t} MPa	**E_1 MPa**	**s_{1t} MPa**	**$E_{1\text{-}12.7}$ MPa**	**$E_{1\text{-}25.4}$ MPa**	**s_{1t} MPa**	**$E_{1\text{-}12.7}$ MPa**	**$E_{1\text{-}25.4}$ MPa**

TENSION	Mean	low (450)	7.0	3120	7.6	2875	2506	7.3	3145	2394
	COV		25.3	19.3	12.7	10.4	14.8	15.4	9.7	15.2
	Mean	med (550)	8.2	3373	10.3	4004	3331	10.7	4054	3712
	COV		17.6	19.8	14.4	15.7	11.4	12.1	8.2	10.5
	Mean	high (650)	10.3	4331	11.5	4913	3770	12.4	5371	5447
	COV		17.3	14.2	12.1	12.5	13.7	11.4	9.5	11.1
COMPRESSION	Mean	low (450)	5.6	2279	8.2	2911	2846	7.0	2250	3061
	COV		21.2	16.6	20.3	19.9	11.6	22.2	16.6	25.7
	Mean	med (550)	7.6	2759	10.7	3638	3298	8.7	2447	3555
	COV		16.8	11.4	14.0	14.6	12.6	14.6	11.0	14.1
	Mean	high (650)	8.8	3239	11.6	4086	3138	11.7	2825	4094
	COV		19.9	12.1	16.6	11.9	11.5	12.3	13.4	7.1

Table 3.1. *Tensile and compression properties*

		Density (kg/m^3)	SIZE 19.05- by 76.2-mm	
			t_{12} MPa	G_{12} MPa
SHEAR	Mean	low (450)	6.2	1014
	COV		18.0	26.6
	Mean	med (550)	8.5	1118
	COV		32.2	18.6
	Mean	high (650)	9.2	1376
	COV		22.2	19.7

Table 3.2. *Shear properties*

Size Effect on Properties

To examine a possible size effect, the data for all the density ranges were combined. The results of the rearrangement are presented in Table 3.3. The numbers shown in Table 3.3 indicate that the tensile properties increased as the specimen size increased, however, the trend was not clear. For compression properties no trends were found with the specimen size.

		Characteristic Size							
		12.7- by 12.7-mm		25.4- by 25.4-mm			50.8- by 50.8-mm		
		s_1 MPa	E_1 MPa	s_1 MPa	$E_{1\text{-}12.7}$ MPa	$E_{1\text{-}25.4}$ MPa	s_1 MPa	$E_{1\text{-}12.7}$ MPa	$E_{1\text{-}25.4}$ MPa
TEN	Mean	8.50	3598	9.71	3936	3208	10.14	4199	3814
	COV	19.41	23.15	18.02	25.63	21.48	22.19	24.98	36.08
	n	67	67	38	38	38	38	38	38
COM	Mean	7.28	2764	10.28	3526	3081	9.05	2531	3586
	COV	20.74	19.68	15.08	20.36	10.81	23.09	16.59	19.30
	n	66	66	39	39	39	39	39	39

Table 3.3. *Tensile and compression properties at different sizes.*

A summary of analysis of variance (ANOVA) for tensile and compression properties with variables specimen size are shown in Tables 3.4 and 3.5, respectively. For all properties analyzed specimen size had a significant influence, this fact is certified by the high F values presented in Tables 3.4 and 3.5.

Property	ANOVA						
	Source of Variation	*SS*	*df*	*MS*	*F*	*P-value*	*F crit*
Tensile strength	Between Groups	75.07	2	37.53	10.91	<0.0001	3.0603
	Within Groups	481.79	140	3.44			
	Total	556.85	142				
Tensile Modulus (12.7-mm)	Between Groups	9146564	2	4573282.08	5.16	0.0069	3.0603
	Within Groups	124178733	140	886990.95			
	Total	133325297	142				
Tensile Modulus (25.4-mm)	Between Groups	6959921.07	1	6959921.07	5.85	0.018	3.9668
	Within Groups	88042035.29	74	1189757.23			
	Total	95001956.36	75				

Table 3.4. *Summary of analysis of variance for tensile properties.*

Property	ANOVA

	Source of Variation	*SS*	*df*	*MS*	*F*	*P-value*	*F crit*
Compression strength	Between Groups	232.79	2	116.40	40.53	<0.0001	3.0603
	Within Groups	404.93	141	2.87			
	Total	637.72	143				
Compression Modulus (12.7-mm)	Between Groups	21812057	2	10906028.6	33.79	<0.0001	3.0603
	Within Groups	45510551	141	322769.87			
	Total	67322609	143				
Compression Modulus (25.4-mm)	Between Groups	4966475.13	1	4966475.13	16.83	0.0001	3.9668
	Within Groups	22421005.05	76	295013.22			
	Total	27387480.18	77				

Table 3.5. *Summary of analysis of variance for compression properties.*

Differences in mechanical properties as a result of specimen size were determined using Tukey's test. The results of Tukey's test for tensile and compression properties are presented in Tables 3.6 and 3.7, respectively.

Property	**GROUPING**			
	Size	**Mean**	**N**	**Tukey's**
Tensile strength	50.8- by 50.8-mm	10.14	38	A
	25.4- by 25.4-mm	9.71	38	A
	12.7- by 12.7-mm	8.50	67	B
Tensile Modulus (12.7-mm)	50.8- by 50.8-mm	4199	38	A
	25.4- by 25.4-mm	3936	38	A B
	12.7- by 12.7-mm	3598	67	B
Tensile Modulus (25.4-mm)	50.8- by 50.8-mm	3814	38	A
	25.4- by 25.4-mm	3208	38	B

Table 3.6. *Tukey's test results for tensile properties.*

Property	GROUPING			
	Size	Mean	N	Tukey's
Compression strength	25.4- by 25.4-mm	10.28	39	A
	50.8- by 50.8-mm	9.05	39	B
	12.7- by 12.7-mm	7.28	66	C
Compression Modulus (12.7-mm)	25.4- by 25.4-mm	3526	39	A
	12.7- by 12.7-mm	2764	66	B
	50.8- by 50.8-mm	2531	39	B
Compression Modulus (25.4-mm)	50.8- by 50.8-mm	3586	39	A
	25.4- by 25.4-mm	3081	39	B

Table 3.7. *Tukey's test results for compression properties.*

The Tukey's test results shown in Table 3.6 evidenced differences between mean of tensile properties at different sizes, but these differences were concentrated principally between the 12.7- by 12.7-mm specimen size and 50.8- by 50.8-mm specimen size. Therefore, no differences exist between means of specimen size 25.4- by 25.4-mm and 50.8- by 50.8-mm for either tensile modulus using 12.7-mm length-gauge extensometers or tensile strength. The results presented in Table 3.7 indicated differences exist between mean of compression properties. However, in this case, the differences were generalized for all sizes with the exception of compression modulus using 12.7-mm length-gauge extensometers between the 12.7- by 12.7-mm specimen size and the 50.8- by 50.8-mm specimen size.

Effect of Density on Properties

All the relationships between density and the mechanical properties previously determined presented similar behavior, and all mechanical properties are positively related with density. Figures 3.5 shows the relationship between density and shear strength of OSB, this plot was chosen to show the positive influence on the mechanical properties of OSB. All others plot between density and mechanical properties of OSB are presented in Appendix G. It is clear that

all properties are strongly affected by density (Tables 3.1 and 3.2). When density was increased, the strength and stiffness properties also increased. This behavior was to be expected, but the differences were marked by the different slope of each relationship. To develop a better understanding of this relationship, regression analysis was made between the properties and density. The results are presented in Table 3.8, which corresponds to the logarithmic regression model.

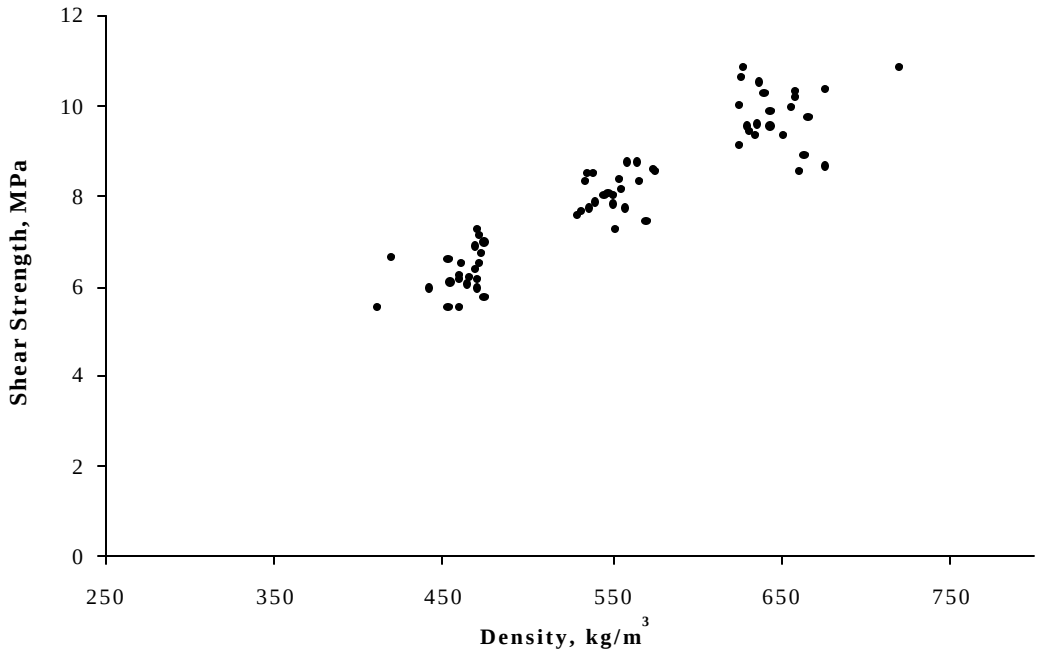

Figure 3.5. *Plot relationship between density and shear strength.*

Property		Regression Equation	r^2	Standard Error
Tension-50.8	s_{1t}=	14.705**Ln(d)** - 82.545	0.87	0.8380
	E_1=	8932**Ln(d)** - 52487	0.86	526.60
Compression-50.8	s_{1c}=	15.49**Ln(d)** - 88.587	0.86	0.7845
	E_1=	3556.5**Ln(d)** - 18832	0.41	537.17
Shear	t_{12}=	9.8195**Ln(d)** - 53.875	0.87	0.5712
	G_{12}=	949.69**Ln(d)** - 4841.3	0.60	118.13

Table 3.8. *Logarithmic regression model between tensile, compression, and shear properties of OSB and density.*

The results of linear regression and logarithmic regression models were very close; however, the logarithmic model was more realistic for wood composites especially at lowest and highest density values. The reason is because the logarithmic regression models present asymptotic behavior at high-density values; however, the linear regression model predicts unrealistic high property values at those density levels. This fact is represented in Figure 3.6.

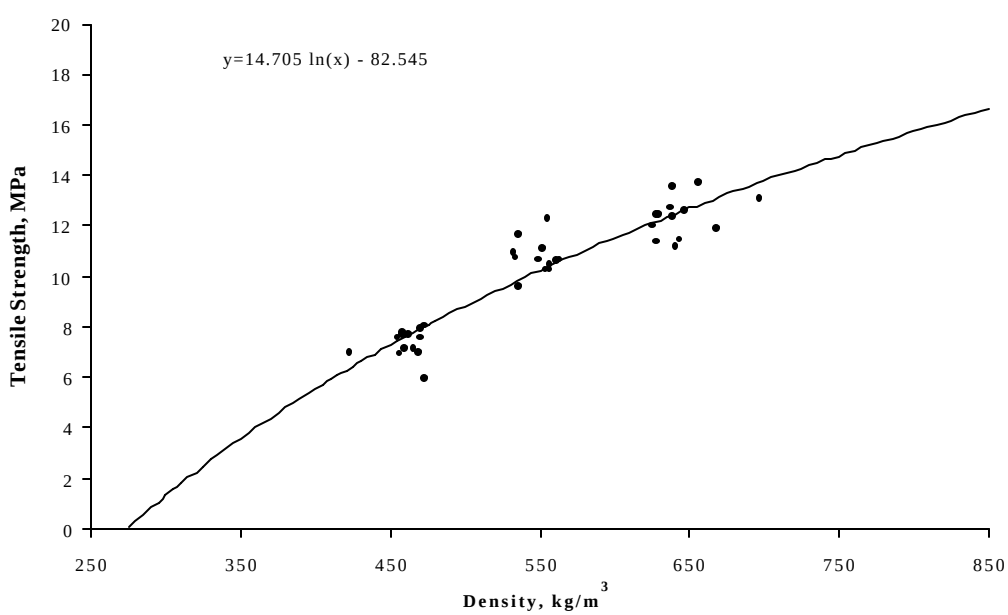

Figure 3.6. *Tensile strength vs. density for specimen size 50.8- by 254.0-mm.*

Validating Input

The actual correlation structure between properties is presented in Table 3.9. The values presented in Table 3.9 correspond to coefficient of determination between different properties. The table is symmetric, and the missing values indicate that the correlation between corresponding properties is not possible to realize with the actual data values because them were obtained at different locations.

Actual	**d**	**E_{1c}**	**E_{1t}**	**G_{12}**	**s_{1c}**	**s_{1c}**	**t_{12}**
d	1.000	0.413	0.857	0.605	0.862	0.866	0.866
E_{1c}	0.413	1.000	*	*	0.357	*	*
E_{1t}	0.857	*	1.000	*	*	0.774	*
G_{12}	0.605	*	*	1.000	*	*	0.206
s_{1c}	0.862	0.357	*	*	1.000	*	*
s_{1c}	0.866	*	0.774	*	*	1.000	*
t_{12}	0.866	*	*	0.206	*	*	1.000

Table 3.9. *Correlation structure for the actual values.*

The confident intervals were determined using the average and standard deviation of r^2, from the 10 simulated batches, through the method described by Snedecor and Cochran (1980). The intervals were constructed using a significance level (α) equal to 0.05, nine degree of freedom, and with ***n*** value equal to 10. The confident intervals are presented in Table 3.10 using a similar structure of Table 3.9, but using an interval rather than a single value of coefficient of determination.

Actual	d	E_{1c}	E_{1t}	G_{12}	s_{1c}	s_{1c}	t_{12}
d	1.000	0.451-0.522	0.850-0.878	0.552-0.617	0.885-0.907	0.858-0.885	0.853-0.881
E_{1c}	0.451-0.522	1.000	*	*	0.291-0.396	*	*
E_{1t}	0.850-0.878	*	1.000	*	*	0.690-0.762	*
G_{12}	0.552-0.617	*	*	1.000	*	*	0.302-0.438
s_{1c}	0.885-0.907	0.291-0.396	*	*	1.000	*	*
s_{1c}	0.858-0.885	*	0.690-0.762	*	*	1.000	*
t_{12}	0.853-0.881	*	*	0.302-0.438	*	*	1.000

Table 3.10. Confident intervals of *correlation structure for the simulated values.*

The confident intervals presented in Table 3.10 indicated that six of the actual coefficients of determination are covered by the confident interval and two (d-E_{1c} and E_{1t}-σ_{1t}) of the others three are just in the limit of the interval. Only one of the coefficient of determination (G_{12}-τ_{12}) falls outside the confident interval. Those previous result reveals that the regression model developed in this research can be safely used to generate property values via Monte Carlo simulation.

The testing results for all specimens tested are presented in Appendix H. Scatterplots between OSB property and density including the logarithmic regression line were made, and for all other properties, and are presented in Appendix I.

Conclusions

Test results revealed a clear relationship between oriented strandboard (OSB) properties and density. All property values increased as density increased; the differences between the relationship model were principally the slope, intercept, and coefficient of determination. The tensile and compression property values showed marked differences. The effect of specimen size was not as clear as the density effect as was shown by the analysis of variance (ANOVA) and Tukey's test. There was an increase in the coefficient of determination as the specimen size increased for the tensile properties; however, this effect was not clearly observed in compression properties. Based on the ANOVA and Tukey's results the more convenient size corresponds to the specimen of 25.4- by 25.4-mm at the central part.

This research developed statistical input models to generate mechanical properties base on regression models using density as a predictor variable. The results obtained by logarithmic regression and linear regression models were comparable, especially in the 450 kg/m^3 to 650 kg/m^3 density range. The logarithmic regression model better describes the reality of wood composites behavior at their lowest and highest density levels.

The results of validation revealed that the regression model developed in this research can be used to simulate mechanical properties at different sizes and anywhere within the panel based on the density values at specific location and size using conditional Monte Carlo simulation.

The methodology used in this investigation can be used to develop other regression models to predict different mechanical or physical properties of wood composites. This initial research reveals a potential for further investigations into predicting wood composite properties based on x-ray density data.

References

ASTM 1996. Standard Test Method for Evaluating Properties of Wood-Based Fiber and Particle Panel Materials. Standard D 1037-96a. American Society of Testing and Materials.

ASTM 1993. Standard Test Method for Shear Properties of Composite Materials by V-Notched Beam Method. Standard D 5379/D 5379M-93. American Society of Testing and Materials.

Bozo, A.M. 2002. Spatial Variation in Wood Composites. Dissertation. Washington State University. Pullman, Washington.

Carll, C.G. 1994. Basic Mechanical Properties of Flakeboard From Ring-cut Flakes of Eastern Hardwoods. Forest Product Journal 44(9):26-32.

Chen, S., R. Wellwood, and D. Kenway. 2000. On-Line Infrared Panel Density Measurement. 34th International Particleboard/Composite Material Symposium. Washington State University, Pullman, Washington.

Dong,C.C. 1979. The Mechanical Properties of Flakeboards Related to Flake Orientation. Dissertation. Washington State University. Pullman, Washington.

Heebink, B. G., W. F. Lehmann, and F. V. Hefty. 1972. Reducing particleboard pressing time: exploratory study. Research paper FPL-180. USDA Forest Service, Forest Products Laboratory. Madison, Wisconsin.

Hse, C. 1975. Properties of flakeboards from hardwoods growing on southern pine sites. Forest Products Journal. 25(3):48-53.

Kollmann, F. and W. Cote. 1968. Principles of Wood Science and Technology. Springer-Verlag New York Inc. 592 p.

Kwon, J. H. and R. L. Geimer. 1998. Impact of Steam pressing variables on the dimensional stabilization of flakeboard. Forest Products Journal. 48(4):55-61.

Mayers, K.L. 2001. Impact of Strand Geometry and Orientation of Mechanical Properies of Strand Composites. Master's Thesis. Washington State University. Pullman, Washington.

Plath, E. and E. Schnitzler. 1974. The density profile, a criterion for evaluating particleboard. Holz asl Roh-und Werkstoff. 32:443-449.

Rice, J. T. and R. H. Carey. 1978. Wood density and board composition effects on phenolic resin-bonded flakeboard. Forest Products Journal. 28(4):21-28.

Shen, K. C. and Carroll, M. N. 1969. A new method for evaluation of internal strength of particleboard. Forest Products Journal. 19(8):17-22.

Shen, K. C. and Carroll, M. N. 1970. Measurement of layer-strength distribution in particleboard. Forest Products Journal. 20(6):53-55.

Snedecor, G. and W. Cochran.1980. Statistical Methods. The Iowa State University Press. 507 p.

Steiner, P. R., S. Chow, and D. Nguyen. 1978. Improving mill waferboard properties by x-ray-densitometry evaluation methods. Forest Products Journal. 28(12):33-34.

Steiner, P. R., L. A. Jozsa, M. L. Parker, and S. Chow. 1978. Application of x-ray densitometry to determine density profile in waferboard: relationship of density to thickness expansion and internal bond strength under various cycles. Wood Science. 11(1):48-55.

Strickler, M. D. 1959. Properties of Douglas-fir flakeboard. Forest Products Journal. 9(7):203-215.

Wong, E. D., M. Zhang, Q. Wang, and S. Kawai. 1998. Effects of mat moisture content and press closing speed on the formation of density profile and properties of particleboard. Journal of Wood Science. 44:287-295

Xu, W. and O. Suchsland. 1998. Modulus of elasticity of wood composite panels with a uniform vertical density profile: a model. Wood and Fiber Science. 30(3):293-300.

Chapter 4

Influence of Spatial Variation in Localized Properties on OSB Performance Criteria

Introduction

Despite the significantly improved technology for manufacturing oriented strandboard (OSB), density variability remains a common problem for OSB manufacturers (Chen et al. 2000). This density variability has been the main concern of previous works (Suchland and Xu 1989, 1991; Xu and Steiner 1995; Dai and Steiner 1993; Steiner and Dai 1994; Lang and Wolcott 1996; Lu et al. 1998; Wang and Lam 1998; Bozo 2002).

All performance criteria are developed toward the end use of the product independent of the means the product was manufactured (APA 1994). The primary goal of quality assurance programs is to assure that the product will satisfy these requirements while optimizing profits. Two critical attributes for the building code compliance of OSB roof and floor sheathing are the maximum deflection and ultimate load of the OSB plate under a concentrated edge load. The concentrated static load (CSL) test mimics the deflection and load condition and is required by the *Voluntary Product Standard PS2*-92 as outlined in the *Performance Standards and Polices for Structural -Use Panels PRP-108*. The CSL test consists of a standardized point load applied to an OSB specimen located on support framing. The maximum load in a CSL test is highly affected by local density variation. Chen et al. (2000) showed that panels with similar global densities exhibit different maximum load depending on the local density variation around the loading zone.

Hoyle et al. (1982) studied the deflection of composite wood panels under concentrated load applying the theory of thin orthotropic plate deflection. In their research on OSB, plywood,

particleboard, and veneer particleboard composites, test result were compared with theoretical deflections due to concentrated load at different test loading conditions. Their conclusion was that deflections calculated by plate theory exceeded measured values, due to the input information used in the finite element analysis. Laufenberg and Xu (1989) developed an orthotropic plate analysis and used it to solve concentrated loading problems. This investigation found discreet correlation between theoretical and tested deflections.

The results of these works show promise in using plate-type analysis for modeling concentrated load cases; however, the experimental tests used in these research did not conform with standard tests such as ASTM E 661-88. Moreover, the loading and boundary conditions were more simplistic. These previous works did not address the variability of mechanical properties that result from horizontal density distributions within OSB panels. Likewise, in their present form, they provide little basis for developing empirical relationships that might guide or integrate with quality assurance programs. The goal of this research is to incorporate the spatial variability in the finite element analysis through the local property consideration rather than global property.

Objectives

The general objective of this study was to model the CSL test criteria according to *Voluntary Product Standard PS 2-92* and *APA PRP-108*, and through the CSL test example determine the influence of spatial distribution in localized mechanical properties on OSB performance. The specific objectives were to:

1. Obtain experimental maximum deflection and ultimate load under the concentrated static load test
2. Obtain maximum deflection and ultimate load employing a finite element model using average and localized properties.
3. Compare the testing results and modeling results of maximum deflection and ultimate load.

Material and Methods

Material Sampling

This research was conducted using 18 commercially produced OSB panels (1.22- by 2.44-m by 19-mm). These panels were taken as a sample from a larger study examining the influence spatial density variation has on mechanical properties. The density values were obtained by scanning x-ray densitometry with a spatial resolution of 12.7- by 12.7-mm (Bozo 2002). A quarter section of each OSB panel was used as a specimen to perform the CSL test (Fig. 4.1). The remaining three-quarters of the panel were used to develop property-density

relations used in this study (Bozo 2002). Details of the horizontal density variation and property-density relations are presented elsewhere (Bozo 2002).

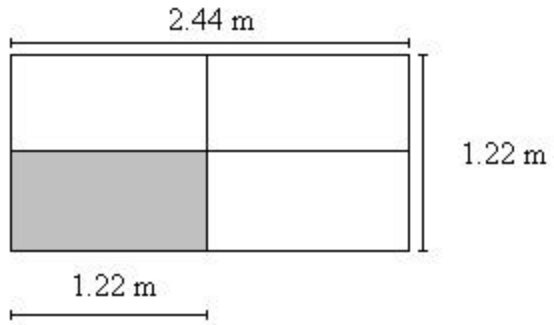

Figure 4.1. *Schematic representation of a quarter panel of OSB sheet.*

Concentrated Static Load Test

The CSL tests were conducted according to PS 2-92 (section 6.4.1) (NIST 1992). The general description, specimen preparation, and test procedure was made using ASTM E-661 (ASTM 1997). The standard specifies three sheathing conditions: full-edge support, partial-edge support, and without-edge support. The sheathing without-edge support condition (Fig. 4.2) was used in this study for representing the most common and disadvantageous for the product. The specimen size (0.61- by 1.22-m.) and framing installation required for the test is shown in Figure 4.2.

During loading, the concentrated static load was applied at the center-span between supports at 63.5 mm from the edge of the panel (Fig. 4.2). As specified, the point load was simulated using a 76.2-mm diameter-loading disk for deflection and a 25.4-mm diameter-loading disk for ultimate load. The procedure for stiffness testing was to load the panel with a constant deflection rate of 2.5 mm/minute, and recording the maximum deflection under the point load

when at a load of 890 N was attained. For strength testing, the load was removed and the loading disk replaced by the 25.4-mm diameter. The panel is subsequently loaded at the rate of 5 mm/minute until failure, recording the ultimate load.

All testing was conducted using a computer controlled, servohydraulic ram equipped with a 450-kg (Interface model 1210AF-1K-B) electronic load cell. An internally mounted linear variable differential transformer (LVDT) was monitored to control the load head rate. Local panel deflections were recorded using a ± 25.4-mm (Sensotec model 060-3618-02 range ± 1.000 inch) range LVDT mounted on the bottom face below the central point of the loading zone.

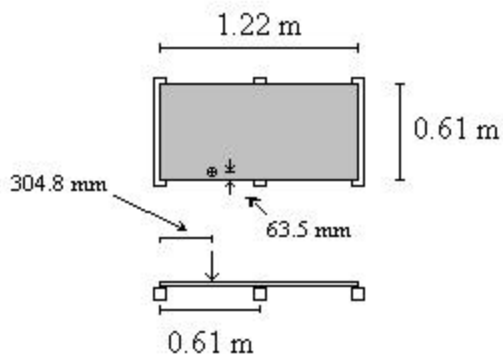

Figure 4.2. *Schematic representation of CSL test*

Finite Element Analysis

A finite element analysis constructed of shell elements was used to model the CSL test with localized mechanical properties. The shell equations used in this analysis assume that stresses and strains are invariant with the thickness direction. This condition is approximated when the plate thickness is small compared with the other dimensions (Szilard 1974). The span to thickness ratio of OSB specimens used in this study was 32 (609.6-mm span and 19.05-mm thickness), well within the specified range of 24 to 64.

The finite element analysis was performed using a commercial code (*Automatic Dynamic Incremental Nonlinear Analysis*, ADINA). The complete specimen was modeled because the loading condition contained no axis of symmetry. The load was modeled as a pressure applied over a circular area equivalent to the loading disk (25.4-mm and 76.4-mm diameter for deflection and ultimate load, respectively). The translations of nodes corresponding to the prescribed nailing pattern used in the physical tests were restricted in all directions. Shell elements were employed to facilitate the use of failure criteria. A schematic representation of the finite element model is presented in Figure 4.3.

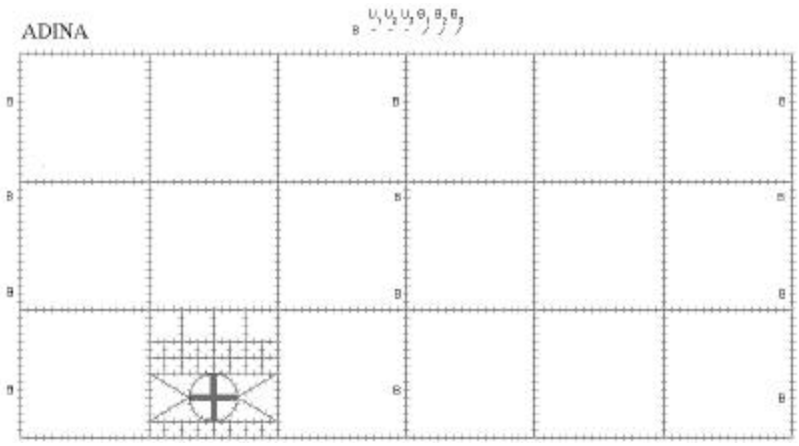

Figure 4.3. *Schematic representation of the finite element model (B represents boundary condition).*

The OSB was modeled as an orthotropic plate, requiring nine independent material properties. A preliminary sensitivity analysis revealed that Young's modulus (E_1) in the machine direction and Poisson's ratio (ν) were the most and least influential properties, respectively (Bozo 2002). In addition, previous research (Bozo 2002) showed that OSB exhibited different strength and stiffness properties when load in the tension or compression modes and all properties varied in density. As such, E_{1t}, σ_{1t}, E_{1c}, σ_{1c}, G_{12}, and τ_{12} were generated for a given density value using Monte Carlo simulation. The regression models used to generate OSB

properties via Monte Carlo simulation are presented in Table 4.1 and were obtained from previous work (Bozo 2002). Transverse strength and stiffness properties (E_{2t}, σ_{2t}, E_{2c}, σ_{2c}) were estimated from property ratios provided by Dong (1979). Poisson's ratio was assumed to be constant at 0.3.

Property		Regression Equation	r^2	Standard Error
Tension-50.8	s_{1t}=	14.705**Ln(d)** - 82.545	0.87	0.8380
	E_{1t}=	8932**Ln(d)** - 52487	0.86	526.60
Compression-50.8	s_{1c}=	15.49**Ln(d)** - 88.587	0.86	0.7845
	E_{1c}=	3556.5**Ln(d)** - 18832	0.41	537.17
Shear	t_{12}=	9.8195**Ln(d)** - 53.875	0.87	0.5712
	G_{12}=	949.69**Ln(d)** - 4841.3	0.60	118.13

Table 4.1. *Logarithmic regression model for tension, compression, and shear properties.*

To study the influence of localized density variations, two analyses were conducted. First, a uniform panel was modeled using the average property values obtained from Monte Carlo simulation for localized density. Second, material properties were assigned to each surface of the model using Monte Carlo simulation from local density values. The numbers of simulations (***n***) necessary for a statistically valid simulation was computed using the Confidence Interval Method (Snedecor and Cochran 1980) and varied for each panel specimen, but in all cases the minimum number was less than 10. To maintain consistency, a constant number of 25 simulations were taken for all specimens for both maximum deflection and ultimate load.

Because the finite element solutions were highly sensitive to the mesh density in the load zones (Bozo 2002), the panel specimen was divided into different zones as shown in Figures 4.4 and 4.5 (maximum deflection and ultimate load, respectively). Zones one through four correspond to the loading disk.

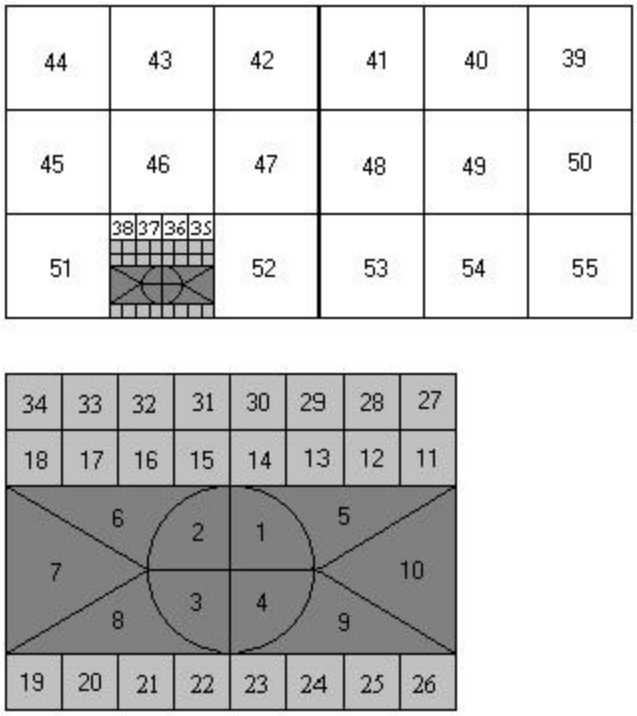

Figure 4.4. *Zones within CSL specimen for maximum deflection.*

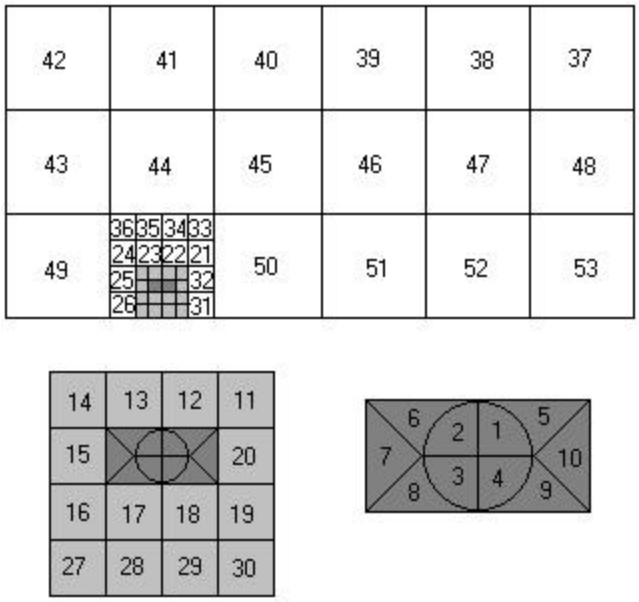

Figure 4.5. *Zones within CSL specimen for ultimate load.*

For simplicity, the maximum stress failure criterion was used to determine ultimate load. Material failure occurs when any of the following inequalities are no longer satisfied at any node:

$$X_c < \sigma_1 < X_t$$
$$Y_c < \sigma_2 < Y_t$$
$$-S_{12} < \tau_{12} < S_{12}$$

where: $(\sigma_1, \sigma_2, \tau_{12})$ denotes the stress vector in the principal material directions
S, *X*, and *Y* represent ultimate stress values for shear and the 1, 2 directions
subscripts *c* and *t* represent compression and tension, respectively
subscripts *1* and *2* represent the longitudinal and transverse panel directions, respectively

A summary of the model condition using in ADINA is presented in Table 4.2 for both maximum deflection and ultimate load. The results obtained from the finite element analysis were compared with the results of the physical tests and the OSB performance criteria.

ADINA condition	Maximum Deflection	Ultimate load
Plate size	609.6- by 1219.2-mm	609.6- by 1219.2-mm
Number of surfaces	53	55
Size of loading zone	76.2 mm diameter	25.4 mm diameter
Material	elastic orthotropic	elastic orthotropic
Boundary condition	x, y, and z translation	x, y, and z translation
Loading pressure	0.1952 MPa	-
Number of step	1	20
Element group	shell element	shell element
Number of nodes per element	4	4
Kinematics formulation	small displacement/strain	small displacement/strain
Numerical integration	8 gauss points	8 gauss points
Stress reference system	global	global
Failure criteria	maximum stress	maximum stress
Element number loading zone	1260	140
Element number total	5966	4758

Table 4.2. *Condition to model maximum deflection and ultimate load for CSL test using ADINA*

Results and Discussion

For this part of the investigation, 18 specimens were extracted from different panels for testing to ensure the requirement of the *Voluntary Product standard PS 2-92* requirement (a

minimum of 10 specimens taken from at least five panels) (NIST 1992). The concentrated static load test produced two results: maximum deflection under 890 N load and ultimate load.

Concentrated Static Load Test Results

The deflection and ultimate load results for all panels tested are presented in Table 4.3 including summary statistics. According to *Voluntary Product Standard PS 2-92* "at least 90 percent of tests shall deflect no more than the specified maximum deflection" (NIST 1992). Based on the thickness of the OSB panels (19.05-mm), the *Single Floor-24* end-use-span rating was used for the concentrated static load test. The *Voluntary Product Standard PS 2-92* specifies a maximum deflection of 2.7-mm (NIST 1992).

Specimen Label	**Maximum Deflection mm**	**Ultimate Load kN**
m1p1	2.15	2.80
m1p2	2.00	3.56
m1p3	2.29	2.80
m1p4	2.20	3.11
m1p5	2.51	2.62
m1p6	2.43	2.48
m2p1	2.13	3.30
m2p2	1.84	3.94
m2p3	2.18	3.17
m2p4	2.22	2.91
m2p5	2.42	2.51
m2p6	2.27	3.49
m3p1	2.03	3.23
m3p2	2.46	2.70
m3p3	1.87	3.48
m3p4	2.46	3.02
m3p5	2.40	2.93
m3p6	2.13	3.32
mean	2.22	3.08
COV	9.12	12.90
minimum	1.84	2.48
maximum	2.51	3.94

Table 4.3. *Maximum deflection and ultimate load values for the CSL tests conducted.*

The experimental maximum deflection values presented in Table 4.3 indicate that all 18 specimens met the requirement specified in the *Voluntary Product standard PS 2-92*. Moreover, the experimental maximum deflection values did not show a high variability as described by the low coefficient of variation (9.12 %) values.

The *Voluntary Product standard PS 2*-92 specifies that all specimens shall support a minimum static load of 2.45 kN (NIST 1992). Interpretation of the results presented in Table 4.3 revealed that all of the specimens tested supported the specified minimum ultimate static load. The mean value of 3.08-kN was 25.7 percent higher than the minimum value defined in the standard. The standard deviation, coefficient of variation, and difference between maximum and minimum values revealed an expected high variation level.

Finite Element Analysis

The results and summary statistics of maximum deflection and ultimate load predicted using finite element analysis and physical testing are presented in Table 4.4. In general, the FE model accurately predicted the test values for both maximum deflection and ultimate load. However, the results obtained using the local densities were more accurate than the results obtained using global density. In general, the finite element values were lower than the test values (mean) and also presented a lower variation level (standard deviation and coefficient of variation).

Specimen	Maximum deflection mm			Ultimate load kN		
	Global	Local	Test	Global	Local	Test
m1p1	2.16	2.14	2.15	2.80	2.55	2.80
m1p2	1.97	1.95	2.00	2.85	2.73	3.56
m1p3	2.15	2.17	2.29	2.80	2.54	2.80
m1p4	2.09	2.21	2.20	2.95	2.82	3.11
m1p5	2.19	2.39	2.51	2.75	2.53	2.62
m1p6	2.23	2.25	2.43	2.73	2.39	2.48
m2p1	2.09	2.10	2.13	3.13	3.18	3.30
m2p2	2.07	1.98	1.84	3.15	3.22	3.94
m2p3	2.10	2.06	2.18	3.02	3.04	3.17
m2p4	2.09	2.08	2.22	2.91	2.65	2.91
m2p5	2.14	2.30	2.42	2.51	2.05	2.51
m2p6	2.16	2.10	2.27	2.96	3.02	3.49
m3p1	2.04	1.99	2.03	3.07	2.93	3.23
m3p2	2.11	2.29	2.46	2.84	2.48	2.70
m3p3	2.08	1.98	1.87	2.96	2.84	3.48
m3p4	2.23	2.39	2.46	2.87	2.76	3.02
m3p5	2.28	2.35	2.40	2.78	2.37	2.93
m3p6	2.19	2.23	2.13	2.98	3.01	3.32
mean	2.13	2.16	2.22	2.89	2.73	3.08
COV	3.52	6.71	9.12	5.42	11.39	12.90
minimum	1.97	1.95	1.84	2.51	2.05	2.48
maximum	2.28	2.39	2.51	3.15	3.22	3.94

Table 4.4. *Finite element results using global and local density: maximum deflection under 890 N Load and ultimate load.*

The prediction accuracy for each specimen was compared in the plots of maximum deflection and ultimate load presented in Figures 4.6, and 4.7, respectively. In these plots, the solid (FE-local densities) and dashed (FE global density) lines represent the linear relationship between test and finite element results using global and local densities, respectively. The dotted line represents the 45 degree line of a perfect prediction. Interpretation of these plots confirm that the finite element results using local densities produced more accurate results across the range than those values obtained using global density. This finding is reaffirmed by the r^2, which are larger when local density values were used. Note that the slope of the prediction line using local densities parallels the 45 degree line as compared to that of the global density. Finally,

standard deviation and COV values were unrealistically low when global density was used, and these values were double in magnitude and more realistic when local densities were used.

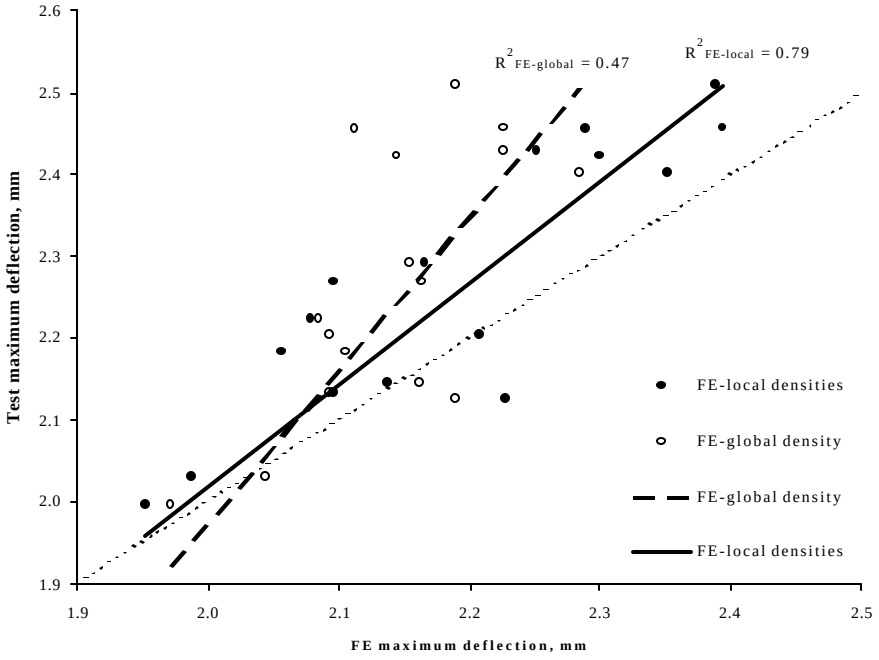

Figure 4.6. *Plot showing the maximum deflection results (finite element vs. test).*

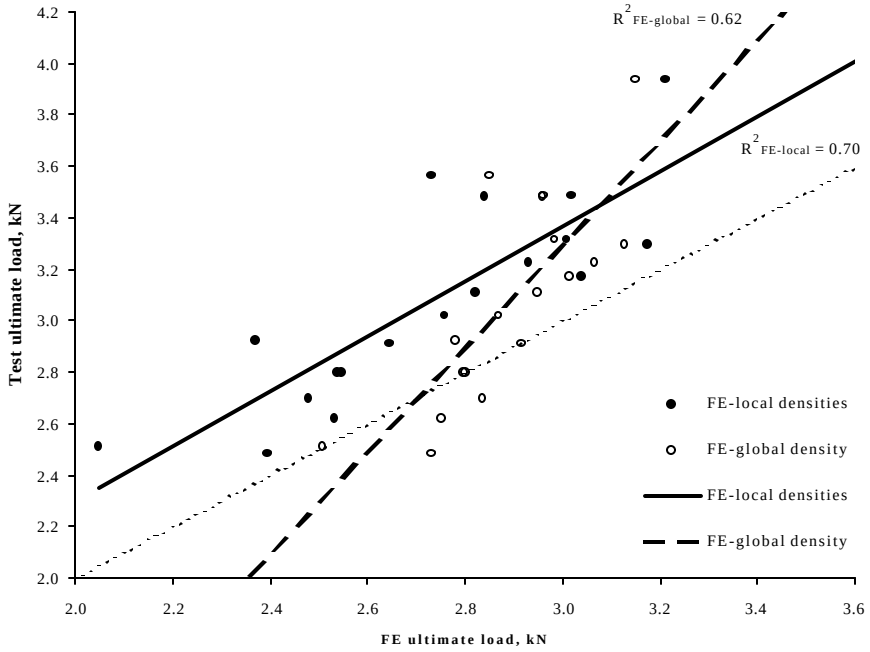

Figure 4.7. *Representation plot of ultimate load results (finite element vs test).*

Conclusions

The experimental maximum deflection and ultimate load results under the concentrate static load test revealed that all 18 panels met the requirements dictated by the *Voluntary Product Standard PS 2-92* (2.70 mm and 2.45 kN, respectively). The mean value of maximum deflection was 2.22 mm with a coefficient of variation (COV) of 9.12 percent, whereas the mean value of ultimate load was 3.08 kN with a COV value equal to 12.9 percent.

In general, the finite element maximum deflection and ultimate load results display reasonable agreement with the experimental results; however, the results obtained using local property variations are more realistic. The coefficient of determination between finite element results and test results for maximum deflection and ultimate load using local properties (based on local density) was 0.79 and 0.70, respectively. Consequently, the methodology based on the finite element method is recommended to simulate concentrated static load test results utilizing local density values.

References

APA-The Engineered Wood Association. 2000. Oriented Strand Board Product Guide. Tacoma, Washington.

APA-The Engineered Wood Association. 1994. PRP-108 Performance Standards and Policies for Structural- Use Panels. Tacoma, Washington.

ASTM 1997. Standard Test Method for Performance of Wood and Wood-Based and Roof Sheating Under Concentrated Static and Impact Loads. Standard E661-88. American Society of Testing and Materials.

Bozo, A. 2002. Spatial Variation in Wood Composites. Washington State University, Pullman, Washington.

Chen, S., R. Wellwood, and D. Kenway. 2000. On-Line Infrared Panel Density Measurement. 34th International Particleboard/Composite Material Symposium. Washington State University, Pullman, Washington.

Cook, R., D. Malkus, and M. Plesha. 1989. Concepts and Application of Finite Element Analysis John Wiley and Sons. New York.

Dong,C.C. 1979. The Mechanical Properties of Flakeboards Related to Flake Orientation. Dissertation. Washington State University. Pullman, Washington.

Guan, N., Y. Wang, and H. Gu. 2001. Specimen Orientation for the Calibration of Direct Scanning x-ray Wood Densitometers. Wood and Fiber Science, 33(1). Pp 26-30.

Hoyle, R.J., R.J. Tichy, and R.Y. Itani. 1982. Composite Wood Panel Deflection Under Concentrated Load. Wood Science Vol. 15, No 2

Laufenberg, T.L. and D.P.Xu. 1989. Concentrate Load and Impact Behavior of Wood-Based Panels. 23d International Particleboard/Composite Material Symposium. Washington State University. Pullman, Washington.

National Institute of Standards and Technology (NIST). 1992. Voluntary Product Standard PS 2-92, Performance Standard for Wood-Based Structural-Use Panels. U.S. Government Printing Office, Washington, DC.

Szilard, R. 1974. Theory and Analysis of Plate. Classical and Numerical Methods. Prentice-Hall, INC. Englewood Cliffs, New Jersey.

Chapter 5

An Inverse Methodology Using Finite Elements for Determining the Elastic Constants of Wood Composites

Introduction

The traditional means of determining mechanical properties is based on statically determinate test configurations that typically investigate pure loading modes such as tension, compression, or shear. In all these tests, the process consists of applying a predetermined load and measuring the resulting displacement (Le Magorou et al. 2001). Together, these quantities define the boundary conditions for the test. They are subsequently used to compute the material constants to be used in predetermined constitutive relations. However, for many cases, the complexity of either the boundary conditions or material response may provide difficulties for a direct solution to the material response problem. Just as advanced numerical techniques may be used for a direct solution with boundary conditions or material response complexities, the inverse solution of the same model may provide benefits for determining material response under the same conditions (Hermanson 1996).

The solution of a direct problem consists of finding effects based on a full description of their causes. In opposition, the inverse problem facilitates finding unknown causes based on observation of their effects (Mosegaard and Tarantola 1995 and 2002). The inverse problem is the numerical solution (for f) of an equation of the form $f \cdot g = h + \{noise\}$, given knowledge of g and h (Hermanson 1996). There are several examples where the inverse problem method had been applied, such as computer axial tomography, radio-astronomical imaging, navigation, model fitting, image analysis, and geophysics (Tan and Fox 2001).

One of the most important advantages of the inverse problem method is that response data may be used to determine the causes for the response. In addition, the inverse problem method facilitates the determination of several stiffness components using a single, mixed-mode test. The inverse problem method also presents disadvantages such as numerical instabilities and nonunique solutions (Tarantola and Valette 1982).

Objectives

While developing techniques to determine structure-property relations in wood composites, this investigation presents a methodology for material characterization using finite elements theory.

The specific objectives of this research are to:

1. Propose an inverse methodology using finite elements for determining the elastic constants of wood composites.
2. Resolve the constant coefficients (*a* and *b*) of given logarithmic regression model using the inverse problem methodology.
3. Compare the constant coefficients (*a* and *b*) obtained using the inverse method with those developed using traditional regression techniques.

Material and Methods

Material Sampling

The material sampling included nine tension and compression specimens of commercial OSB consisting of three different sizes at the central part, 12.7- by 12.7-mm, 12.7- by 25.4-mm, and 12.7-by 50.8-mm (three specimens for each size). The mechanical response of these specimens was obtained from previous research documented by Bozo (2002). All the specimens chosen for this analysis had an approximate density value of 550 kg/m^3 at the central part of the specimen.

Inverse Problem Method

The inverse problem method is described in this section to develop a relationship between the displacements and loads observed from the experimental tension and compression test results. The inverse problem method is analogous to a finite element analysis where the stiffness matrix $\left(k_{ij}^{lm}\right)$ relates the nodal loads $\left(p_i^l\right)$ and the nodal displacements $\left(d_j^m\right)$ as:

$$p_i^i = k_{ij}^{lm} \cdot d_j^m \qquad \text{Equation 5.1}$$

where, i and j represent the degrees of freedom (u_x *and* u_y), and l and m represent the node number. In the finite element method, a known displacement or force is prescribed at a node, k_{ij}^{lm}, and the corresponding unknown force or displacement is computed (Hermanson 1996). In the inverse method, forces and displacements are known at the boundary, but the stiffness matrix, k_{ij}^{lm}, is unknown. The stiffness matrix includes both the material constitutive matrix ***C*** and strain-displacement relations ***B*.**

$$k_{ij}^{lm} = \int_V B_{ia}^{l\ T} \cdot C_{ab} \cdot B_{bj}^m \cdot dV \qquad \text{Equation 5.2}$$

Where $\boldsymbol{a}$ and $\boldsymbol{b}$ span 1→4 which represents the four unique strains. The strain-displacement relation matrix $\boldsymbol{B}$ as well the material constitutive matrix $\boldsymbol{C}$ of Equation 5.2 are unknown for the test. However, the displacement field can be assumed using the shape functions as with the finite element method. Substituting Equation 5.2 into Equation 5.1 gives the following:

$$p_i^l = \left[\int_V B_{ia}^{l\ T} \cdot C_{ab} \cdot B_{bj}^m \cdot dV\right] \cdot d_j^m \qquad \text{Equation 5.3}$$

The type of element formulation determines the strain-displacement relations, $\boldsymbol{B}$. In this research, a plane bilinear isoparametric element was used (Cook et al. 1989). Consequently, the only unknown is the material constitutive matrix $\boldsymbol{C}$. Using Gauss quadrature (Cook et al. 1989), the Equation 5.3 can be expanded as:

$$p_i^l = \left[\sum_{m=1}^{ngp}\sum_{n=1}^{ngp} B_{ia}^{l\ T} \cdot C_{ab} \cdot B_{bj}^m \cdot wt_m \cdot wt_n \cdot t \cdot |J|\right] \cdot d_j^m \qquad \text{Equation 5.4}$$

where,

wt_m and wt_n	= weigth factor
t	= thickness of the panel
$\lvert J \rvert$	= determinant of Jacobian
ngp	= number of gauss points

By using indicial notation, Equation 5.4 is rewritten as:

$$p_i^l = \left[\sum_{m=1}^{ngp}\sum_{n=1}^{ngp} B_{ia}^{l\ T} \cdot B_{bj}^m \cdot wt_m \cdot wt_n \cdot t \cdot |J| \cdot d_j^m\right] \cdot C_{ab} \qquad \text{Equation 5.5}$$

or in matrix form as:

$$p = A \cdot C \qquad \text{Equation 5.6}$$

The constitutive matrix, ***C*** can be solved as:

$$C = A^{-1} \cdot p \qquad \text{Equation 5.7}$$

A schematic representation of a four-node plane bilinear isoparametric element is shown in Figure 5.1. The load and deformation imposed on each node is revealed in the testing results.

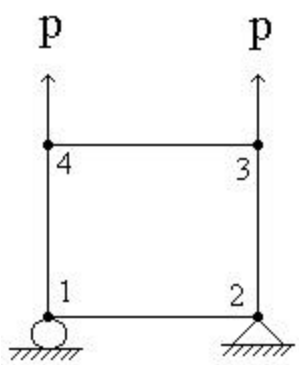

Figure 5.1. *Schematic representation of element in tension.*

In this case, the load vector is represented by 0, *p* and -*p* values, and the displacement vector by 0 and *d* values. All values in the x-direction are considered zero, for both load and displacement. The displacement values for nodes 1 and 2 are zero as imposed by the boundary condition. The load and displacement vector can then be defined as follows:

$$p = \begin{bmatrix} 0 & -p & 0 & -p & 0 & p & 0 & p \end{bmatrix}^T \qquad d = \begin{bmatrix} 0 & 0 & 0 & 0 & 0 & d & 0 & d \end{bmatrix}^T$$

The constitutive matrix ***C*** corresponds to the two-dimensional case and the general form is shown in Equation 5.5. Substituting into Equation 5.4 yields Equation 5.6, and C_{22} can easily be obtained.

$$C = \begin{bmatrix} C_{11} & C_{12} & 0 \\ C_{21} & C_{22} & 0 \\ 0 & 0 & C_{66} \end{bmatrix} \qquad \text{Equation 5.8}$$

$$\begin{bmatrix} 0 \\ -p \\ 0 \\ -p \\ 0 \\ p \\ 0 \\ p \end{bmatrix} = \begin{bmatrix} \sum_{i=1}^{9}\left[(B(i)_{26} + B(i)_{28}) \cdot B(i)_{11}\right] \cdot C_{12} \cdot w(i)_1 \cdot w(i)_2 \cdot t \cdot |J| \cdot d \\ \sum_{i=1}^{9}\left[(B(i)_{26} + B(i)_{28}) \cdot B(i)_{22}\right] \cdot C_{22} \cdot w(i)_1 \cdot w(i)_2 \cdot t \cdot |J| \cdot d \\ \sum_{i=1}^{9}\left[(B(i)_{26} + B(i)_{28}) \cdot B(i)_{13}\right] \cdot C_{12} \cdot w(i)_1 \cdot w(i)_2 \cdot t \cdot |J| \cdot d \\ \sum_{i=1}^{9}\left[(B(i)_{26} + B(i)_{28}) \cdot B(i)_{24}\right] \cdot C_{22} \cdot w(i)_1 \cdot w(i)_2 \cdot t \cdot |J| \cdot d \\ \sum_{i=1}^{9}\left[(B(i)_{26} + B(i)_{28}) \cdot B(i)_{15}\right] \cdot C_{12} \cdot w(i)_1 \cdot w(i)_2 \cdot t \cdot |J| \cdot d \\ \sum_{i=1}^{9}\left[(B(i)_{26} + B(i)_{28}) \cdot B(i)_{26}\right] \cdot C_{22} \cdot w(i)_1 \cdot w(i)_2 \cdot t \cdot |J| \cdot d \\ \sum_{i=1}^{9}\left[(B(i)_{26} + B(i)_{28}) \cdot B(i)_{17}\right] \cdot C_{12} \cdot w(i)_1 \cdot w(i)_2 \cdot t \cdot |J| \cdot d \\ \sum_{i=1}^{9}\left[(B(i)_{26} + B(i)_{28}) \cdot B(i)_{28}\right] \cdot C_{22} \cdot w(i)_1 \cdot w(i)_2 \cdot t \cdot |J| \cdot d \end{bmatrix} \qquad \text{Equation 5.9}$$

Results

Specimen Characterization and Test Results

Specimen	Thickness mm	Width mm	Strain mm/mm	Displacement mm	Stress MPa	Load N
T-12.7-1	19.47	13.74	0.0008560	0.0109	2.68	717
T-12.7-2	19.15	13.86	0.0009450	0.0120	3.41	906
T-12.7-3	19.30	14.34	0.0008620	0.0109	3.16	875
T-25.4-1	19.25	25.83	0.0002300	0.0029	0.35	175
T-25.4-2	19.30	26.14	0.0005470	0.0069	0.77	389
T-25.4-3	18.97	25.60	0.0006630	0.0084	1.04	506
T-50.8-1	19.29	52.45	0.0006040	0.0077	0.47	477
T-50.8-2	19.05	46.72	0.0005840	0.0074	0.53	470
T-50.8-3	19.22	52.29	0.0000950	0.0012	0.08	77
C-12.7-1	19.01	12.75	0.0014470	0.0184	3.01	729
C-12.7-2	19.69	12.83	0.0006535	0.0083	2.86	723
C-12.7-3	18.85	12.84	0.0006520	0.0083	1.42	343
C-25.4-1	19.49	25.26	0.0008570	0.0109	1.12	552
C-25.4-2	19.39	25.58	0.0008560	0.0109	1.16	577
C-25.4-3	19.14	25.67	0.0018880	0.0240	2.59	1274
C-50.8-1	19.47	50.58	0.0009860	0.0125	0.47	465
C-50.8-2	19.28	50.43	0.0006120	0.0078	0.29	286
C-50.8-3	19.25	51.18	0.0009210	0.0117	0.41	407

Table 5.1. *Specimen characterization and test results*

The specimen characteristics along with load and deflection results from the physical tests are presented in Table 5.1. In the case of uniaxial tension and compression, the constitutive term of interest is C_{22}, for which, an identity is formulated using the nomenclature of the inverse problem method (Equation 5.10). The term H^{-1} is subsequently defined in Equation 5.11. However, from the material constitutive relationship it is know that C_{22} in terms of material properties is defined as Equation 5.12.

$$c_{22} = H^{-1} \cdot p \qquad \text{Equation 5.10}$$

$$H^{-1} = \left(\sum_{i=1}^{9} \left[(B(i)_{26} + B(i)_{28}) \cdot B(i)_{22} \right] \cdot C_{22} \cdot w(i)_1 \cdot w(i)_2 \cdot t \cdot |J| \cdot d \right)^{-1} \quad \text{Equation 5.11}$$

$$C_{22} = \frac{E_2}{(1 - \boldsymbol{n}_{21} \cdot \boldsymbol{n}_{12})} \quad \text{Equation 5.12}$$

Rearranging Equation 5.12 and substituting into Equation 5.10, yields:

$$E_2 = H^{-1} \cdot p \cdot (1 - \boldsymbol{n}_{21} \cdot \boldsymbol{n}_{12}) \quad \text{Equation 5.13}$$

Substituting E_2, as defined in the logarithmic regression model, into Equation 5.13, the following is obtained:

$$a \cdot Ln(D) + b = H^{-1} \cdot p \cdot (1 - \boldsymbol{n}_{21} \cdot \boldsymbol{n}_{12}) \quad \text{Equation 5.14}$$

For each specimen size there were three specimens; consequently, the coefficients *a* and *b* on Equation 5.14 were solved by singular value decomposition using three simultaneous equations representing the three test specimens. The results for coefficients *a* and *b*, as well the values developed from the regression models are presented in Table 5.2.

Size	**Singular value decomposition**		**Regression model**	
	a	***b***	***a***	***b***
T 12.7-mm	3440	-18060	3466	-18228
T 25.4-mm	6944	-39820	6354	-36100
T 50.8-mm	6020	-33690	6857	-39020
C 12.7-mm	2919	-15660	2669	-14055
C 25.4-mm	3595	-19070	3942	-21335
C 50.8-mm	2260	-11720	2060	-10454

Table 5.2. *Values of coefficients a and b using singular value decomposition and regression models.*

Visual appraisal of the values for *a* and *b* (Tab. 5.2) indicates little difference between values developed by the inverse method and those resulting from the traditional regression analysis. However, the previous assurance is more clearly appreciated in Figure 5.2. Each plot shows two data series of density versus modulus of elasticity, the first series corresponds to the values generated using the coefficients *a* and *b* from the singular value decomposition, and the second series corresponds to the values using the coefficients *a* and *b* from the traditional regression model.

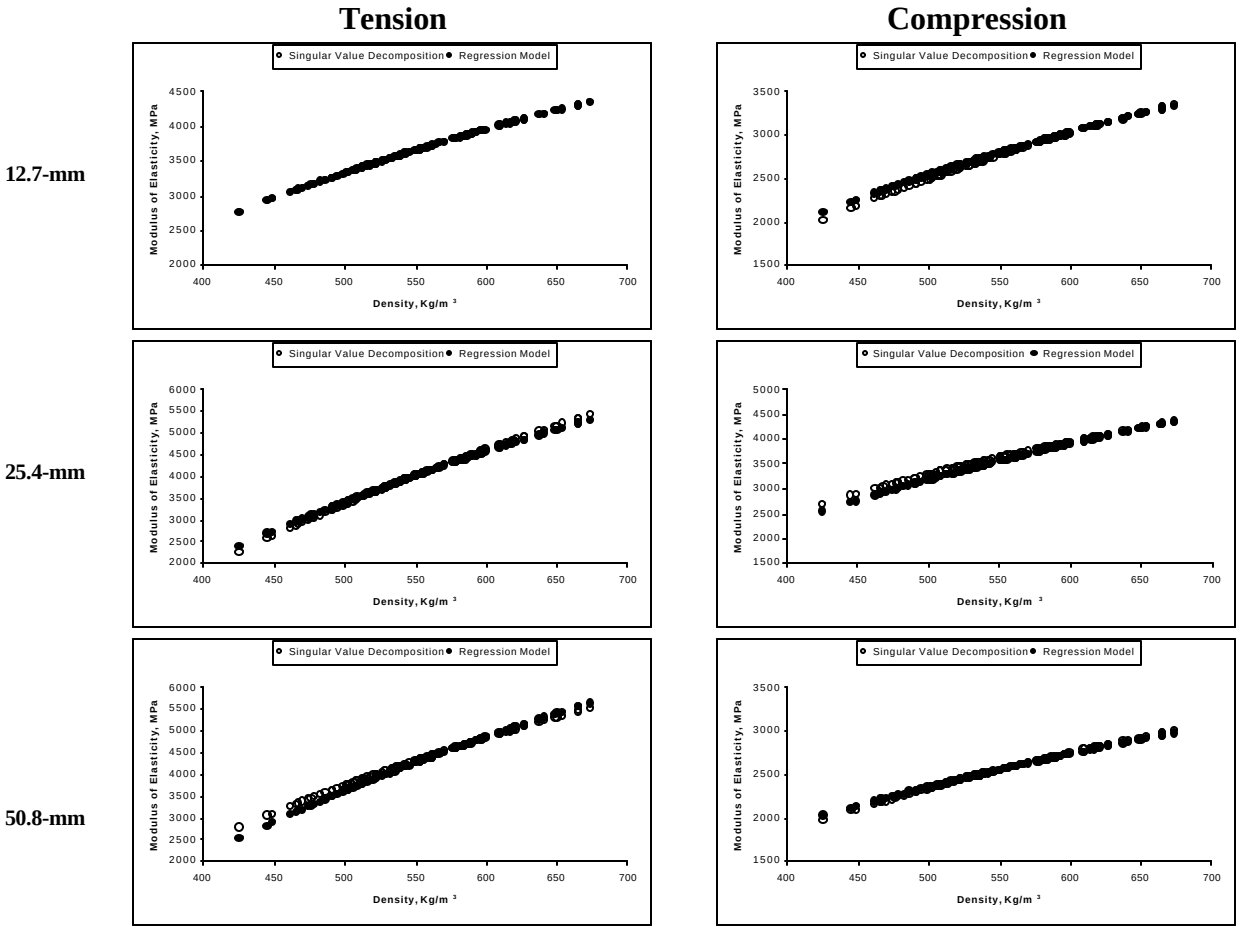

Figure 5.2. *Overlapping of curves obtained using singular value decomposition results and the traditional regression model results.*

The test of comparison of the means (Snedecor and Cochrane 1980) was used to verify whether the series are equal or not. Table 5.3 shows the results of the hypothesis test for coefficients *a* and *b* from the singular value decomposition and regression models. The results indicate no significant differences.

	Tension			**Compression**		
	12.7-mm	**25.4-mm**	**50.8-mm**	**12.7-mm**	**25.4-mm**	**50.8-mm**
S_p	340.80	656.88	636.80	276.03	372.33	213.41
t_{cal}	0.0811	0.0343	0.5314	-0.6976	1.4220	-0.1285
$a/2$	0.005	0.005	0.005	0.005	0.005	0.005
t_{table}	±2.807	±2.807	±2.807	±2.807	±2.807	±2.807
Reject H_o	**no**	**no**	**no**	**no**	**no**	**no**

Table 5.3. *Hypothesis test of comparison of means results.*

In general, the inverse method produces similar results to that of the traditional regression with a minimum of samples. Although the method was applied successfully to both tension and compression tests, it is clear that the tension results are somewhat better.

Conclusions

The inverse methodology using finite elements for determining the elastic constants of wood composites described in this research is only a preliminary application and must be considered as an exploratory method for further investigation. However, the inverse problem method proved very useful and warrants further development. This method is a supplement to the finite element formulation by extending the analysis beyond solving only the boundary value problem.

The results obtained for the regression coefficient (*a* and *b*), applying the inverse problem methodology, agree with values obtained by applying traditional regression techniques for all

loading modes and specimen sizes studied. However, the solutions obtained using singular value decomposition presented instability problems and were not unique. The results obtained using tension models were better than those obtained using compression models. However, the difference in results is not due to the inverse problem method, but due to other factors.

References

Hermanson, J.C. 1996. The Triaxial Behavior of Redwood Using a new Confined Compression Device. Dissertation. University of Wisconsin. Madison, Wisconsin, USA.

Le Magorou, L., F. Bos, and F. Rouger. 2000. An Inverse Problem Approach to Identify Viscoelastic Behavior of Structural Wood Based Panels. Word Conference on Timber Engineering. British Columbia, Canada.

Liu, J.Y., W.T. Simpson, and S.P. Verrill. 2000. An Inverse Moisture Diffusion Algorithm for the Determination of Diffusion Coefficient. The 12th International Drying Symposium. Noordwijkerhout, Netherlands.

Mosegaard, K. 1995. Monte Carlo Sampling of Solution to Inverse Problem. Journal of Geophysics Resarch, Vol 100, No B7, 12,431-12,447.

Snedecor, G.W. and W.G. Cochran. 1989. Statistical Methods. The Iowa State University Press. Ames, Iowa, USA.

Tarantola, A. and B. Valette. 1982. Generalized Noinlinear Inverse Problem Solved Using the Least Squares Criterion. Reviws of Geophysics and Space Physics, Vol 20 No 2. 219-

Chapter 6

Summary of Conclusion

Two complementary methods to assess variability in the localized density of oriented strandboard (OSB) panels were presented using graphical and analytical methods. Graphical methods provided a means of visualizing the data and their variability. Density patterns were evident in the contour plots and represented large-scale panel structure. Correlation and periodicity among neighboring specimens can be quantified using analytical methods such as spectral analysis and geostatistics. Spectral analysis and geostatistics indicated correlation between neighboring density specimens, and were used to identify spatial dependence within the density data. The spatial dependence results obtained by variogram, correlogram, and spectral density were consistently equivalent. The results observed in this research suggest that the use of local density rather than global density as a predictor of physical or mechanical properties would be more effective because the local density involves the neighborhood effect. The results presented in this investigation revealed that the global panel density was the poorest predictor of CSL behavior. In contrast, the mean density for an area of 254.0- by 190.5-mm and 203.2- by 165.1-mm around the load point, represented the highest correlation for maximum deflection and ultimate load, respectively. In both cases, the distance from the periphery of the circular loading area and the outer edge of the rectangular area was 88.9 mm. These results agree with the statistical range of influence for density in the longitudinal and transverse directions, which was between 200 and 400 mm and between 150 and 300 mm, respectively.

Test results revealed a clear relationship between oriented strandboard (OSB) properties and density. All property values increased as density increased; the differences between the relationship model were principally the slope, intercept, and coefficient of determination. The

effect of specimen size was not as clear as the density effect as was shown by the analysis of variance (ANOVA) and Tukey's test. Based on the ANOVA and Tukey's results the more convenient size corresponds to the specimen of 25.4- by 25.4-mm at the central part. This research developed statistical input models to generate mechanical properties base on regression models using density as a predictor variable. The logarithmic regression model better describes the reality of wood composites behavior at their lowest and highest density levels. The results of validation revealed that the regression model developed in this research can be used to simulate mechanical properties at different sizes and anywhere within the panel based on the density values at specific location and size using conditional Monte Carlo simulation.

The experimental maximum deflection and ultimate load results under the concentrate static load test revealed that all 18 panels met the requirements dictated by the *Voluntary Product Standard PS 2-92* (2.70 mm and 2.45 kN, respectively). The mean value of maximum deflection was 2.22 mm with a coefficient of variation (COV) of 9.12 percent, whereas the mean value of ultimate load was 3.08 kN with a COV value equal to 12.9 percent. In general, the finite element maximum deflection and ultimate load results display reasonable agreement with the experimental results; however, the results obtained using local property variations are more realistic. The coefficient of determination between finite element results and test results for maximum deflection and ultimate load using local properties was 0.79 and 0.70, respectively.

The inverse methodology using finite elements for determining the elastic constants of wood composites described in this research is only a preliminary application and must be considered as an exploratory method for further investigation. However, the inverse problem method proved very useful and warrants further development. This method is a supplement to the finite element formulation by extending the analysis beyond solving only the boundary value

problem. The results obtained for the regression coefficient (*a* and *b*), applying the inverse problem methodology, agree with values obtained by applying traditional regression techniques for all loading modes and specimen sizes studied. However, the solutions obtained using singular value decomposition presented instability problems and were not unique. The results obtained using tension models were better than those obtained using compression models. However, the difference in results is not due to the inverse problem method, but due to other factors.

Appendix A

Graphical Results

Data plots,
Color-scale plots,
Three-dimensional plots,
and
Contour plots

density	25	76	127	178	229	279	330	381	432	483	533	584	635	686	737	787	838	889	940	991	1041	1092	1143	1194	mm
25	559	600	591	566	552	549	572	521	486	508	545	642	544	631	570	520	602	558	623	629	580	598	608	571	
76	596	586	575	580	508	545	559	525	525	548	562	593	550	586	557	559	531	515	557	594	544	536	574	549	
127	589	591	605	542	547	584	571	554	535	578	551	587	611	577	562	602	535	561	582	564	601	565	571	541	
178	552	577	551	584	543	560	542	480	514	495	559	597	585	595	592	636	555	560	560	555	587	537	570	576	
229	571	539	547	577	550	516	543	520	523	500	601	614	553	572	583	619	555	558	597	605	559	542	545	527	
279	535	568	542	529	598	563	585	549	546	519	520	574	545	554	607	563	553	558	548	545	532	469	515	581	
330	575	579	582	590	509	577	556	551	579	557	491	579	558	560	610	609	572	540	532	578	554	598	540	572	
381	616	549	596	548	546	601	575	546	586	550	557	531	561	596	633	561	610	605	626	572	539	596	509	594	
432	601	608	572	570	549	551	535	549	530	559	580	564	590	611	573	587	599	616	590	567	527	551	523	544	
483	628	558	544	616	622	606	570	577	524	518	607	585	590	521	567	606	589	604	565	545	490	549	484	455	
533	603	585	615	608	574	608	583	501	501	525	531	572	578	553	579	573	631	565	592	585	510	533	506	536	
584	541	568	582	601	592	557	553	499	537	505	520	525	533	563	582	565	600	535	530	530	542	589	601	546	
635	549	603	564	604	581	616	612	543	485	512	521	594	557	522	560	546	574	574	540	601	535	534	595	560	
686	587	547	577	554	493	539	633	554	497	486	552	575	543	504	541	567	609	616	565	577	538	528	567	572	
737	576	532	558	580	551	564	533	534	544	587	586	585	581	526	522	554	548	554	590	616	554	493	537	526	
787	535	500	599	582	537	562	538	605	563	585	515	585	574	572	527	508	593	538	611	608	542	499	528	528	
838	516	505	600	562	522	545	505	503	577	607	559	552	521	551	566	542	543	537	554	547	552	532	566	538	
889	550	580	566	553	526	586	501	524	547	568	528	566	569	586	503	564	601	624	540	565	566	588	564	552	
940	568	548	570	590	551	561	559	555	560	562	549	574	507	545	506	571	567	566	564	589	531	532	533	573	
991	528	555	559	530	543	619	577	565	569	570	520	553	545	587	585	552	526	603	580	646	579	580	617	595	
1041	492	589	528	559	583	539	586	551	591	566	553	571	568	577	539	554	530	580	568	576	597	575	536	552	
1092	504	550	537	539	528	523	551	542	567	540	539	580	602	529	582	539	535	555	535	506	563	538	516	533	
1143	571	583	588	520	457	566	591	532	545	496	502	516	563	482	613	561	527	561	497	511	509	513	544	555	
1194	546	600	556	574	568	566	527	468	521	542	521	552	527	549	598	596	584	561	510	573	511	575	535	530	
1245	517	565	564	584	573	584	548	525	503	530	554	532	546	574	559	602	539	570	571	605	533	581	559	514	
1295	531	561	609	552	544	582	598	571	535	505	516	499	528	547	576	597	549	554	559	564	534	624	542	589	
1346	510	508	576	531	545	590	566	577	568	536	559	522	529	558	554	579	620	605	614	538	509	574	516	513	
1397	519	570	575	508	537	541	542	610	561	544	628	543	575	526	551	618	623	622	633	573	541	533	562	606	
1448	540	558	554	569	570	574	559	571	542	522	579	543	531	551	576	560	589	617	607	543	579	542	565	642	
1499	548	511	555	552	565	528	595	579	558	547	549	562	570	572	578	551	557	564	548	556	568	586	584	572	
1549	550	523	548	578	546	558	574	571	551	575	573	560	594	580	577	647	617	618	585	590	562	562	585	521	
1600	527	460	497	567	533	540	533	609	584	554	529	597	601	627	664	590	600	626	630	606	553	531	568	572	
1651	561	503	547	548	514	575	548	587	561	516	542	569	554	546	567	567	563	612	612	560	491	472	519	488	
1702	563	564	543	528	541	569	569	604	573	503	524	555	563	596	569	537	573	629	584	553	551	540	511	505	
1753	513	532	543	516	549	600	590	493	529	574	584	610	598	515	544	566	553	539	558	521	515	549	559	526	
1803	555	560	563	523	551	571	579	538	510	591	555	593	593	538	555	596	557	504	566	502	546	526	508	528	
1854	528	571	553	585	597	555	535	526	573	504	560	519	524	549	617	590	631	541	530	511	531	491	540	572	
1905	618	575	624	594	559	585	572	534	515	524	567	537	517	544	590	600	625	586	579	533	531	535	602	544	
1956	606	563	628	566	557	579	509	504	502	549	565	514	528	567	629	619	607	610	544	538	526	514	562	495	
2007	540	557	598	551	549	605	545	480	477	501	515	511	525	537	544	568	552	605	590	568	561	576	554	524	
2057	507	549	619	536	544	585	602	478	526	511	533	553	556	529	560	561	580	590	558	541	578	537	538	564	
2108	642	591	560	549	550	598	569	511	521	519	559	482	554	557	576	595	575	567	512	602	576	513	576	517	
2159	566	536	574	618	585	564	562	525	541	520	476	570	583	541	568	603	583	571	555	572	517	545	564	499	
2210	504	549	563	546	553	584	527	527	540	525	465	534	496	544	531	561	574	611	508	575	531	538	530	506	
2261	483	540	535	552	551	612	537	528	556	530	552	521	500	501	492	584	550	594	518	573	538	493	519	490	
2311	523	517	533	532	564	588	567	560	554	526	562	560	549	562	624	585	566	586	573	548	542	501	515	548	
2362	532	558	593	517	511	550	550	548	550	573	565	557	563	515	591	578	582	605	580	514	480	502	520	583	
2413	551	540	568	499	558	541	554	517	523	577	548	540	573	554	648	656	612	582	582	619	556	526	516	572	

mm

Figure A.1. *Data plot of density (kg/m^3) of panel m1p1 (window size 50- by 50-mm)*

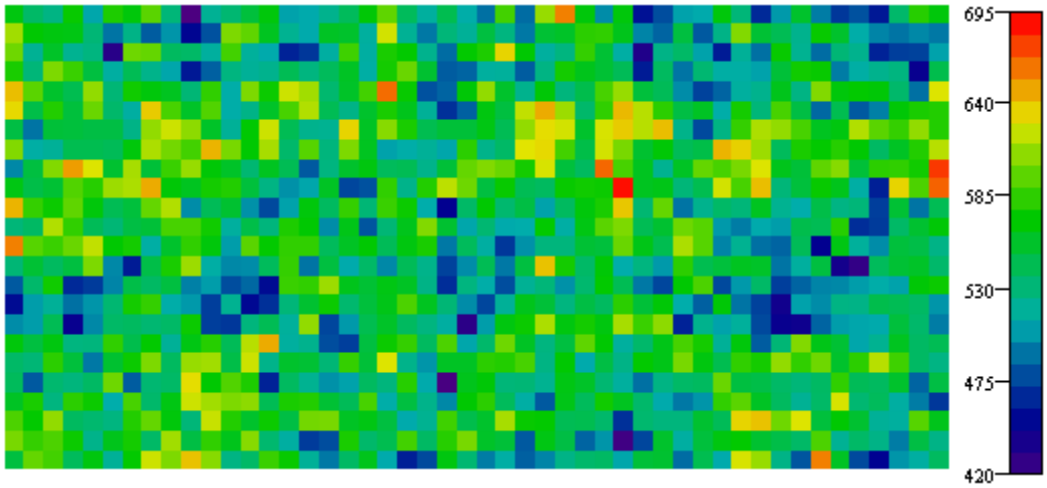

Figure A.2. *Color-scale plot of density (kg/m^3) of panel m1p1 (window size 50- by 50- mm).*

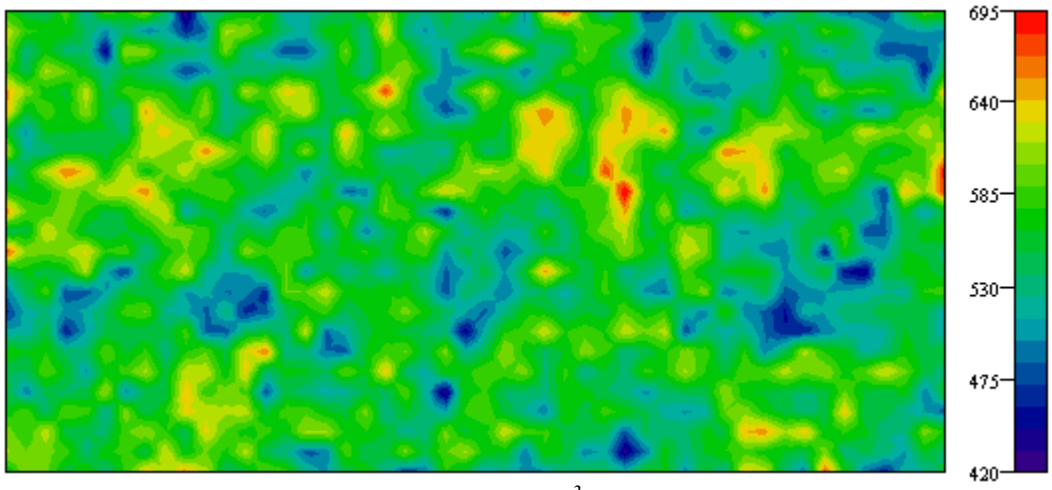

FigureA.3. *Three-dimensional plot of density (kg/m^3) of panel m1p1 (window size 50- by 50- mm).*

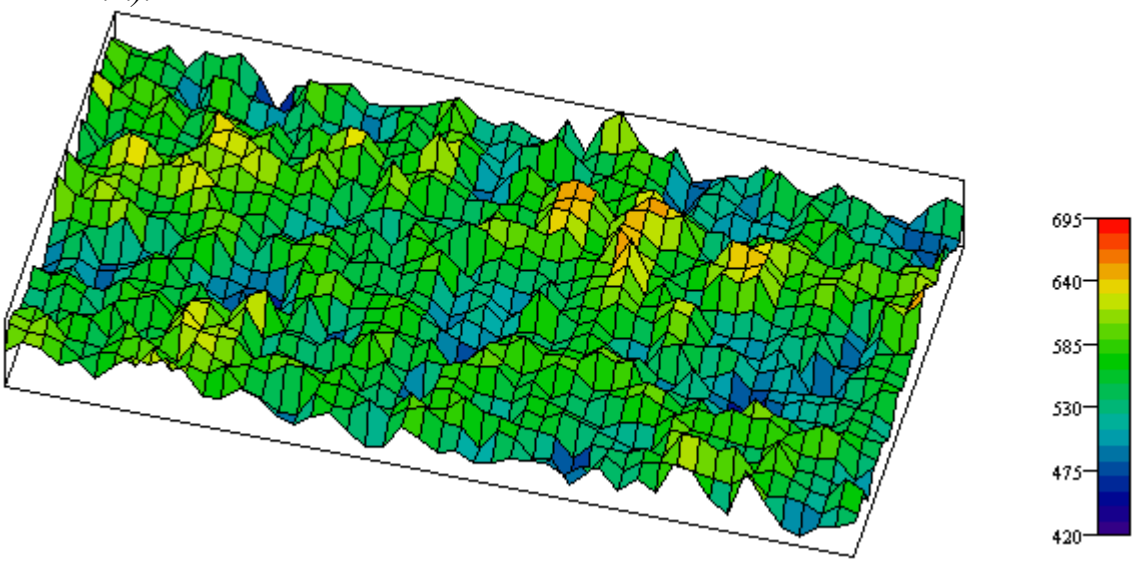

FigureA.4. *Contour plot of density (kg/m^3) of panel m1p1 (window size 50- by 50- mm).*

density	25	76	127	178	229	279	330	381	432	483	533	584	635	686	737	787	838	889	940	991	1041	1092	1143	1194	mm
25	541	522	510	597	569	535	502	519	608	634	604	583	593	577	652	687	645	580	633	695	578	566	591	630	
76	584	539	541	588	586	545	553	577	601	587	571	561	560	593	656	656	645	599	584	579	527	574	541	536	
127	582	531	610	597	569	549	577	578	525	558	585	593	542	626	652	623	644	609	563	575	481	512	555	540	
178	558	566	600	556	514	556	526	528	520	599	609	580	615	644	631	581	580	610	607	582	530	572	582	568	
229	582	586	586	562	556	538	561	600	587	591	622	569	554	607	671	659	603	570	645	612	612	568	553	543	
279	624	566	575	549	566	548	610	569	589	570	547	578	577	649	605	643	564	595	615	636	597	544	555	571	
330	646	584	557	568	550	535	544	543	576	608	540	610	582	636	562	610	613	623	636	632	592	570	574	526	
381	597	526	573	623	564	523	535	531	521	636	590	571	559	558	573	608	597	600	573	630	525	563	569	543	
432	565	561	611	641	520	528	581	596	515	601	624	550	583	557	604	608	599	544	601	666	580	567	551	515	
483	595	642	545	626	528	537	568	572	587	587	576	660	606	536	620	601	607	649	600	673	570	531	534	520	
533	607	545	543	545	565	594	541	575	544	616	588	675	588	565	618	643	588	602	654	630	607	570	564	551	
584	658	594	598	601	595	563	540	502	545	565	580	611	637	628	595	621	584	646	639	652	582	584	581	583	
635	574	557	602	552	570	588	596	545	583	577	582	575	620	596	581	580	657	628	608	643	559	623	624	595	
686	569	620	537	577	547	575	591	573	548	592	608	612	612	631	597	608	716	667	619	644	575	580	597	561	
737	582	565	597	597	576	574	610	567	584	596	638	615	627	579	623	632	644	593	575	659	570	608	589	544	
787	573	570	602	627	615	559	559	570	548	558	584	610	639	590	639	583	618	593	640	615	580	595	590	628	
838	504	554	557	516	520	494	551	555	577	593	577	599	652	625	653	612	609	628	603	629	630	581	582	501	
889	480	554	538	554	565	535	548	524	585	568	556	592	611	599	628	564	625	598	599	596	577	577	565	569	
940	557	539	550	553	524	552	574	541	563	563	605	599	602	605	621	594	624	594	611	580	565	506	547	585	
991	591	559	544	555	537	538	599	529	569	625	553	601	626	595	683	640	596	540	567	599	579	529	520	546	
1041	608	572	581	542	567	513	547	499	557	544	588	614	624	624	654	596	592	583	597	607	570	522	524	581	
1092	609	604	571	545	518	488	501	501	558	538	596	587	579	566	639	602	574	643	612	603	579	530	584	585	
1143	569	531	504	532	515	518	488	559	579	500	552	593	560	582	622	602	623	622	649	605	608	547	572	575	
1194	622	564	542	580	519	508	579	552	532	506	557	581	545	576	592	571	559	634	600	600	571	547	614	650	
1245	566	515	578	637	529	533	544	545	541	536	506	589	588	590	588	616	614	560	657	592	579	561	584	531	
1295	537	584	614	503	526	578	543	534	519	523	547	584	595	640	584	593	575	546	648	656	602	561	598	609	
1346	559	612	560	568	521	523	534	537	547	555	556	554	603	677	628	633	625	585	580	601	558	576	636	587	
1397	569	589	614	591	587	530	552	540	545	603	505	505	581	625	613	598	622	595	570	580	593	557	577	550	
1448	571	570	579	550	538	565	568	535	519	612	585	524	569	585	572	634	633	638	586	548	534	488	576	580	
1499	583	600	617	575	533	524	539	540	514	551	588	562	534	514	570	577	644	645	659	600	590	518	607	589	
1549	565	576	579	611	524	534	525	505	535	527	539	559	628	562	579	606	657	598	566	573	627	566	600	542	
1600	598	584	617	572	548	585	553	553	547	541	501	508	608	598	677	586	629	612	620	605	588	562	555	567	
1651	588	561	635	584	508	558	543	488	502	532	484	542	625	601	639	616	605	572	631	618	566	631	584	560	
1702	530	540	607	595	547	617	514	490	479	526	525	548	584	546	635	577	587	587	572	582	606	617	585	565	
1753	585	619	669	575	550	573	585	502	500	532	556	562	583	595	632	637	579	584	584	568	564	563	566	599	
1803	607	595	598	566	547	555	574	535	517	494	525	563	555	560	604	623	590	636	616	566	543	521	548	590	
1854	647	581	568	617	567	559	576	543	531	496	502	536	567	529	537	642	556	525	513	575	599	556	563	565	
1905	561	572	588	578	554	564	536	593	551	564	532	517	547	539	561	612	570	523	477	538	572	539	518	562	
1956	568	545	620	556	535	572	542	560	584	588	569	537	567	592	570	601	531	554	536	573	486	471	526	539	
2007	599	596	589	521	493	576	575	541	534	549	573	540	581	577	597	622	593	614	576	615	505	457	499	550	
2057	580	575	555	531	501	533	558	520	573	526	541	621	599	603	583	625	563	554	608	573	505	513	515	546	
2108	509	496	523	521	502	548	496	514	525	519	548	622	646	655	628	621	605	584	614	560	523	501	505	521	
2159	509	529	550	564	559	592	559	572	587	591	555	604	636	580	574	602	536	550	570	558	519	524	595	528	
2210	538	513	581	562	556	560	578	495	553	590	580	589	564	576	629	608	528	525	520	523	595	485	514	530	
2261	583	483	520	539	546	575	517	546	577	553	574	608	590	642	657	606	580	502	542	586	578	530	503	495	
2311	546	487	559	577	551	557	505	564	590	517	595	616	587	586	561	556	596	590	565	555	529	518	531	529	
2362	512	532	566	545	549	555	560	565	514	562	649	641	554	585	596	584	556	608	513	546	504	514	538	471	
2413	516	549	546	508	549	553	507	554	525	629	622	619	592	632	594	603	546	591	557	536	539	517	495	489	

mm

Figure A.5. *Data plot of density (kg/m^3) of panel m1p2 (window size 50- by 50-mm)*

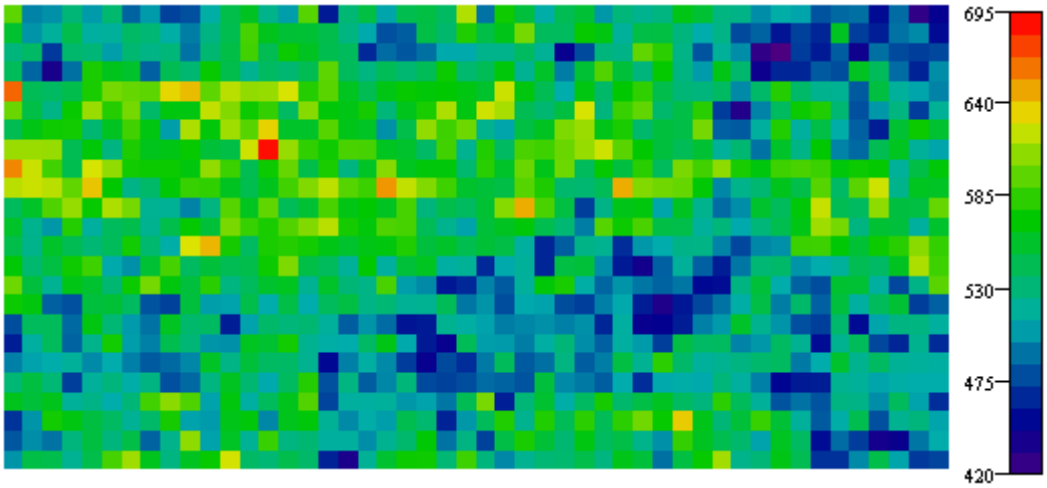

Figure A.6. *Color-scale plot of density (kg/m^3) of panel m1p2 (window size 50- by 50- mm).*

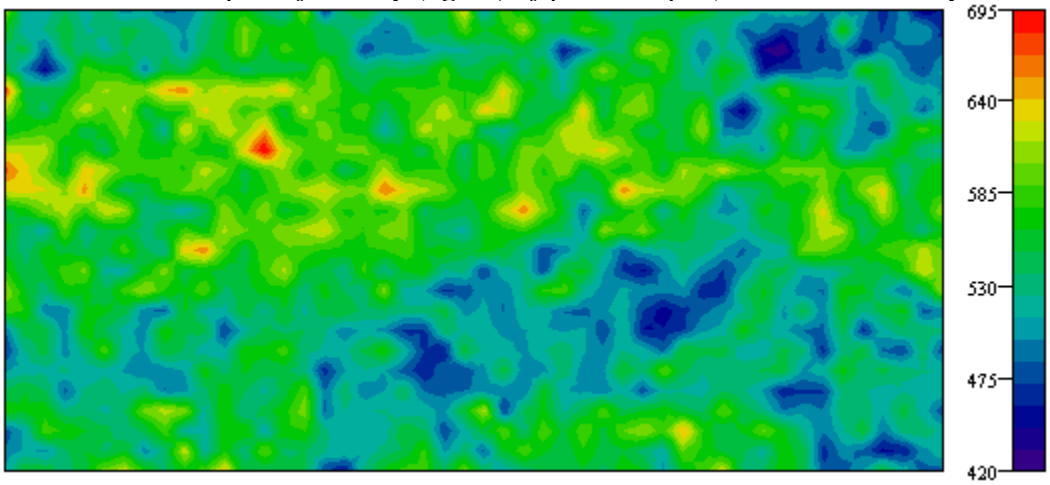

FigureA.7. *Three-dimensional plot of density (kg/m^3) of panel m1p2 (window size 50- by 50- mm).*

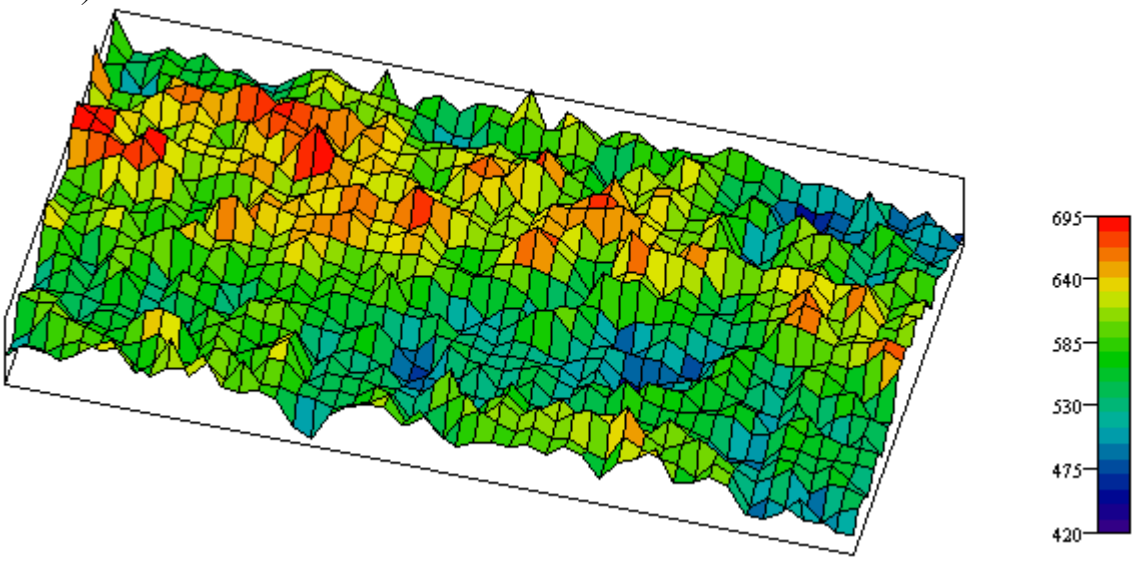

FigureA.8. *Contour plot of density (kg/m^3) of panel m1p2 (window size 50- by 50- mm).*

density	25	76	127	178	229	279	330	381	432	483	533	584	635	686	737	787	838	889	940	991	1041	1092	1143	1194	mm
25	586	576	582	525	561	582	585	573	565	577	574	489	521	586	540	532	580	579	595	634	614	604	604	724	
76	593	556	533	575	562	547	598	580	547	547	525	503	507	537	446	545	563	529	567	640	583	592	613	681	
127	581	530	528	579	569	579	598	519	532	559	531	577	500	525	465	549	556	522	549	654	567	632	647	635	
178	628	513	548	571	581	571	626	585	564	574	562	541	542	560	603	552	566	573	608	599	553	632	615	645	
229	573	544	545	542	582	513	596	542	541	528	507	510	562	582	556	570	517	577	587	584	619	619	606	678	
279	477	562	500	590	557	513	550	517	577	568	533	512	506	605	559	550	550	562	562	614	587	610	586	620	
330	561	523	485	582	623	585	541	540	586	563	555	534	550	578	584	506	516	555	569	585	592	621	577	600	
381	554	550	560	568	566	631	612	549	557	570	563	530	553	595	566	549	573	602	586	567	575	597	614	614	
432	514	503	530	586	580	559	605	532	549	543	606	596	569	613	561	546	563	554	510	579	532	631	580	594	
483	551	580	541	567	591	582	630	560	568	585	591	583	561	620	577	549	490	466	519	519	571	568	623	598	
533	510	508	557	533	591	591	662	617	594	566	601	588	582	613	646	562	535	492	529	594	612	603	604	550	
584	529	501	526	498	573	544	672	597	558	566	503	563	524	559	569	552	534	578	603	583	561	574	591	505	
635	568	571	495	511	530	536	629	567	527	542	560	571	569	602	530	566	537	563	576	574	539	540	573	578	
686	583	554	543	498	533	513	532	534	574	581	589	601	580	614	611	597	552	571	549	566	577	582	558	581	
737	559	542	511	544	532	519	475	517	557	642	578	611	536	562	593	567	539	571	539	574	589	540	564	508	
787	504	539	508	547	522	519	523	567	592	551	582	550	571	579	558	532	502	533	536	546	574	617	531	602	
838	521	545	545	570	562	559	523	553	598	598	587	615	609	602	549	531	518	525	522	583	550	597	583	588	
889	548	522	539	589	504	604	485	613	641	601	626	618	635	578	563	596	581	565	516	537	564	567	676	655	
940	564	541	541	554	574	518	556	591	562	605	581	564	601	603	595	629	612	574	524	556	559	502	630	637	
991	584	601	611	543	556	583	655	569	548	642	650	589	601	630	583	573	584	549	575	561	574	597	596	590	
1041	574	569	559	518	562	597	600	559	594	619	583	600	641	618	559	547	497	525	576	579	525	553	583	594	
1092	566	552	563	555	558	585	600	566	590	602	595	657	588	566	544	525	511	582	573	571	557	572	550	549	
1143	553	535	525	571	585	567	573	605	591	625	602	610	593	590	593	583	533	606	573	526	577	591	566	556	
1194	540	539	519	480	562	532	582	537	537	583	551	602	619	614	626	590	559	590	577	531	533	543	586	606	
1245	549	576	538	509	518	532	546	606	585	551	589	588	602	570	548	525	505	549	566	592	552	553	552	569	
1295	531	514	520	549	542	524	564	566	561	530	653	540	576	604	594	541	534	591	607	563	542	604	553	575	
1346	526	524	527	533	534	533	603	621	577	600	594	568	532	600	599	578	548	570	564	517	505	587	562	560	
1397	525	516	528	576	547	527	576	623	573	581	554	564	587	603	573	572	581	592	544	562	562	606	594	614	
1448	482	559	523	580	506	512	538	571	596	598	616	571	606	585	534	618	599	581	560	541	557	570	610	542	
1499	519	526	510	524	528	528	592	598	620	588	589	578	533	563	501	461	532	567	578	536	578	540	660	610	
1549	485	568	572	547	538	606	578	641	601	623	603	593	548	597	530	518	534	538	523	562	570	581	565	595	
1600	476	581	568	532	565	584	565	586	576	530	603	581	537	618	533	566	545	523	514	580	601	619	547	571	
1651	548	524	529	520	571	567	529	579	638	634	669	573	556	613	604	607	547	543	511	532	529	559	506	571	
1702	514	494	495	511	517	590	573	607	610	585	565	588	562	565	602	533	515	531	506	515	542	603	542	577	
1753	452	526	559	528	517	534	586	599	572	636	528	568	581	532	538	563	523	513	504	562	550	586	554	561	
1803	505	516	543	452	486	541	621	569	563	588	568	568	551	543	531	570	528	505	529	580	521	575	618	570	
1854	509	496	466	454	569	532	517	567	558	536	554	522	555	529	504	546	509	499	478	537	560	575	599	557	
1905	501	512	529	476	523	505	508	517	565	566	566	528	563	503	485	534	502	493	476	555	549	550	588	540	
1956	579	488	544	516	533	552	558	527	582	558	556	538	591	516	498	545	535	523	534	564	553	578	529	545	
2007	553	536	498	530	553	550	568	538	528	546	519	555	552	537	477	512	488	501	534	530	526	603	595	587	
2057	504	517	527	508	550	543	523	520	499	566	555	618	515	519	523	524	515	525	538	556	563	605	573	556	
2108	510	490	523	530	553	544	548	578	560	575	566	494	514	540	576	534	511	515	518	538	609	626	611	597	
2159	555	549	561	558	582	547	578	551	564	576	576	552	543	561	495	516	546	532	539	502	528	550	536	566	
2210	564	525	500	561	612	576	597	560	606	604	580	551	578	576	572	559	574	561	561	572	596	539	535	576	
2261	531	527	527	554	555	539	591	589	619	683	561	546	635	581	565	522	535	538	527	587	582	582	535	519	
2311	510	463	524	513	567	580	611	651	574	666	569	618	594	561	489	523	554	535	562	549	566	574	588	536	
2362	544	507	548	535	534	467	540	547	563	630	579	547	520	545	562	538	583	534	629	588	554	529	566	531	
2413	562	559	547	527	559	583	566	552	558	617	603	590	545	595	644	522	521	540	549	568	574	506	570	516	

mm

Figure A.9. *Data plot of density (kg/m^3) of panel m1p4 (window size 50- by 50-mm)*

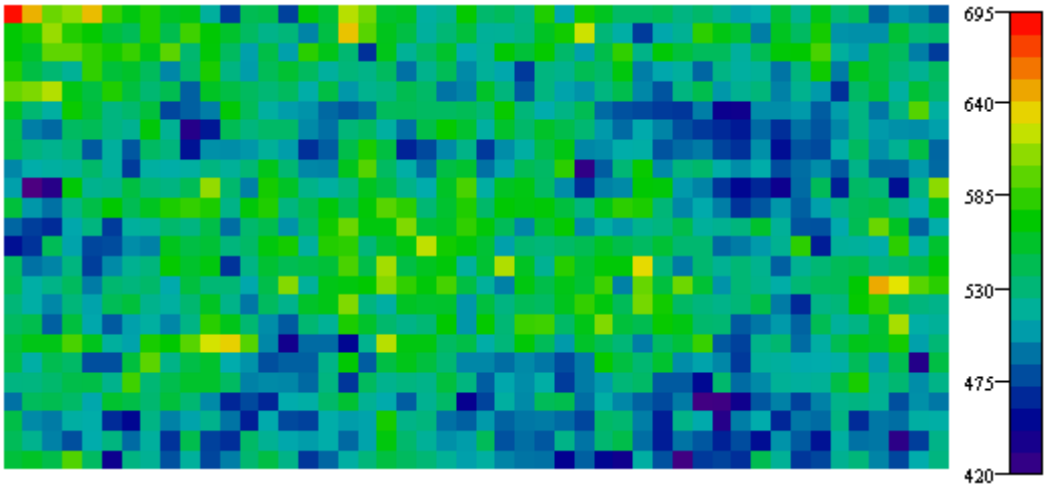

Figure A.10. *Color-scale plot of density (kg/m^3) of panel m1p4 (window size 50- by 50- mm).*

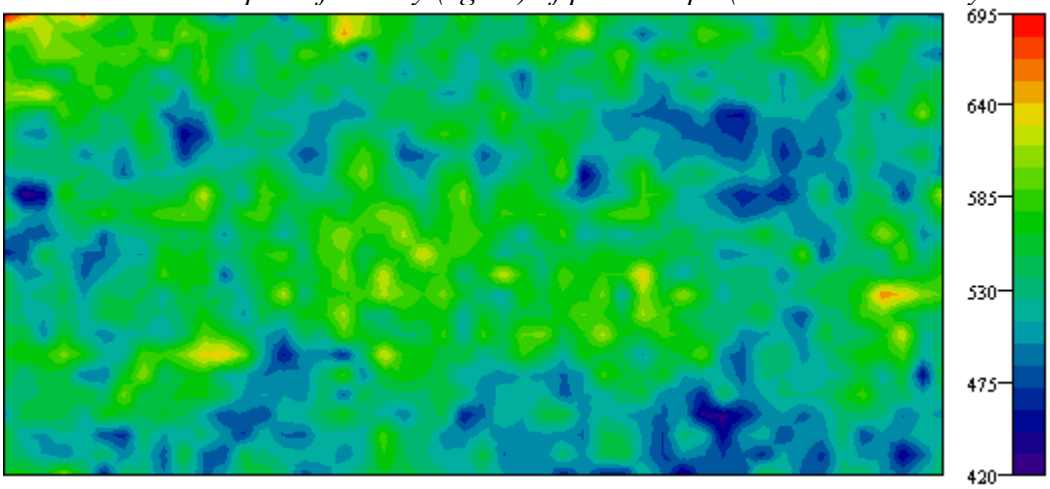

FigureA.11. *Three-dimensional plot of density (kg/m^3) of panel m1p4 (window size 50- by 50- mm).*

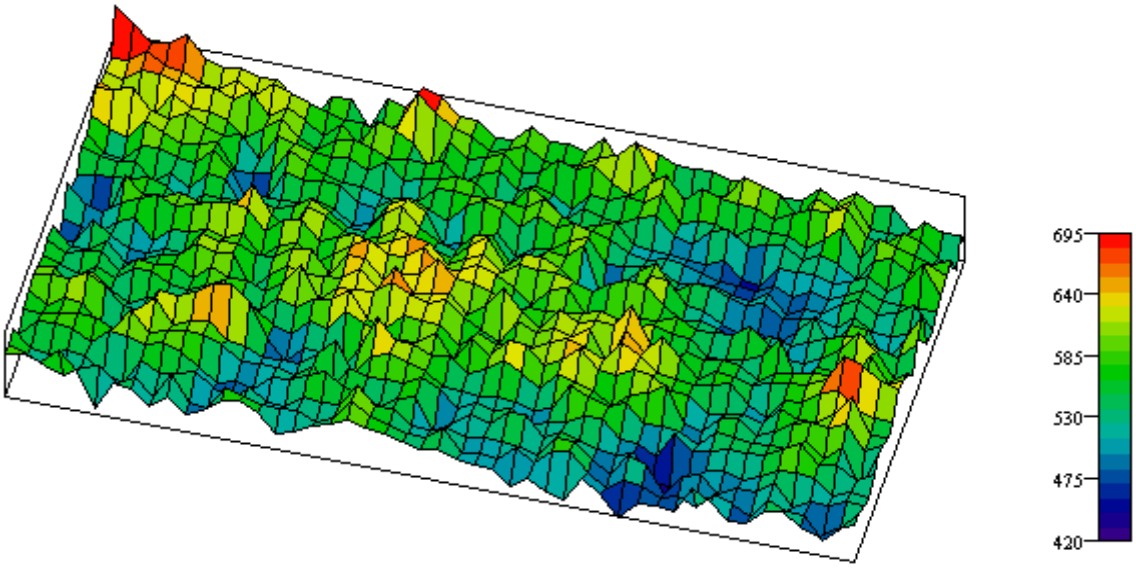

FigureA.12. *Contour plot of density (kg/m^3) of panel m1p4 (window size 50- by 50- mm).*

density	25	76	127	178	229	279	330	381	432	483	533	584	635	686	737	787	838	889	940	991	1041	1092	1143	1194	mm
25	576	576	595	560	606	621	588	547	549	577	581	625	565	556	606	534	541	539	562	578	559	487	603	551	
76	574	574	563	599	610	619	572	536	579	569	600	588	550	628	548	587	571	547	552	560	562	539	555	572	
127	575	544	545	560	610	575	581	570	591	535	579	628	577	621	576	525	568	497	529	533	564	587	547	610	
178	564	551	513	527	605	623	569	581	586	516	566	577	541	609	602	487	615	610	541	526	520	542	575	612	
229	548	543	538	502	514	582	596	552	570	528	593	581	505	586	568	543	561	582	604	584	538	568	603	544	
279	598	526	546	517	494	610	541	558	601	608	602	572	511	459	514	581	566	595	625	626	597	557	616	575	
330	565	530	574	547	496	584	561	623	609	594	592	543	487	498	567	590	579	597	589	607	562	617	587	571	
381	546	544	522	546	533	525	591	635	599	533	533	525	525	501	511	554	614	604	579	522	506	558	575	557	
432	523	540	498	484	514	515	570	596	541	522	557	578	553	559	529	588	603	584	511	507	511	577	608	604	
483	552	570	527	516	530	570	553	554	562	566	549	562	536	561	521	577	576	559	512	533	557	543	611	612	
533	549	527	579	570	568	569	579	550	579	549	540	553	543	592	558	562	575	536	486	514	534	489	571	630	
584	587	548	568	545	610	601	583	602	563	615	615	560	565	582	606	528	549	527	583	593	549	592	601	625	
635	576	531	554	501	567	558	599	619	613	612	566	572	576	579	601	596	575	560	570	588	581	617	560	589	
686	547	615	574	557	603	568	598	654	552	604	540	533	535	534	552	548	532	490	522	523	517	593	566	609	
737	592	594	577	596	595	557	629	628	600	593	537	518	543	551	557	553	520	494	523	500	543	529	558	553	
787	580	565	564	600	576	556	565	638	603	614	539	467	495	500	521	514	494	529	528	515	519	532	574	597	
838	550	574	599	528	556	582	620	593	522	577	590	557	553	516	547	531	552	547	601	615	551	542	571	618	
889	538	591	552	504	562	552	586	620	543	602	579	513	568	561	583	579	586	573	520	578	563	534	543	538	
940	538	537	574	511	617	571	617	597	598	565	567	551	551	574	566	541	535	526	518	591	559	533	560	546	
991	485	531	606	557	614	555	595	558	567	552	578	570	540	615	566	546	542	505	510	536	563	563	575	517	
1041	543	547	530	526	612	583	560	566	568	539	506	574	512	609	574	502	560	512	520	550	544	513	519	574	
1092	590	574	543	552	585	540	582	511	550	539	549	576	630	554	530	519	514	550	566	561	540	560	532	549	
1143	582	561	554	569	555	519	588	578	526	541	556	567	604	520	552	540	556	561	615	481	537	536	572	606	
1194	553	525	519	520	529	541	574	518	512	520	558	575	524	541	521	531	515	563	612	541	575	571	598	583	
1245	524	574	512	574	529	537	526	536	554	522	554	559	533	515	504	526	550	560	540	600	499	529	521	510	
1295	529	562	578	569	560	540	533	505	597	577	562	542	559	546	508	501	550	530	527	556	499	498	577	527	
1346	573	545	525	526	536	530	501	541	555	549	603	527	546	514	521	449	491	505	525	551	588	595	550	597	
1397	513	487	549	461	452	587	524	563	540	545	561	510	537	550	561	476	423	552	527	555	537	531	593	615	
1448	618	525	504	539	516	535	532	572	523	523	506	495	497	539	560	527	451	517	562	524	501	599	568	589	
1499	560	546	526	566	572	501	548	593	559	551	528	487	555	575	548	545	495	513	531	540	567	586	556	597	
1549	572	556	545	530	547	546	585	597	596	537	531	516	552	559	593	584	599	545	519	513	526	563	547	603	
1600	572	529	515	480	541	524	569	605	555	558	559	561	540	560	575	554	541	486	529	563	528	553	564	619	
1651	608	542	571	539	566	589	636	580	517	546	584	508	511	504	562	502	520	524	548	542	545	497	549	584	
1702	591	574	529	588	529	583	613	574	496	517	564	552	505	519	524	524	511	535	567	570	541	560	556	573	
1753	602	567	518	551	508	609	581	541	502	524	532	522	561	619	506	516	538	518	504	508	524	592	517	567	
1803	620	548	572	518	515	564	573	530	561	555	548	555	558	536	497	537	533	512	504	519	536	564	606	553	
1854	568	539	517	487	522	579	535	522	575	610	592	539	529	534	484	507	487	507	524	588	544	527	533	561	
1905	509	524	530	502	471	538	527	533	557	574	522	556	498	560	545	454	479	503	507	584	518	559	544	538	
1956	523	546	587	523	563	542	549	531	521	563	612	587	557	546	559	518	495	504	559	568	496	536	553	519	
2007	521	548	590	559	539	584	531	579	545	557	580	568	563	567	531	490	513	543	551	542	461	511	530	543	
2057	556	496	543	562	606	567	574	561	540	614	546	612	556	561	535	544	557	584	598	573	462	537	582	588	
2108	640	566	504	567	642	584	621	522	496	545	556	597	564	552	508	524	496	537	525	496	497	560	569	595	
2159	611	550	530	568	611	588	617	538	524	553	553	545	551	526	526	532	546	522	489	500	552	515	565	578	
2210	589	550	532	491	508	513	577	531	506	558	497	540	535	514	565	570	549	547	471	524	560	533	565	571	
2261	607	538	574	577	519	549	577	565	550	548	527	571	554	504	538	543	529	492	478	526	541	497	566	563	
2311	555	522	567	572	525	566	574	551	551	524	555	506	553	487	529	503	489	533	523	548	553	532	543	511	
2362	514	590	580	624	573	540	581	571	536	514	537	516	518	570	518	511	528	538	483	511	605	535	522	526	
2413	575	588	622	601	548	546	581	597	605	547	592	592	589	580	530	530	543	572	520	536	530	546	513	482	

mm

Figure A.13. *Data plot of density (kg/m^3) of panel m1p5 (window size 50- by 50-mm)*

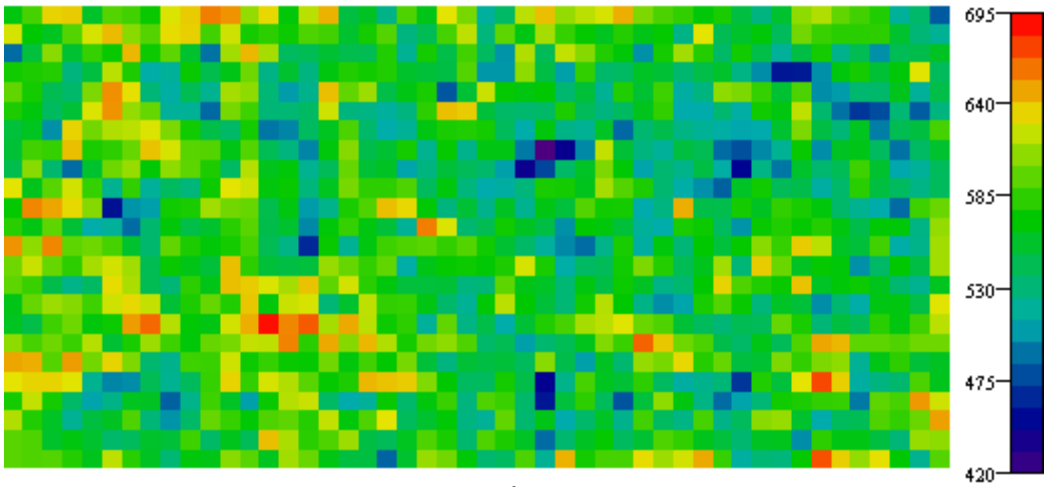

Figure A.14. *Color-scale plot of density (kg/m^3) of panel m1p5 (window size 50- by 50- mm).*

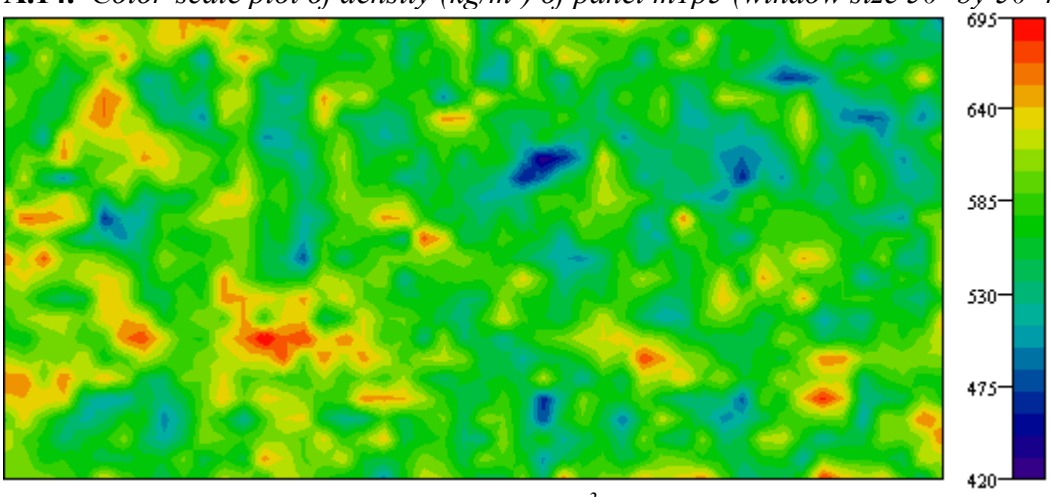

FigureA.15. *Three-dimensional plot of density (kg/m^3) of panel m1p5 (window size 50- by 50- mm).*

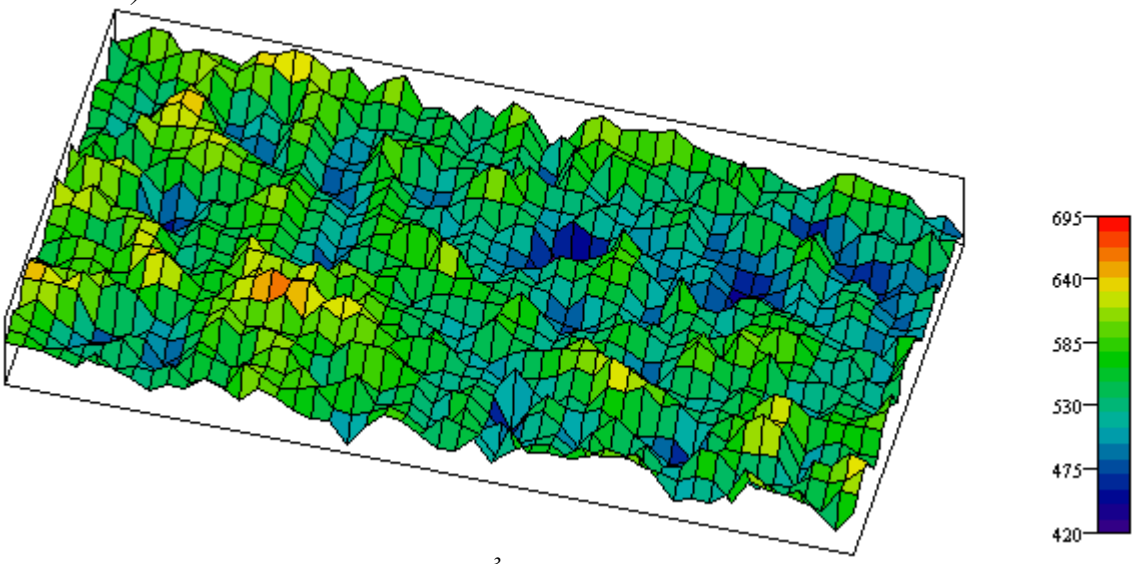

FigureA.16. *Contour plot of density (kg/m^3) of panel m1p5 (window size 50- by 50- mm).*

density	25	76	127	178	229	279	330	381	432	483	533	584	635	686	737	787	838	889	940	991	1041	1092	1143	1194	mm
25	529	606	577	551	552	534	530	592	648	604	535	571	610	514	553	560	530	549	531	569	521	508	572	596	
76	532	571	561	521	603	611	597	530	616	560	571	540	529	540	583	581	534	534	504	541	535	562	612	577	
127	519	571	563	519	616	562	612	604	592	573	608	556	542	567	582	581	517	484	563	532	534	547	592	592	
178	589	639	549	566	676	565	648	612	628	589	582	519	546	546	559	585	554	531	537	554	562	611	577	564	
229	602	605	565	627	611	586	573	617	597	620	578	564	545	512	529	541	523	550	535	588	567	567	545	539	
279	553	561	552	561	572	589	603	616	593	583	598	515	504	511	518	530	524	516	503	604	574	548	577	623	
330	531	525	528	552	556	562	627	608	558	531	585	573	551	544	576	517	542	573	542	604	568	591	589	652	
381	526	515	512	530	519	550	589	544	523	496	592	620	606	563	573	561	560	555	541	599	533	543	538	601	
432	577	572	560	539	557	557	521	483	424	442	581	622	571	564	592	570	528	499	555	519	562	552	605	564	
483	563	559	546	536	549	532	569	524	455	477	606	618	584	599	599	560	546	533	509	534	546	574	637	603	
533	563	569	506	533	600	595	562	544	501	510	532	574	614	672	628	564	530	574	571	547	547	638	620	604	
584	576	516	534	509	619	584	622	586	537	544	527	552	581	592	579	581	532	508	521	515	554	624	598	589	
635	498	511	499	522	610	518	597	596	588	603	543	562	600	605	602	557	561	579	539	522	564	597	586	607	
686	523	515	547	568	574	517	558	635	571	566	550	543	590	613	593	567	611	588	548	539	547	591	544	539	
737	483	525	556	577	574	567	544	562	528	490	532	531	591	562	554	535	548	574	599	544	522	565	538	585	
787	547	515	515	586	556	562	524	539	567	494	537	486	535	532	558	505	565	541	531	566	542	579	538	521	
838	574	508	590	596	630	557	533	539	530	533	560	516	538	524	547	513	492	504	520	543	567	518	530	546	
889	559	513	588	519	504	522	518	496	534	523	552	513	514	521	585	541	498	558	555	538	468	459	460	587	
940	583	564	579	543	531	534	567	521	504	508	490	495	524	525	524	534	494	526	554	567	589	544	540	596	
991	570	529	530	475	518	526	492	499	493	540	504	497	532	543	510	502	517	542	516	588	545	521	550	545	
1041	554	457	432	473	472	516	498	536	539	512	533	499	562	537	554	529	492	498	504	572	526	488	508	531	
1092	578	478	505	552	589	594	493	525	568	520	494	527	515	466	549	555	496	515	538	529	533	498	537	536	
1143	551	525	462	490	533	547	557	505	535	585	535	551	557	497	519	539	546	498	482	584	567	528	521	576	
1194	557	504	503	604	593	531	543	513	503	574	526	552	567	493	502	527	592	522	518	577	530	561	520	512	
1245	527	507	507	547	544	492	555	572	516	616	615	594	534	505	575	523	528	493	484	573	566	562	570	548	
1295	500	510	538	510	504	524	544	539	504	503	600	595	525	545	572	531	560	544	615	545	531	537	542	588	
1346	493	495	523	487	506	527	546	505	492	506	516	568	521	555	541	535	542	554	572	568	560	605	569	615	
1397	554	588	481	501	502	507	556	556	515	515	523	607	583	540	482	560	569	544	520	491	586	621	543	577	
1448	527	520	495	461	479	528	571	590	523	555	579	575	552	528	479	525	549	507	520	515	605	565	576	603	
1499	576	562	566	509	509	580	604	583	542	586	577	499	503	505	514	505	534	552	524	578	559	576	596	567	
1549	541	518	554	517	491	573	633	584	575	636	592	564	609	509	511	509	513	562	559	538	526	511	579	594	
1600	514	529	516	524	535	532	558	574	540	589	554	513	535	532	550	531	511	572	504	488	608	562	630	628	
1651	574	526	532	554	560	536	539	499	551	602	562	487	569	552	543	520	511	541	519	507	593	597	629	546	
1702	572	478	507	527	601	575	567	593	537	537	552	551	584	534	565	473	473	505	557	582	525	570	624	570	
1753	471	594	510	503	604	577	554	612	595	556	581	584	530	533	506	494	450	505	512	554	531	583	610	593	
1803	496	528	510	495	556	500	574	600	571	599	555	591	585	587	543	515	500	494	509	538	578	533	650	651	
1854	499	517	522	566	548	519	548	585	575	630	544	550	545	552	564	516	559	486	536	569	562	582	575	564	
1905	587	589	544	544	569	548	517	542	608	564	550	571	548	562	596	549	585	538	536	511	505	603	583	507	
1956	531	532	553	534	548	569	544	578	615	584	562	605	544	581	604	543	512	549	530	531	530	578	580	610	
2007	543	541	528	539	550	608	547	581	572	581	565	582	543	540	550	512	521	536	545	471	516	554	586	611	
2057	563	539	558	618	500	589	566	535	549	573	545	629	548	534	546	565	522	529	522	459	506	522	560	601	
2108	541	512	568	586	560	562	577	543	572	569	517	614	550	587	554	578	537	505	548	478	473	556	566	574	
2159	575	521	519	554	562	568	600	533	570	574	599	581	518	559	561	508	457	494	462	509	506	534	563	572	
2210	572	601	517	543	544	542	604	630	580	560	549	588	549	588	589	482	435	578	526	558	526	563	561	528	
2261	535	539	544	537	527	621	638	602	635	635	552	500	560	609	647	542	564	594	557	559	489	562	544	535	
2311	543	558	571	558	574	615	635	573	601	613	538	590	611	614	569	561	555	528	555	539	544	499	545	590	
2362	465	579	559	547	600	601	563	569	595	621	591	581	595	600	530	503	562	556	546	502	543	535	578	609	
2413	483	556	540	595	592	625	561	585	599	615	620	598	618	600	562	588	560	594	572	577	524	544	585	606	
mm																									

Figure A.17. *Data plot of density (kg/m^3) of panel m1p5 (window size 50- by 50-mm)*

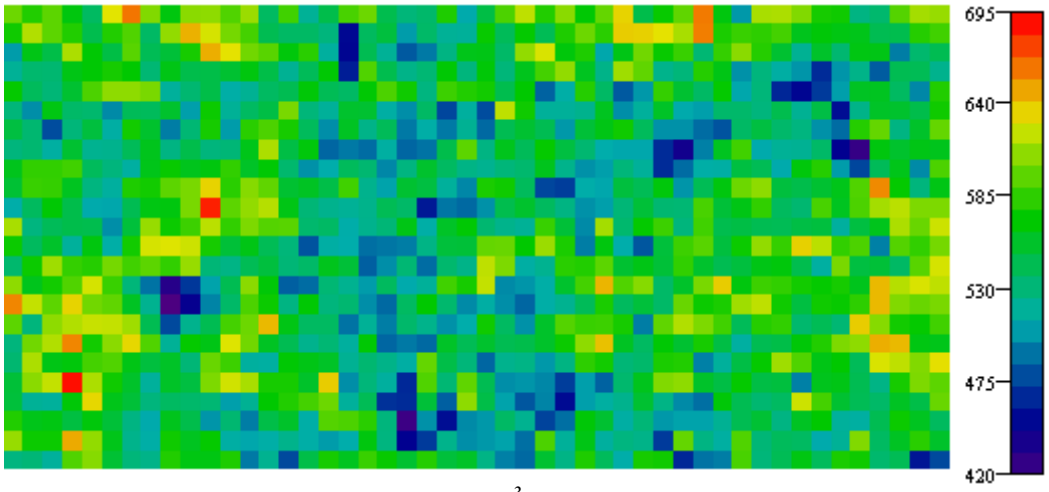

Figure A.18. *Color-scale plot of density (kg/m^3) of panel m1p5 (window size 50- by 50- mm).*

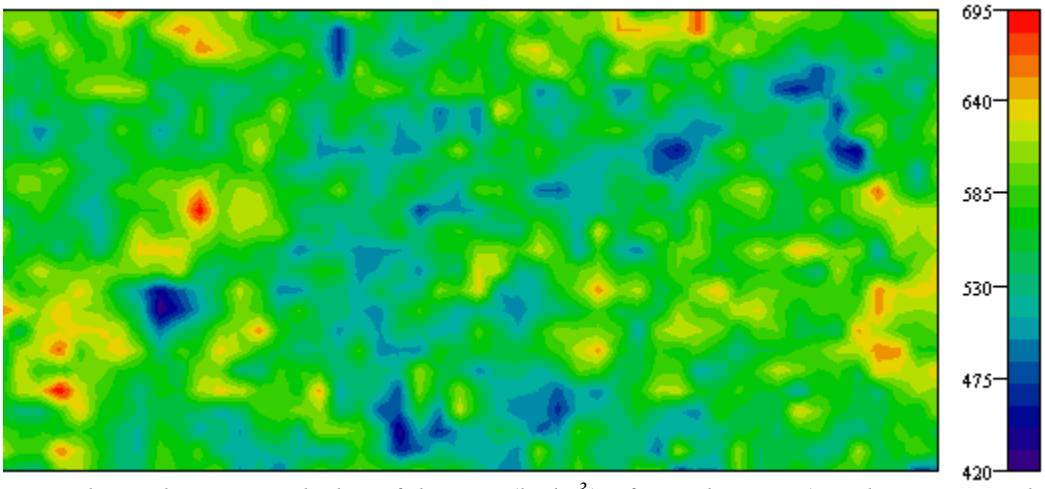

FigureA.19. *Three-dimensional plot of density (kg/m^3) of panel m1p5 (window size 50- by 50- mm).*

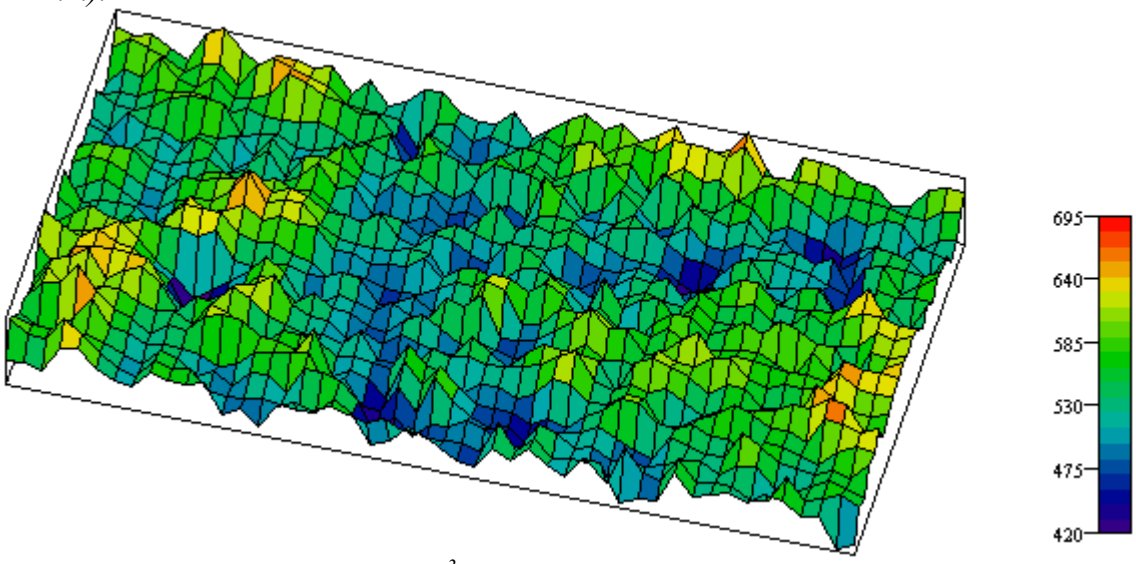

FigureA.20. *Contour plot of density (kg/m^3) of panel m1p5 (window size 50- by 50- mm).*

density	25	76	127	178	229	279	330	381	432	483	533	584	635	686	737	787	838	889	940	991	1041	1092	1143	1194	mm
25	580	546	530	588	543	544	543	570	574	625	576	601	579	589	613	600	601	648	606	570	511	616	539	590	
76	591	568	545	536	576	570	531	577	593	564	570	585	569	565	544	640	629	599	582	539	556	540	575	579	
127	555	521	527	535	592	599	517	535	497	486	560	524	602	588	612	632	593	660	579	571	568	566	542	536	
178	542	478	581	573	545	612	516	516	566	504	599	598	587	616	632	639	588	639	578	546	547	490	544	548	
229	537	522	552	584	566	524	554	485	488	557	554	546	554	577	651	584	578	557	557	548	511	508	546	632	
279	466	559	528	575	519	530	552	539	475	539	507	569	578	582	615	588	549	556	560	519	523	571	583	621	
330	549	531	525	575	523	529	515	549	527	500	487	543	546	579	557	603	577	555	578	537	490	529	559	602	
381	559	523	546	506	541	536	533	482	508	508	522	520	526	561	570	615	570	557	519	622	547	545	582	622	
432	624	524	537	548	533	601	619	470	495	532	513	527	572	562	575	594	573	595	561	550	522	515	539	540	
483	554	542	535	538	532	538	548	520	503	521	507	565	614	607	541	544	560	553	549	551	544	603	551	558	
533	520	522	542	575	532	527	554	546	531	547	526	559	548	569	619	597	569	581	570	631	572	596	562	549	
584	556	547	583	524	535	543	535	537	516	516	486	582	552	575	629	550	549	608	585	559	569	586	560	585	
635	538	600	597	515	522	561	559	498	544	577	528	491	493	553	585	529	547	565	537	558	568	589	543	551	
686	556	585	616	640	543	540	531	555	523	582	534	506	443	538	593	565	596	566	558	586	516	610	560	589	
737	562	516	526	579	574	577	585	566	595	564	563	566	485	547	598	581	534	593	590	590	581	564	546	586	
787	553	456	549	544	559	595	581	567	583	529	530	547	519	523	570	582	559	578	522	540	575	572	656	650	
838	510	506	531	549	567	570	579	522	536	556	540	528	554	540	546	603	548	588	598	598	575	537	598	594	
889	493	480	578	573	510	528	576	511	557	562	505	495	524	505	571	605	546	636	605	556	565	552	523	569	
940	533	545	580	558	531	582	579	540	559	547	535	509	547	539	587	576	543	621	581	608	608	556	611	633	
991	518	553	578	560	526	562	589	558	526	513	547	526	524	542	555	566	573	546	562	578	582	551	611	618	
1041	542	561	541	558	516	560	520	588	545	577	521	551	566	575	586	622	616	587	596	565	608	581	552	574	
1092	578	560	560	557	524	531	569	563	593	562	566	581	578	581	528	597	617	650	564	557	524	592	589	584	
1143	601	565	559	560	559	533	584	476	599	580	506	589	553	500	495	562	596	608	586	587	552	607	624	583	
1194	583	569	591	602	541	605	600	487	556	579	571	535	566	575	608	560	605	609	577	598	598	618	550	626	
1245	567	584	620	589	585	627	601	554	619	540	549	529	606	597	600	510	542	588	548	578	597	596	571	654	
1295	548	569	579	537	542	611	591	574	615	566	558	580	544	566	579	574	590	562	527	604	561	540	553	587	
1346	577	578	577	510	566	610	637	580	587	571	517	551	549	565	558	588	576	637	593	605	600	609	568	614	
1397	592	567	548	543	533	597	578	554	552	541	509	548	561	611	594	581	589	582	603	567	589	601	541	589	
1448	590	561	536	581	546	587	518	551	536	519	500	541	547	572	617	581	633	611	599	575	545	548	618	550	
1499	538	587	607	571	584	535	538	579	581	530	454	552	602	604	599	568	666	601	573	556	527	570	586	598	
1549	539	528	562	506	554	563	582	586	563	515	510	548	534	549	553	577	596	561	544	578	548	557	619	537	
1600	532	548	573	596	580	543	573	577	587	556	507	538	590	576	592	537	605	560	644	575	572	580	626	567	
1651	570	552	575	542	541	567	582	567	591	576	512	549	535	538	575	591	578	615	593	606	596	594	547	568	
1702	530	556	555	527	565	579	570	559	543	621	544	501	556	584	594	622	562	616	595	615	590	562	551	577	
1753	574	572	580	550	536	518	538	557	561	596	563	570	565	584	654	668	597	601	556	557	566	507	540	552	
1803	592	583	573	588	600	540	565	598	586	554	541	501	603	624	633	567	580	622	577	562	550	523	536	581	
1854	547	562	572	587	582	590	517	563	566	530	586	563	577	592	578	550	567	563	577	570	527	520	557	584	
1905	549	513	591	530	584	602	565	573	543	553	578	631	575	591	565	560	571	607	570	592	501	495	552	609	
1956	574	550	605	564	548	583	602	556	543	594	597	608	617	529	561	581	555	554	555	520	487	488	503	539	
2007	567	540	578	574	577	553	592	516	531	522	585	581	567	549	568	572	605	557	575	523	488	493	541	529	
2057	616	536	599	559	586	589	588	536	562	585	590	529	498	554	591	632	642	566	555	575	568	517	513	578	
2108	568	494	569	599	602	598	590	571	569	575	507	533	571	585	558	588	608	662	632	588	505	519	525	537	
2159	562	559	608	616	626	575	533	550	615	566	563	568	607	591	618	557	631	628	491	608	503	532	544	564	
2210	594	553	551	564	579	552	625	534	555	578	521	571	595	592	559	535	611	602	560	587	518	512	528	548	
2261	598	587	581	575	593	599	630	552	569	569	583	573	588	604	569	536	549	521	538	579	518	489	500	543	
2311	610	593	621	547	565	581	595	554	527	551	573	540	580	555	570	557	567	585	533	505	526	537	494	542	
2362	550	503	566	544	535	561	581	601	542	537	532	531	600	569	560	575	583	627	546	535	491	513	485	574	
2413	553	554	535	545	557	615	602	597	571	551	615	513	532	560	579	566	615	590	539	525	536	541	521	528	

mm

Figure A.21. *Data plot of density (kg/m^3) of panel m2p1 (window size 50- by 50-mm)*

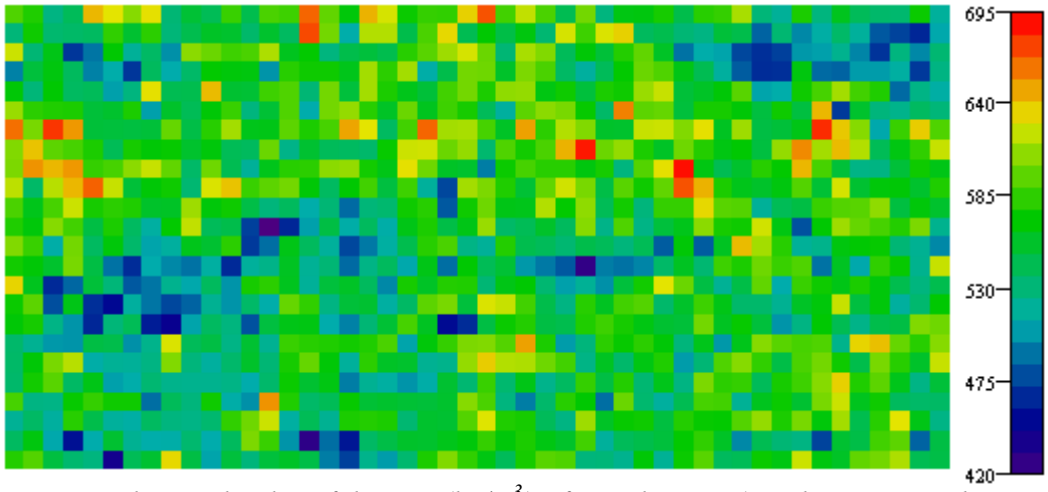

Figure A.22. *Color-scale plot of density (kg/m^3) of panel m2p1 (window size 50- by 50- mm).*

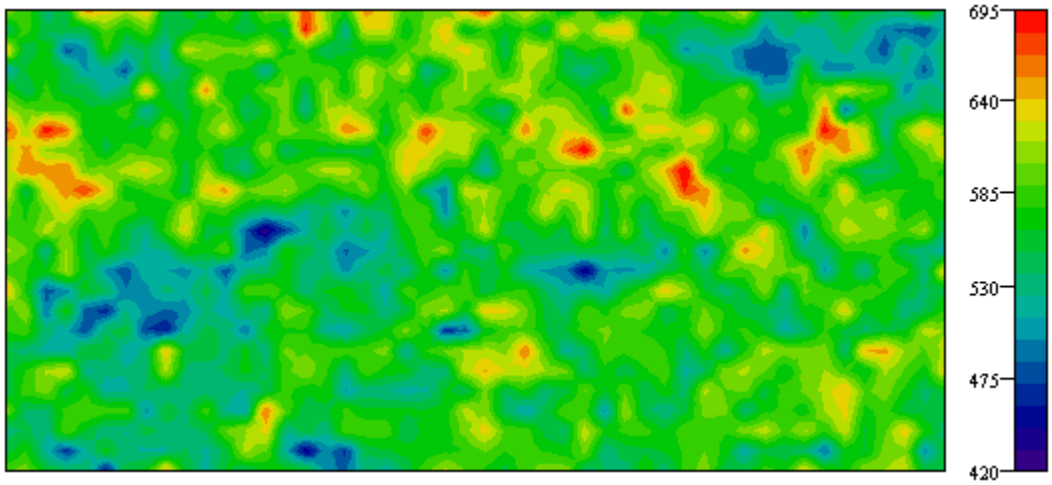

FigureA.23. *Three-dimensional plot of density (kg/m^3) of panel m2p1 (window size 50- by 50- mm).*

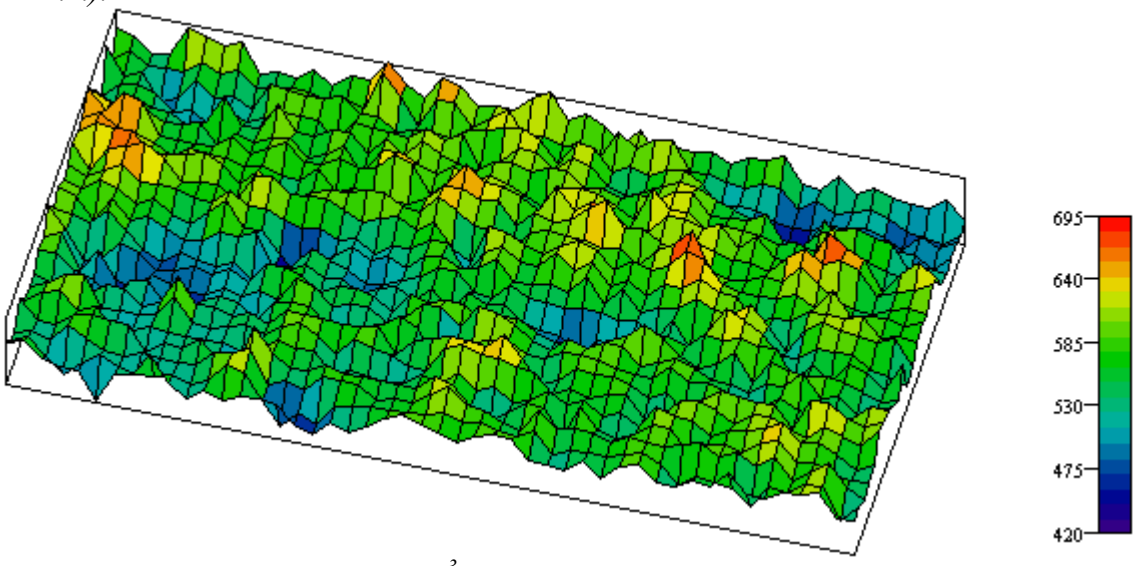

FigureA.24. *Contour plot of density (kg/m^3) of panel m2p1 (window size 50- by 50- mm).*

density	25	76	127	178	229	279	330	381	432	483	533	584	635	686	737	787	838	889	940	991	1041	1092	1143	1194	mm
25	511	526	592	611	569	614	586	587	552	571	552	563	590	610	635	657	589	584	550	610	542	489	540	537	
76	518	589	624	566	533	596	551	605	603	538	560	513	606	548	538	645	625	507	478	624	635	573	538	531	
127	514	554	577	533	579	596	578	550	579	557	591	575	602	605	516	592	631	618	544	655	638	611	576	559	
178	535	614	630	615	562	622	611	547	531	578	579	591	621	601	567	571	590	610	594	600	513	587	608	584	
229	511	590	591	596	540	571	560	557	521	607	592	593	618	617	581	610	619	579	552	614	579	634	676	598	
279	509	570	546	619	542	565	547	569	564	570	649	570	589	599	617	650	584	579	577	591	577	538	611	594	
330	475	540	546	604	566	576	584	596	591	512	572	592	600	645	659	564	569	600	629	605	623	533	560	587	
381	530	536	538	597	555	550	538	587	550	500	495	539	635	603	570	525	549	587	587	644	601	580	528	575	
432	566	598	614	591	616	586	597	578	584	513	529	578	601	629	594	643	577	610	644	629	580	504	555	473	
483	494	550	578	617	616	616	598	590	628	551	546	562	599	589	553	602	624	565	539	567	547	573	582	457	
533	484	553	555	545	633	565	594	565	585	560	528	556	572	547	532	554	540	531	566	598	580	575	569	552	
584	485	554	582	487	573	612	635	616	538	515	543	538	555	544	567	530	539	569	563	567	569	616	600	616	
635	545	545	592	576	562	608	604	557	560	550	575	561	596	577	577	588	596	630	619	580	565	541	548	598	
686	521	568	580	579	605	635	597	572	579	532	550	541	664	612	546	619	588	666	575	527	506	573	516	573	
737	552	593	573	533	589	613	592	605	573	514	531	550	576	612	541	616	616	617	586	582	515	521	517	512	
787	594	583	630	586	576	550	637	638	589	554	621	592	577	597	576	550	641	648	545	557	511	507	527	575	
838	567	554	567	594	522	510	600	586	501	514	547	587	615	566	571	606	612	602	573	591	613	527	529	523	
889	529	563	531	560	560	555	587	583	565	570	605	609	596	495	558	588	558	598	626	532	573	528	573	535	
940	562	607	622	637	633	604	577	532	514	568	610	620	603	530	527	563	587	589	589	573	519	528	541	602	
991	564	589	619	628	581	566	616	587	565	603	598	568	596	538	515	562	606	562	567	579	557	536	548	557	
1041	564	578	636	555	571	562	562	546	600	627	579	610	594	554	611	579	540	584	528	587	489	565	591	602	
1092	620	555	570	571	549	542	569	565	541	599	559	582	616	577	626	567	556	530	519	484	546	547	562	566	
1143	559	565	555	630	609	582	588	604	503	592	514	542	601	575	621	550	570	586	494	498	531	549	561	599	
1194	566	503	566	586	528	539	568	605	543	548	524	569	590	626	651	616	582	555	536	569	564	586	570	542	
1245	529	493	523	548	524	559	591	559	542	553	526	515	531	581	594	574	613	556	541	583	569	529	553	542	
1295	551	546	502	467	485	567	575	546	550	543	541	518	580	555	576	553	566	561	576	523	535	522	532	556	
1346	561	466	538	501	527	579	564	561	537	559	587	566	547	547	613	636	586	615	626	558	554	575	576	613	
1397	543	522	556	529	552	578	575	576	546	541	516	522	515	587	639	595	588	590	597	590	600	578	551	599	
1448	538	563	577	566	549	557	591	572	536	527	515	559	596	553	583	550	619	619	546	578	582	519	519	528	
1499	546	577	553	549	523	547	599	523	506	547	523	551	565	573	588	599	575	558	575	560	562	452	482	519	
1549	568	601	549	542	508	541	569	580	602	561	534	522	559	539	595	615	528	565	628	556	485	504	516	554	
1600	572	533	534	519	537	519	550	575	567	595	555	570	576	583	573	572	551	550	622	559	513	506	524	582	
1651	531	564	574	556	528	617	619	609	591	630	561	541	532	528	617	581	572	540	555	527	497	517	525	520	
1702	537	583	609	582	512	542	540	589	560	599	520	597	583	570	597	532	568	583	506	508	509	484	546	532	
1753	563	594	611	579	533	528	519	549	552	525	502	548	555	571	490	547	555	548	512	573	550	536	549	542	
1803	591	591	572	565	557	558	543	555	544	474	534	550	586	557	560	554	591	612	563	578	547	523	500	550	
1854	557	573	551	587	593	622	561	551	524	537	525	553	567	534	569	528	554	574	546	526	485	530	524	572	
1905	542	534	562	609	596	573	576	550	541	582	514	503	565	546	521	515	557	526	530	557	514	463	518	589	
1956	576	544	533	581	585	568	565	504	537	562	484	529	583	599	547	523	483	524	509	528	463	424	516	573	
2007	538	614	552	511	561	508	547	558	549	554	552	514	508	569	566	553	574	571	553	557	521	487	536	529	
2057	520	540	607	514	555	564	555	504	540	566	539	506	541	528	574	604	512	552	589	535	504	500	531	526	
2108	585	589	535	595	591	587	539	540	552	543	521	540	558	539	560	541	512	550	548	537	509	545	512	513	
2159	579	581	579	562	524	578	561	561	523	502	542	597	567	558	507	582	506	546	557	515	498	524	552	504	
2210	592	580	527	559	558	544	566	554	523	544	532	513	566	565	550	543	501	543	540	515	487	480	520	508	
2261	580	527	528	596	572	557	532	516	510	541	543	541	572	551	619	570	560	554	546	490	497	510	511	478	
2311	592	553	541	552	508	544	542	562	502	535	555	564	547	554	560	517	534	535	491	500	522	494	580	542	
2362	607	586	568	571	502	547	502	524	536	536	589	564	555	548	527	531	566	572	498	510	506	518	502	505	
2413	666	546	574	562	514	525	529	567	564	571	599	592	625	592	579	559	553	549	539	535	504	513	527	509	

mm

Figure A.25. *Data plot of density (kg/m^3) of panel m2p2 (window size 50- by 50-mm)*

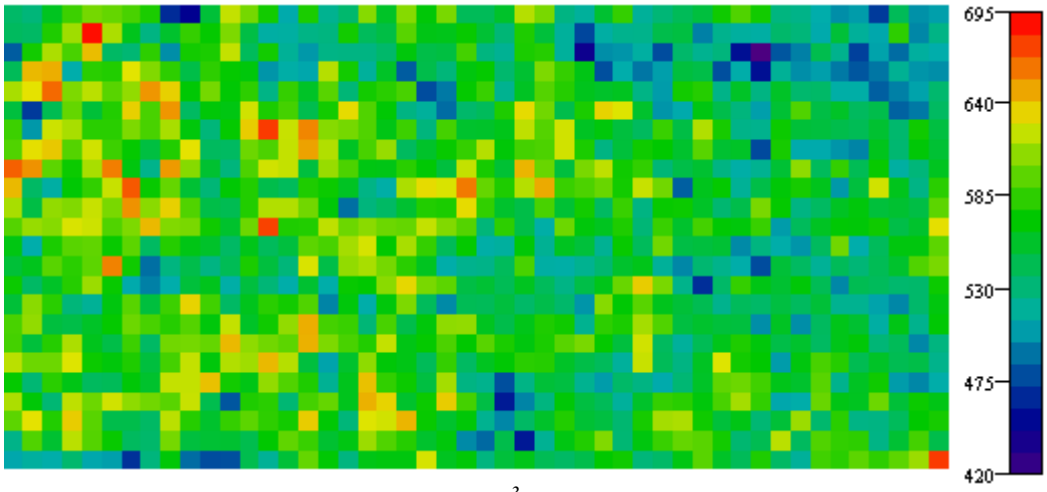

Figure A.26. *Color-scale plot of density (kg/m^3) of panel m2p2 (window size 50- by 50- mm).*

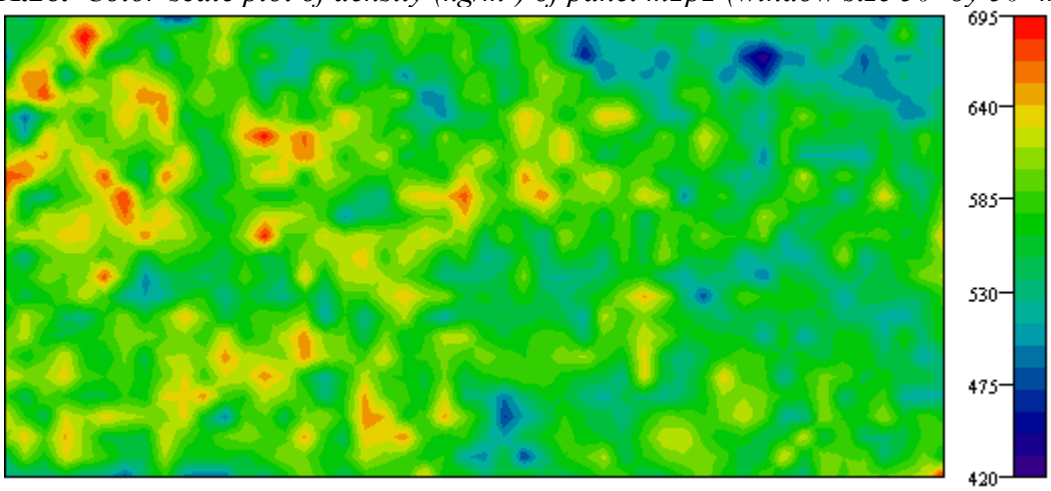

FigureA.27. *Three-dimensional plot of density (kg/m^3) of panel m2p2 (window size 50- by 50- mm).*

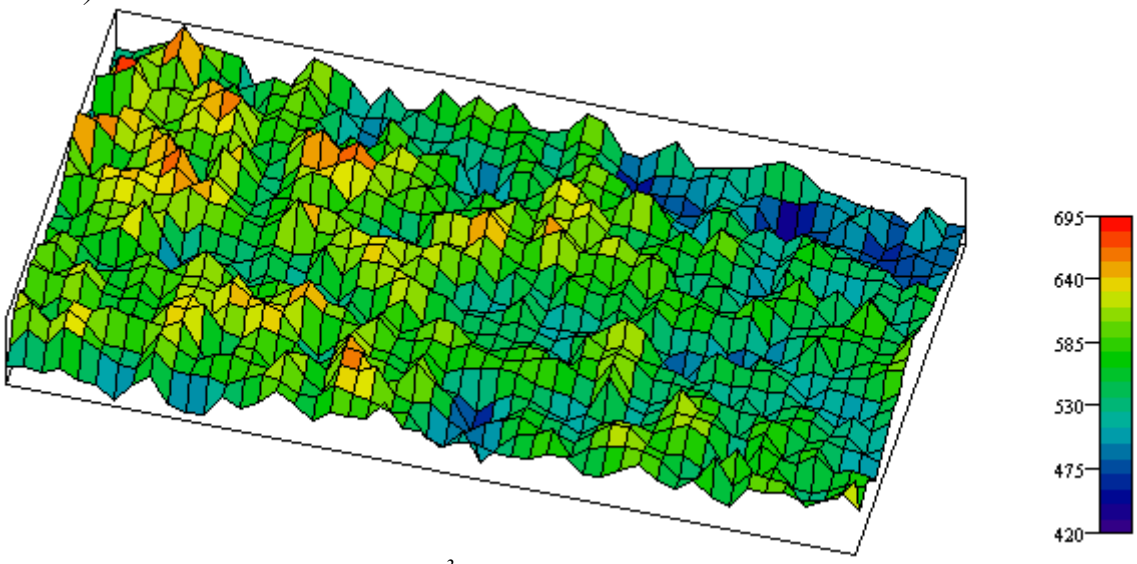

FigureA.28. *Contour plot of density (kg/m^3) of panel m2p2 (window size 50- by 50- mm).*

density	25	76	127	178	229	279	330	381	432	483	533	584	635	686	737	787	838	889	940	991	1041	1092	1143	1194	mm
25	623	576	585	593	558	503	555	547	558	560	566	595	637	562	574	554	561	556	561	556	579	569	552	561	
76	619	554	607	556	582	564	581	462	600	565	561	553	540	662	608	557	584	532	581	491	523	545	554	567	
127	608	615	617	577	587	576	592	473	530	538	586	554	569	645	575	637	603	564	564	562	491	522	552	540	
178	614	616	621	577	543	540	551	562	571	552	615	575	601	584	585	603	517	534	576	570	480	518	554	582	
229	571	598	589	554	547	537	561	554	484	503	561	565	613	578	565	511	520	549	590	642	495	461	524	546	
279	566	553	540	574	514	501	522	550	514	523	537	598	572	596	541	577	531	564	603	608	499	543	554	602	
330	594	550	569	640	585	548	533	502	518	546	545	529	589	582	547	574	551	574	593	591	541	585	573	638	
381	549	599	565	561	554	524	500	548	500	541	597	549	589	590	667	556	552	568	559	579	477	532	573	615	
432	527	575	556	535	547	535	574	529	515	514	552	520	584	564	688	577	581	553	588	530	508	551	570	537	
483	591	545	513	526	586	568	593	574	575	537	507	568	517	553	594	574	565	575	610	564	499	557	517	519	
533	586	638	538	518	561	536	554	504	569	507	573	568	543	558	616	618	538	584	571	535	557	517	552	543	
584	622	596	582	549	590	573	588	526	580	538	587	539	564	576	641	631	603	565	522	571	610	541	581	629	
635	533	541	580	559	549	563	545	572	562	517	589	597	602	599	592	605	590	590	545	574	679	592	594	614	
686	538	546	547	562	520	571	571	598	558	520	578	611	611	607	591	641	566	555	552	600	559	563	620	549	
737	520	547	551	566	566	563	548	536	546	496	583	589	588	594	579	611	555	527	548	593	515	572	630	537	
787	578	580	516	533	536	593	538	561	545	558	626	585	569	576	585	634	593	583	527	550	609	573	565	497	
838	546	576	561	548	555	605	552	563	577	608	629	590	554	540	561	625	593	581	606	557	594	538	587	582	
889	554	539	554	532	571	604	577	544	586	602	553	551	568	581	582	592	612	605	647	584	600	583	577	564	
940	555	549	575	573	554	616	582	560	526	532	570	546	596	648	589	535	542	568	556	589	635	576	580	604	
991	545	550	575	556	552	558	571	540	539	463	567	618	571	596	576	598	559	592	581	578	568	605	568	600	
1041	570	574	596	547	573	586	567	577	522	528	594	567	562	561	628	553	506	581	548	569	568	620	580	588	
1092	584	561	549	588	556	563	571	563	535	527	548	536	553	568	567	558	547	589	590	599	613	582	536	573	
1143	564	591	559	592	542	517	625	560	573	552	505	499	538	543	568	594	532	553	533	548	589	579	518	568	
1194	581	572	564	550	581	540	577	515	570	612	509	522	515	533	571	514	516	523	565	554	562	538	548	556	
1245	569	567	606	578	611	606	564	542	538	503	544	491	559	527	483	548	551	540	546	578	632	554	517	558	
1295	594	538	510	525	581	586	606	543	542	546	581	560	626	563	513	556	546	477	555	550	589	509	558	563	
1346	589	557	543	548	607	599	578	520	505	526	501	516	576	559	552	540	558	486	532	546	535	512	522	469	
1397	556	579	612	542	578	561	550	531	531	533	508	531	561	527	556	519	553	514	527	557	538	546	562	551	
1448	580	590	590	531	580	558	533	553	496	521	542	515	562	521	519	523	571	556	561	519	551	548	594	588	
1499	623	589	603	549	605	566	578	567	535	570	557	535	525	570	559	545	553	549	567	544	537	602	541	609	
1549	575	563	606	513	537	567	543	524	599	568	550	535	559	526	556	518	569	537	593	584	547	545	566	570	
1600	593	562	606	621	567	554	524	585	596	565	517	508	517	544	555	508	543	518	533	540	538	525	572	618	
1651	604	577	607	587	589	619	525	500	563	534	567	537	543	560	550	516	508	547	490	544	585	572	567	600	
1702	633	571	507	478	517	616	558	530	644	602	532	564	586	576	574	602	609	600	552	534	590	523	591	554	
1753	535	516	531	528	509	592	561	593	556	526	572	661	625	580	566	575	592	569	553	550	548	598	560	558	
1803	543	530	547	586	533	544	571	565	533	558	548	574	600	588	582	596	550	584	539	544	571	645	610	560	
1854	585	508	538	550	597	587	602	572	560	565	524	536	566	583	546	554	622	589	580	600	590	534	609	569	
1905	584	527	587	618	574	594	575	579	544	563	548	544	555	594	571	574	588	578	535	563	503	560	592	554	
1956	626	584	587	568	547	557	604	551	563	555	520	535	544	600	575	566	605	518	544	578	537	515	545	519	
2007	576	559	601	604	582	554	599	590	554	547	578	602	553	568	599	600	578	573	571	584	540	511	577	580	
2057	601	573	611	570	598	581	594	559	539	504	555	536	502	539	617	584	608	619	551	599	566	565	561	582	
2108	575	565	584	583	568	624	559	629	552	517	542	579	553	508	650	613	594	602	582	593	523	546	570	627	
2159	569	583	575	558	599	605	556	557	591	574	540	537	597	572	574	625	630	573	569	576	575	578	569	594	
2210	579	598	514	573	617	577	560	561	521	582	538	544	552	591	545	651	594	593	621	584	570	549	546	648	
2261	593	547	604	620	582	586	578	558	559	572	535	548	541	591	579	615	564	642	620	576	589	529	534	556	
2311	575	565	535	588	584	577	536	536	530	588	556	608	562	536	621	591	583	580	599	543	582	595	541	588	
2362	520	585	568	556	537	564	545	552	543	510	612	599	558	597	577	617	596	625	581	549	610	644	594	610	
2413	514	599	568	523	536	552	527	549	591	579	581	592	555	641	622	635	604	618	599	538	567	603	560	589	

mm

Figure A.29. *Data plot of density (kg/m^3) of panel m2p3 (window size 50- by 50-mm)*

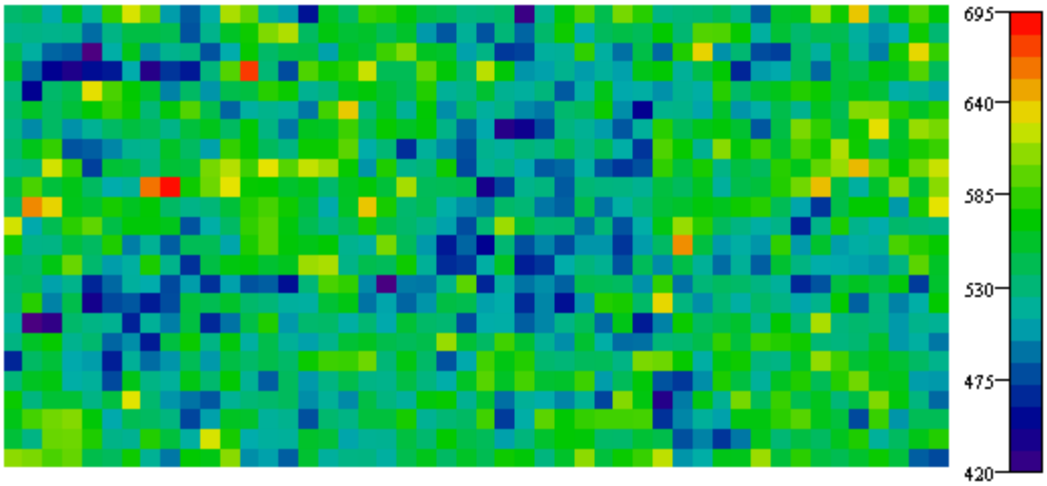

Figure A.30. *Color-scale plot of density (kg/m^3) of panel m2p3 (window size 50- by 50- mm).*

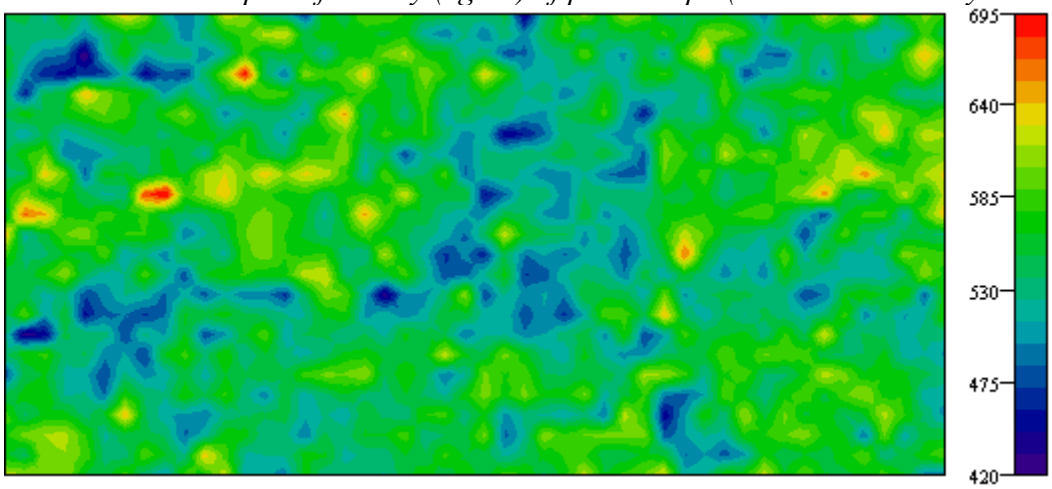

FigureA.31. *Three-dimensional plot of density (kg/m^3) of panel m2p3 (window size 50- by 50- mm).*

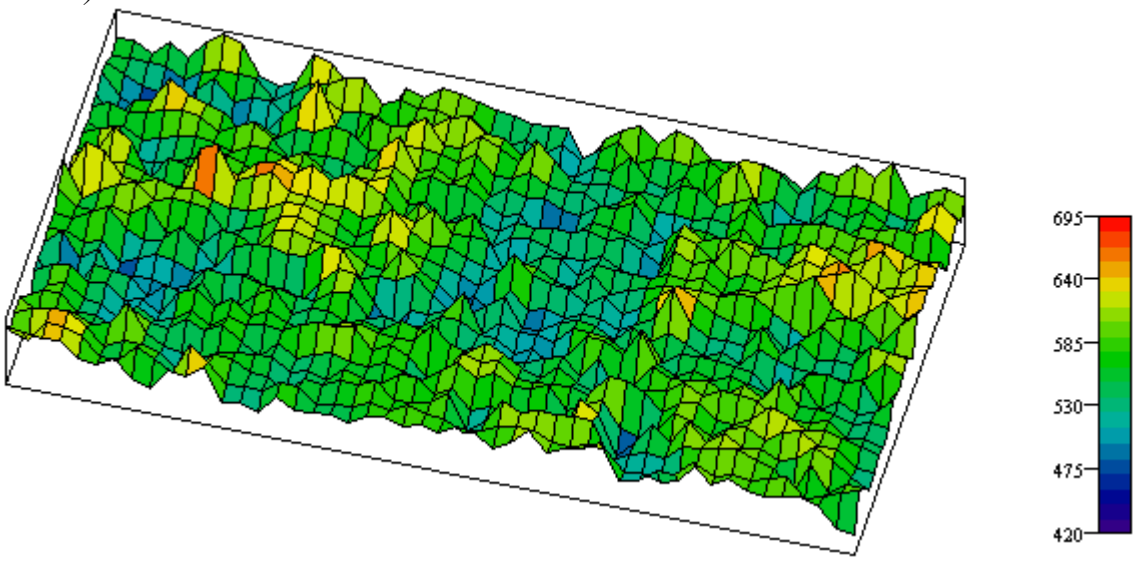

FigureA.32. *Contour plot of density (kg/m^3) of panel m2p3 (window size 50- by 50- mm).*

density	25	76	127	178	229	279	330	381	432	483	533	584	635	686	737	787	838	889	940	991	1041	1092	1143	1194	mm
25	580	622	629	564	608	579	624	605	561	593	619	645	584	594	601	652	634	628	641	585	583	638	555	569	
76	618	610	589	558	561	562	586	611	582	610	612	562	572	569	590	594	588	616	578	556	509	566	562	613	
127	561	558	582	588	554	588	556	512	627	595	606	543	519	558	585	585	566	591	589	558	518	539	543	551	
178	584	587	560	520	590	533	559	605	622	623	615	595	532	568	576	594	567	638	615	566	566	613	592	571	
229	512	554	544	513	645	562	656	626	593	605	586	583	588	564	585	537	527	542	660	579	576	564	542	574	
279	531	630	573	580	557	590	626	644	585	615	578	618	575	561	571	606	518	524	610	559	560	531	601	541	
330	551	597	552	571	622	604	609	639	570	659	597	632	603	603	568	572	539	568	547	547	568	609	604	635	
381	546	588	556	568	636	624	578	599	594	636	614	578	608	608	568	582	558	544	539	521	519	572	583	607	
432	640	643	579	576	555	576	558	561	579	614	657	629	574	565	574	570	577	543	538	553	544	560	531	605	
483	642	591	551	554	605	558	612	619	621	596	622	689	588	553	547	553	577	574	574	556	541	548	536	586	
533	558	542	537	553	605	609	644	638	593	579	578	610	593	571	591	542	567	576	560	538	577	584	595	524	
584	634	644	587	570	586	572	616	642	621	625	599	640	593	581	591	565	579	578	615	574	590	567	548	563	
635	599	635	563	565	570	617	618	610	593	625	614	624	561	608	573	570	560	581	637	564	592	618	553	576	
686	610	589	520	564	625	649	663	613	576	607	613	556	544	625	579	583	600	559	582	578	583	610	559	614	
737	641	613	577	553	564	680	641	620	578	578	583	609	553	566	625	579	536	500	575	583	561	583	591	587	
787	617	575	591	631	597	592	597	594	554	564	620	563	528	548	569	572	575	598	519	507	554	584	580	632	
838	618	598	603	589	603	591	607	563	577	600	667	565	569	589	582	558	604	575	573	621	634	573	581	562	
889	576	637	627	595	624	577	608	568	618	607	584	570	578	557	574	614	626	616	567	582	590	589	571	539	
940	634	660	546	599	606	604	646	565	561	572	616	608	554	526	574	631	597	564	512	556	600	639	620	621	
991	585	615	551	565	572	617	594	546	565	570	582	560	567	559	594	628	531	498	553	582	610	669	607	565	
1041	605	623	565	560	604	606	602	613	592	604	549	524	520	548	555	612	585	594	551	490	580	627	606	563	
1092	616	621	567	524	554	568	587	631	582	554	606	570	524	542	529	546	619	555	540	533	601	593	529	566	
1143	555	534	541	603	605	581	619	591	586	562	640	614	597	552	560	578	591	548	544	525	580	592	642	648	
1194	505	535	569	580	616	592	599	535	593	566	609	580	529	604	553	566	561	577	575	567	551	554	561	581	
1245	526	586	602	502	559	564	555	555	619	617	555	561	538	552	559	589	574	522	562	611	603	607	537	589	
1295	552	585	552	514	590	609	581	597	537	558	558	546	527	565	553	575	542	519	539	614	582	623	589	611	
1346	530	548	557	533	551	553	555	506	541	575	584	531	520	539	509	565	539	511	594	583	606	602	558	605	
1397	557	537	556	530	538	558	604	561	556	586	573	551	521	509	494	486	512	571	577	588	586	591	597	692	
1448	554	528	561	533	564	609	539	520	554	557	571	594	561	517	556	558	583	554	537	569	580	629	524	590	
1499	523	534	570	628	566	582	541	558	542	544	507	539	536	526	524	537	567	556	569	568	583	522	500	549	
1549	528	536	485	520	554	510	550	558	551	543	536	561	547	552	516	525	498	553	511	563	629	593	512	570	
1600	492	545	499	510	573	556	548	598	566	515	539	593	557	525	529	495	536	545	555	591	515	563	554	577	
1651	515	522	500	545	575	591	577	570	608	543	600	564	561	561	514	502	548	590	602	597	582	527	549	586	
1702	514	523	505	543	567	611	577	581	653	587	608	541	561	568	561	536	614	546	587	576	554	555	613	626	
1753	510	484	534	535	532	587	626	535	581	569	551	512	558	549	545	544	563	551	560	553	581	588	614	638	
1803	485	467	500	531	555	588	572	543	545	584	530	531	561	536	565	525	480	597	565	566	559	541	588	621	
1854	555	517	537	572	547	593	517	598	590	607	537	505	526	554	572	545	551	619	588	597	555	524	564	572	
1905	615	575	533	506	500	560	522	522	577	600	580	551	547	557	530	514	519	566	510	504	553	576	606	581	
1956	529	543	533	563	542	548	557	550	542	602	588	564	569	611	572	588	541	516	491	457	515	580	588	626	
2007	490	554	505	515	612	598	532	577	556	621	661	593	587	583	588	538	535	492	525	518	514	537	495	545	
2057	527	498	493	535	497	534	542	569	565	554	582	605	563	581	562	502	536	500	530	533	506	483	536	556	
2108	511	536	536	578	544	557	574	617	593	544	606	599	579	576	572	525	560	524	537	515	526	513	530	535	
2159	532	484	539	517	531	516	566	588	613	548	620	606	566	609	611	577	556	556	567	521	507	524	547	554	
2210	493	501	605	517	568	524	492	552	584	600	599	586	514	568	597	577	553	552	527	523	535	481	517	582	
2261	532	499	524	550	552	509	536	534	542	544	588	555	534	567	595	566	466	467	478	532	531	547	568	580	
2311	559	584	496	490	552	563	585	533	573	591	591	543	496	586	607	524	454	501	540	572	553	551	581	546	
2362	564	527	528	529	537	505	529	599	633	593	606	591	561	530	594	513	488	534	472	637	607	566	560	539	
2413	537	558	535	522	567	593	615	591	561	611	596	566	609	555	624	551	593	557	539	551	539	523	575	570	

mm

Figure A.33. *Data plot of density (kg/m^3) of panel m2p4 (window size 50- by 50-mm)*

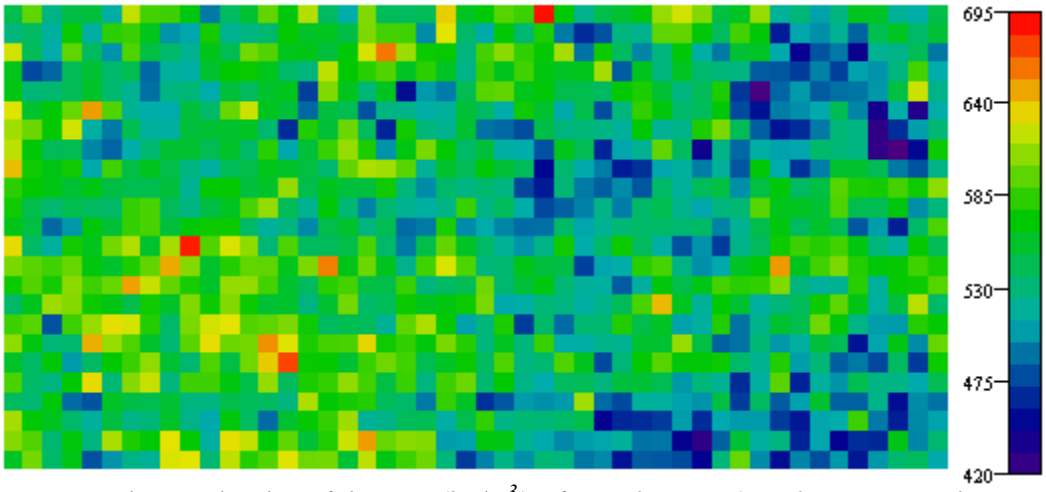

Figure A.34. *Color-scale plot of density (kg/m^3) of panel m2p4 (window size 50- by 50- mm).*

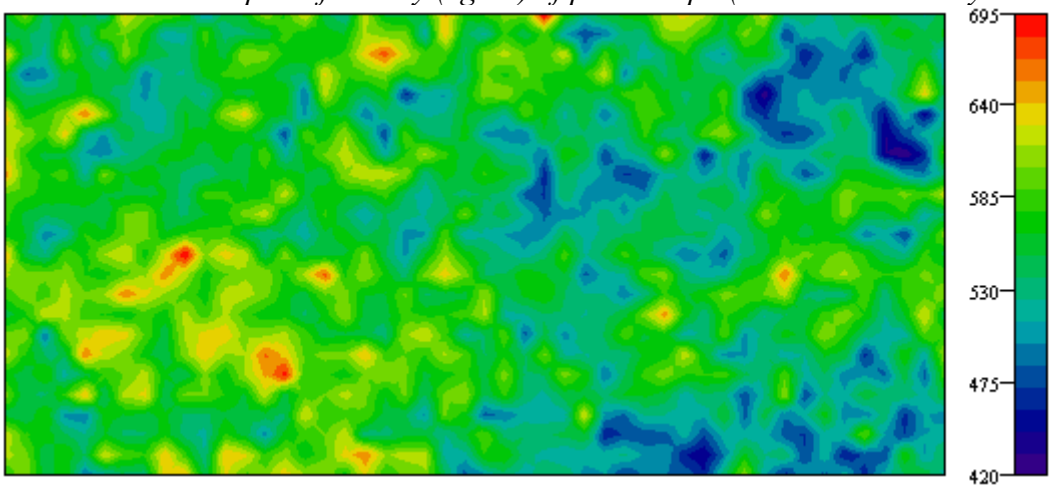

FigureA.35. *Three-dimensional plot of density (kg/m^3) of panel m2p4 (window size 50- by 50- mm).*

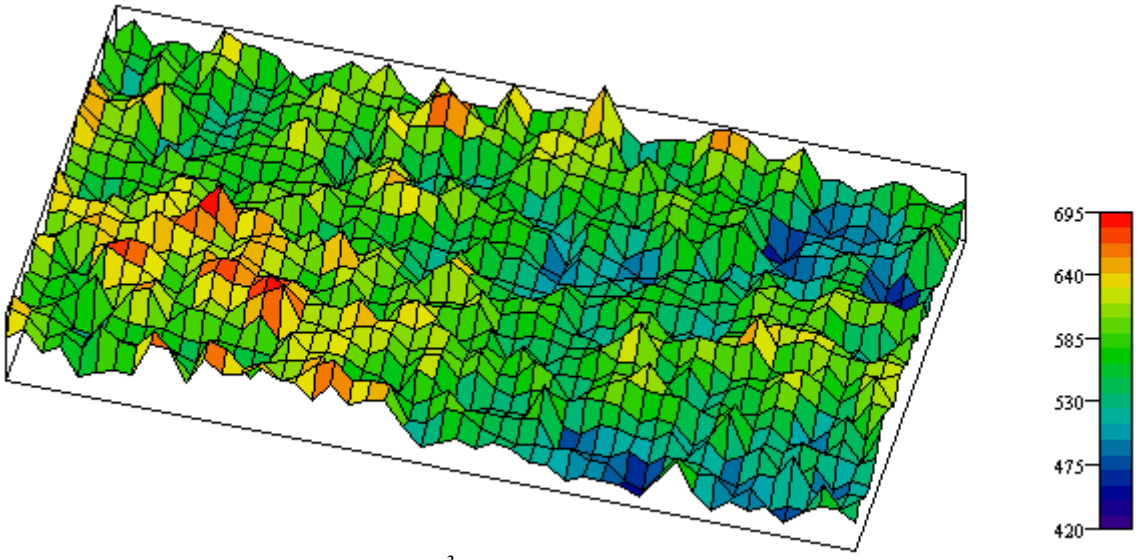

FigureA.36. *Contour plot of density (kg/m^3) of panel m2p4 (window size 50- by 50- mm).*

density	25	76	127	178	229	279	330	381	432	483	533	584	635	686	737	787	838	889	940	991	1041	1092	1143	1194	mm
25	558	559	536	546	526	554	562	511	553	573	563	594	579	612	597	514	550	514	509	546	532	556	536	601	
76	558	586	504	517	516	574	579	510	528	573	579	589	574	624	609	567	549	581	543	545	509	567	520	607	
127	563	582	558	586	495	574	556	508	508	548	599	579	552	601	534	555	562	545	553	552	499	566	574	598	
178	548	518	534	581	528	550	590	528	606	546	583	562	531	562	562	562	551	565	523	534	499	544	573	522	
229	599	535	546	600	534	566	580	550	542	578	556	571	554	546	551	500	526	516	513	526	534	553	562	558	
279	568	539	541	529	546	521	618	564	565	603	570	544	551	522	523	474	490	510	545	592	572	561	569	629	
330	606	501	493	485	549	614	613	581	571	592	592	539	518	531	506	558	467	558	529	573	563	584	575	656	
381	534	587	546	498	560	596	581	619	608	548	542	551	540	542	528	542	509	513	549	499	533	591	587	626	
432	500	549	526	526	537	543	610	618	617	577	541	551	529	529	546	583	567	497	581	527	557	540	575	606	
483	510	562	522	517	508	519	545	540	587	544	614	502	531	542	531	589	623	577	612	533	536	565	597	555	
533	535	515	516	542	518	533	554	563	576	527	600	497	523	560	577	548	558	550	536	604	598	591	635	573	
584	553	562	522	557	526	520	551	518	536	591	529	527	501	570	558	523	539	548	566	566	576	555	591	652	
635	509	558	564	536	542	486	558	550	522	546	485	481	507	557	592	491	538	543	573	585	590	533	599	691	
686	539	565	572	545	541	554	574	515	523	560	559	516	574	574	602	577	577	515	550	573	546	540	636	686	
737	565	586	587	541	555	582	596	592	552	553	548	566	600	561	581	576	559	653	618	557	551	591	616	595	
787	556	516	551	569	532	531	575	599	554	488	549	571	536	558	566	565	576	610	583	561	570	593	636	626	
838	598	617	559	535	505	484	580	553	512	539	584	561	547	573	556	576	540	564	533	594	666	617	627	621	
889	576	623	587	558	533	562	550	533	553	556	579	525	525	547	532	563	540	577	555	598	625	609	639	619	
940	618	539	511	516	508	564	550	525	569	533	565	549	548	582	574	514	578	529	557	547	585	607	653	575	
991	600	544	526	583	559	563	526	527	558	540	539	513	542	519	599	581	619	549	549	581	622	589	631	669	
1041	600	582	520	606	557	565	539	537	550	544	554	530	541	505	502	519	576	575	542	585	586	545	561	607	
1092	563	580	477	540	582	545	522	528	511	597	547	541	537	546	531	531	555	576	581	604	587	559	546	588	
1143	593	562	517	563	570	604	534	543	567	554	554	586	558	558	504	505	535	590	517	553	567	614	613	584	
1194	560	596	577	535	542	557	507	528	547	605	531	539	582	586	554	557	546	569	515	525	558	608	650	595	
1245	546	628	585	564	572	603	583	500	551	590	535	584	583	560	603	546	539	570	509	548	523	588	634	618	
1295	518	589	565	530	540	578	582	534	566	620	499	558	600	549	602	533	574	559	552	548	563	547	589	610	
1346	563	578	577	601	569	545	551	511	539	559	490	527	553	558	559	540	534	580	575	530	523	533	541	597	
1397	567	545	581	552	619	565	551	598	593	581	558	545	536	562	553	572	564	545	547	553	540	526	515	588	
1448	566	585	583	507	591	597	556	617	601	614	524	547	513	509	524	531	529	556	572	562	570	527	546	554	
1499	579	583	553	527	491	541	581	568	584	623	564	521	528	526	555	501	524	599	542	546	508	543	583	548	
1549	609	573	610	543	555	557	570	557	582	553	569	600	566	536	573	527	545	554	584	587	561	537	550	556	
1600	608	551	556	547	547	532	526	537	572	584	548	553	532	519	533	547	557	601	583	559	621	593	567	575	
1651	614	559	552	584	559	560	536	549	543	601	553	572	547	575	519	539	529	572	552	547	608	537	580	585	
1702	590	584	570	560	588	535	600	613	622	566	527	544	513	557	547	511	452	567	571	534	587	578	630	650	
1753	646	589	545	523	566	558	596	570	572	583	592	559	565	604	606	521	478	515	555	578	595	567	558	611	
1803	602	580	580	516	530	565	576	600	581	600	579	557	589	580	571	511	532	609	569	566	511	566	635	591	
1854	554	538	572	530	596	627	557	605	634	575	520	547	598	590	515	510	548	617	536	598	532	597	636	600	
1905	499	546	623	562	546	580	573	605	575	592	555	643	576	509	585	555	533	597	583	612	562	594	575	585	
1956	552	600	573	585	566	511	636	614	583	546	576	625	595	548	575	518	565	560	530	553	532	558	569	620	
2007	550	565	564	542	573	568	631	613	630	587	573	602	621	598	568	562	577	547	536	597	549	535	606	592	
2057	554	570	607	563	587	573	637	565	560	567	527	547	536	550	535	539	538	551	564	568	567	578	632	528	
2108	556	556	567	562	533	554	544	506	538	605	559	540	551	561	568	571	528	517	574	558	595	627	601	603	
2159	555	570	544	576	520	552	529	555	547	564	583	569	506	582	469	524	503	490	552	571	574	611	599	587	
2210	560	551	504	570	599	564	549	583	559	553	563	615	568	571	546	592	555	549	602	595	563	600	619	596	
2261	532	509	523	535	557	576	562	548	605	536	584	550	559	611	592	622	565	591	609	595	525	586	591	649	
2311	550	544	538	588	620	605	568	539	531	571	579	528	552	519	546	576	589	577	583	595	603	555	609	618	
2362	527	488	483	526	573	538	555	512	536	545	516	536	509	548	561	576	590	599	611	597	608	564	529	562	
2413	524	503	524	517	577	611	554	478	535	563	537	535	552	581	539	514	543	591	474	532	533	538	618	659	

mm

Figure A.37. *Data plot of density (kg/m^3) of panel m2p5 (window size 50- by 50-mm)*

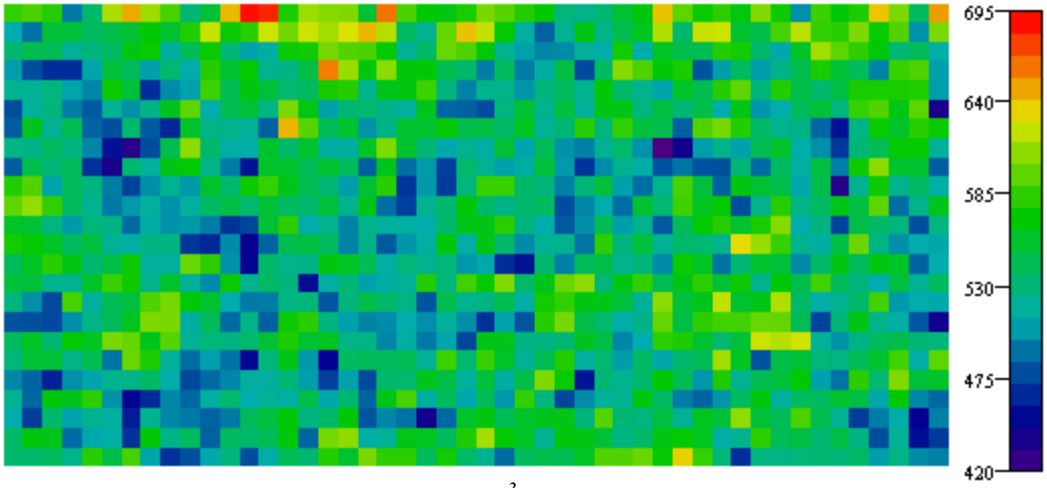

Figure A.38. *Color-scale plot of density (kg/m^3) of panel m2p5 (window size 50- by 50- mm).*

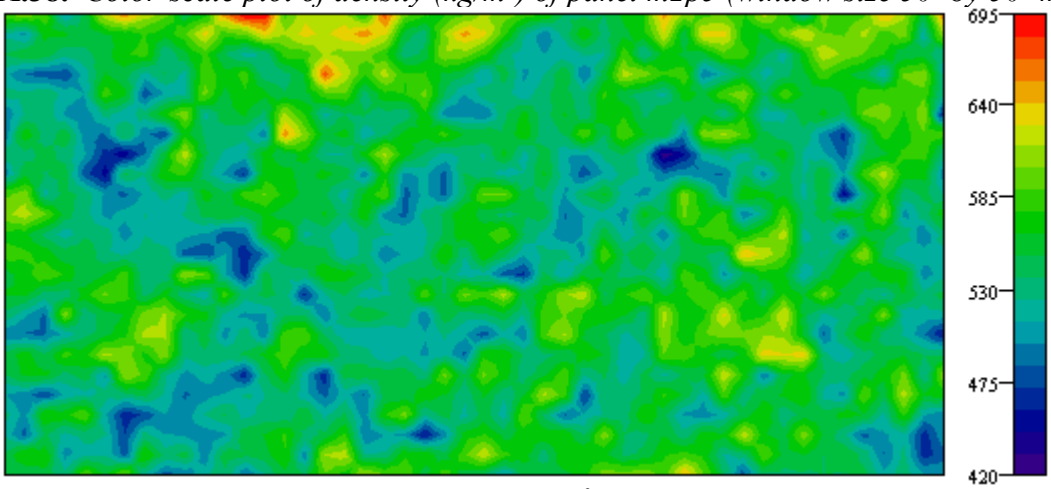

FigureA.39. *Three-dimensional plot of density (kg/m^3) of panel m2p5 (window size 50- by 50- mm).*

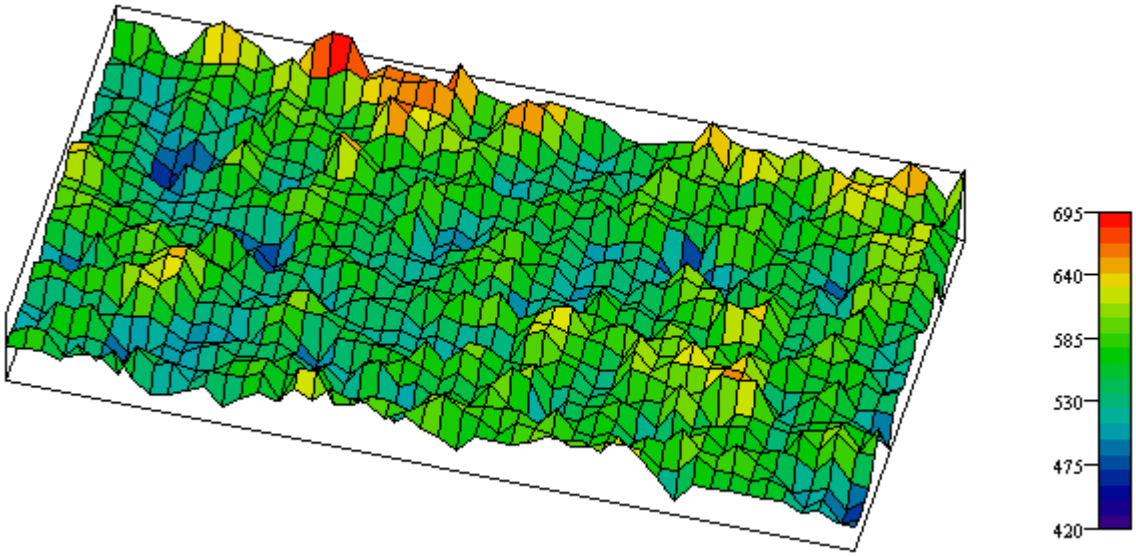

FigureA.40. *Contour plot of density (kg/m^3) of panel m2p5 (window size 50- by 50- mm).*

density	25	76	127	178	229	279	330	381	432	483	533	584	635	686	737	787	838	889	940	991	1041	1092	1143	1194	mm
25	531	552	587	574	577	571	609	616	617	635	534	518	544	587	554	588	518	590	609	594	611	664	570	648	
76	548	517	583	589	560	542	606	568	676	563	541	537	522	538	511	575	570	564	601	560	601	621	575	581	
127	564	557	565	563	572	522	575	527	610	570	553	568	565	570	542	557	578	578	573	563	568	591	577	555	
178	532	520	583	579	520	605	525	540	644	554	554	543	540	552	580	610	586	528	595	592	566	593	550	581	
229	550	566	608	571	562	568	532	565	580	523	567	587	579	575	563	600	572	525	539	583	631	582	585	606	
279	540	535	508	561	532	583	555	616	588	567	559	570	617	610	536	551	566	585	526	528	564	554	620	582	
330	534	568	546	543	579	597	527	569	606	550	542	577	621	574	577	581	529	543	550	559	519	566	615	620	
381	523	539	584	577	572	597	580	613	623	537	534	579	643	621	568	560	525	540	554	581	573	547	574	593	
432	609	557	523	552	624	610	618	650	570	582	584	547	570	620	555	543	482	524	532	581	567	536	591	637	
483	531	563	537	582	585	586	617	542	538	611	561	513	586	600	588	558	505	526	567	545	573	515	558	582	
533	557	518	538	537	489	567	633	586	586	576	565	523	541	585	565	484	503	525	545	537	603	588	504	594	
584	583	526	536	541	550	598	610	624	583	609	608	602	568	564	578	552	517	537	475	487	553	536	555	572	
635	581	542	529	537	571	558	584	555	541	537	556	591	592	581	556	581	536	511	513	564	592	547	535	534	
686	487	583	537	551	569	540	536	596	575	568	591	561	545	517	522	519	544	503	559	510	546	509	574	568	
737	536	552	532	531	532	581	517	568	556	531	533	503	602	548	531	548	560	584	571	579	514	578	579	580	
787	547	468	522	526	524	539	542	564	508	539	563	566	611	557	554	558	522	563	537	571	577	603	561	583	
838	476	479	544	582	541	596	510	606	556	510	525	544	511	559	518	547	500	555	555	535	551	605	582	569	
889	511	553	588	582	510	597	557	568	595	531	546	558	492	577	560	532	519	550	562	539	545	528	524	551	
940	592	574	587	591	551	527	565	562	570	563	566	551	538	570	575	524	537	523	528	559	578	562	557	541	
991	523	561	535	571	601	562	562	608	585	554	580	571	510	534	509	546	534	529	509	536	594	580	607	551	
1041	552	557	481	558	573	527	571	544	574	495	535	556	543	531	532	503	543	549	548	535	527	573	595	579	
1092	574	576	570	556	467	570	581	566	566	544	505	586	572	611	562	506	515	600	516	549	564	576	552	614	
1143	580	562	567	592	488	543	568	548	587	532	535	521	548	582	578	510	543	575	545	568	566	573	566	606	
1194	557	532	581	523	511	545	508	548	580	520	547	528	548	579	604	592	575	553	633	579	537	528	660	621	
1245	556	544	597	581	567	552	543	577	570	535	595	543	507	520	507	544	544	542	544	527	539	525	534	591	
1295	541	571	564	617	566	579	573	561	548	517	568	577	506	511	492	495	483	510	547	563	505	567	532	615	
1346	600	527	514	518	566	585	538	588	550	523	552	588	546	604	535	504	505	562	543	584	554	597	587	614	
1397	538	556	506	505	580	571	596	583	605	551	584	591	518	571	554	514	507	589	533	611	469	584	567	595	
1448	605	611	571	558	547	563	611	566	573	539	577	601	529	579	589	526	513	557	553	598	524	563	558	629	
1499	566	613	548	511	543	548	532	558	533	576	626	596	592	596	539	593	575	552	558	583	614	564	544	574	
1549	537	509	562	559	555	513	608	583	548	588	610	575	610	582	551	543	540	515	528	585	570	527	545	531	
1600	602	590	563	559	553	557	604	563	551	603	574	571	587	595	600	539	553	537	547	540	520	547	552	595	
1651	601	604	622	564	572	604	584	603	641	601	555	566	617	547	579	495	535	474	509	526	539	539	575	571	
1702	582	584	581	561	593	586	537	516	548	604	654	550	562	596	595	509	502	582	498	500	538	565	573	522	
1753	566	566	574	531	571	544	546	556	567	574	588	584	561	605	606	535	500	566	512	520	532	549	571	612	
1803	574	563	627	572	595	560	541	563	584	550	547	585	535	592	594	565	503	546	509	483	512	544	525	525	
1854	601	539	529	595	551	581	547	519	551	574	583	551	528	499	505	533	485	521	526	473	479	494	569	529	
1905	553	570	552	495	472	569	585	573	522	567	565	586	568	480	542	555	487	537	490	568	549	565	543	611	
1956	539	538	522	531	520	583	579	574	556	603	538	542	574	565	575	482	528	504	527	521	545	590	560	611	
2007	520	543	521	586	566	547	538	542	566	639	577	522	561	561	587	485	459	516	492	508	555	625	579	590	
2057	497	495	543	622	636	569	571	567	570	569	605	624	600	569	546	532	527	544	507	497	539	630	581	619	
2108	524	565	549	613	600	529	584	568	556	537	574	561	572	570	539	529	489	480	478	501	538	582	604	595	
2159	544	577	584	571	571	507	616	565	523	522	552	600	574	560	564	552	488	510	524	484	487	568	640	658	
2210	505	571	571	509	582	536	519	546	557	516	538	532	494	533	526	561	487	513	576	511	550	574	598	635	
2261	575	578	554	546	504	535	528	576	524	556	585	561	508	551	546	582	526	517	537	516	570	634	537	514	
2311	567	563	553	525	562	559	576	613	562	517	580	574	553	569	569	543	499	510	523	570	568	588	580	532	
2362	566	605	575	544	543	580	575	564	545	574	565	611	560	552	505	480	526	531	584	618	500	532	558	591	
2413	472	534	513	614	559	545	601	520	556	593	555	568	557	603	567	500	542	573	564	601	512	510	520	601	
mm																									

Figure A.41. *Data plot of density (kg/m^3) of panel m2p6 (window size 50- by 50-mm)*

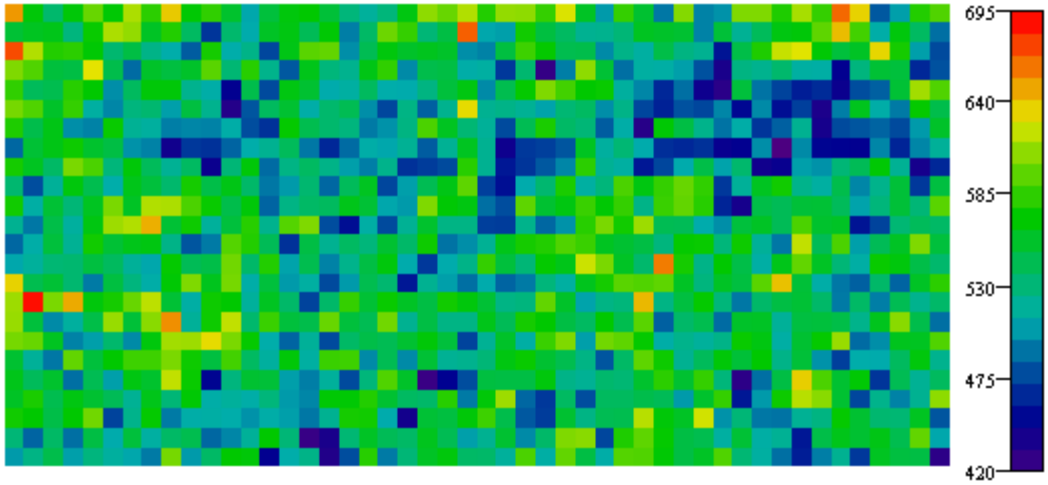

Figure A.42. *Color-scale plot of density (kg/m^3) of panel m2p6 (window size 50- by 50- mm).*

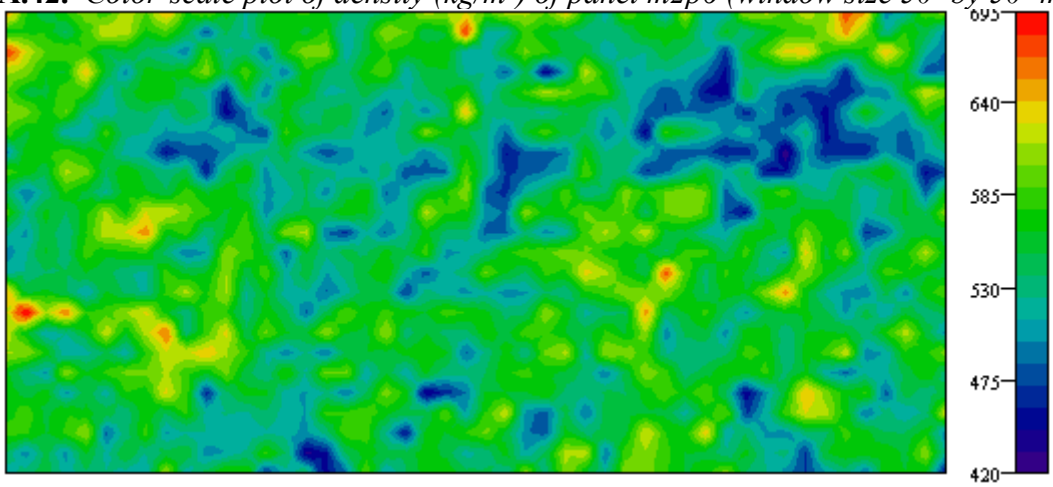

FigureA.43. *Three-dimensional plot of density (kg/m^3) of panel m2p6 (window size 50- by 50- mm).*

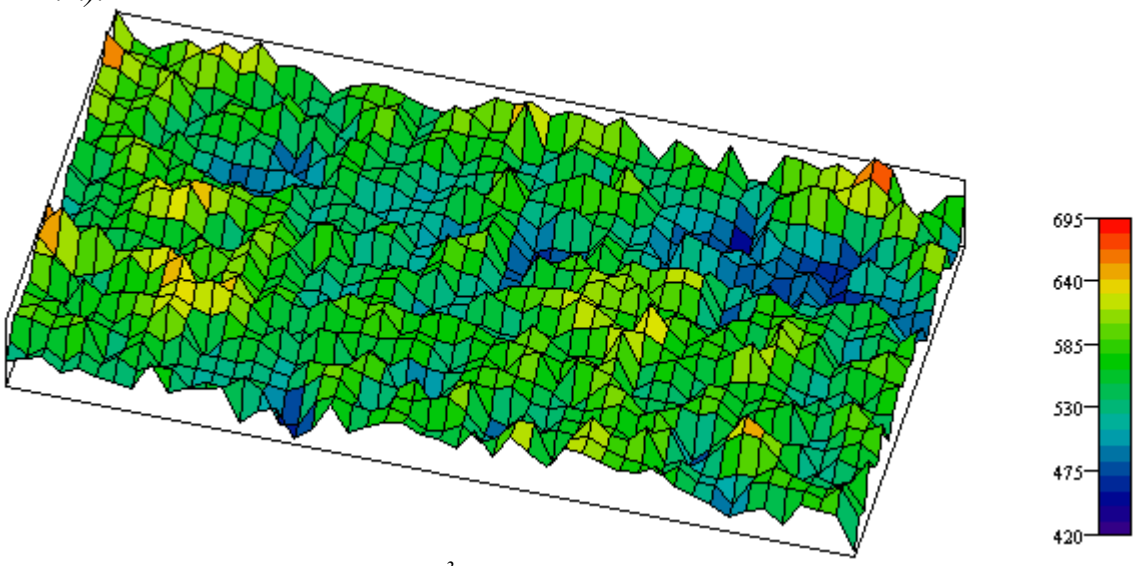

FigureA.44. *Contour plot of density (kg/m^3) of panel m2p6 (window size 50- by 50- mm).*

density	25	76	127	178	229	279	330	381	432	483	533	584	635	686	737	787	838	889	940	991	1041	1092	1143	1194	mm
25	570	509	579	509	534	504	578	547	597	571	557	556	572	609	575	692	618	633	642	624	591	598	586	622	
76	600	545	551	516	556	548	547	505	624	562	554	556	617	638	631	666	594	653	642	621	615	553	554	550	
127	575	511	565	519	553	553	559	507	538	579	580	514	599	608	678	601	613	630	595	653	575	582	579	576	
178	586	587	528	524	555	573	496	513	574	576	602	548	557	596	643	553	545	604	610	644	600	612	643	636	
229	553	541	554	586	562	567	605	620	606	601	605	526	591	574	618	592	546	602	638	660	562	626	575	529	
279	532	529	562	543	598	638	602	555	560	606	603	569	592	578	603	573	542	539	578	673	593	577	548	538	
330	550	530	546	540	534	579	598	578	575	592	565	610	629	615	635	564	565	587	580	598	589	542	541	536	
381	577	549	578	511	579	560	552	570	566	547	548	560	600	568	583	579	607	628	578	574	552	538	577	547	
432	598	582	609	589	593	548	555	546	539	530	542	554	558	541	627	612	566	611	583	576	548	577	580	565	
483	559	570	573	608	546	590	546	518	467	514	567	544	525	591	546	591	621	586	561	576	585	525	535	607	
533	533	546	580	534	572	594	564	519	500	506	545	512	515	589	559	549	618	622	601	563	615	541	567	561	
584	562	586	562	531	494	515	509	555	534	557	526	562	552	639	576	576	640	612	604	545	608	499	548	587	
635	617	560	611	515	591	600	552	562	546	553	552	561	529	605	614	604	567	567	593	587	608	534	533	535	
686	569	542	582	555	585	535	544	583	559	560	572	537	558	579	540	540	541	535	566	565	546	546	530	569	
737	591	559	596	572	545	513	529	563	533	512	557	523	534	597	649	546	531	524	534	529	499	540	568	657	
787	584	606	566	552	571	556	521	499	498	525	543	553	548	571	567	523	508	523	570	575	588	568	587	674	
838	571	605	593	515	570	562	564	514	596	552	606	515	563	567	605	588	547	556	595	627	577	565	603	619	
889	547	557	570	571	546	607	603	530	563	549	550	529	559	497	597	564	538	559	556	583	564	567	605	610	
940	515	568	572	588	632	602	613	585	542	560	538	533	589	575	558	542	607	627	584	562	526	636	627	583	
991	544	478	539	585	554	524	585	597	528	507	543	519	512	564	532	577	597	600	606	595	567	637	586	593	
1041	586	509	591	559	506	496	533	537	467	514	553	506	529	562	506	542	601	612	633	607	602	568	577	593	
1092	581	587	562	594	518	521	491	569	486	500	578	572	549	560	545	569	584	574	601	626	577	533	589	582	
1143	529	573	603	540	535	550	540	516	548	448	487	529	521	559	602	550	558	586	594	575	593	578	509	619	
1194	554	565	539	510	562	521	565	534	573	545	538	559	579	561	601	614	626	594	569	581	628	544	576	652	
1245	544	561	559	594	540	601	513	487	511	544	514	537	605	539	510	548	584	525	571	625	559	565	597	644	
1295	575	556	573	573	568	554	525	506	513	481	396	468	543	556	614	636	640	628	596	605	544	590	619	659	
1346	516	521	533	564	531	561	504	500	527	499	473	508	596	604	568	623	627	610	580	559	560	570	575	603	
1397	493	570	586	544	504	546	486	506	496	482	529	495	523	628	585	584	626	633	563	617	548	588	586	600	
1448	555	539	575	540	541	547	511	565	514	554	555	521	499	614	589	594	572	607	571	569	526	588	605	608	
1499	514	568	550	553	544	508	487	506	532	561	494	546	543	652	596	608	604	566	599	547	510	625	623	574	
1549	510	571	527	516	530	519	571	537	500	522	569	577	601	640	579	533	548	564	587	587	563	632	649	660	
1600	468	550	518	470	550	526	525	514	532	545	547	592	609	608	590	552	585	634	527	562	621	579	565	622	
1651	482	463	556	513	511	546	526	534	547	538	563	557	537	570	598	554	549	636	580	550	594	525	592	577	
1702	519	539	558	518	491	492	578	556	473	544	575	591	577	576	539	539	584	572	577	565	559	492	593	607	
1753	587	559	573	577	529	559	592	517	540	540	580	581	556	601	574	632	617	615	646	623	540	504	562	557	
1803	555	542	580	644	552	562	627	510	535	541	559	567	615	590	598	598	606	620	621	597	527	531	637	584	
1854	527	588	572	592	575	552	511	523	568	575	534	527	526	553	560	580	606	575	584	636	578	547	586	555	
1905	543	536	650	553	534	505	522	524	560	529	498	537	543	546	600	565	548	585	619	655	572	615	528	584	
1956	524	548	613	541	541	517	526	474	531	531	536	555	541	591	627	555	538	578	575	554	566	542	576	581	
2007	564	566	564	550	565	521	484	501	499	522	542	525	565	582	617	585	508	587	637	561	578	554	561	559	
2057	541	530	566	491	520	490	542	516	519	500	569	520	512	559	542	580	609	625	616	595	532	559	505	495	
2108	551	519	565	587	505	514	552	524	469	519	540	527	555	548	579	553	537	587	601	591	524	522	522	523	
2159	568	523	549	521	494	590	548	525	540	523	571	596	546	529	592	567	505	579	644	611	501	522	515	500	
2210	576	554	525	516	474	524	522	520	502	550	554	531	550	560	610	557	549	537	597	565	442	493	554	561	
2261	505	547	510	550	577	550	561	577	521	525	541	513	512	557	619	582	548	513	531	567	494	549	565	532	
2311	596	544	534	535	583	589	543	549	596	514	618	585	540	539	614	575	571	558	562	555	555	461	555	549	
2362	545	546	529	532	564	552	588	535	559	604	563	502	557	615	578	572	500	496	557	532	545	531	570	561	
2413	564	501	500	553	607	520	524	544	570	601	507	489	557	606	544	571	562	534	582	474	529	544	542	565	
mm																									

Figure A.45. *Data plot of density (kg/m^3) of panel m3p1 (window size 50- by 50-mm)*

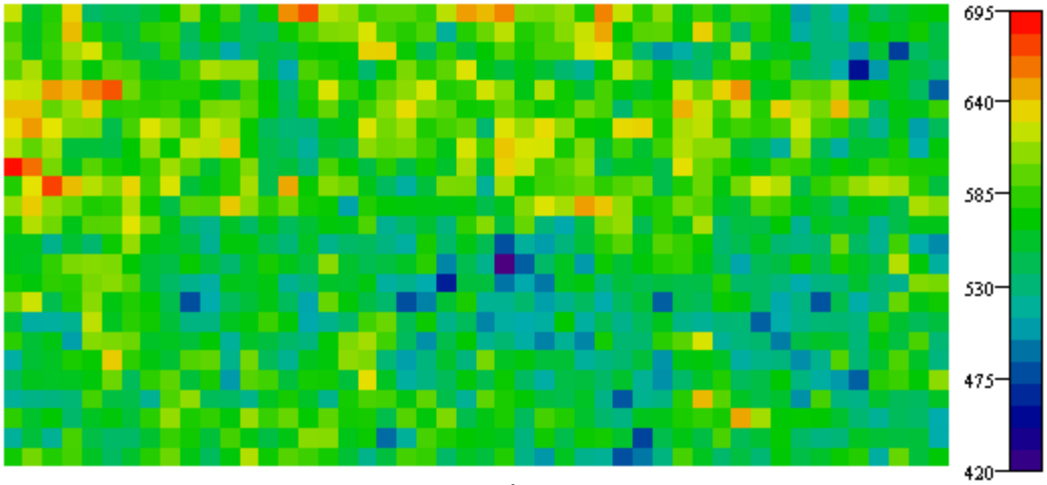

Figure A.46. *Color-scale plot of density (kg/m^3) of panel m3p1 (window size 50- by 50- mm).*

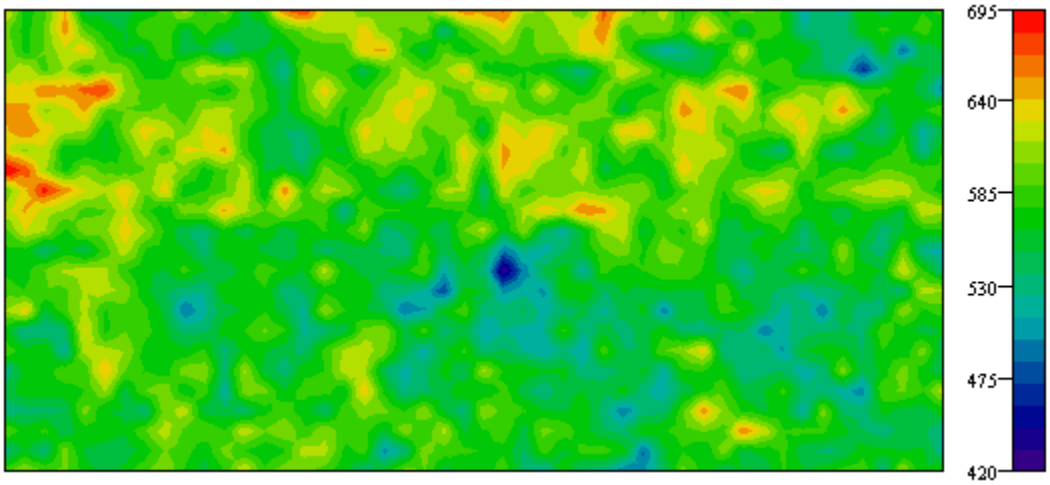

FigureA.47. *Three-dimensional plot of density (kg/m^3) of panel m3p1 (window size 50- by 50- mm).*

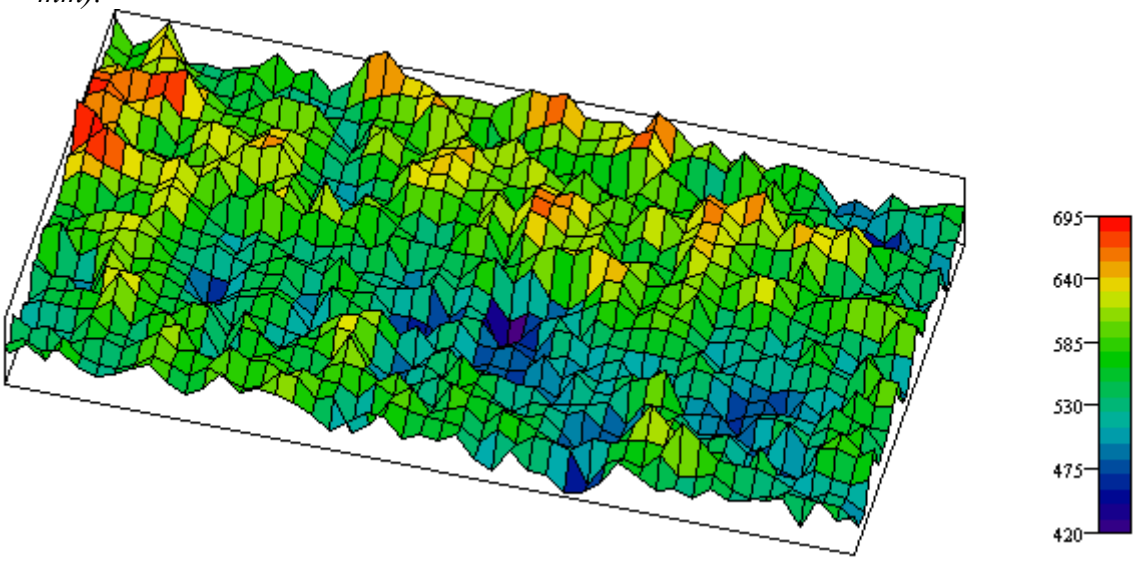

FigureA.48. *Contour plot of density (kg/m^3) of panel m3p1 (window size 50- by 50- mm).*

density	25	76	127	178	229	279	330	381	432	483	533	584	635	686	737	787	838	889	940	991	1041	1092	1143	1194	mm
25	549	511	532	551	552	592	560	610	472	492	563	551	600	578	614	573	552	569	617	540	536	511	553	570	
76	584	536	540	602	592	578	544	537	528	522	531	567	653	606	608	546	572	565	606	579	564	549	643	606	
127	629	524	528	519	537	560	588	506	510	536	584	516	561	563	574	544	538	596	593	529	529	548	571	614	
178	567	575	535	521	558	540	557	537	543	545	557	516	550	526	544	610	518	556	564	461	524	533	552	543	
229	566	554	536	532	630	538	569	534	561	529	528	518	526	512	540	588	588	556	559	527	502	541	522	534	
279	591	591	616	561	559	555	534	559	538	498	552	525	549	524	583	529	555	562	598	549	537	535	490	547	
330	485	548	550	573	543	528	529	499	498	530	489	527	518	488	554	550	574	596	552	538	497	547	550	529	
381	484	601	553	522	511	506	511	481	528	549	587	515	518	544	550	557	587	608	568	597	546	573	482	470	
432	510	525	565	523	517	581	557	518	518	496	565	577	579	498	577	557	540	588	511	547	522	527	525	557	
483	543	549	571	519	571	609	564	536	506	469	518	570	573	532	539	557	529	573	564	561	550	572	529	586	
533	515	560	566	577	565	602	523	530	539	516	549	567	570	603	540	510	576	573	636	538	570	568	534	618	
584	539	591	550	577	613	556	536	509	521	464	564	607	571	598	595	594	586	604	593	504	526	555	548	536	
635	534	568	532	529	511	547	487	500	499	486	532	591	587	563	558	600	598	583	592	605	599	582	590	574	
686	586	545	529	590	595	563	526	488	488	473	515	525	534	549	508	559	600	607	568	574	549	551	553	666	
737	570	618	481	578	562	557	532	493	493	542	550	530	476	530	529	606	589	618	570	586	543	588	536	577	
787	582	594	525	501	488	558	544	504	520	528	521	481	480	544	499	544	562	563	574	636	619	529	541	569	
838	527	559	526	557	501	589	556	527	564	520	504	497	557	559	562	613	556	639	645	588	601	544	552	552	
889	605	584	602	616	515	489	500	491	531	604	579	548	592	578	544	605	593	667	637	587	578	535	566	625	
940	572	551	563	532	543	538	531	549	540	550	535	600	613	600	632	608	612	540	589	603	524	556	613	581	
991	536	501	532	538	466	557	531	535	550	542	566	572	615	628	612	627	592	582	553	595	583	576	538	623	
1041	525	560	550	555	464	589	544	520	552	555	531	573	597	585	626	577	592	598	594	600	560	562	586	582	
1092	541	531	521	541	545	518	627	575	547	542	512	471	535	588	650	598	569	604	567	579	529	600	571	522	
1143	519	457	525	564	513	528	548	558	535	536	508	512	564	530	626	625	636	668	605	579	562	569	554	580	
1194	562	566	598	554	525	534	584	521	560	523	512	554	605	591	622	600	626	635	586	576	595	629	578	585	
1245	566	513	520	578	475	470	517	531	533	563	500	528	640	591	610	561	603	608	640	600	560	601	644	585	
1295	536	585	507	549	470	592	573	541	589	563	570	569	616	563	515	582	582	587	585	556	562	596	634	551	
1346	511	539	519	520	523	556	566	575	564	534	587	573	533	564	585	652	592	629	587	593	610	572	615	535	
1397	552	539	554	565	530	503	579	587	559	574	595	620	613	599	612	602	537	644	601	566	577	535	527	541	
1448	540	553	600	580	545	519	506	535	575	615	594	579	536	565	633	547	563	598	584	552	536	602	589	593	
1499	543	513	493	586	535	521	487	497	544	593	614	604	561	609	564	583	578	584	560	550	609	594	611	591	
1549	513	499	555	517	551	515	495	431	489	581	541	591	601	607	586	598	643	612	562	559	621	590	596	620	
1600	530	495	520	557	536	475	515	446	491	544	566	575	613	613	631	593	653	597	567	562	645	616	610	598	
1651	530	510	542	498	502	555	564	537	533	579	654	604	626	637	631	635	641	585	581	632	638	574	603	642	
1702	551	551	538	524	518	504	547	507	536	565	625	606	574	579	625	689	644	549	596	620	620	582	500	563	
1753	580	571	534	536	512	524	557	560	560	584	621	604	641	632	661	650	614	583	563	624	576	577	520	581	
1803	546	537	588	528	519	593	544	545	574	528	597	612	664	621	636	595	605	611	603	565	654	558	491	574	
1854	538	540	531	513	504	573	529	522	574	568	583	580	630	583	603	603	580	590	559	553	597	519	547	545	
1905	525	591	521	512	496	524	531	568	615	549	575	611	605	612	630	610	646	604	567	560	542	565	551	588	
1956	537	565	525	546	548	622	562	555	573	562	614	579	584	674	637	645	656	644	624	574	565	587	591	604	
2007	520	515	555	505	548	544	551	600	577	572	580	552	589	592	647	606	619	621	624	561	596	604	588	602	
2057	536	522	548	566	556	565	571	602	572	584	550	575	625	597	675	621	574	643	637	614	562	563	529	505	
2108	551	597	586	560	562	558	627	556	587	575	624	569	599	604	648	614	641	625	584	599	615	529	533	549	
2159	542	588	517	541	560	591	571	546	565	600	604	547	568	650	620	650	684	597	595	595	572	546	527	560	
2210	505	592	542	482	558	603	578	559	568	556	602	580	590	583	574	665	689	649	600	621	547	510	522	514	
2261	577	583	564	541	529	588	549	590	584	574	572	608	584	654	642	641	636	640	554	608	530	531	521	568	
2311	527	562	573	626	580	617	579	643	604	607	581	622	637	624	645	614	600	666	609	630	549	537	503	563	
2362	571	569	583	606	604	601	567	640	662	613	542	634	645	657	659	664	612	636	631	602	537	578	526	538	
2413	554	547	580	584	543	546	586	622	622	623	563	564	556	606	628	587	646	604	608	566	552	545	576	508	

mm

Figure A.49. *Data plot of density (kg/m^3) of panel m3p2 (window size 50- by 50-mm)*

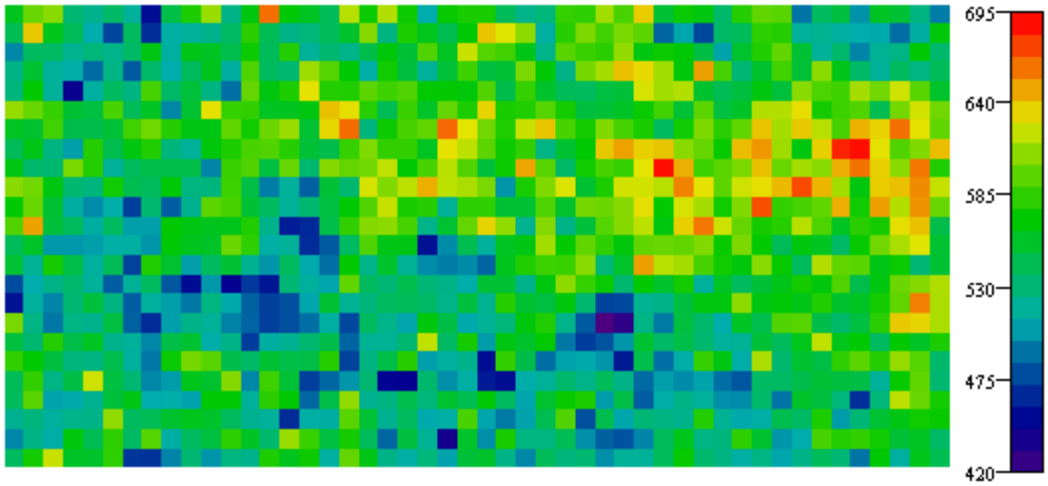

Figure A.50. *Color-scale plot of density (kg/m^3) of panel m3p2 (window size 50- by 50- mm).*

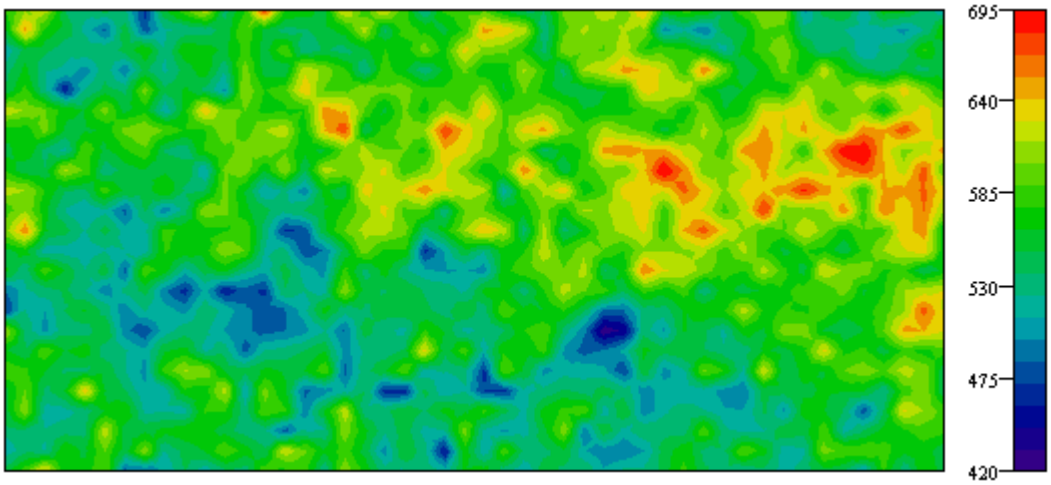

FigureA.51. *Three-dimensional plot of density (kg/m^3) of panel m3p2 (window size 50- by 50- mm).*

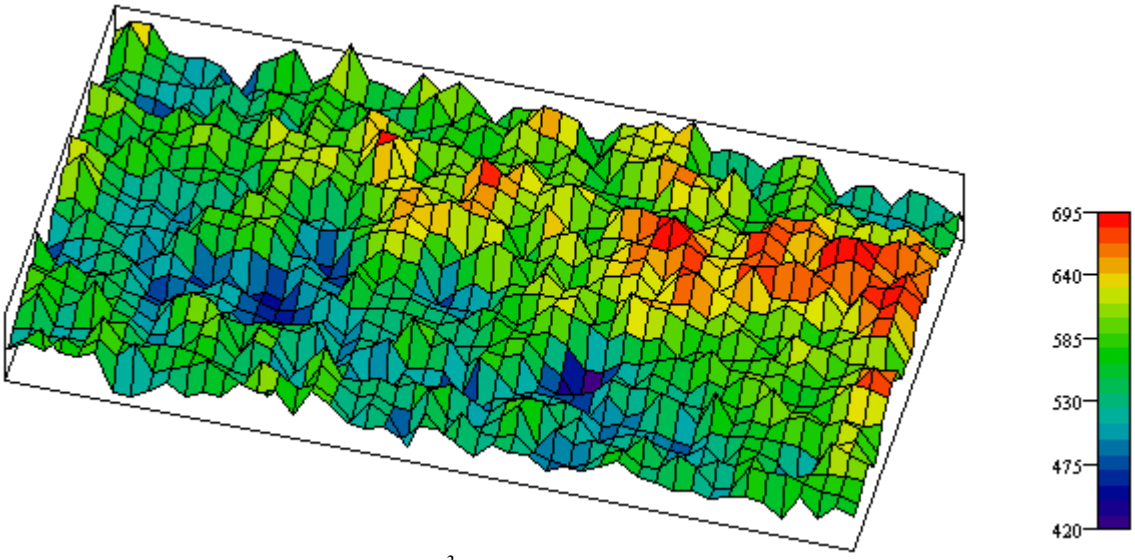

FigureA.52. *Contour plot of density (kg/m^3) of panel m3p2 (window size 50- by 50- mm).*

density	25	76	127	178	229	279	330	381	432	483	533	584	635	686	737	787	838	889	940	991	1041	1092	1143	1194	mm
25	584	565	535	533	549	573	561	610	653	587	619	649	547	669	635	670	652	638	604	613	565	551	562	589	
76	507	593	562	519	528	553	553	499	596	598	653	636	595	604	631	666	687	621	636	623	558	616	566	622	
127	554	547	512	530	497	576	545	544	566	572	584	596	586	629	628	671	639	626	620	620	603	575	515	606	
178	596	565	610	517	494	554	564	616	544	580	578	605	588	616	639	623	602	612	649	591	564	488	476	557	
229	540	556	607	523	558	547	553	529	522	566	544	559	614	607	659	615	594	589	627	535	574	535	510	555	
279	551	545	539	587	529	627	589	596	504	597	585	609	618	625	585	662	628	602	632	576	607	562	578	554	
330	584	518	554	596	565	587	578	574	521	581	545	557	613	540	584	599	618	605	621	520	541	554	538	522	
381	602	578	586	621	602	585	552	550	531	553	561	545	636	604	622	627	629	575	591	553	572	565	578	565	
432	643	569	553	598	608	611	597	549	582	567	582	525	550	576	557	647	598	581	569	555	492	515	513	514	
483	524	621	601	539	568	613	522	513	592	570	579	503	543	603	556	540	524	544	620	569	513	501	540	524	
533	615	640	589	613	586	596	529	546	579	561	509	528	525	558	591	535	609	571	600	595	532	500	535	523	
584	583	602	582	576	573	527	536	490	538	570	604	503	471	568	579	577	565	596	629	558	539	536	539	537	
635	545	604	560	569	562	557	553	516	569	537	623	543	517	614	622	627	552	603	639	575	565	506	568	520	
686	506	568	594	519	548	567	522	508	562	526	543	547	577	636	629	590	584	626	638	602	581	579	550	532	
737	516	608	542	506	527	518	495	501	479	462	489	576	547	598	662	554	549	599	546	554	572	543	574	587	
787	516	577	560	561	521	538	571	559	508	514	502	510	521	534	596	578	572	604	555	558	588	588	581	584	
838	533	574	573	587	564	534	561	562	583	587	570	551	552	567	630	630	597	595	601	526	526	572	496	572	
889	632	576	576	614	620	576	522	550	538	519	560	516	552	502	567	600	563	593	579	506	524	551	541	570	
940	549	533	578	550	626	540	515	502	480	528	554	498	528	533	563	578	607	630	609	539	528	568	553	539	
991	527	534	539	597	595	517	503	538	538	542	518	567	579	531	602	566	596	625	584	505	510	548	581	534	
1041	514	532	540	584	585	542	543	576	533	491	545	600	608	580	591	582	582	584	609	546	447	503	558	536	
1092	501	568	523	575	539	503	525	556	527	527	571	552	571	550	587	563	542	545	569	604	516	478	554	611	
1143	605	580	548	566	586	552	534	538	532	503	544	537	533	520	563	536	561	539	588	616	555	515	578	581	
1194	572	546	556	570	600	584	538	545	522	499	507	512	536	572	615	591	552	563	575	566	558	567	568	567	
1245	526	514	494	497	553	544	529	490	530	580	591	503	580	597	595	603	549	565	562	533	538	544	589	577	
1295	530	514	546	549	575	575	565	533	583	505	527	544	566	601	613	651	587	594	530	532	586	582	587	590	
1346	531	506	530	583	510	544	533	528	533	531	544	607	582	602	611	642	588	572	571	552	538	569	579	614	
1397	602	563	609	632	564	573	533	582	570	572	523	608	538	559	631	595	619	623	584	551	559	532	603	581	
1448	565	541	586	521	549	533	572	577	565	544	553	579	553	542	579	606	610	561	561	540	543	578	609	551	
1499	529	547	534	542	534	597	571	530	525	548	515	553	553	590	512	528	555	568	530	577	629	577	531	554	
1549	512	505	551	566	522	584	598	526	490	488	503	510	536	583	538	523	550	573	575	568	592	545	601	574	
1600	501	483	546	535	596	518	538	495	530	483	514	529	554	560	563	567	604	589	569	568	546	562	655	579	
1651	542	524	561	526	527	554	574	485	559	568	558	560	531	533	558	601	602	607	579	553	472	558	600	561	
1702	541	520	518	469	488	518	537	505	552	498	580	537	568	586	584	595	593	589	605	519	413	477	468	554	
1753	475	558	550	546	499	575	558	543	504	497	537	525	507	500	554	609	563	609	585	541	550	521	532	554	
1803	508	541	565	542	557	552	535	537	563	557	571	611	567	530	578	531	616	594	579	528	568	562	551	535	
1854	512	565	532	496	512	515	511	496	552	540	591	606	592	541	638	535	565	587	579	541	592	537	522	531	
1905	517	569	595	595	572	500	471	530	549	525	540	548	558	519	615	621	573	576	571	579	558	551	539	518	
1956	542	562	588	567	548	529	497	522	538	578	597	546	570	519	598	590	609	626	558	583	560	560	483	505	
2007	524	524	554	539	556	530	570	530	572	563	556	588	569	547	620	579	567	598	579	587	606	524	494	451	
2057	561	615	560	543	543	535	508	548	490	521	558	538	604	554	616	592	623	582	552	561	530	568	497	483	
2108	532	549	599	573	552	531	493	534	544	575	579	568	599	623	616	588	595	578	521	589	598	584	545	492	
2159	466	562	525	534	487	542	533	487	529	573	571	546	531	578	629	575	550	517	527	574	543	506	547	524	
2210	498	485	502	469	462	536	542	505	494	526	563	511	513	589	632	583	583	562	597	582	513	519	556	597	
2261	539	527	542	525	484	564	587	588	555	534	584	500	538	589	591	626	612	578	573	614	560	485	527	577	
2311	595	547	543	551	505	510	543	554	596	556	531	568	606	559	570	535	593	628	559	547	534	533	517	571	
2362	588	559	526	534	506	535	514	545	591	557	538	592	571	553	572	589	598	590	551	511	511	479	519	528	
2413	572	598	572	573	545	580	561	528	532	528	536	509	560	594	569	582	585	611	596	570	505	542	559	555	
mm																									

Figure A.53. *Data plot of density (kg/m^3) of panel m3p3 (window size 50- by 50-mm)*

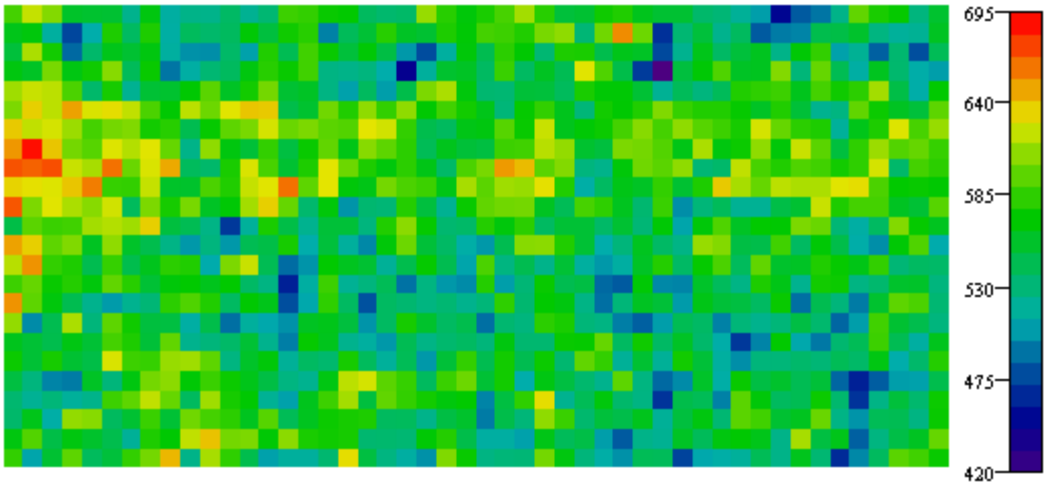

Figure A.54. *Color-scale plot of density (kg/m^3) of panel m3p3 (window size 50- by 50- mm).*

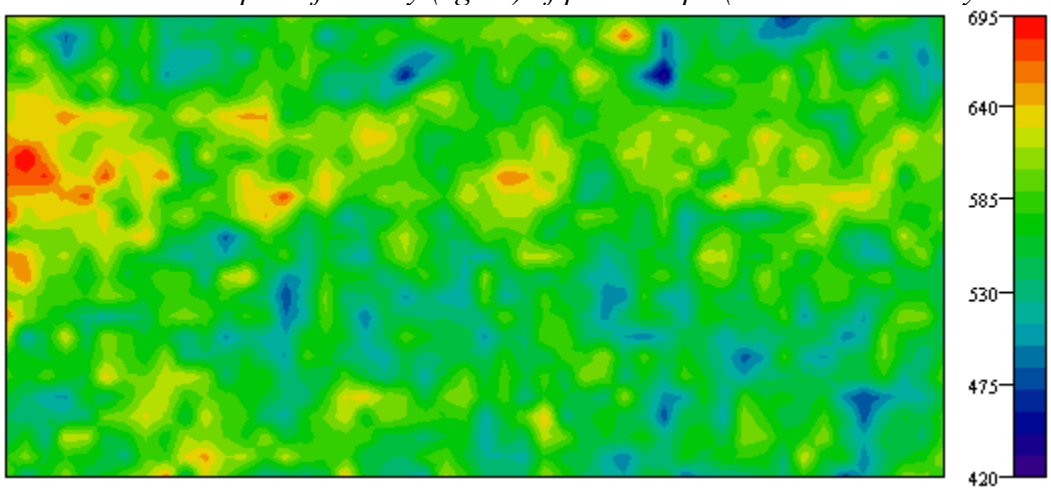

FigureA.55. *Three-dimensional plot of density (kg/m^3) of panel m3p3 (window size 50- by 50- mm).*

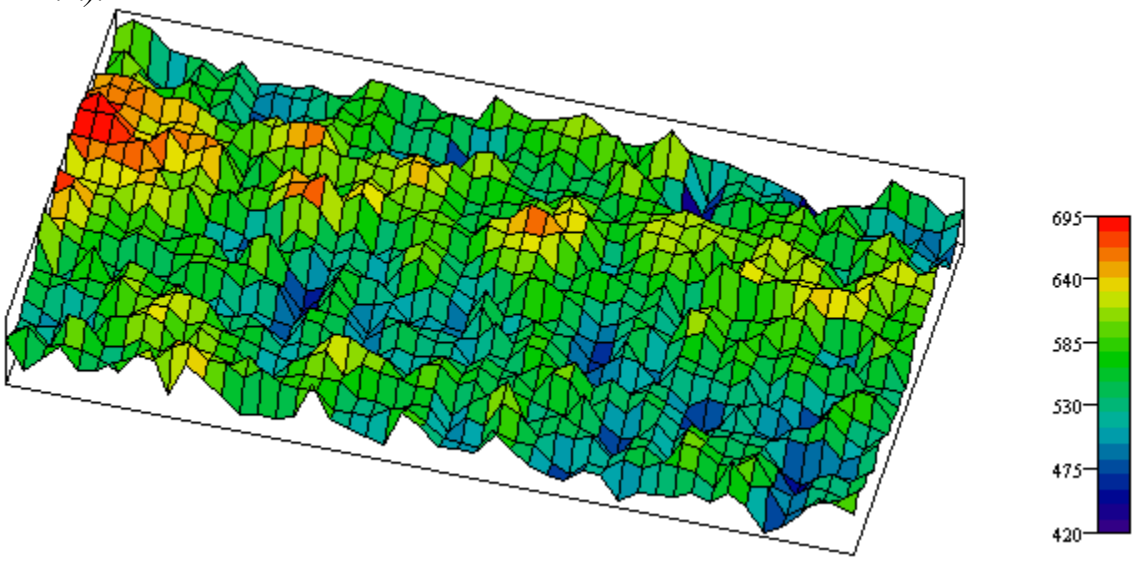

FigureA.56. *Contour plot of density (kg/m^3) of panel m3p3 (window size 50- by 50- mm).*

density	25	76	127	178	229	279	330	381	432	483	533	584	635	686	737	787	838	889	940	991	1041	1092	1143	1194	mm
25	580	564	540	599	600	585	580	558	569	630	586	601	623	578	482	526	531	596	536	540	550	584	538	533	
76	558	568	547	610	643	657	560	506	561	561	603	551	603	576	499	556	549	544	515	584	554	554	578	679	
127	467	524	566	548	568	537	557	480	519	481	571	624	557	555	530	554	550	531	521	568	543	547	606	613	
178	494	523	567	518	504	480	491	493	527	510	574	616	566	560	521	524	562	576	603	539	543	494	613	609	
229	595	551	535	529	557	572	552	556	552	551	598	595	471	536	522	531	527	539	562	510	555	569	547	576	
279	555	608	505	540	560	584	593	571	579	581	586	536	518	514	526	459	475	535	507	496	530	560	575	544	
330	550	552	570	524	576	551	589	552	545	585	554	527	534	557	554	461	523	553	550	558	592	578	596	593	
381	555	555	591	631	598	581	555	512	532	572	511	487	503	534	549	513	556	555	593	557	585	618	656	591	
432	583	512	520	572	593	592	551	554	539	594	561	577	540	560	539	554	568	633	566	536	589	650	618	634	
483	561	450	478	521	613	565	522	527	562	560	574	545	526	564	556	603	565	579	577	639	564	571	576	640	
533	488	478	500	542	573	584	584	540	542	583	582	575	523	504	481	493	533	566	549	591	544	543	574	558	
584	504	508	544	525	521	598	585	603	529	527	578	513	545	507	494	519	557	559	515	570	556	554	502	599	
635	503	533	515	570	554	572	547	582	523	551	554	546	498	530	545	569	554	553	547	582	599	530	534	572	
686	517	550	529	527	549	576	564	580	573	555	535	564	476	502	526	569	493	511	570	602	583	576	573	574	
737	547	550	537	539	575	562	586	585	601	543	537	513	484	531	581	562	490	572	586	579	551	610	563	594	
787	559	567	554	536	593	574	531	572	559	527	534	512	553	524	523	557	537	516	563	560	531	554	569	610	
838	566	531	525	550	544	542	542	575	591	534	575	564	568	607	542	558	587	555	564	536	526	519	566	564	
889	550	540	524	546	524	554	627	541	562	510	615	587	569	593	552	554	558	530	515	515	600	590	636	643	
940	554	519	509	522	577	546	528	493	556	571	588	524	536	562	524	499	515	517	534	524	589	587	612	634	
991	523	507	506	473	504	567	510	481	492	555	540	559	529	513	498	530	521	527	548	555	568	553	498	591	
1041	487	565	548	486	543	556	533	461	537	543	503	508	491	512	522	515	497	482	499	502	567	561	546	584	
1092	530	568	553	468	519	511	503	515	553	556	525	494	519	527	539	563	540	566	525	514	537	600	578	572	
1143	471	557	508	507	537	492	493	489	521	582	574	528	563	478	573	498	588	566	489	475	538	571	534	565	
1194	472	484	546	470	507	535	491	520	576	590	550	565	544	496	529	541	618	566	542	478	499	550	571	564	
1245	511	506	499	490	545	581	540	518	532	536	560	531	540	522	534	548	565	516	557	569	556	551	571	580	
1295	509	497	487	464	536	546	565	538	526	481	483	525	528	552	541	499	523	544	505	559	519	543	561	583	
1346	498	511	523	556	565	473	540	541	608	465	483	513	513	585	533	564	544	583	536	532	518	569	562	502	
1397	553	529	584	593	559	525	545	540	534	507	507	524	552	551	564	513	571	571	523	549	523	549	591	587	
1448	558	624	590	607	573	515	567	545	516	550	491	528	520	561	559	550	537	535	554	500	531	534	584	595	
1499	543	535	531	550	538	539	547	601	565	532	497	529	562	582	611	544	548	583	528	505	484	612	602	568	
1549	559	526	537	573	519	543	563	573	544	557	527	551	571	605	623	517	523	572	552	479	521	556	591	552	
1600	539	556	523	549	489	605	586	533	571	605	490	561	529	536	601	552	523	577	562	493	574	533	631	506	
1651	608	543	546	556	570	602	568	541	603	588	558	565	598	529	553	588	558	578	559	549	529	565	555	523	
1702	520	531	508	539	575	558	561	551	542	570	579	500	569	537	538	597	580	564	509	557	569	615	543	548	
1753	574	531	468	624	605	639	599	594	557	575	585	535	498	561	567	560	609	533	483	505	557	564	562	636	
1803	601	547	561	591	607	644	631	626	570	552	602	578	564	602	621	603	578	548	518	481	531	510	577	548	
1854	584	528	556	659	601	637	616	612	557	571	554	567	586	612	581	581	588	592	524	557	537	562	565	547	
1905	549	569	549	593	619	584	567	564	590	608	586	598	557	541	554	554	574	593	574	500	552	585	579	578	
1956	549	593	509	526	585	616	563	540	596	621	583	565	589	547	584	545	565	581	599	503	517	494	555	558	
2007	569	597	521	592	611	611	580	553	584	616	615	613	615	513	596	587	579	536	538	504	532	496	529	609	
2057	573	574	522	552	590	563	587	592	634	572	586	572	523	519	579	619	608	545	516	510	538	566	526	581	
2108	558	521	527	527	583	561	520	536	554	582	597	536	567	536	572	565	534	529	479	552	520	538	501	546	
2159	514	548	533	569	602	573	533	507	592	603	578	538	575	582	502	528	526	527	501	548	507	505	559	550	
2210	525	555	486	504	536	572	547	549	577	598	516	561	521	538	558	565	570	514	518	533	489	551	537	548	
2261	531	518	500	479	603	595	609	585	582	577	649	556	520	556	552	552	534	489	553	567	520	561	542	556	
2311	526	487	536	489	571	564	571	584	553	588	520	574	555	511	545	542	552	532	535	553	535	546	548	588	
2362	549	567	530	538	545	523	490	566	557	602	533	561	546	533	543	526	545	562	600	553	517	520	532	560	
2413	486	520	538	534	593	504	467	563	611	574	591	560	585	569	513	554	558	501	643	584	521	522	557	523	

mm

Figure A.57. *Data plot of density (kg/m^3) of panel m3p4 (window size 50- by 50-mm)*

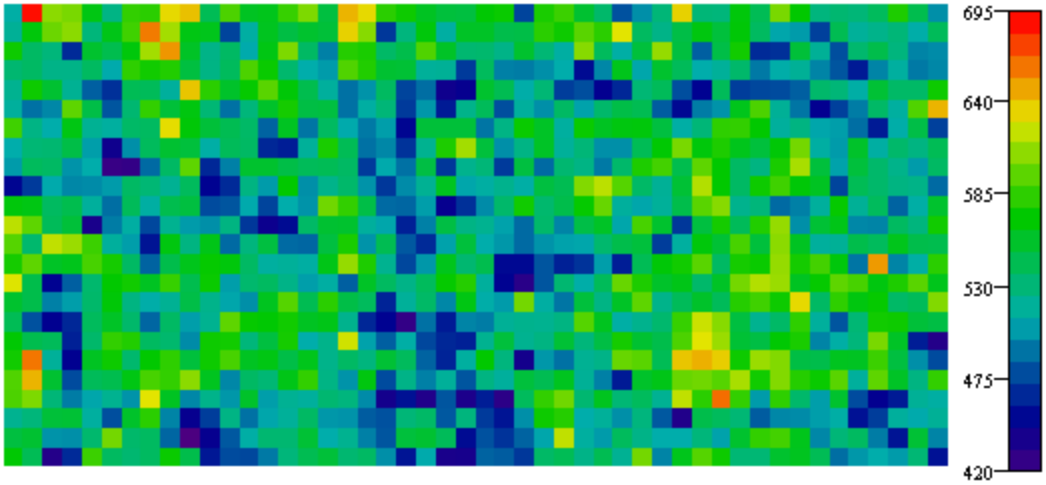

Figure A.58. *Color-scale plot of density (kg/m^3) of panel m3p4 (window size 50- by 50- mm).*

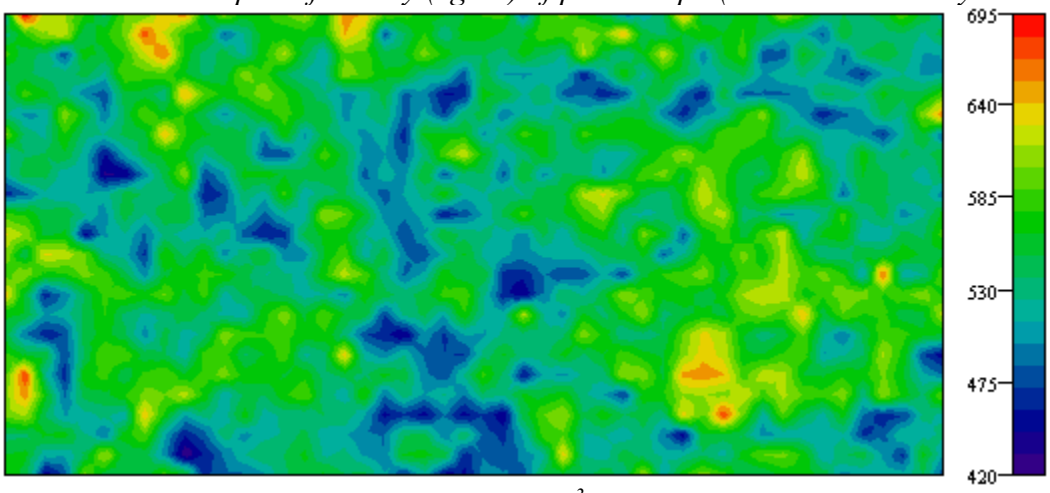

FigureA.59. *Three-dimensional plot of density (kg/m^3) of panel m3p4 (window size 50- by 50- mm).*

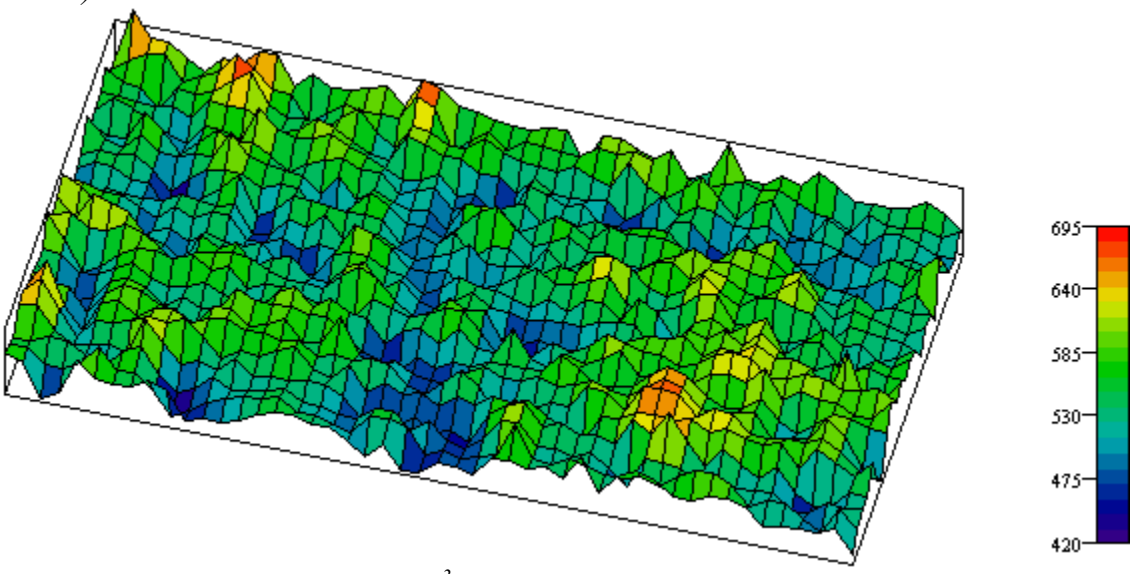

FigureA.60. *Contour plot of density (kg/m^3) of panel m3p4 (window size 50- by 50- mm).*

density	25	76	127	178	229	279	330	381	432	483	533	584	635	686	737	787	838	889	940	991	1041	1092	1143	1194	mm
25	464	535	555	516	603	545	494	466	544	546	487	501	565	530	541	553	504	535	562	562	526	519	463	510	
76	501	573	529	536	538	487	492	552	499	486	487	542	558	534	495	523	531	600	594	572	553	521	484	557	
127	529	525	553	549	501	485	522	563	491	463	539	571	542	536	549	529	517	474	544	561	512	520	511	618	
178	506	512	537	499	482	534	532	559	523	486	533	528	537	523	540	496	506	498	512	517	471	502	522	563	
229	564	590	556	535	546	508	527	535	523	496	599	526	564	588	569	535	531	542	482	532	478	529	528	531	
279	569	577	520	536	511	505	493	554	520	473	532	536	561	541	556	564	518	560	522	572	526	525	511	521	
330	498	540	497	564	521	538	503	575	511	546	516	551	529	528	512	525	480	524	559	632	555	564	498	538	
381	542	531	496	507	492	512	523	535	534	557	546	575	547	551	527	544	499	509	538	549	498	497	520	538	
432	486	494	488	534	524	534	518	571	560	564	524	558	557	514	588	516	488	513	494	524	511	539	562	615	
483	523	555	570	563	561	573	566	552	570	549	529	543	488	523	533	539	477	566	521	539	542	526	543	610	
533	524	561	580	517	544	530	542	499	582	532	557	517	547	516	531	577	531	516	552	482	497	514	522	541	
584	498	546	557	541	565	571	511	518	571	516	556	589	529	551	535	593	503	483	503	584	534	492	499	489	
635	568	573	566	556	553	630	596	568	555	489	500	537	550	526	531	549	528	505	490	562	545	530	515	546	
686	541	518	573	589	578	571	565	569	492	482	491	462	473	507	530	561	509	513	555	521	562	515	559	582	
737	573	592	591	577	590	595	555	571	541	536	548	492	504	506	489	520	500	513	557	548	531	563	560	566	
787	562	616	585	574	602	538	571	582	566	544	529	580	553	546	483	525	590	532	511	571	576	595	593	540	
838	542	579	535	576	645	526	513	535	586	529	525	588	529	507	469	540	562	584	523	607	553	553	644	594	
889	514	498	538	507	524	555	509	535	565	506	525	535	513	519	501	558	508	522	596	598	558	577	600	590	
940	585	514	530	519	491	497	483	535	566	559	518	485	505	512	559	564	493	503	624	643	598	569	590	646	
991	589	531	543	528	508	473	533	530	512	506	495	558	557	529	571	601	557	582	559	605	621	583	559	592	
1041	589	520	512	566	554	495	516	494	519	522	524	529	565	564	554	556	522	572	528	583	598	557	539	644	
1092	492	519	497	556	533	508	562	554	529	479	535	564	548	565	558	547	544	596	561	564	566	616	575	651	
1143	517	570	540	561	545	566	616	562	533	522	594	560	571	535	527	531	572	559	558	564	551	569	612	620	
1194	509	542	527	557	550	536	549	505	544	501	502	485	556	540	512	566	578	527	571	563	498	508	530	597	
1245	494	516	546	563	554	555	564	486	510	502	548	594	592	529	534	532	582	572	554	533	477	545	529	587	
1295	505	569	560	552	559	591	568	492	503	514	514	579	573	523	556	560	528	570	525	531	545	599	526	563	
1346	525	530	575	570	541	555	565	505	526	478	472	480	543	525	538	578	540	524	515	573	560	568	553	543	
1397	514	512	516	618	536	560	587	529	560	546	541	524	511	550	547	584	536	548	534	584	565	596	560	550	
1448	550	514	509	574	559	553	525	557	554	570	551	521	509	547	534	510	534	532	531	582	603	552	586	589	
1499	542	508	543	576	531	533	534	541	563	591	578	589	623	607	522	559	551	554	549	582	565	603	632	614	
1549	474	520	504	577	523	549	510	498	560	632	564	572	581	529	502	490	577	581	587	572	577	551	559	633	
1600	540	530	476	528	530	501	531	513	522	581	570	612	579	484	512	506	518	545	568	610	553	583	579	519	
1651	516	513	562	583	525	508	535	544	512	516	577	626	607	503	545	495	530	567	612	584	602	576	585	583	
1702	502	492	512	586	494	523	507	552	467	551	534	688	606	506	517	525	527	572	575	481	586	558	502	624	
1753	534	481	484	514	481	535	554	510	520	532	556	675	661	546	503	518	487	503	553	514	576	547	541	589	
1803	526	479	480	519	503	470	495	464	524	468	530	708	702	557	548	551	531	533	531	538	580	531	551	625	
1854	461	558	535	516	508	532	535	547	504	564	536	707	639	527	544	520	548	583	622	554	558	549	568	553	
1905	509	558	505	498	474	496	548	509	538	531	597	611	581	538	620	561	557	618	522	579	608	588	617	572	
1956	522	518	531	510	525	539	526	539	576	567	546	566	586	568	583	573	564	584	538	612	568	595	623	591	
2007	511	553	538	510	490	520	565	504	531	567	529	599	536	554	557	527	560	552	565	582	529	548	570	590	
2057	516	566	537	536	547	549	540	545	499	547	497	528	556	538	543	550	547	527	520	546	527	605	578	556	
2108	527	577	491	579	545	527	528	558	514	533	518	516	558	535	518	543	589	536	574	534	509	580	592	604	
2159	551	561	541	549	491	517	502	550	560	540	538	596	591	606	515	578	570	585	558	563	528	541	574	601	
2210	535	519	528	474	505	597	540	509	469	511	538	530	546	586	572	589	579	587	569	594	521	512	564	579	
2261	506	556	496	517	578	586	555	582	507	521	509	497	585	585	542	560	622	632	581	533	596	568	547	623	
2311	471	610	527	515	572	561	556	593	582	544	527	455	573	583	585	594	530	565	591	561	576	555	610	665	
2362	562	545	567	543	562	559	600	565	540	512	533	518	509	569	604	543	561	605	592	648	675	610	647	667	
2413	538	560	545	516	589	583	593	542	569	533	567	569	541	571	586	556	555	646	585	583	681	626	591	622	

mm

Figure A.61. *Data plot of density (kg/m^3) of panel m3p5 (window size 50- by 50-mm)*

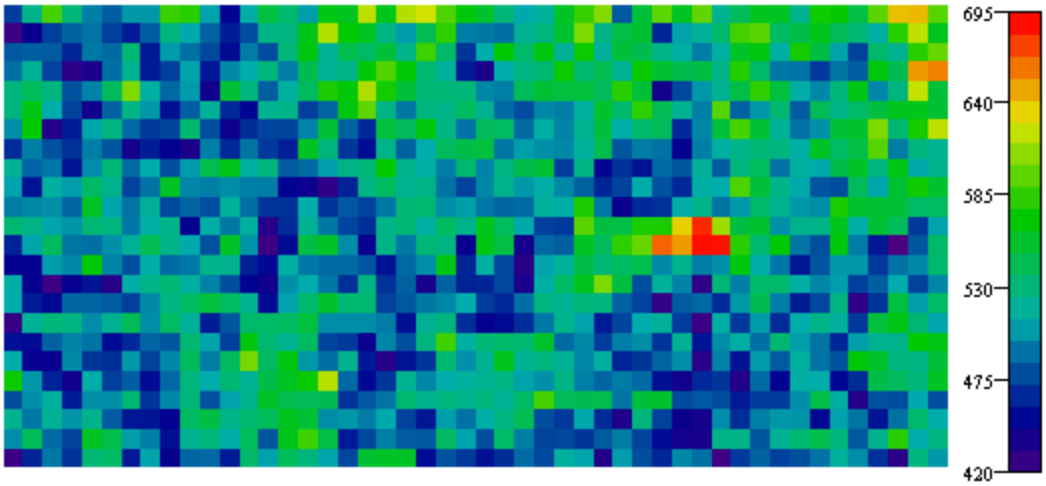

Figure A.62. *Color-scale plot of density (kg/m^3) of panel m3p5 (window size 50- by 50- mm).*

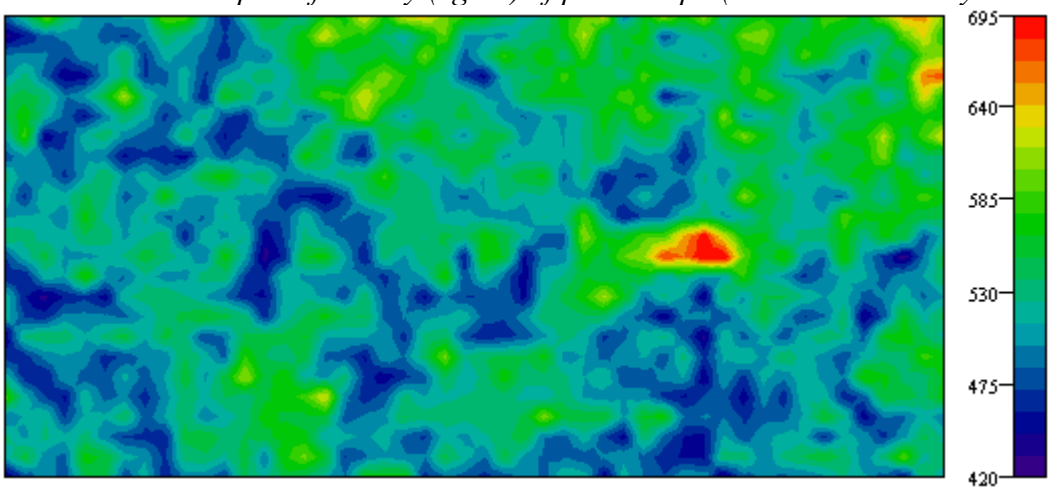

FigureA.63. *Three-dimensional plot of density (kg/m^3) of panel m3p5 (window size 50- by 50- mm).*

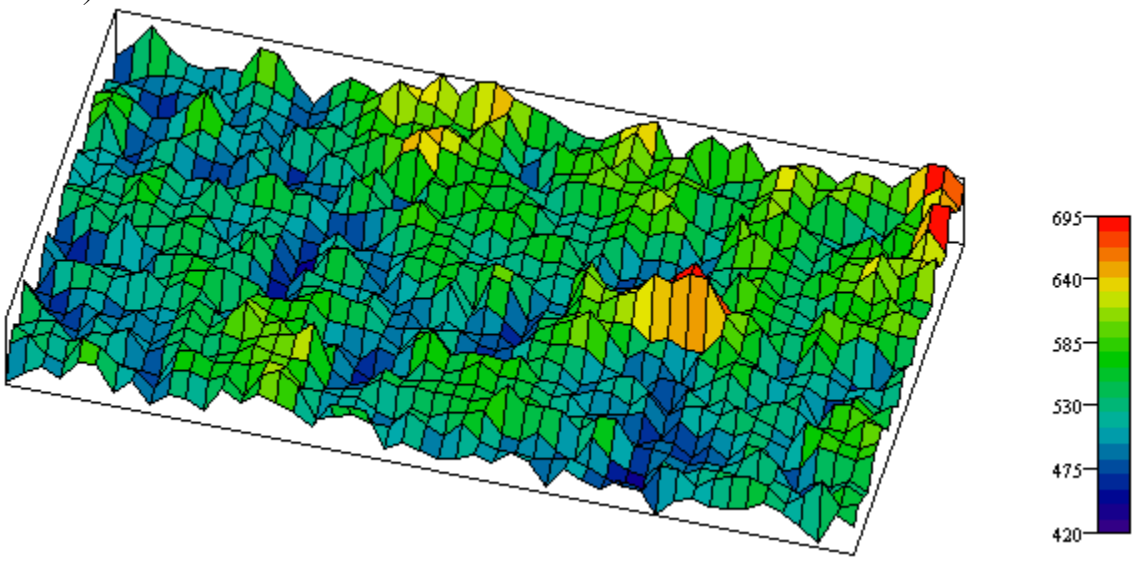

FigureA.64. *Contour plot of density (kg/m^3) of panel m3p5 (window size 50- by 50- mm).*

density	25	76	127	178	229	279	330	381	432	483	533	584	635	686	737	787	838	889	940	991	1041	1092	1143	1194	mm
25	561	522	571	518	554	581	556	577	598	568	607	541	524	558	523	523	577	599	603	602	564	515	591	577	
76	528	558	565	540	541	579	601	599	537	564	560	551	555	592	600	577	574	578	581	561	512	512	557	586	
127	564	561	527	557	525	568	527	584	533	577	588	510	510	509	590	572	566	628	630	549	534	534	559	498	
178	554	547	571	594	558	523	560	601	504	521	556	542	566	547	574	607	581	613	604	541	558	527	517	554	
229	532	572	594	536	629	561	567	547	491	542	544	561	581	592	629	567	594	570	609	526	517	535	582	617	
279	558	554	623	546	540	607	581	557	546	541	594	546	555	593	576	619	604	547	596	561	642	584	647	576	
330	543	545	542	534	582	552	537	534	557	520	589	535	523	528	543	595	585	576	565	522	511	539	606	592	
381	634	592	557	511	627	607	573	519	575	556	501	509	561	561	634	599	463	573	575	551	523	554	564	623	
432	588	589	531	532	568	547	557	546	567	566	540	494	495	536	604	588	515	544	608	566	552	606	584	633	
483	548	612	580	561	531	551	593	582	536	517	510	530	502	533	613	522	603	572	572	519	539	540	549	575	
533	564	528	550	552	606	537	577	564	543	604	562	557	469	533	537	546	590	577	590	546	590	582	561	575	
584	632	543	563	560	580	561	543	515	586	578	543	490	523	498	536	565	539	533	558	601	514	536	499	578	
635	545	502	519	551	497	528	552	487	541	560	555	504	531	512	529	562	579	593	604	539	515	499	528	598	
686	549	532	558	521	474	529	578	566	528	510	590	529	601	565	595	590	599	603	530	600	555	545	585	585	
737	557	595	475	510	504	508	536	604	481	502	551	550	550	601	623	518	564	545	534	555	531	551	564	563	
787	575	588	538	570	546	539	553	562	581	554	564	606	612	611	607	544	561	566	603	553	472	574	569	589	
838	543	563	534	556	567	512	521	589	536	549	593	572	579	586	577	619	580	633	545	536	518	549	616	588	
889	583	557	549	538	571	548	577	533	520	508	544	523	550	538	566	548	530	523	545	523	516	540	530	559	
940	519	579	530	526	515	544	543	511	549	530	530	497	495	548	561	556	511	543	565	533	522	545	511	485	
991	544	566	548	565	561	546	527	476	549	534	543	538	551	574	526	541	555	603	537	516	539	513	507	497	
1041	504	518	549	498	562	559	532	531	489	538	506	542	519	529	521	548	538	551	535	613	585	553	503	524	
1092	529	477	541	507	544	547	516	536	522	576	467	494	514	559	504	519	529	508	555	536	588	561	555	584	
1143	533	507	540	508	498	540	509	526	521	495	514	498	499	513	511	528	530	562	562	564	522	492	491	567	
1194	514	532	536	548	488	461	493	531	568	501	560	534	490	561	577	500	545	529	519	604	569	489	549	541	
1245	567	547	538	524	500	477	524	489	503	442	457	494	538	564	568	575	584	565	557	536	505	493	529	536	
1295	485	495	508	509	562	535	488	504	474	456	455	497	597	585	561	595	540	559	537	544	522	530	569	546	
1346	550	557	498	538	551	495	531	506	490	489	515	528	547	552	541	575	595	567	535	571	498	537	577	523	
1397	470	515	546	569	486	513	534	541	536	446	510	535	527	498	514	584	578	603	505	567	502	536	515	553	
1448	455	549	508	514	509	509	525	567	522	506	537	524	541	523	435	475	492	568	534	548	570	505	509	512	
1499	479	458	491	517	520	498	492	516	495	500	524	556	542	545	509	549	579	544	540	572	524	583	555	537	
1549	474	494	517	498	504	514	540	472	534	529	555	557	577	577	596	521	529	501	536	496	515	596	550	511	
1600	486	505	540	517	520	538	509	557	566	486	491	508	531	557	603	571	487	544	557	543	505	512	504	523	
1651	500	552	548	555	557	508	470	483	498	510	570	513	489	597	576	562	510	575	576	537	497	454	468	532	
1702	501	522	516	502	519	519	479	470	495	572	584	489	552	566	582	594	552	566	527	559	546	553	485	499	
1753	455	505	598	539	510	520	498	554	527	560	592	517	506	561	564	558	519	514	571	571	565	543	562	551	
1803	506	524	521	504	541	535	527	552	535	538	550	515	492	562	556	543	480	537	528	547	577	557	557	518	
1854	518	491	481	534	507	527	500	529	512	506	551	487	546	539	528	543	541	579	512	528	558	541	539	518	
1905	514	513	528	489	484	473	568	507	520	522	484	479	490	500	557	528	546	598	555	558	526	484	523	515	
1956	464	480	489	507	505	560	548	543	540	542	460	485	513	583	575	507	582	534	538	541	515	563	542	553	
2007	488	488	471	539	496	539	522	534	534	532	506	516	547	538	579	535	543	540	523	516	495	528	560	512	
2057	470	537	521	521	516	522	526	529	527	534	541	550	528	523	554	532	532	537	552	522	473	487	484	545	
2108	470	517	547	522	555	571	546	568	496	542	569	553	550	579	578	560	527	542	537	529	451	482	566	521	
2159	426	463	484	513	522	543	552	485	482	527	603	572	555	532	552	511	494	483	518	536	501	508	550	552	
2210	461	500	557	493	524	535	556	509	569	541	549	591	566	520	627	554	511	536	542	554	573	513	518	529	
2261	476	494	543	522	542	511	530	531	579	550	543	524	537	517	547	517	537	569	535	558	598	516	548	503	
2311	505	561	589	538	537	609	576	532	556	591	582	578	567	521	548	523	564	568	549	532	585	575	488	476	
2362	466	597	539	529	529	597	632	583	581	583	613	610	610	629	585	554	538	564	574	537	534	581	543	554	
2413	510	570	537	526	541	563	564	587	570	611	563	594	561	565	553	561	557	575	569	551	529	592	478	532	

mm

Figure A.65. *Data plot of density (kg/m^3) of panel m3p6 (window size 50- by 50-mm)*

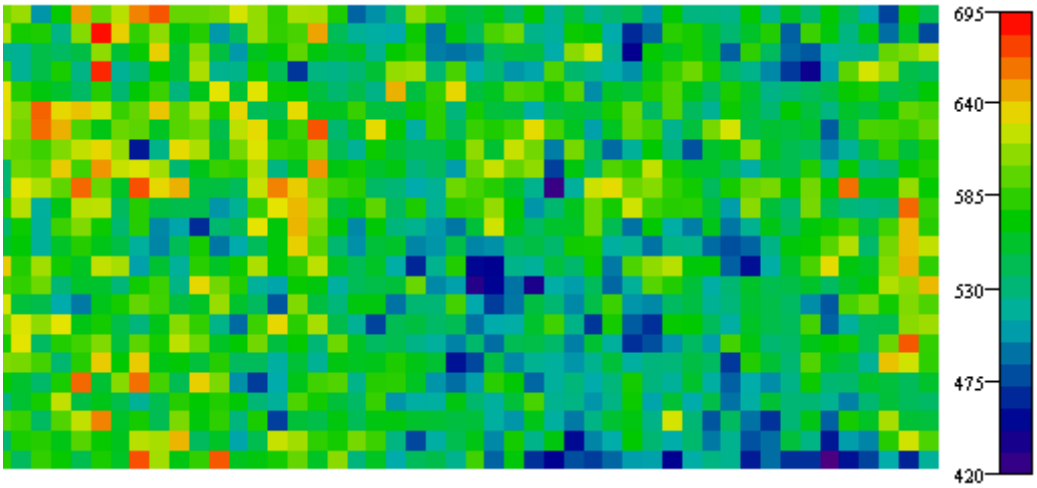

Figure A.66. *Color-scale plot of density (kg/m^3) of panel m3p6 (window size 50- by 50- mm).*

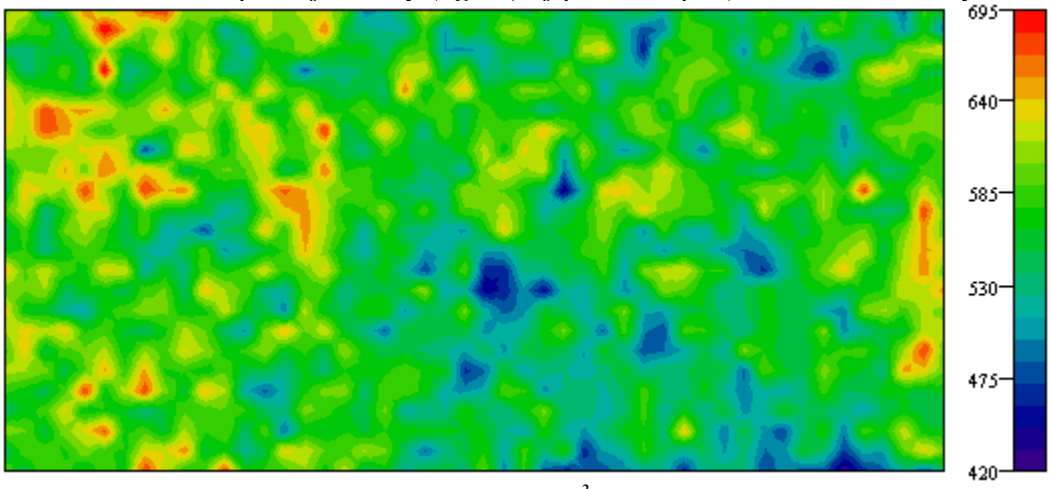

FigureA.67. *Three-dimensional plot of density (kg/m^3) of panel m3p6 (window size 50- by 50- mm).*

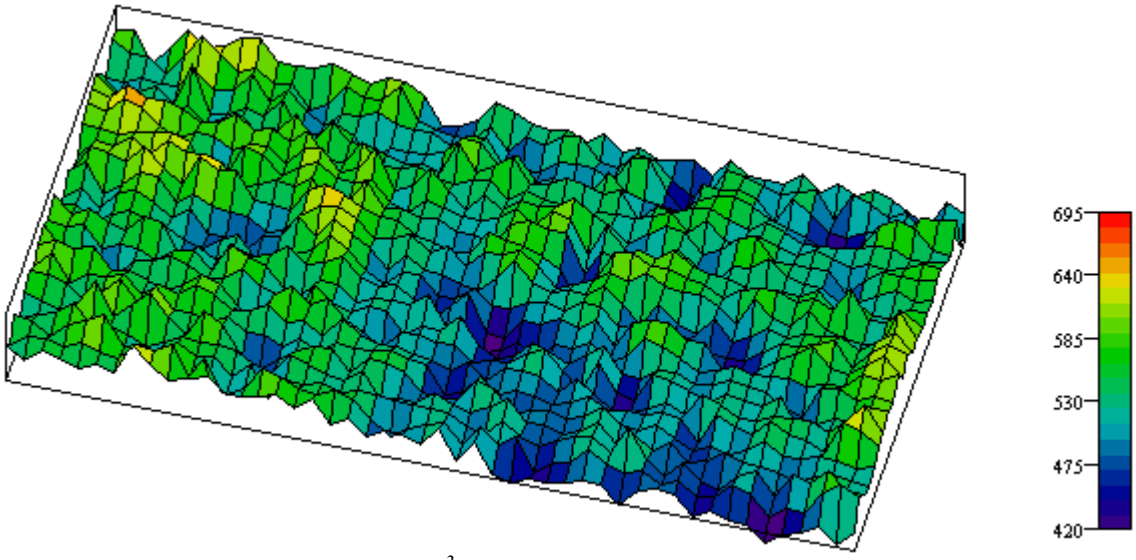

FigureA.68. *Contour plot of density (kg/m^3) of panel m3p6 (window size 50- by 50- mm).*

Appendix B

Histograms and PDF

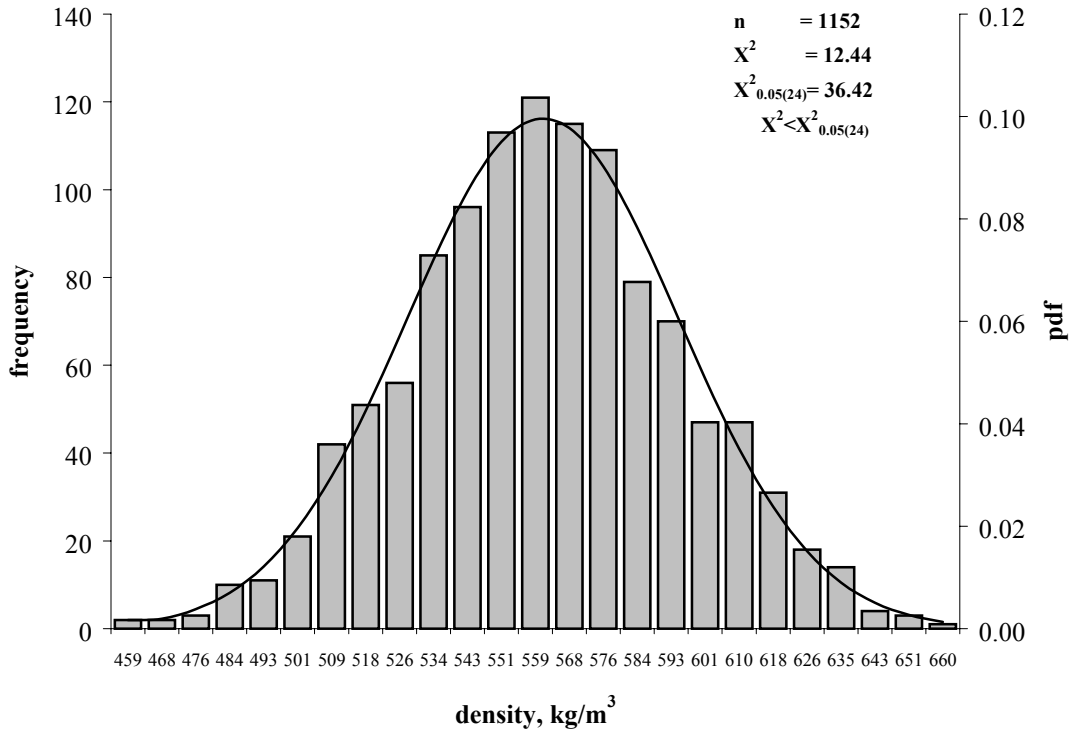

Figure B.1. *Histogram and PDF for density data values of m1p1.*

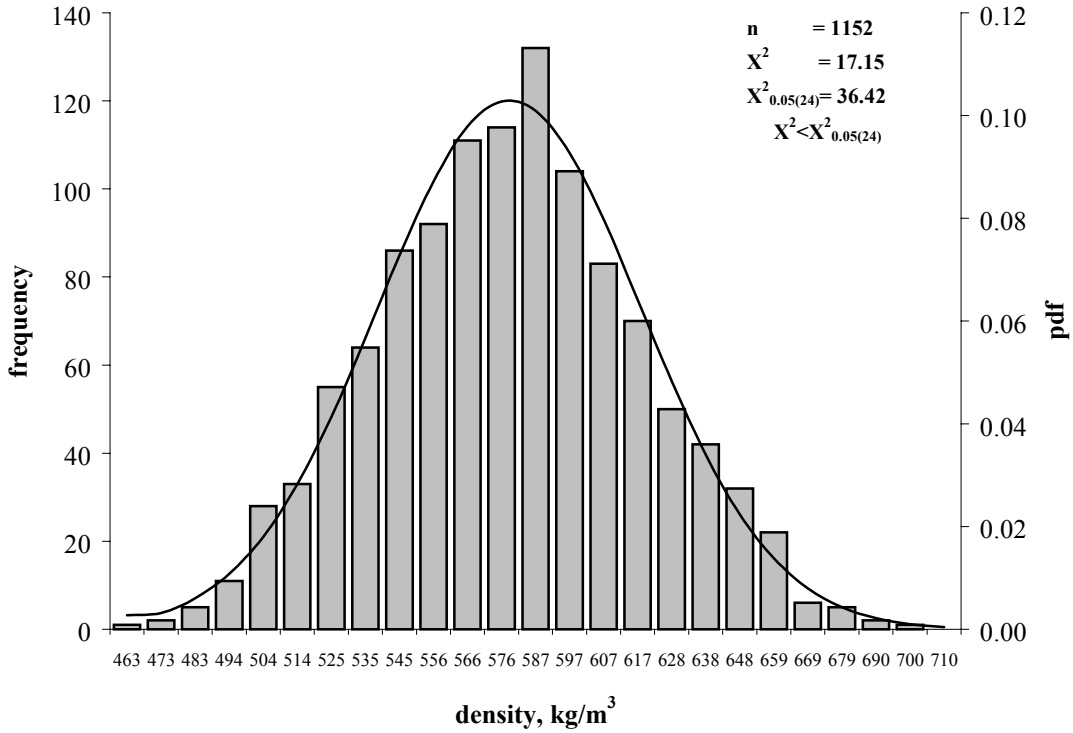

Figure B.2. *Histogram and PDF for density data values of m1p2.*

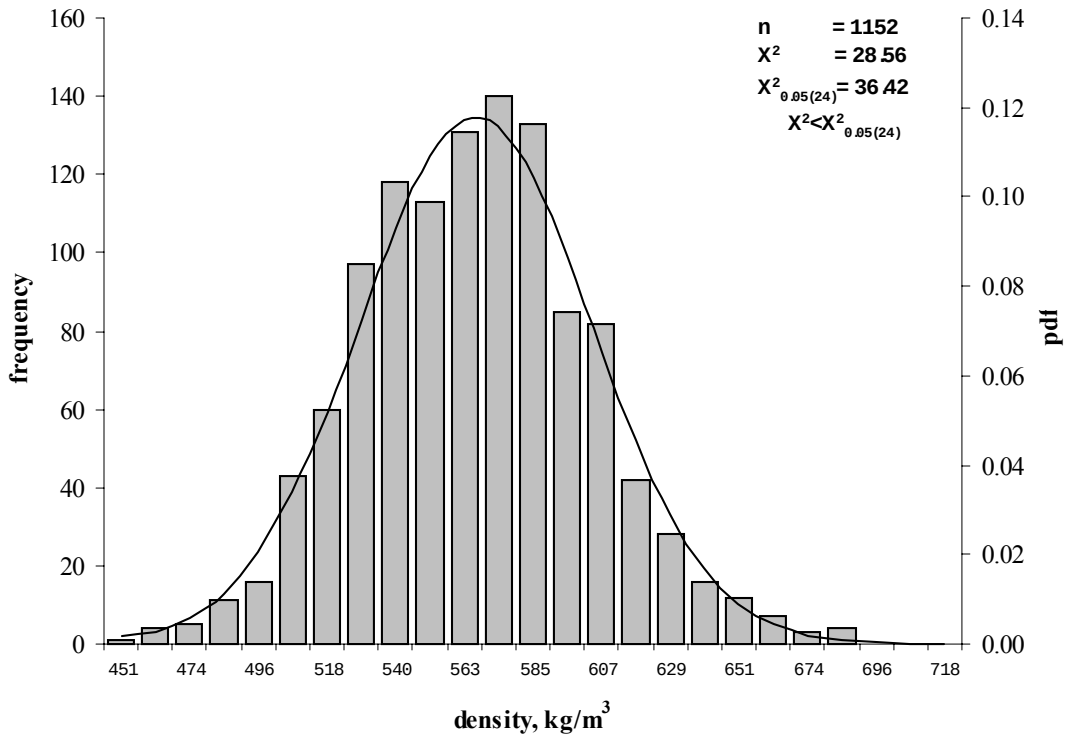

Figure B.3. *Histogram and PDF for density data values of m1p4.*

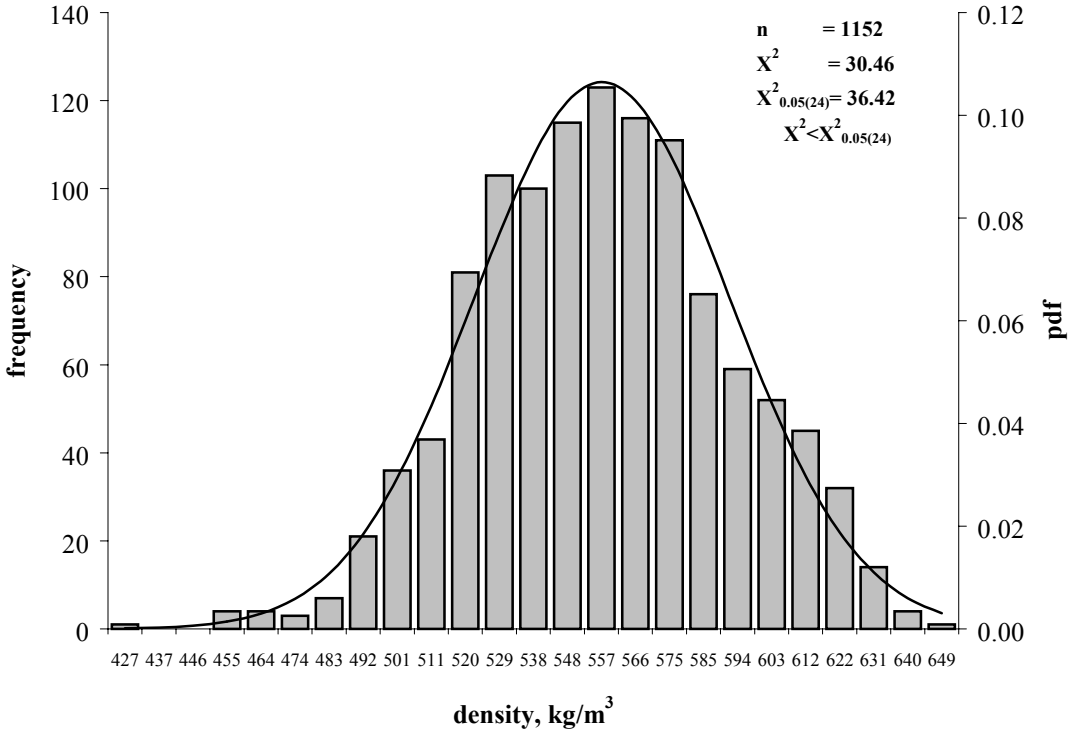

Figure B.4. *Histogram and PDF for density data values of m1p5.*

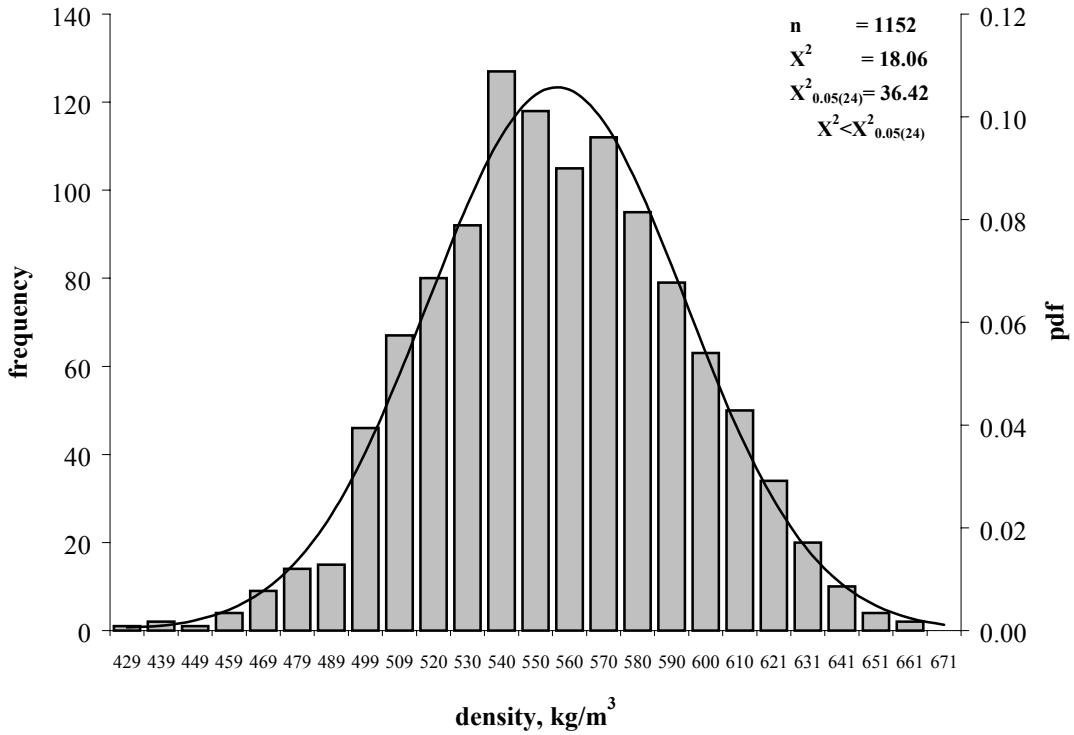

Figure B.5. *Histogram and PDF for density data values of m1p6.*

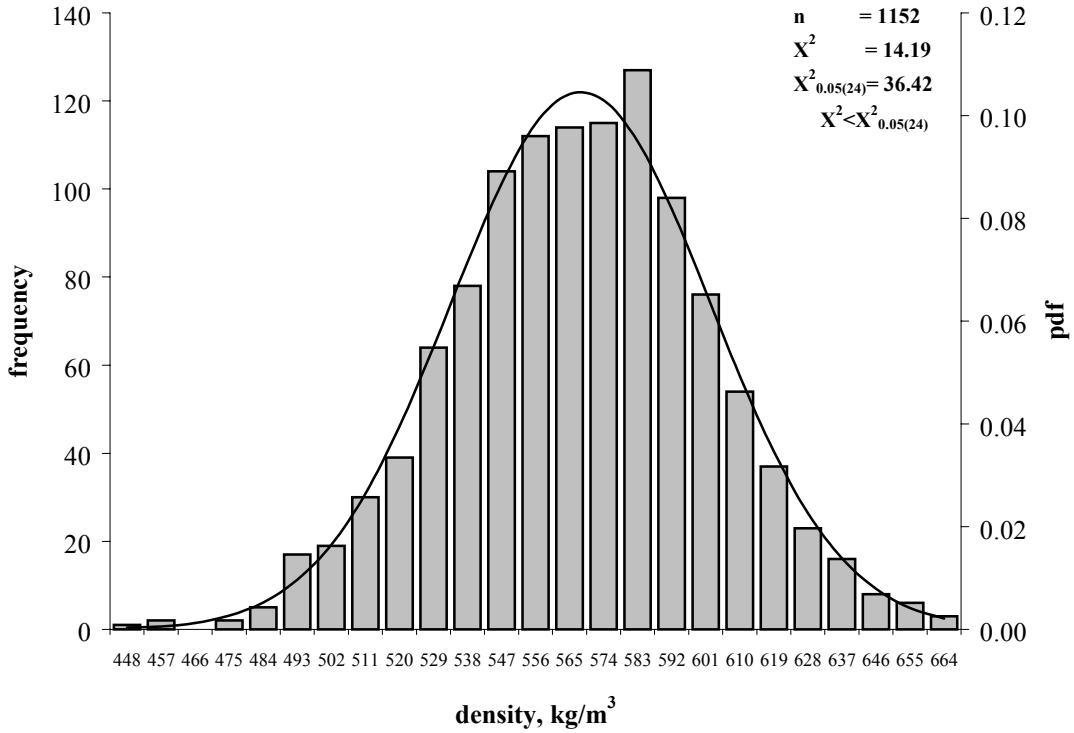

Figure B.6. *Histogram and PDF for density data values of m2p1.*

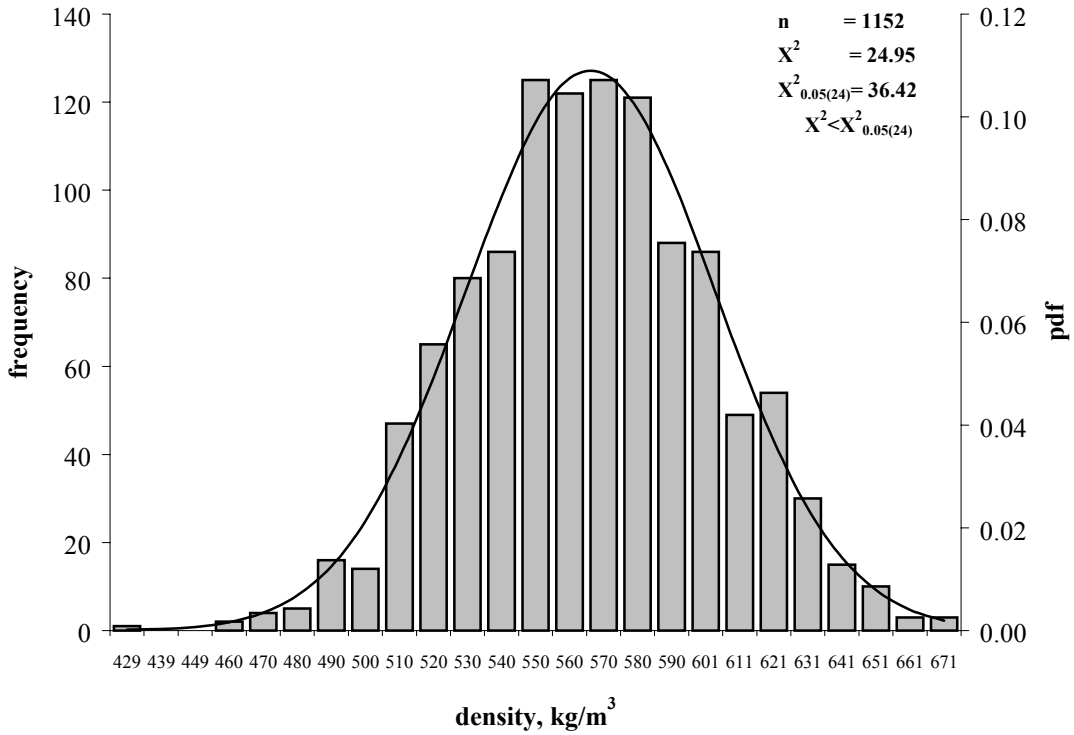

Figure B.7. *Histogram and PDF for density data values of m2p2.*

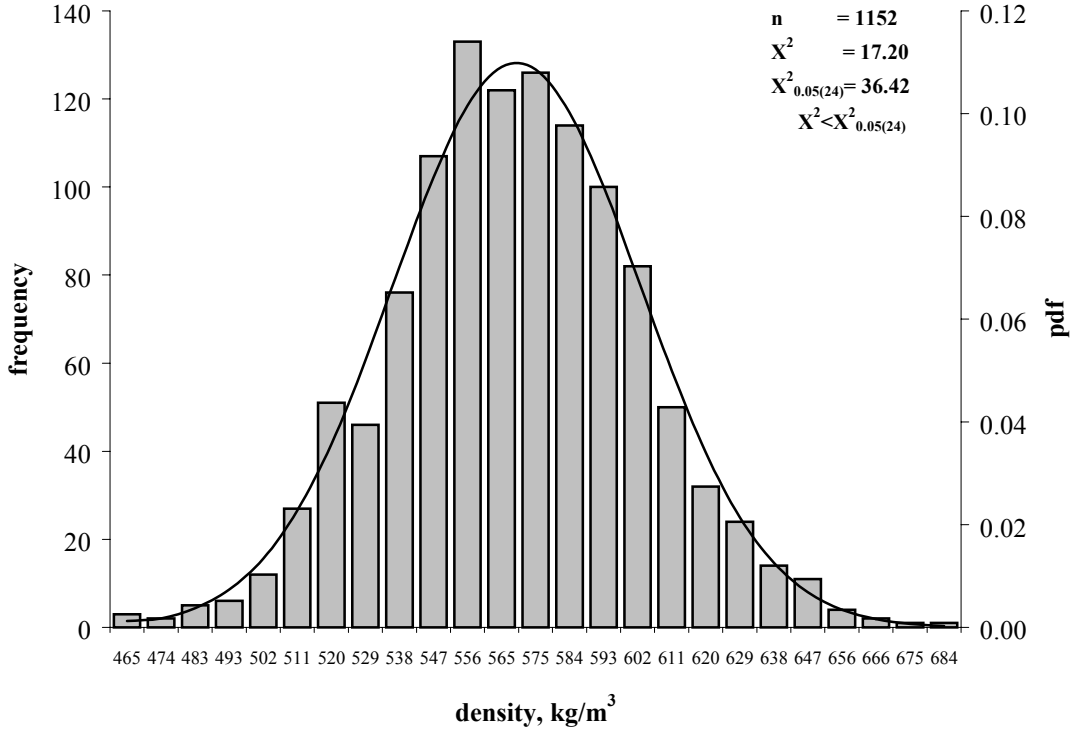

Figure B.8. *Histogram and PDF for density data values of m2p3.*

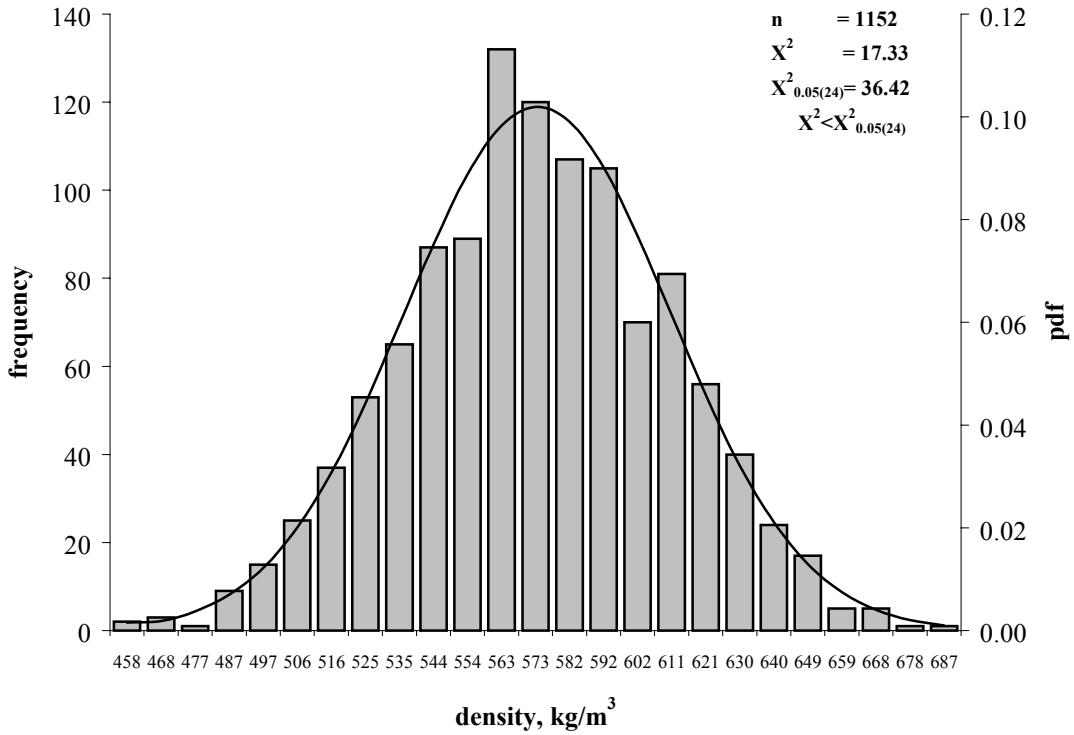

Figure B.9. *Histogram and PDF for density data values of m2p4.*

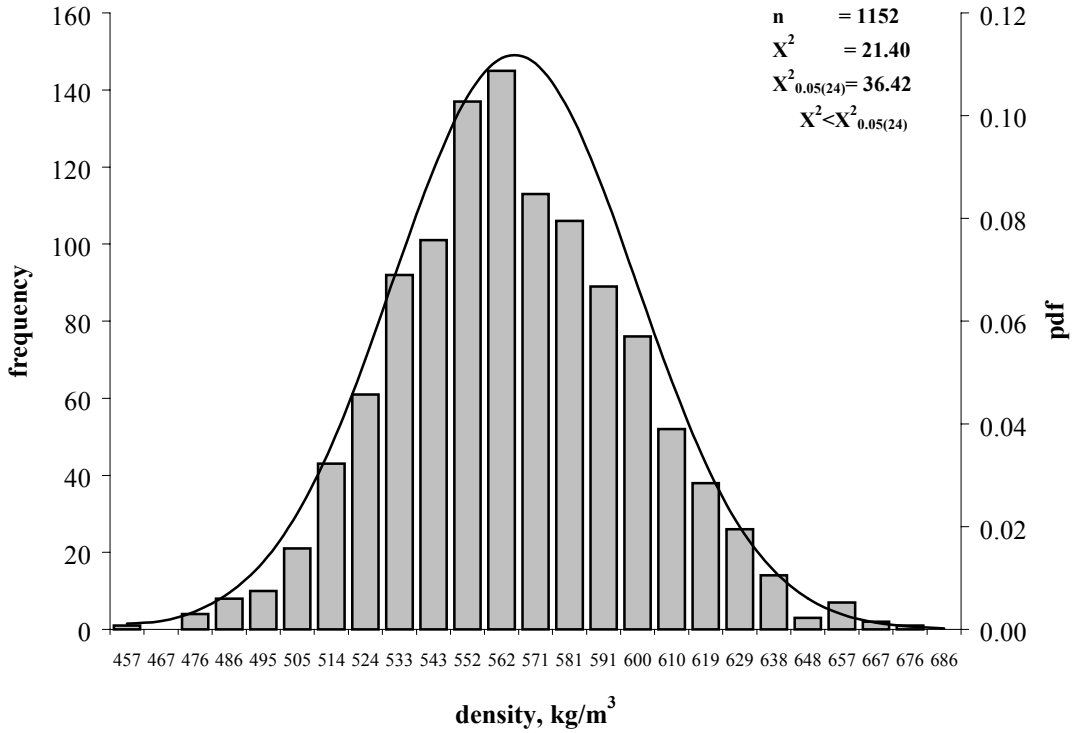

Figure B.10. *Histogram and PDF for density data values of m2p5.*

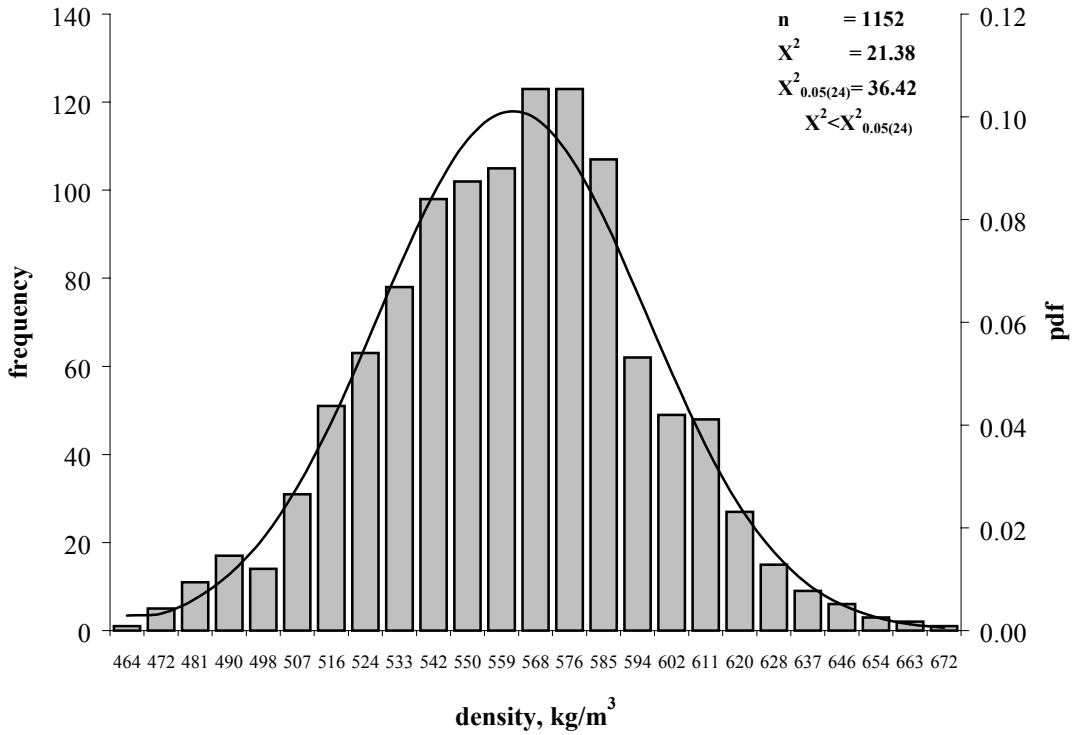

Figure B.11. *Histogram and PDF for density data values of m2p6.*

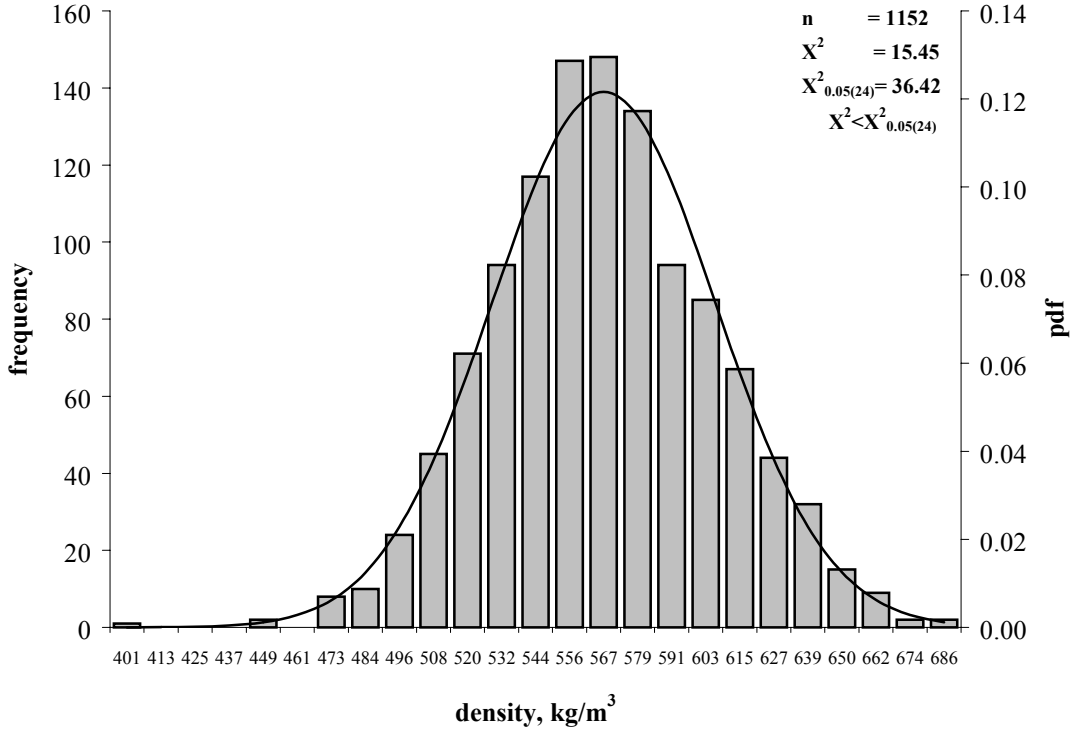

Figure B.12. *Histogram and PDF for density data values of m3p1.*

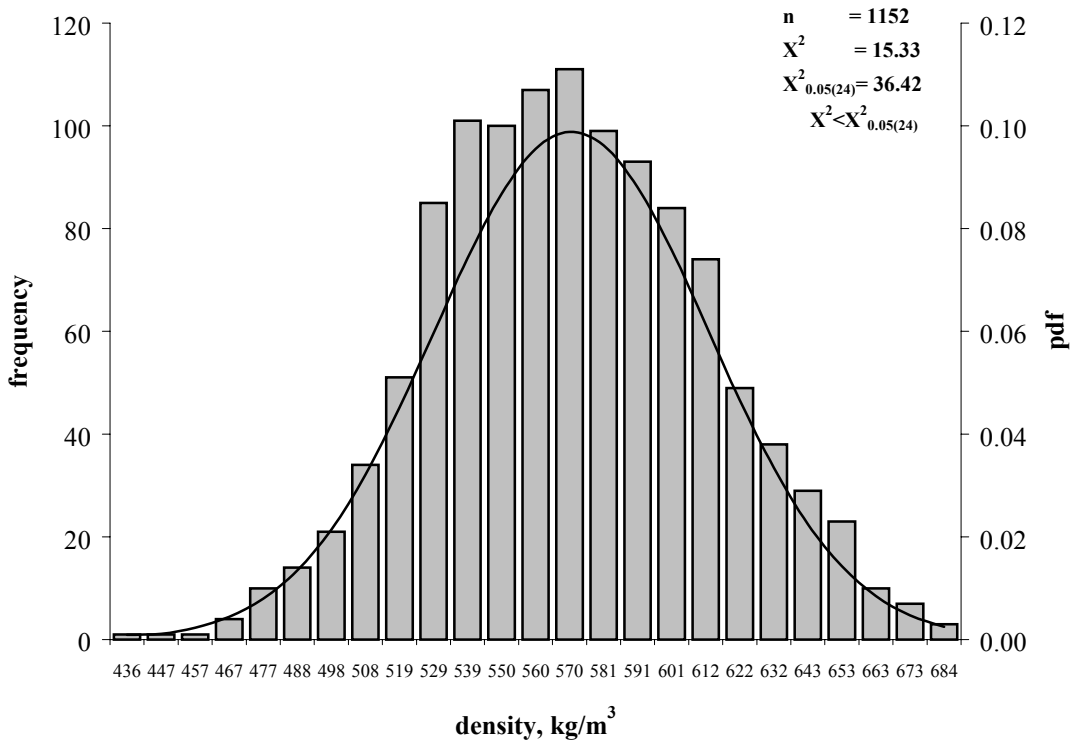

Figure B.13. *Histogram and PDF for density data values of m3p2.*

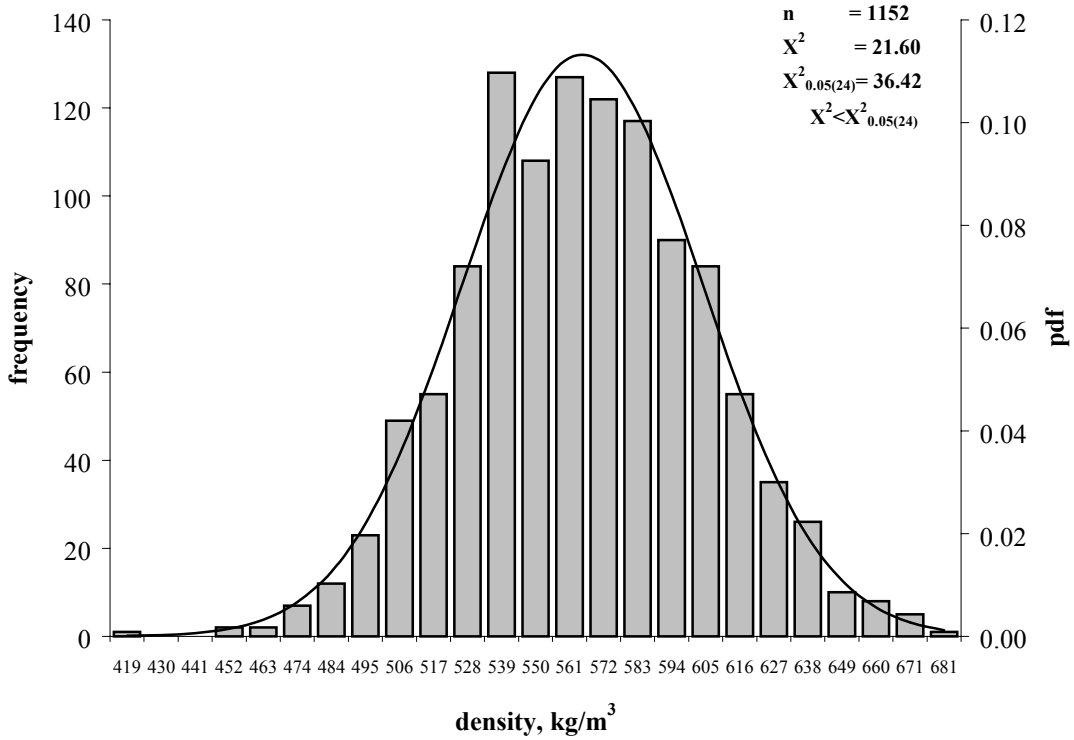

Figure B.14. *Histogram and PDF for density data values of m3p3.*

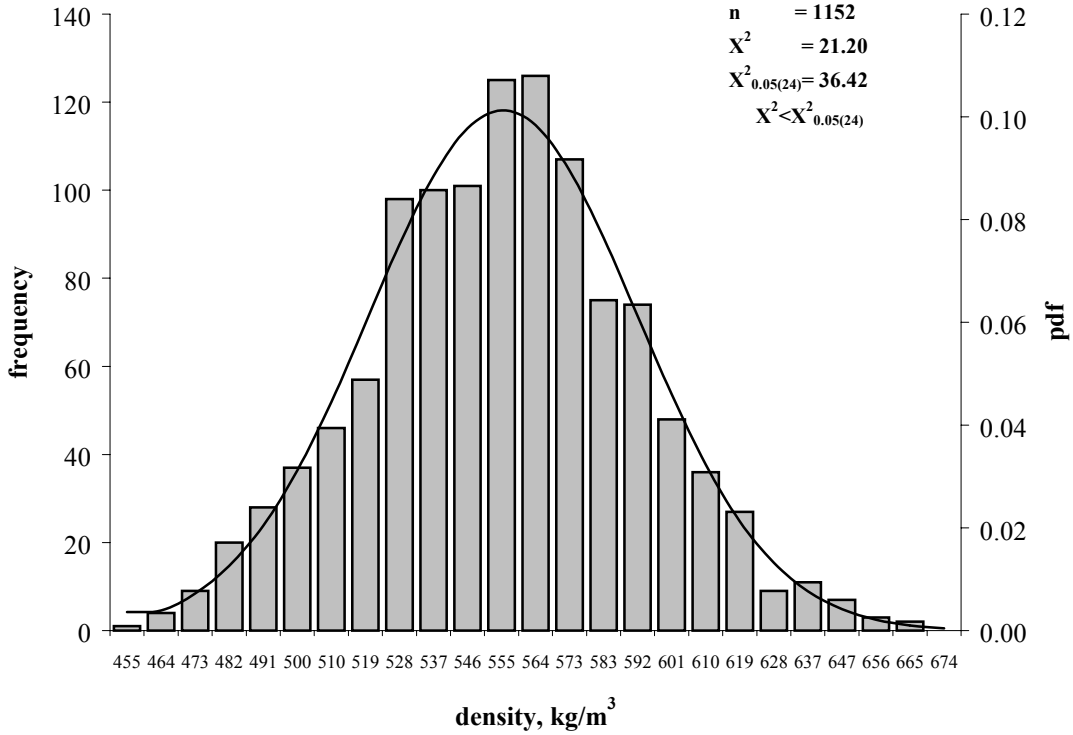

Figure B.15. *Histogram and PDF for density data values of m3p4.*

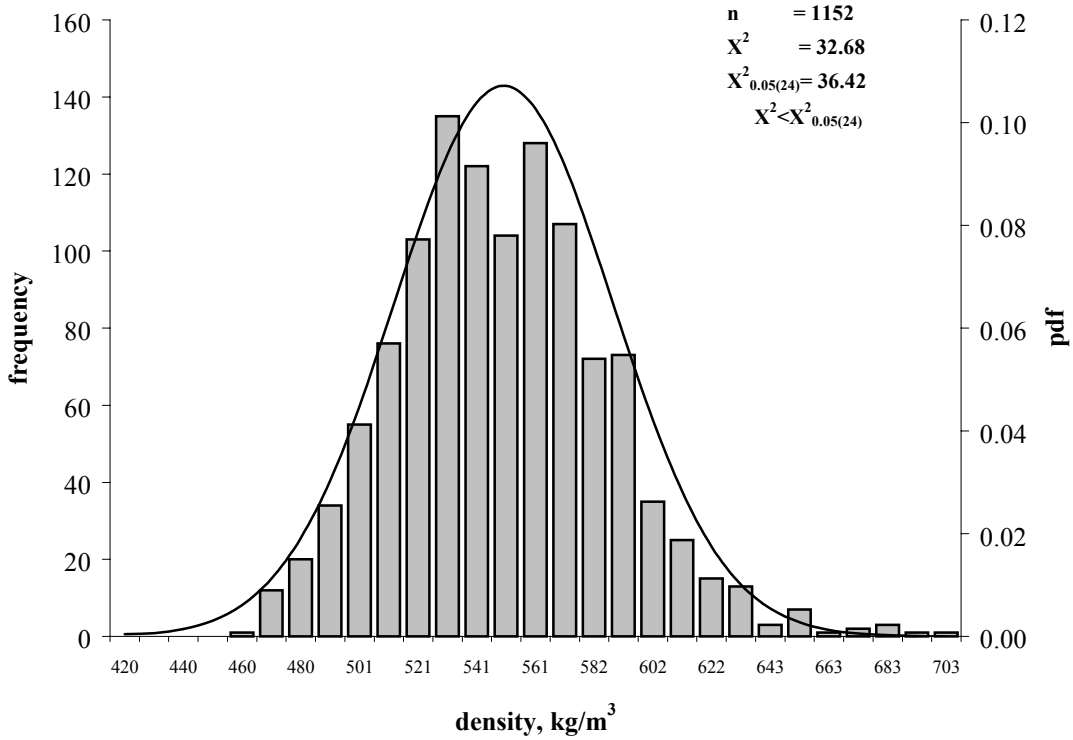

Figure B.16. *Histogram and PDF for density data values of m3p5.*

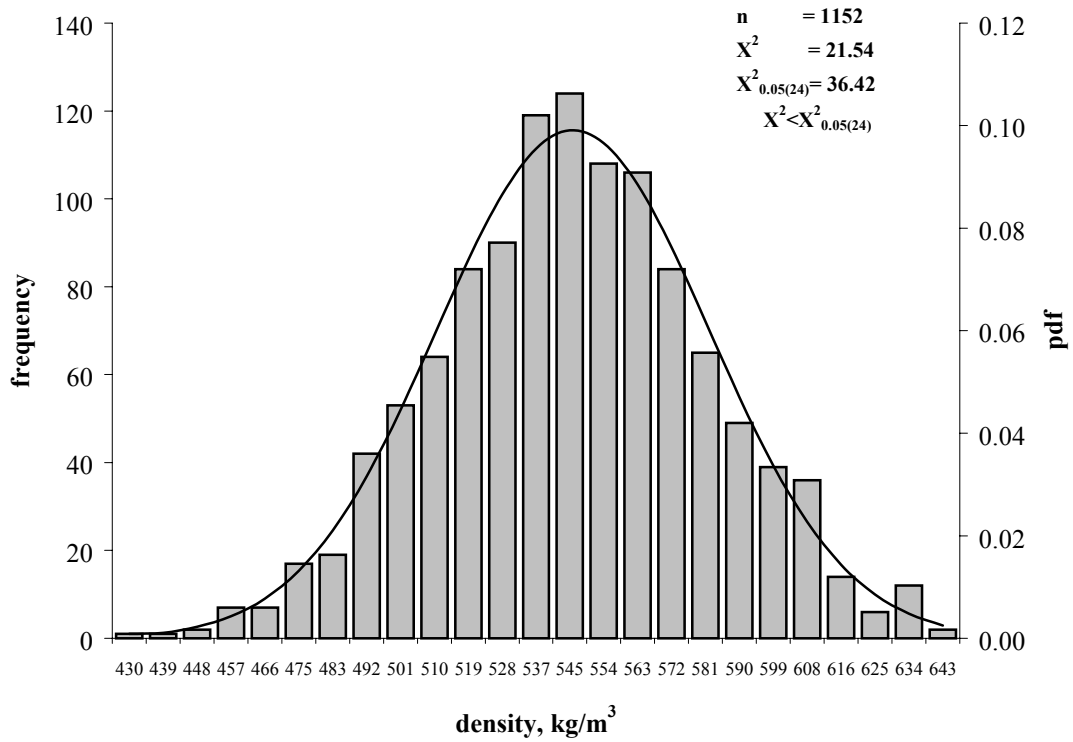

Figure B.17. *Histogram and PDF for density data values of m3p6.*

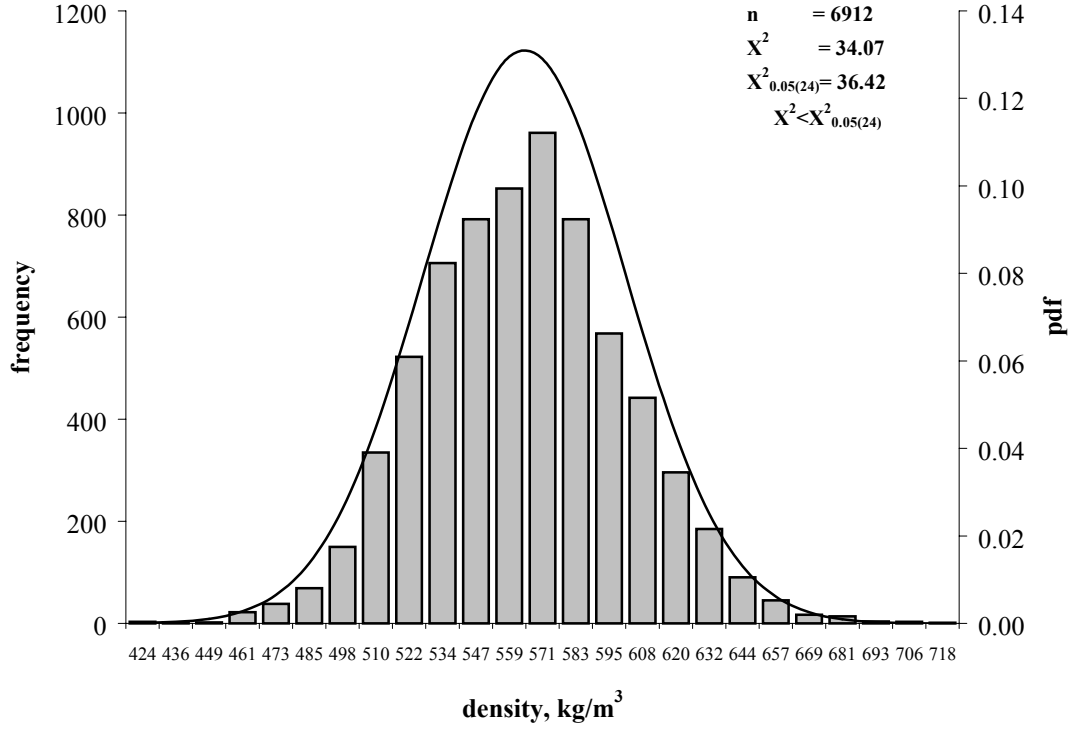

Figure B.18. *Histogram and PDF for density data values of master-1.*

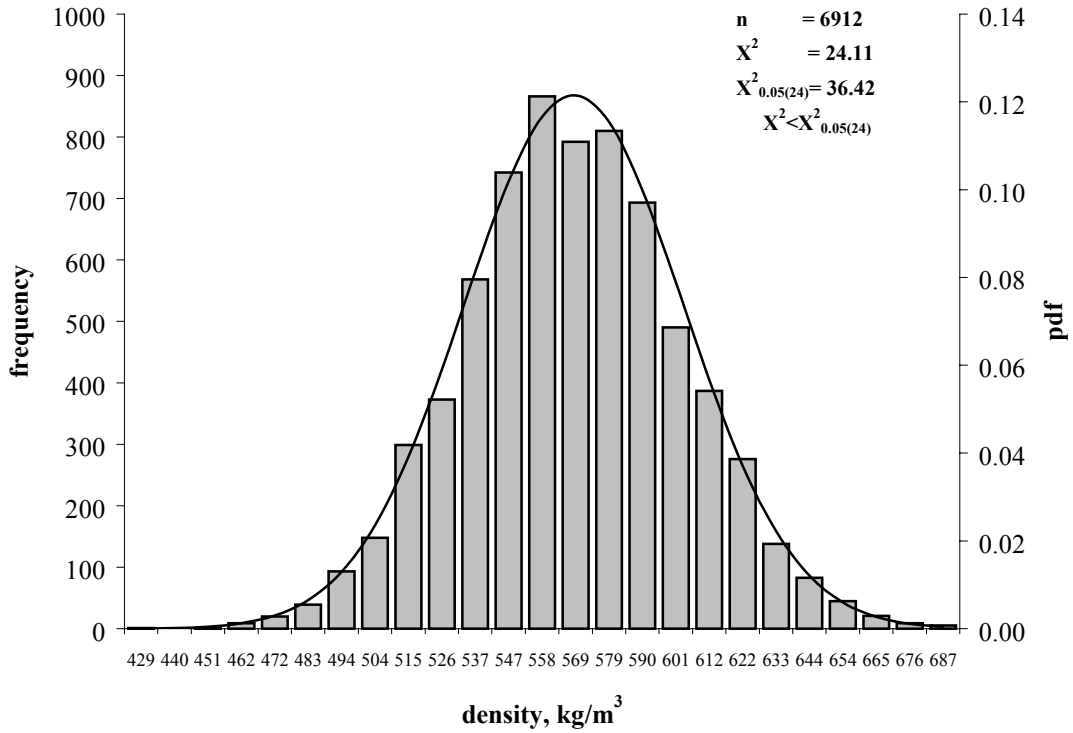

Figure B.19. *Histogram and PDF for density data values of master-2.*

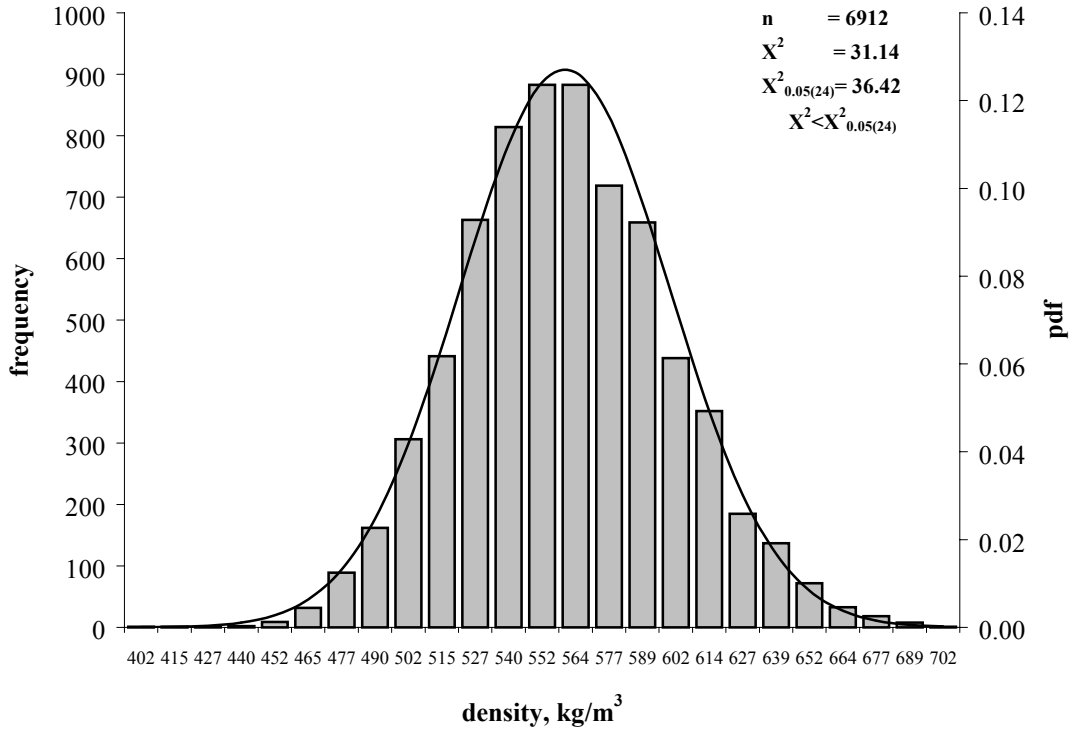

Figure B.20. *Histogram and PDF for density data values of master-3.*

Appendix C

Proportional Effect

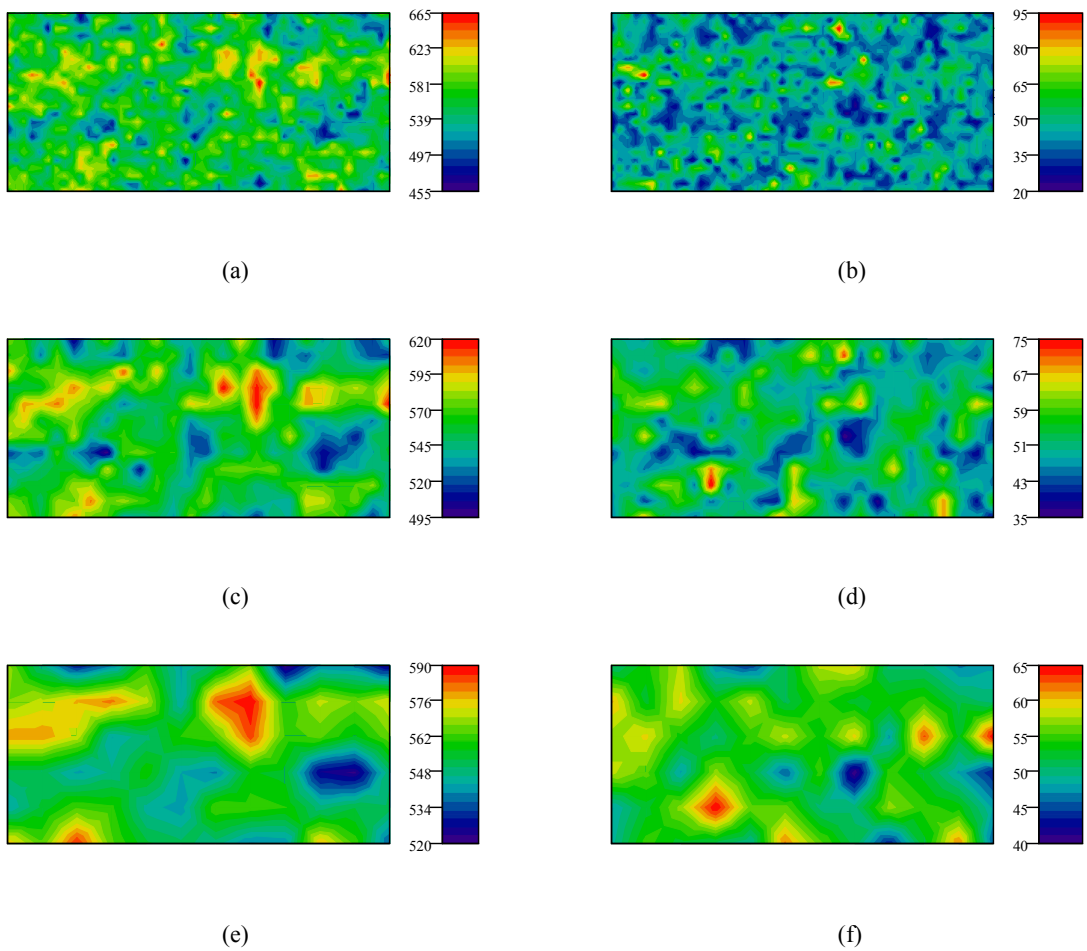

Figure C.1. *m1p1: (a) contour plot of density for windows size 50- by 50-mm, (b) contour plot of standard deviation for windows size 50- by 50-mm, (c) contour plot of density for windows size 100- by 100-mm, (d) contour plot of standard deviation for windows size 100- by 100-mm, (e) contour plot of density for windows size 200- by 200-mm, and (f) contour plot of standard deviation for windows size 200- by 200-mm.*

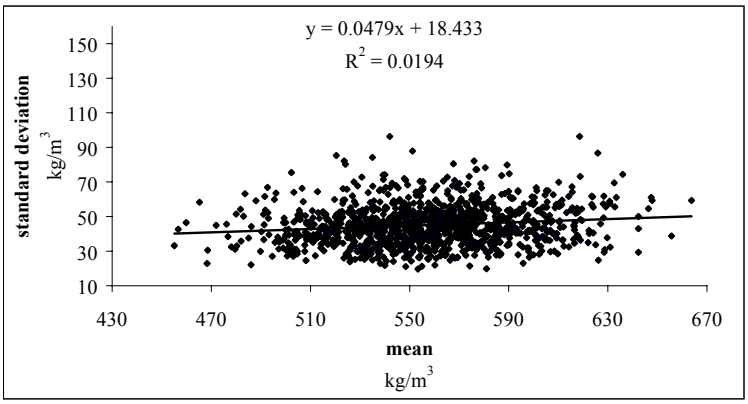

(a)

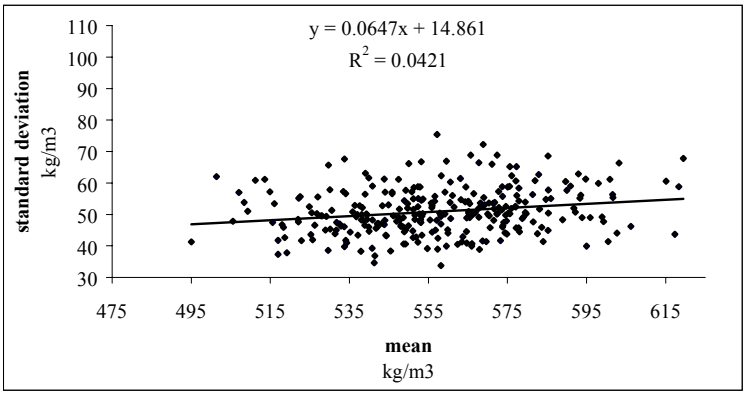

(b)

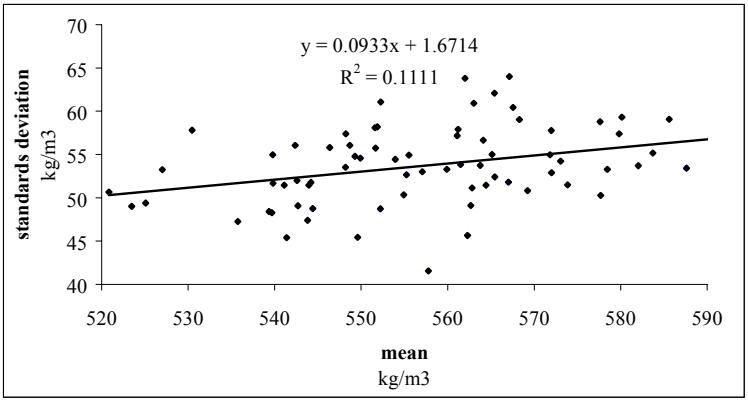

(c)

Figure C.2. *Proportional effect m1p1: (a) windows size 50- by 50-mm, (b) window size 100- by 100-mm, and (c) windows size 200- by 200-mm.*

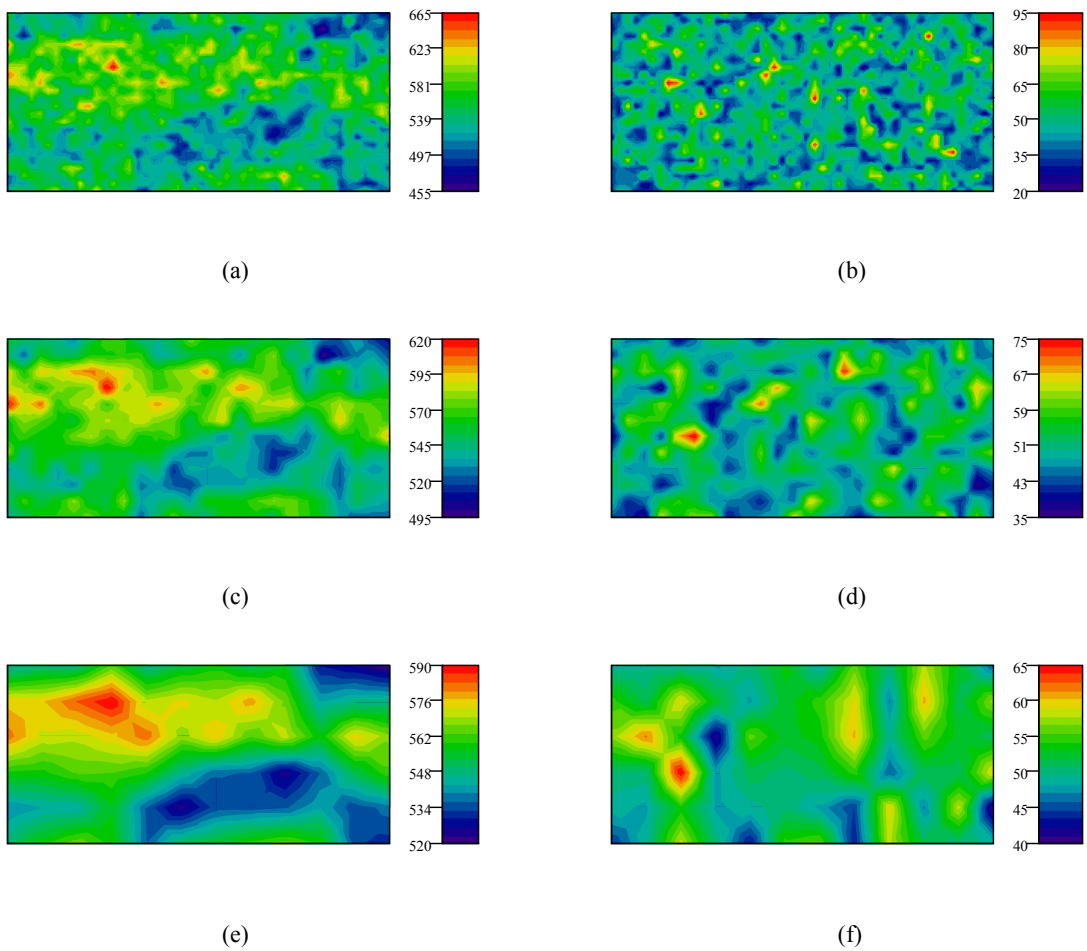

Figure C.3. *m1p2: (a) contour plot of density for windows size 50- by 50-mm, (b) contour plot of standard deviation for windows size 50- by 50-mm, (c) contour plot of density for windows size 100- by 100-mm, (d) contour plot of standard deviation for windows size 100- by 100-mm, (e) contour plot of density for windows size 200- by 200-mm, and (f) contour plot of standard deviation for windows size 200- by 200-mm.*

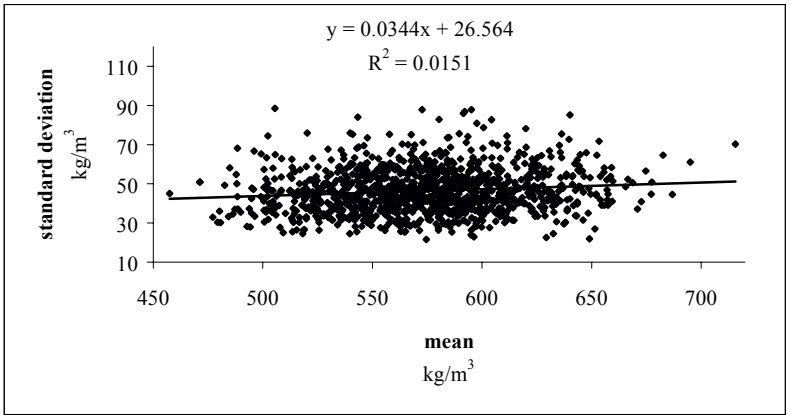

(a)

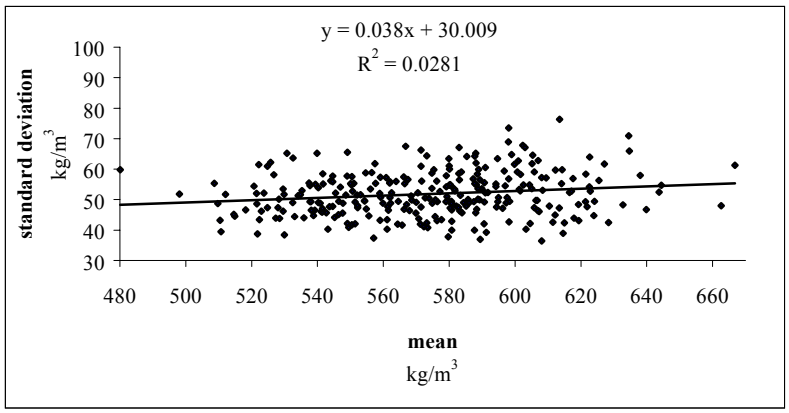

(b)

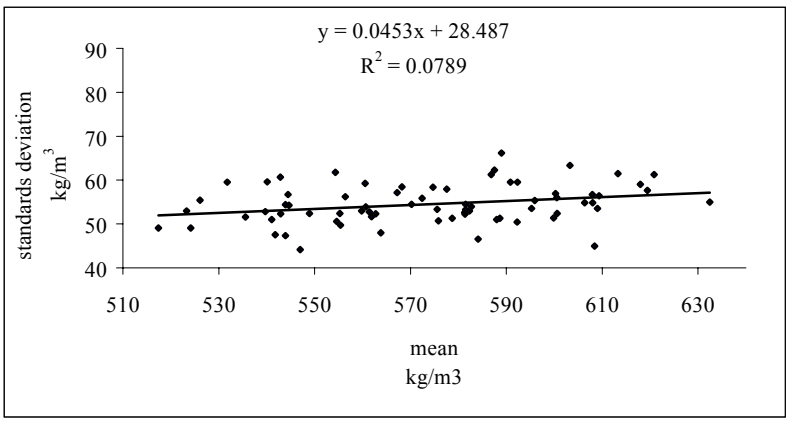

(c)

Figure C.4. *Proportional effect m1p2: (a) windows size 50- by 50-mm, (b) window size 100- by 100-mm, and (c) windows size 200- by 200-mm.*

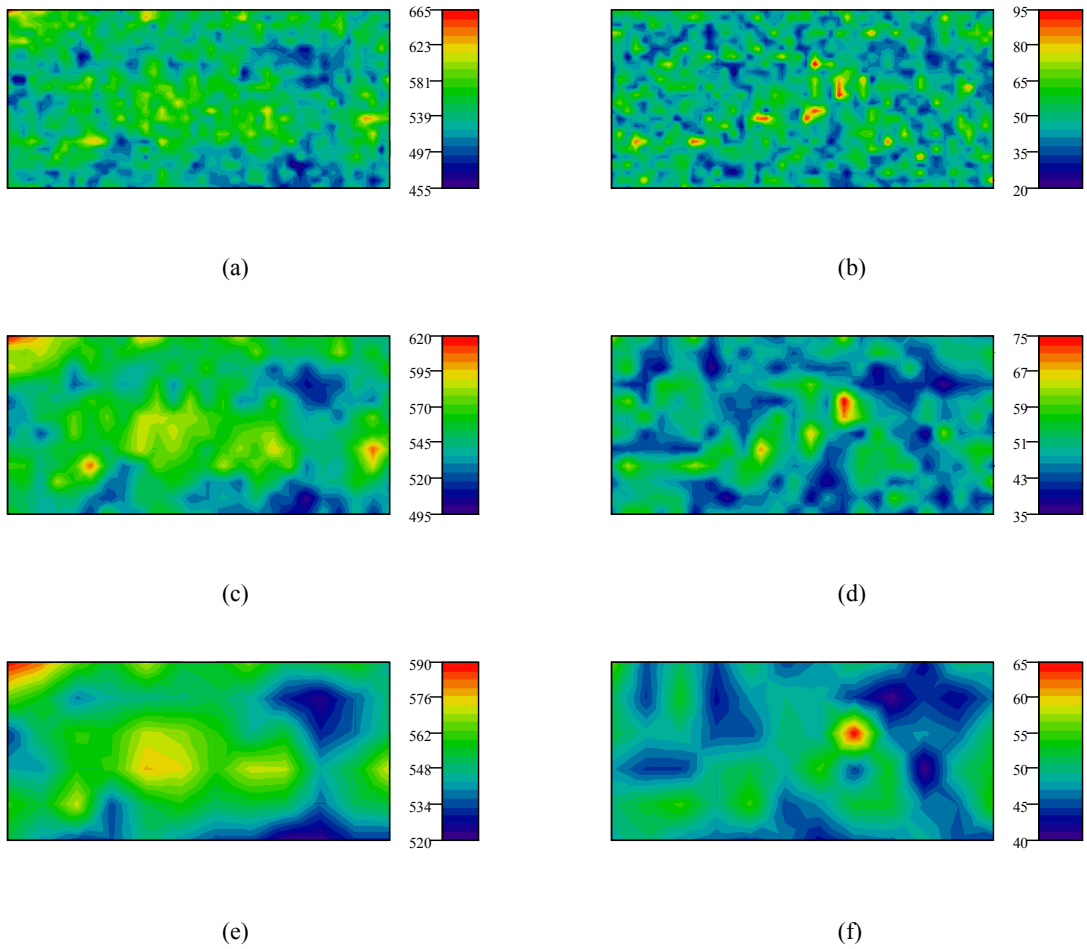

Figure C.5. *m1p4: (a) contour plot of density for windows size 50- by 50-mm, (b) contour plot of standard deviation for windows size 50- by 50-mm, (c) contour plot of density for windows size 100- by 100-mm, (d) contour plot of standard deviation for windows size 100- by 100-mm, (e) contour plot of density for windows size 200- by 200-mm, and (f) contour plot of standard deviation for windows size 200- by 200-mm.*

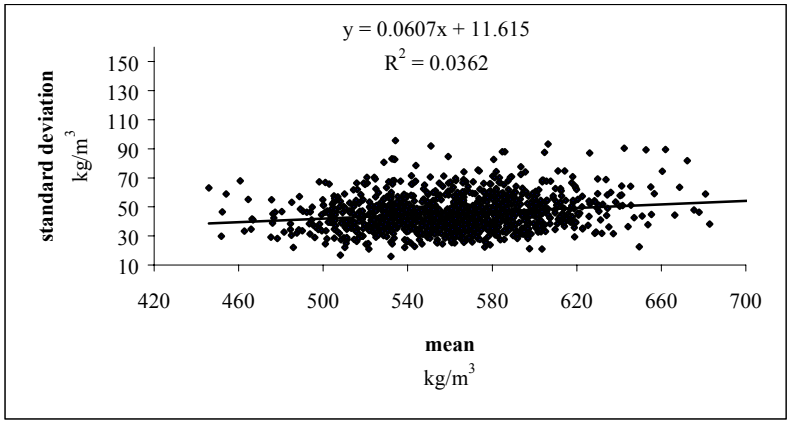

(a)

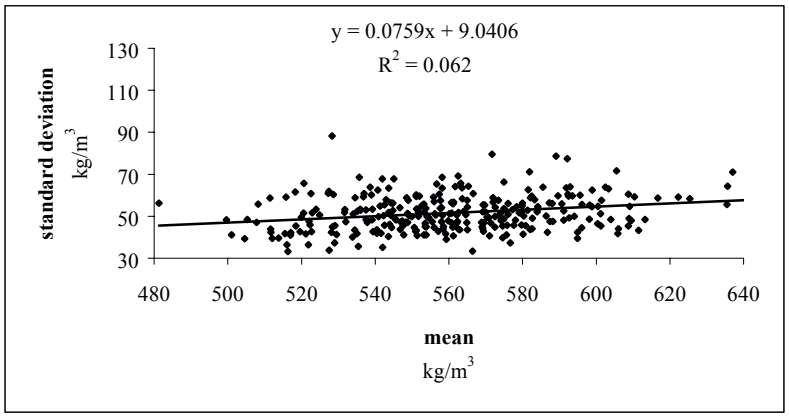

(b)

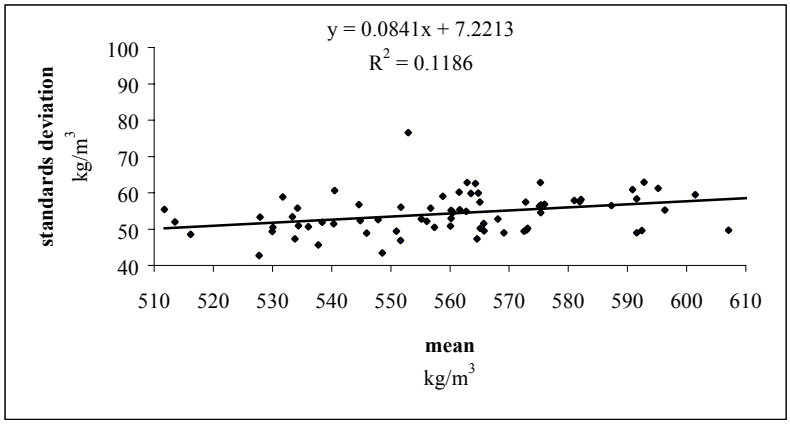

(c)

Figure C.6. *Proportional effect m1p4: (a) windows size 50- by 50-mm, (b) window size 100- by 100-mm, and (c) windows size 200- by 200-mm.*

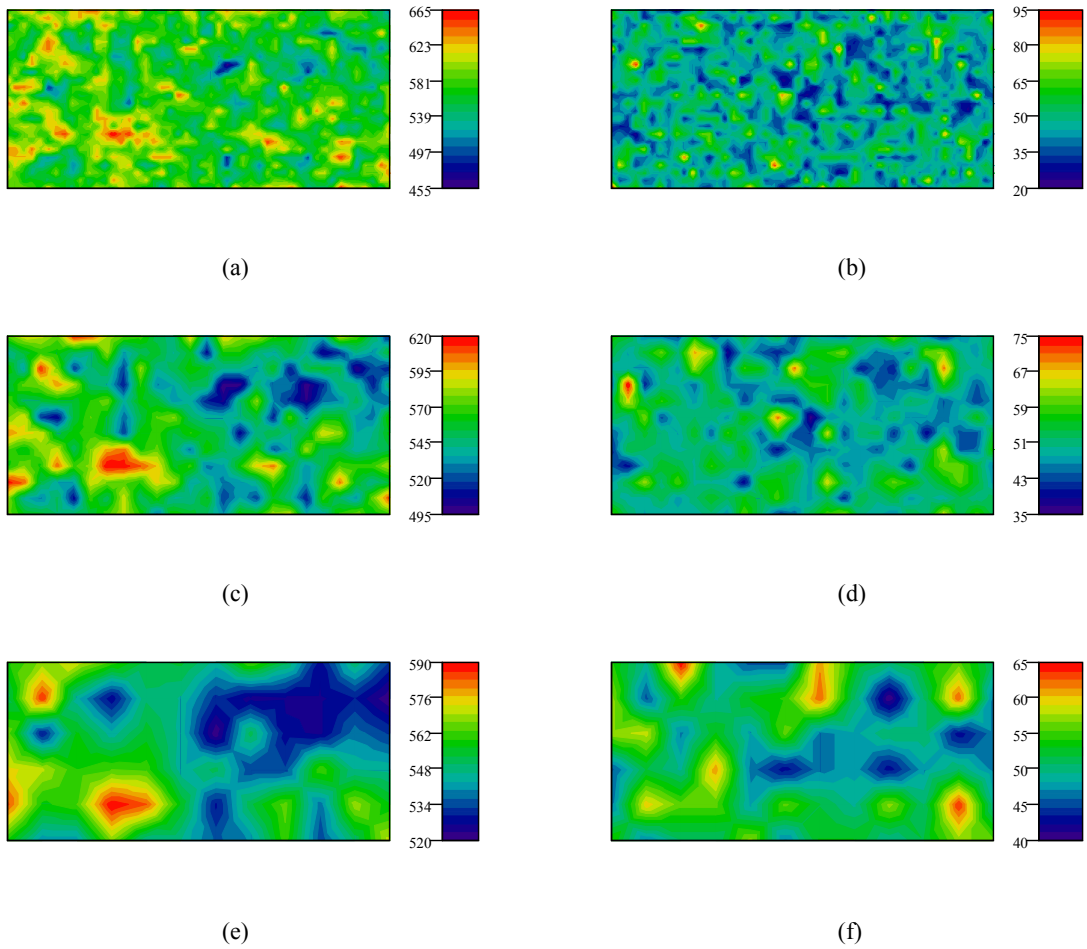

FigureC.7. m1p5: *(a) contour plot of density for windows size 50- by 50-mm, (b) contour plot of standard deviation for windows size 50- by 50-mm, (c) contour plot of density for windows size 100- by 100-mm, (d) contour plot of standard deviation for windows size 100- by 100-mm, (e) contour plot of density for windows size 200- by 200-mm, and (f) contour plot of standard deviation for windows size 200- by 200-mm.*

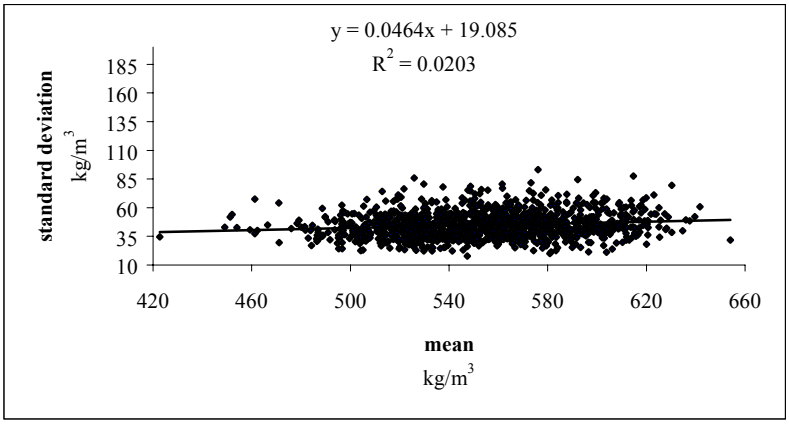

(a)

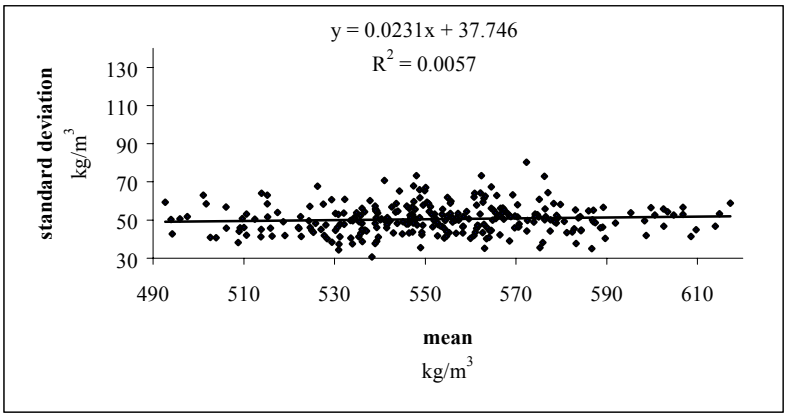

(b)

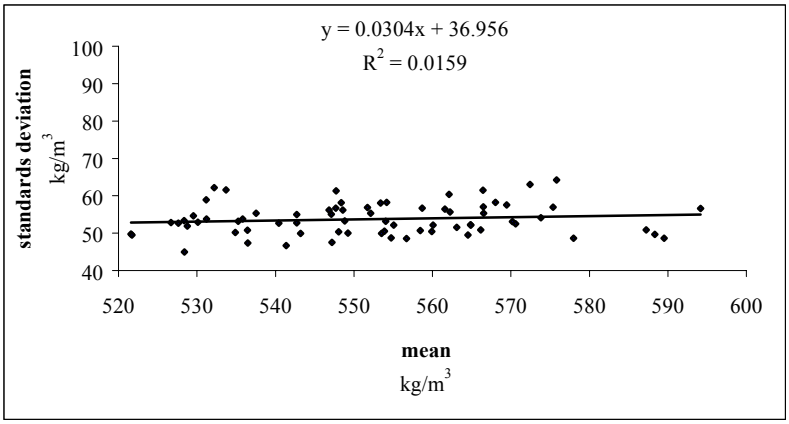

(c)

Figure C.8. *Proportional effect m1p5: (a) windows size 50- by 50-mm, (b) window size 100- by 100-mm, and (c) windows size 200- by 200-mm.*

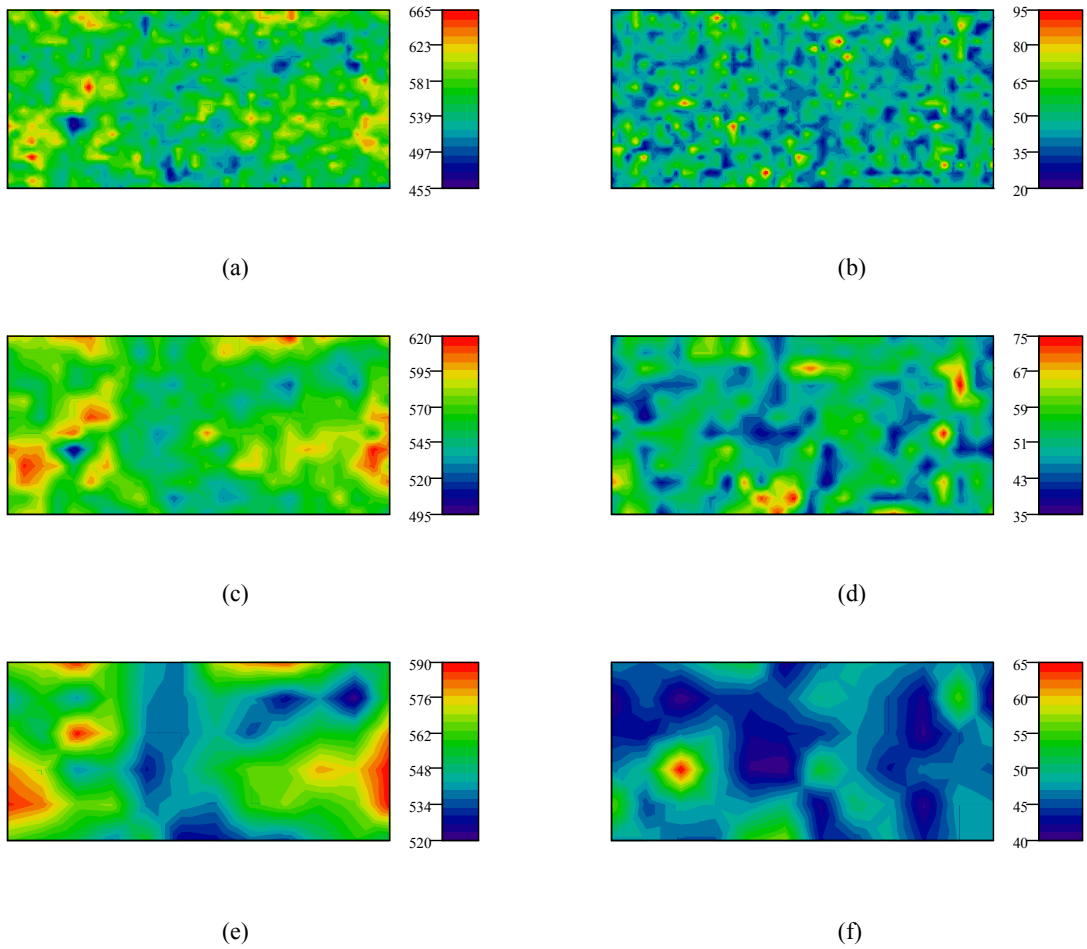

FigureC.9. *m1p6: (a) contour plot of density for windows size 50- by 50-mm, (b) contour plot of standard deviation for windows size 50- by 50-mm, (c) contour plot of density for windows size 100- by 100-mm, (d) contour plot of standard deviation for windows size 100- by 100-mm, (e) contour plot of density for windows size 200- by 200-mm, and (f) contour plot of standard deviation for windows size 200- by 200-mm.*

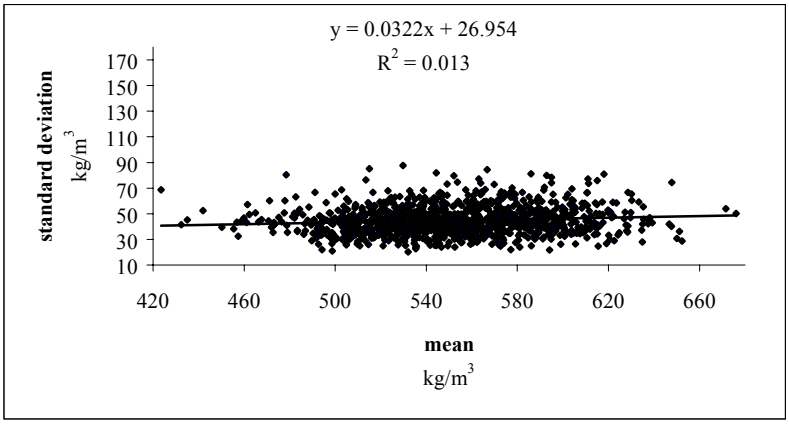

(a)

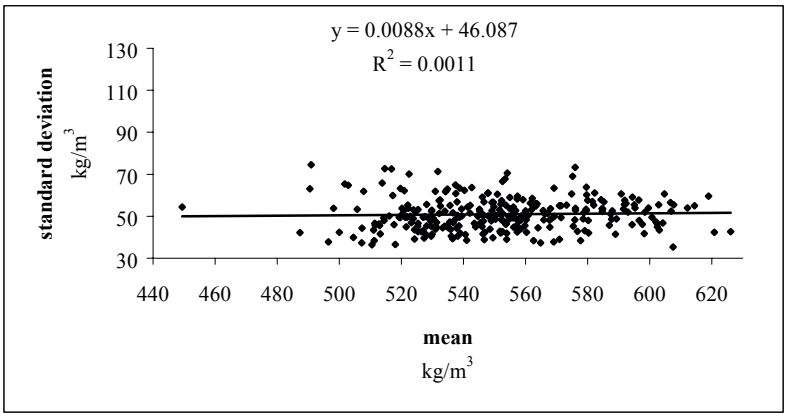

(b)

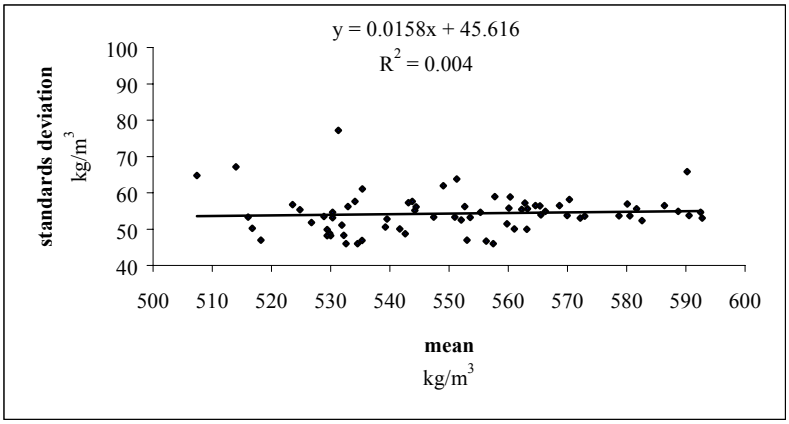

(c)

Figure C.10. *Proportional effect m1p6: (a) windows size 50- by 50-mm, (b) window size 100- by 100-mm, and (c) windows size 200- by 200-mm.*

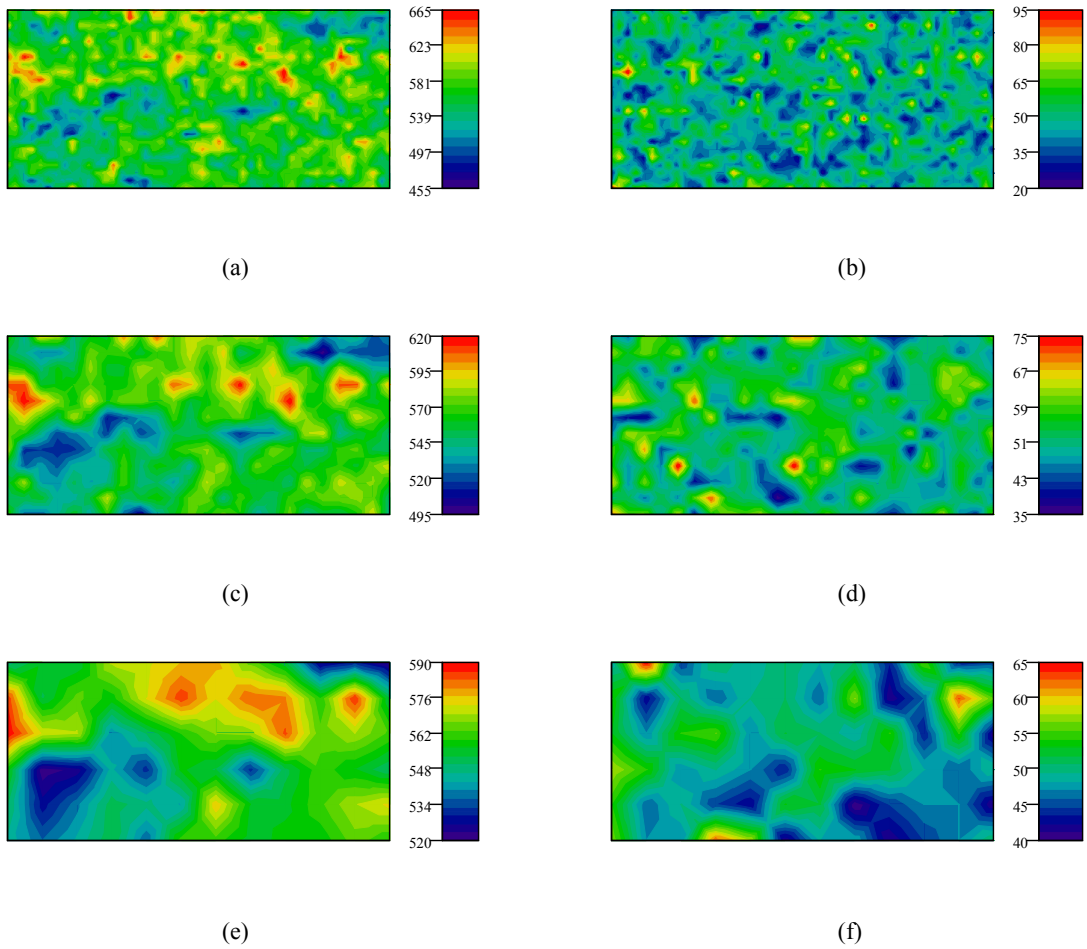

Figure C.11. *m2p1: (a) contour plot of density for windows size 50- by 50-mm, (b) contour plot of standard deviation for windows size 50- by 50-mm, (c) contour plot of density for windows size 100- by 100-mm, (d) contour plot of standard deviation for windows size 100- by 100-mm, (e) contour plot of density for windows size 200- by 200-mm, and (f) contour plot of standard deviation for windows size 200- by 200-mm.*

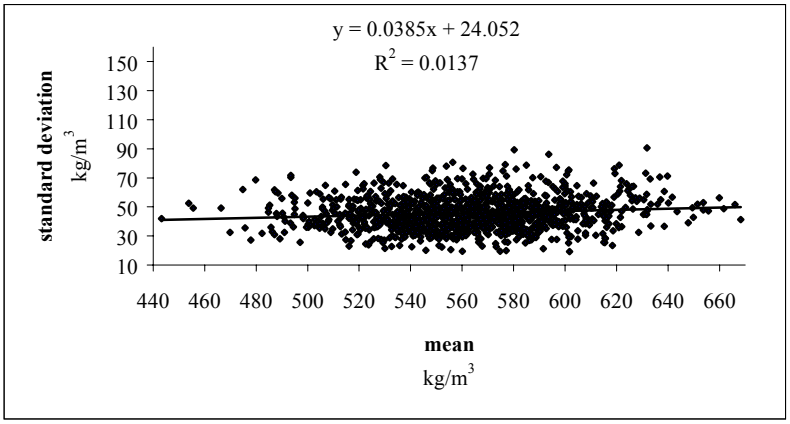

(a)

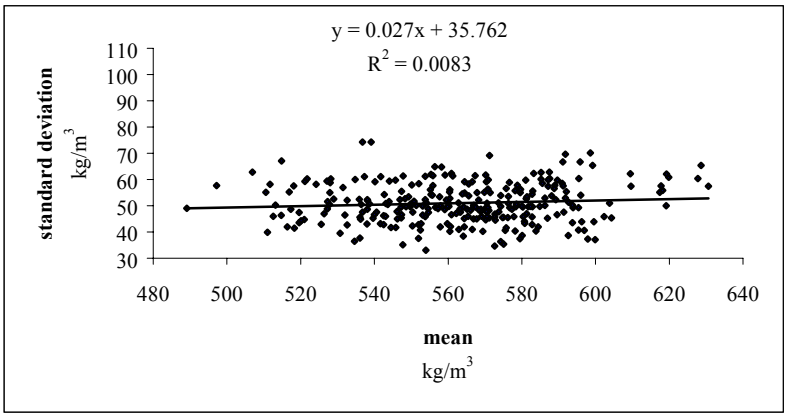

(b)

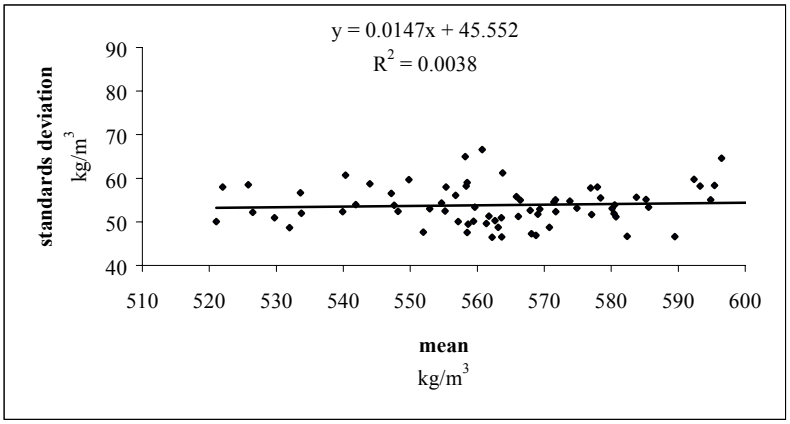

(c)

Figure C.12. *Proportional effect m2p1: (a) windows size 50- by 50-mm, (b) window size 100- by 100-mm, and (c) windows size 200- by 200-mm.*

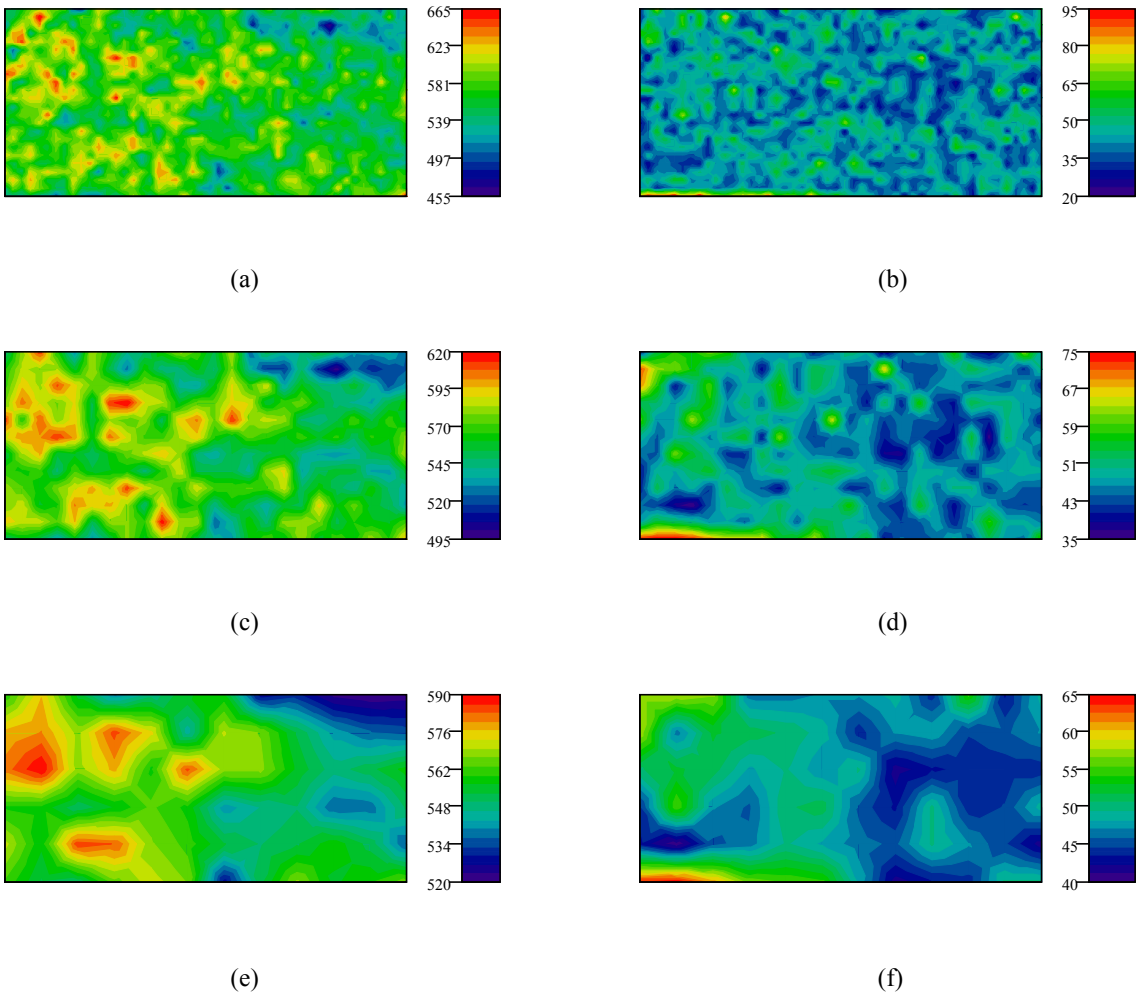

Figure C.13. *m2p2: (a) contour plot of density for windows size 50- by 50-mm, (b) contour plot of standard deviation for windows size 50- by 50-mm, (c) contour plot of density for windows size 100- by 100-mm, (d) contour plot of standard deviation for windows size 100- by 100-mm, (e) contour plot of density for windows size 200- by 200-mm, and (f) contour plot of standard deviation for windows size 200- by 200-mm.*

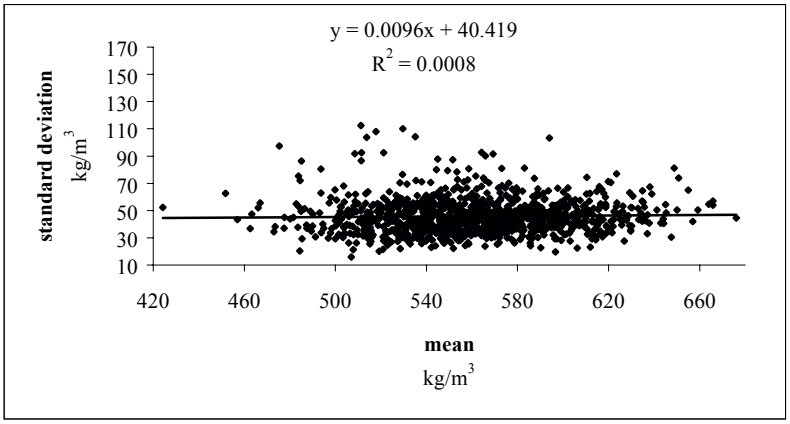

(a)

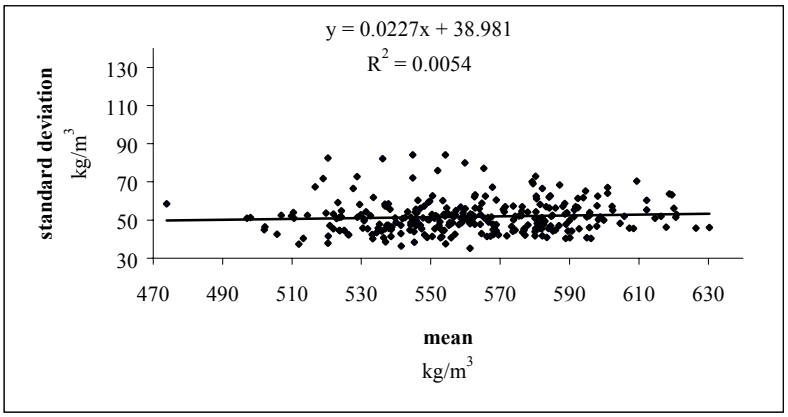

(b)

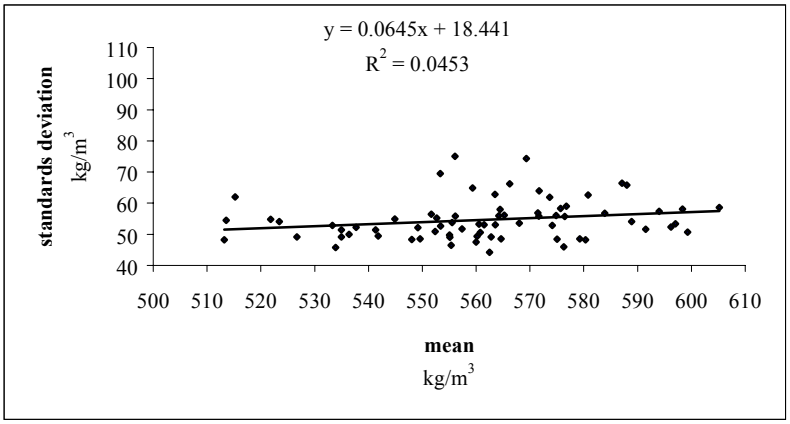

(c)

Figure C.14. *Proportional effect m2p2: (a) windows size 50- by 50-mm, (b) window size 100- by 100-mm, and (c) windows size 200- by 200-mm.*

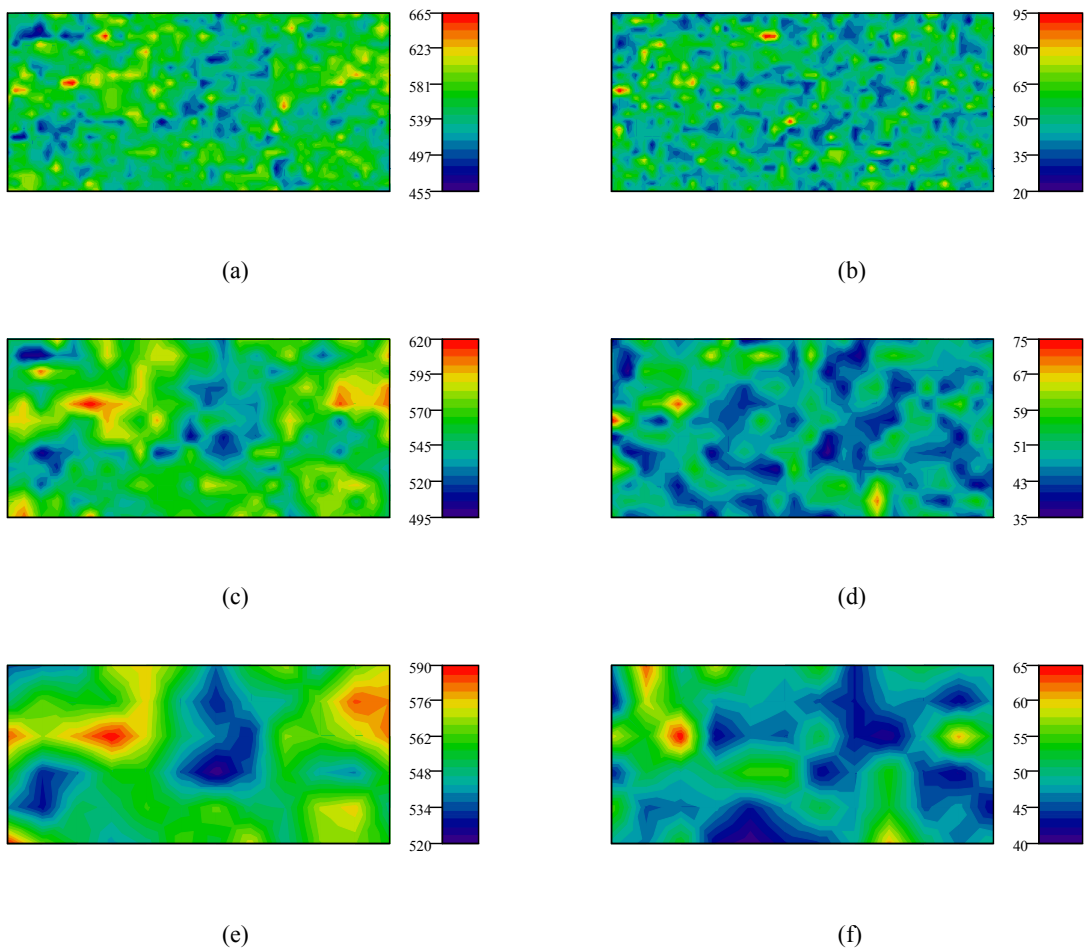

Figure C.15. *m2p3: (a) contour plot of density for windows size 50- by 50-mm, (b) contour plot of standard deviation for windows size 50- by 50-mm, (c) contour plot of density for windows size 100- by 100-mm, (d) contour plot of standard deviation for windows size 100- by 100-mm, (e) contour plot of density for windows size 200- by 200-mm, and (f) contour plot of standard deviation for windows size 200- by 200-mm.*

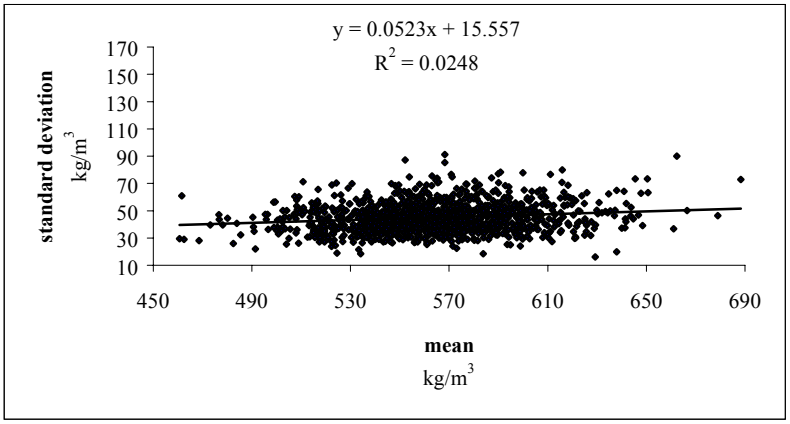

(a)

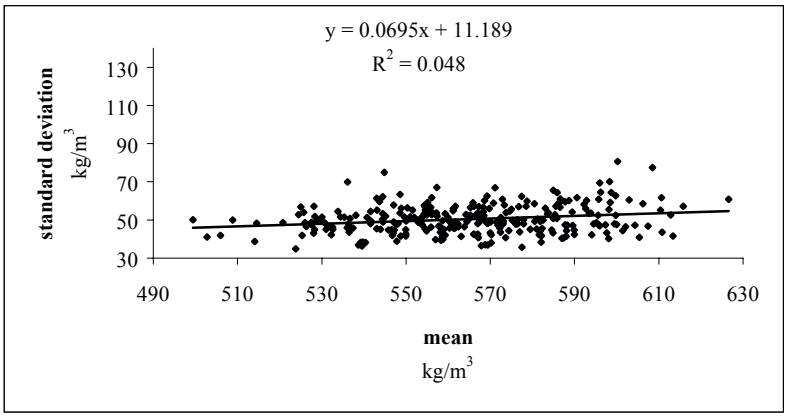

(b)

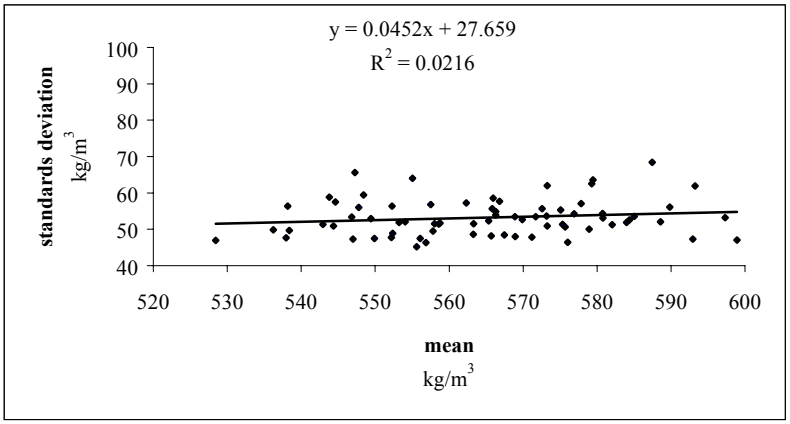

(c)

Figure C.16. *Proportional effect m2p3: (a) windows size 50- by 50-mm, (b) window size 100- by 100-mm, and (c) windows size 200- by 200-mm.*

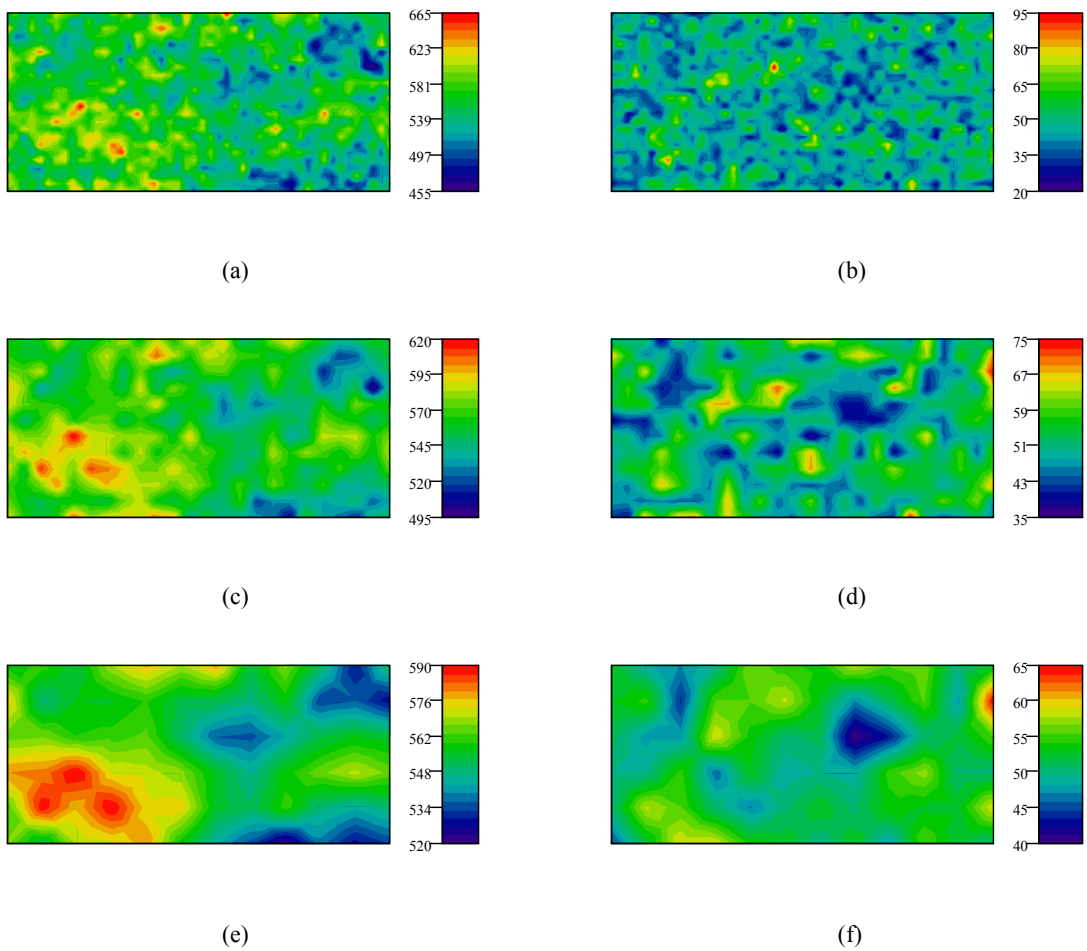

Figure C.17. *m2p4: (a) contour plot of density for windows size 50- by 50-mm, (b) contour plot of standard deviation for windows size 50- by 50-mm, (c) contour plot of density for windows size 100- by 100-mm, (d) contour plot of standard deviation for windows size 100- by 100-mm, (e) contour plot of density for windows size 200- by 200-mm, and (f) contour plot of standard deviation for windows size 200- by 200-mm.*

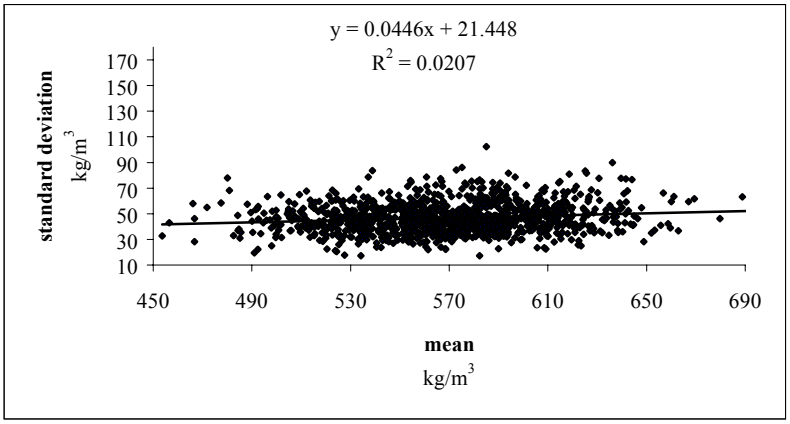

(a)

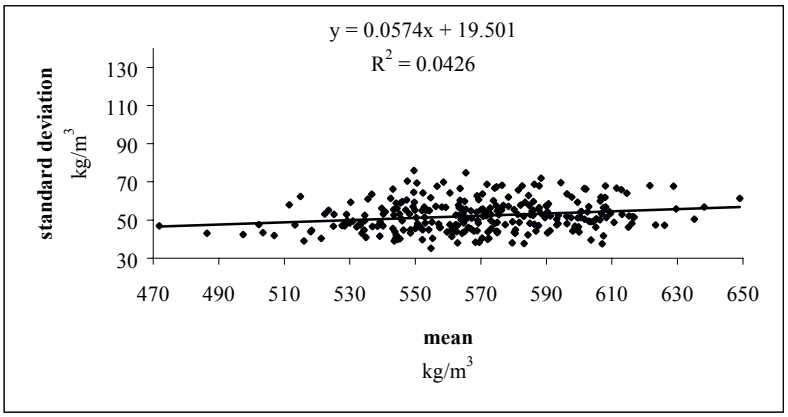

(b)

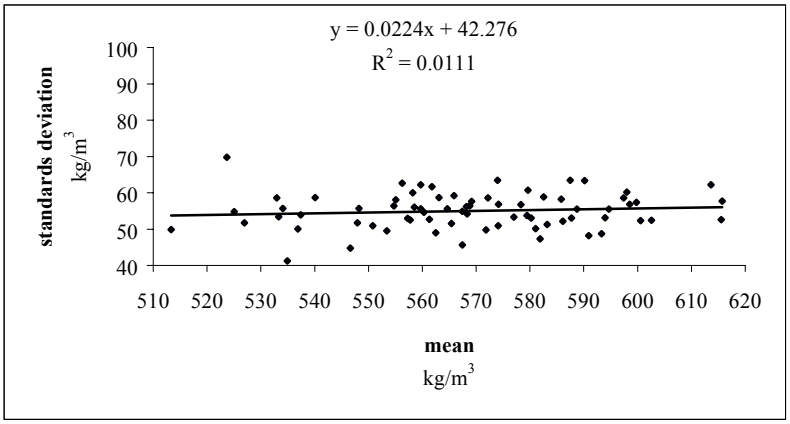

(c)

Figure C.18. *Proportional effect m2p4: (a) windows size 50- by 50-mm, (b) window size 100- by 100-mm, and (c) windows size 200- by 200-mm.*

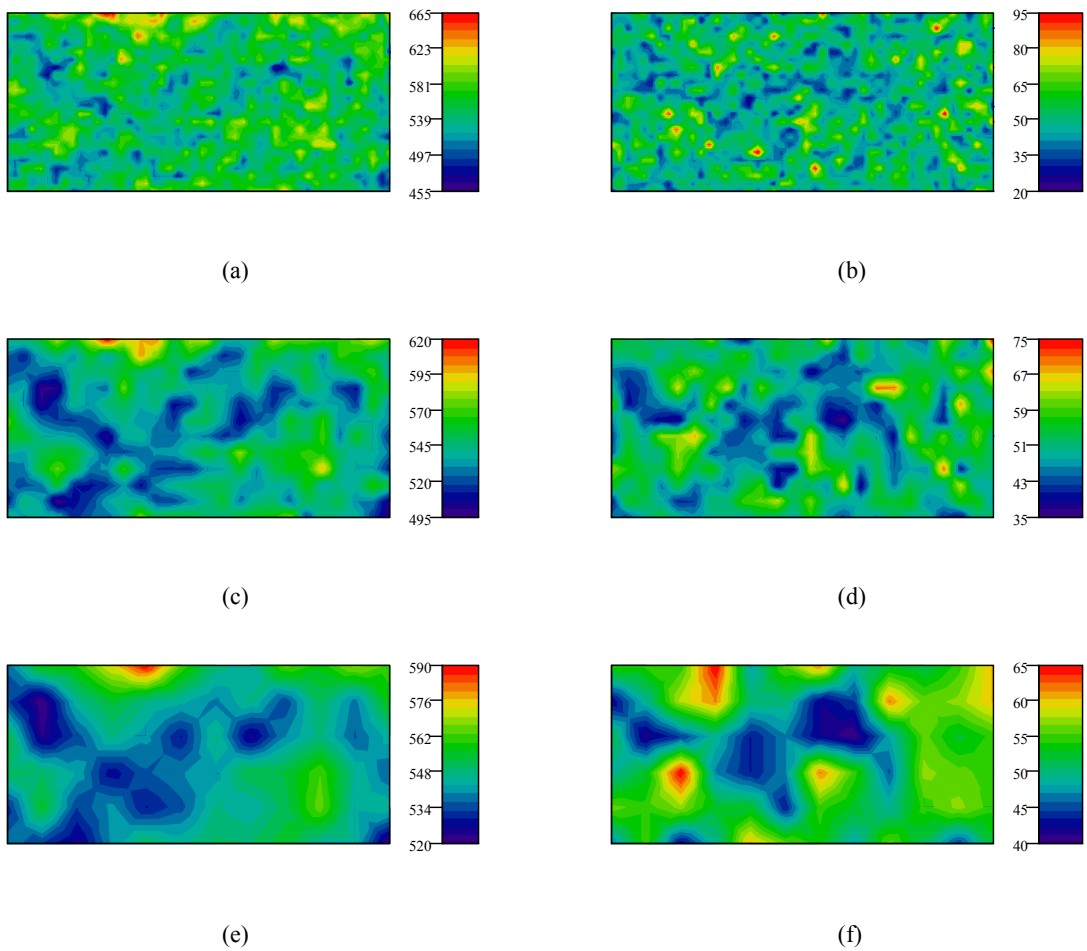

Figure C.19. *m2p5: (a) contour plot of density for windows size 50- by 50-mm, (b) contour plot of standard deviation for windows size 50- by 50-mm, (c) contour plot of density for windows size 100- by 100-mm, (d) contour plot of standard deviation for windows size 100- by 100-mm, (e) contour plot of density for windows size 200- by 200-mm, and (f) contour plot of standard deviation for windows size 200- by 200-mm.*

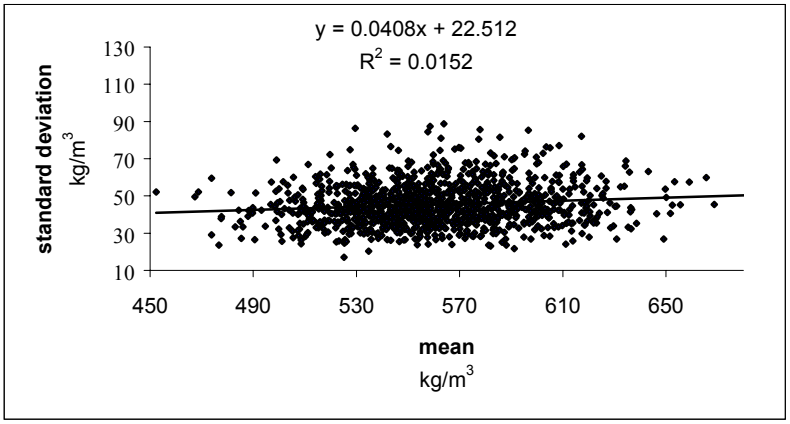

(a)

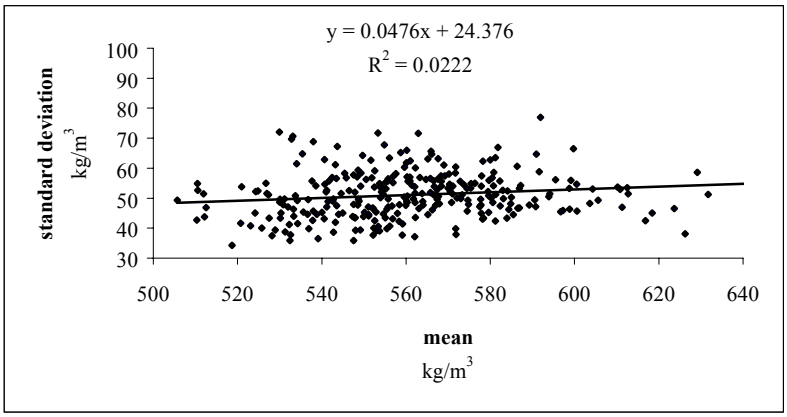

(b)

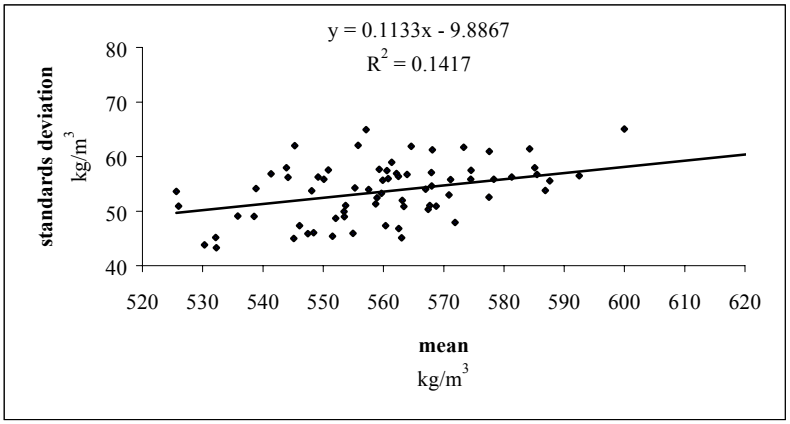

(c)

Figure C.20. *Proportional effect m2p5: (a) windows size 50- by 50-mm, (b) window size 100- by 100-mm, and (c) windows size 200- by 200-mm.*

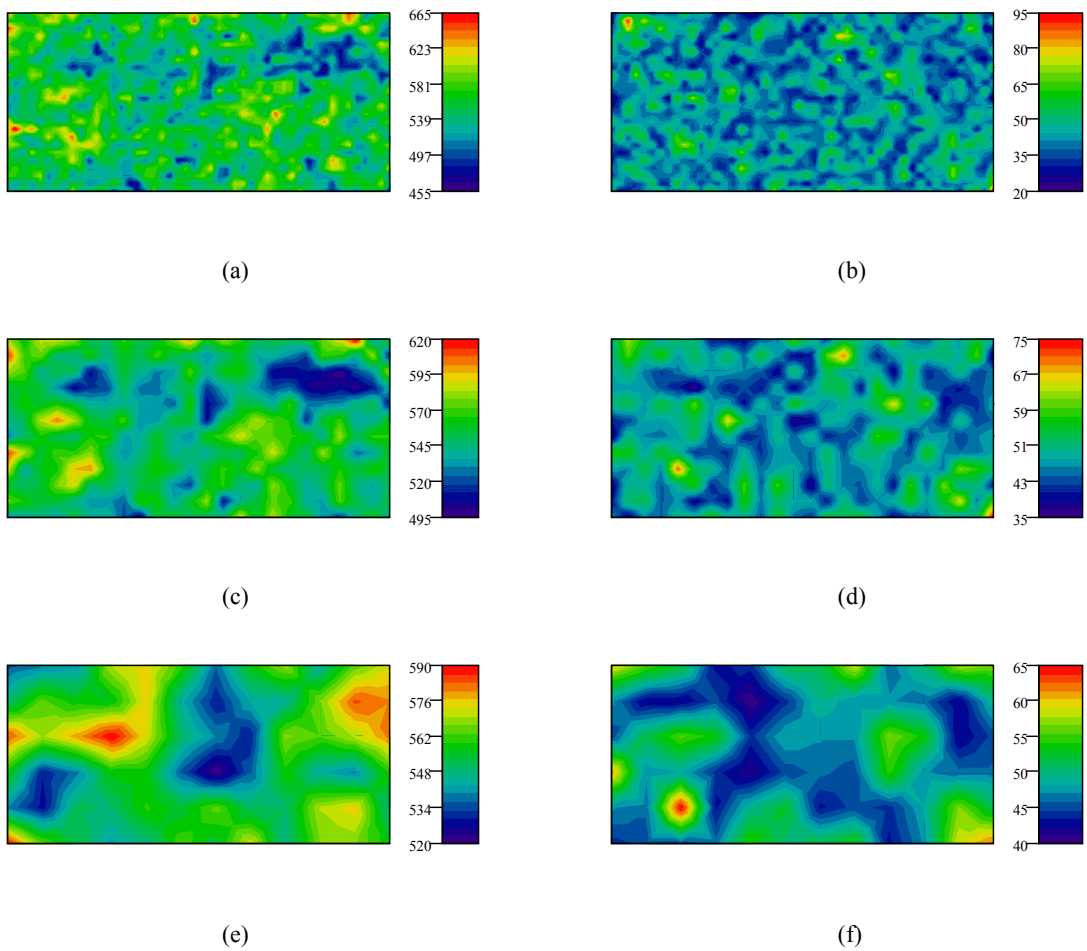

Figure C.21. *m2p6: (a) contour plot of density for windows size 50- by 50-mm, (b) contour plot of standard deviation for windows size 50- by 50-mm, (c) contour plot of density for windows size 100- by 100-mm, (d) contour plot of standard deviation for windows size 100- by 100-mm, (e) contour plot of density for windows size 200- by 200-mm, and (f) contour plot of standard deviation for windows size 200- by 200-mm.*

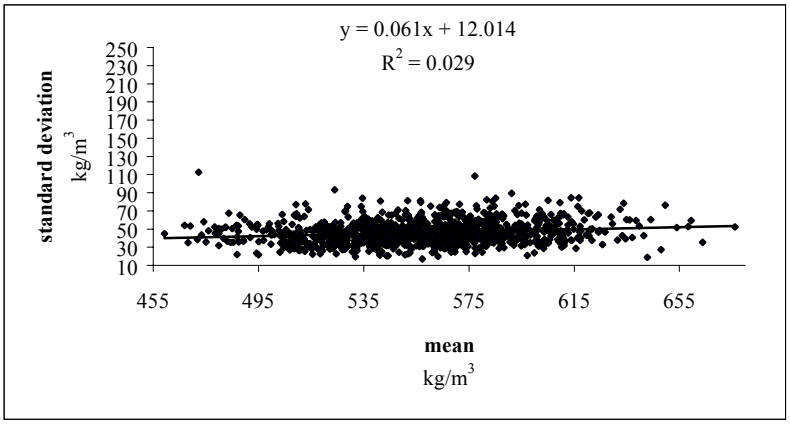

(a)

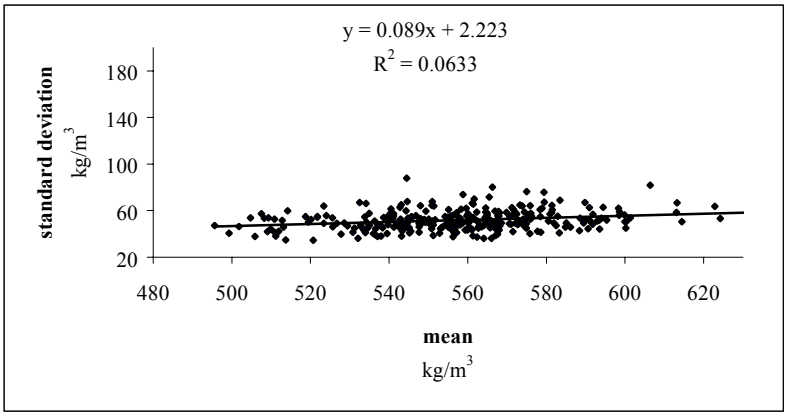

(b)

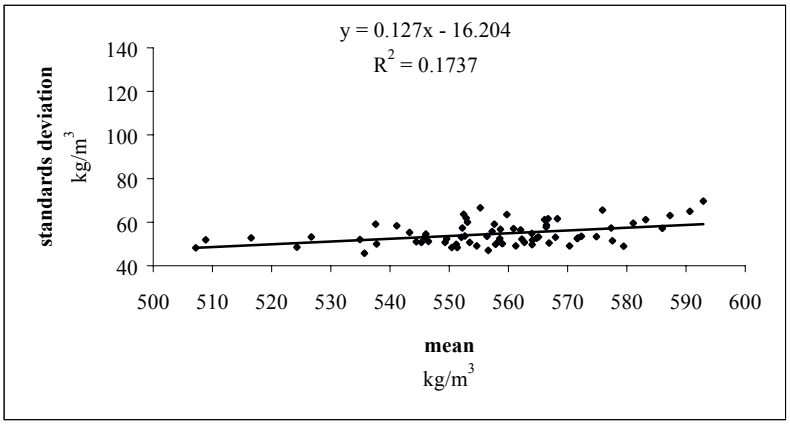

(c)

Figure C.22. *Proportional effect m2p6: (a) windows size 50- by 50-mm, (b) window size 100- by 100-mm, and (c) windows size 200- by 200-mm.*

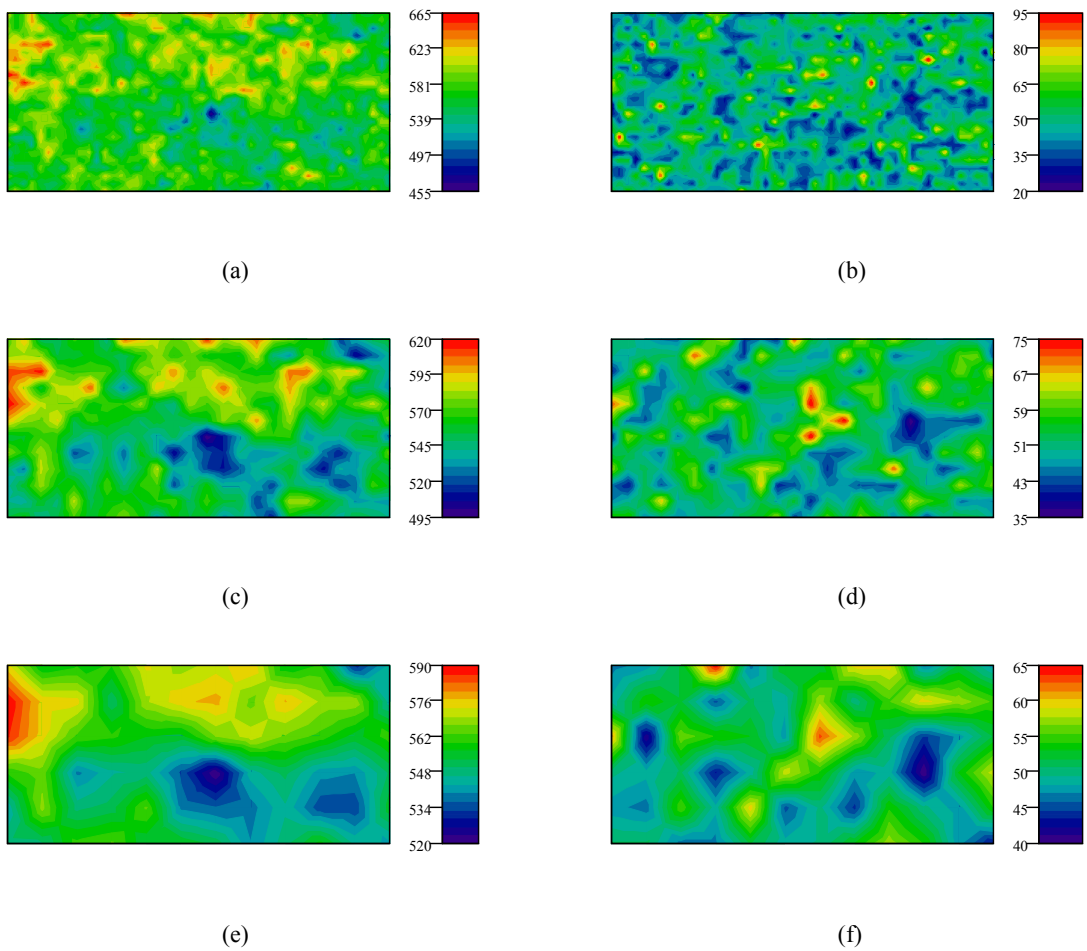

Figure C.23. *m3p1: (a) contour plot of density for windows size 50- by 50-mm, (b) contour plot of standard deviation for windows size 50- by 50-mm, (c) contour plot of density for windows size 100- by 100-mm, (d) contour plot of standard deviation for windows size 100- by 100-mm, (e) contour plot of density for windows size 200- by 200-mm, and (f) contour plot of standard deviation for windows size 200- by 200-mm.*

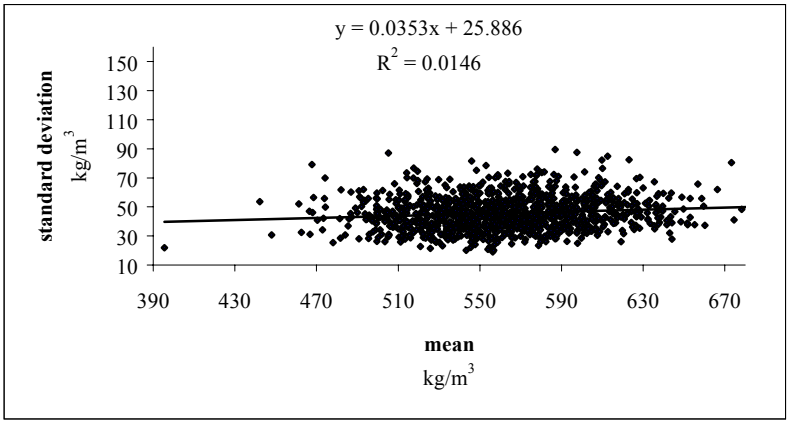

(a)

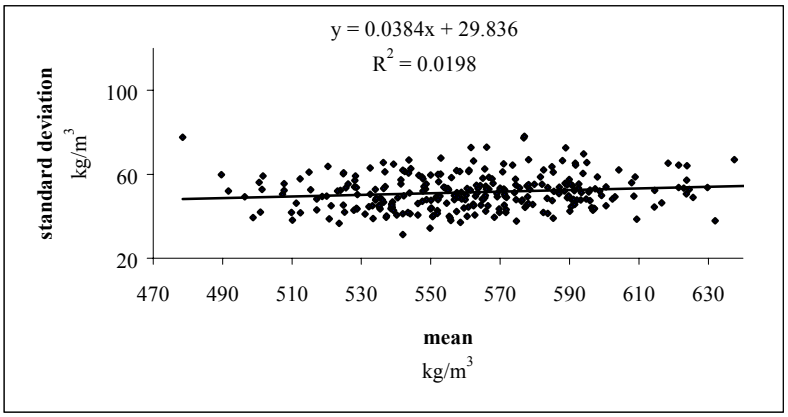

(b)

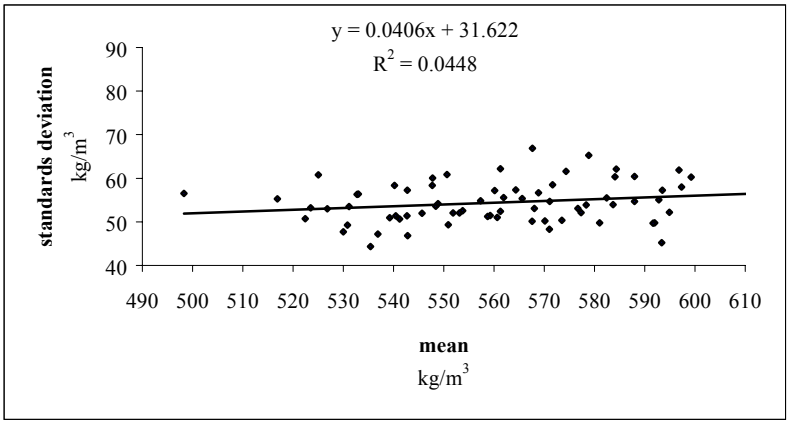

(c)

Figure C.24. *Proportional effect m3p1: (a) windows size 50- by 50-mm, (b) window size 100- by 100-mm, and (c) windows size 200- by 200-mm.*

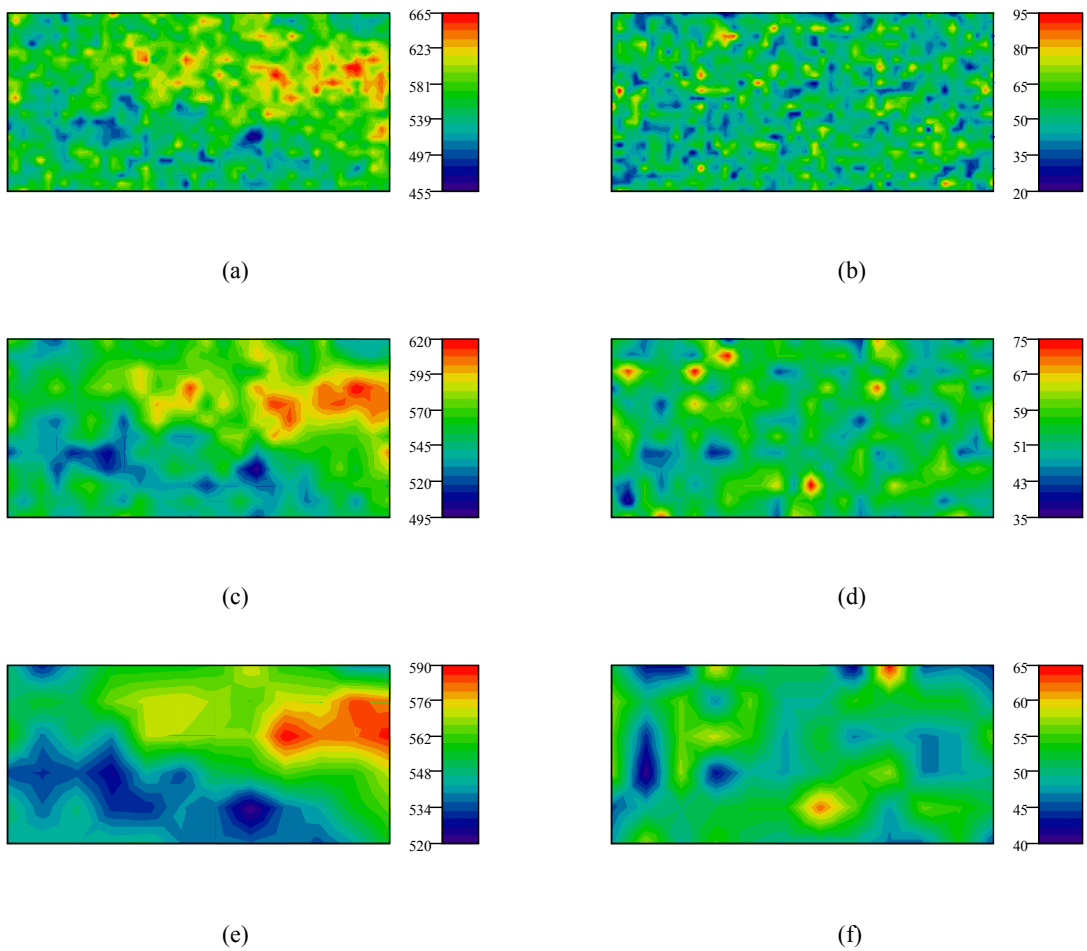

Figure C.25. *m3p2: (a) contour plot of density for windows size 50- by 50-mm, (b) contour plot of standard deviation for windows size 50- by 50-mm, (c) contour plot of density for windows size 100- by 100-mm, (d) contour plot of standard deviation for windows size 100- by 100-mm, (e) contour plot of density for windows size 200- by 200-mm, and (f) contour plot of standard deviation for windows size 200- by 200-mm.*

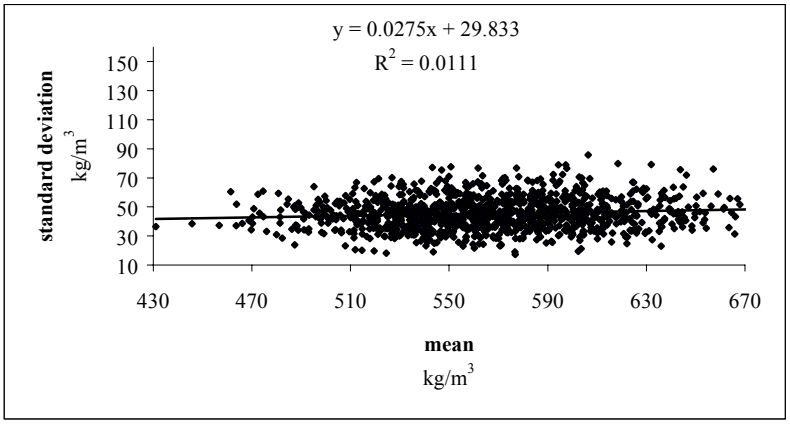

(a)

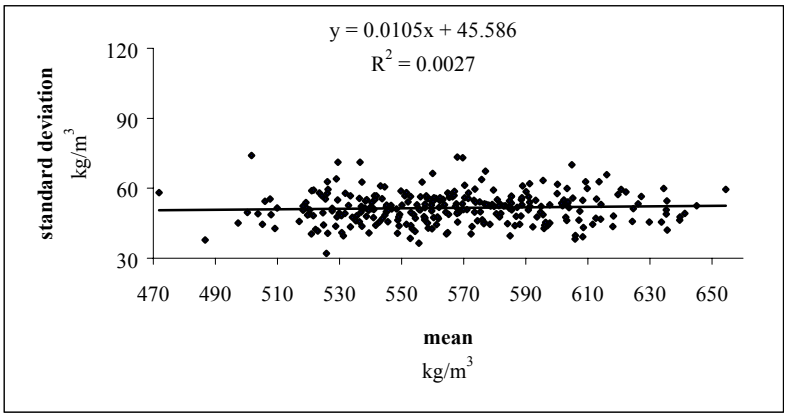

(b)

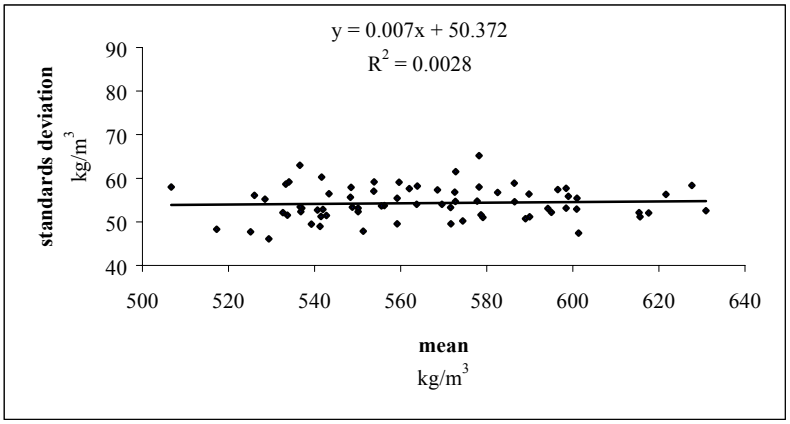

(c)

Figure C.26. *Proportional effect m3p2: (a) windows size 50- by 50-mm, (b) window size 100- by 100-mm, and (c) windows size 200- by 200-mm.*

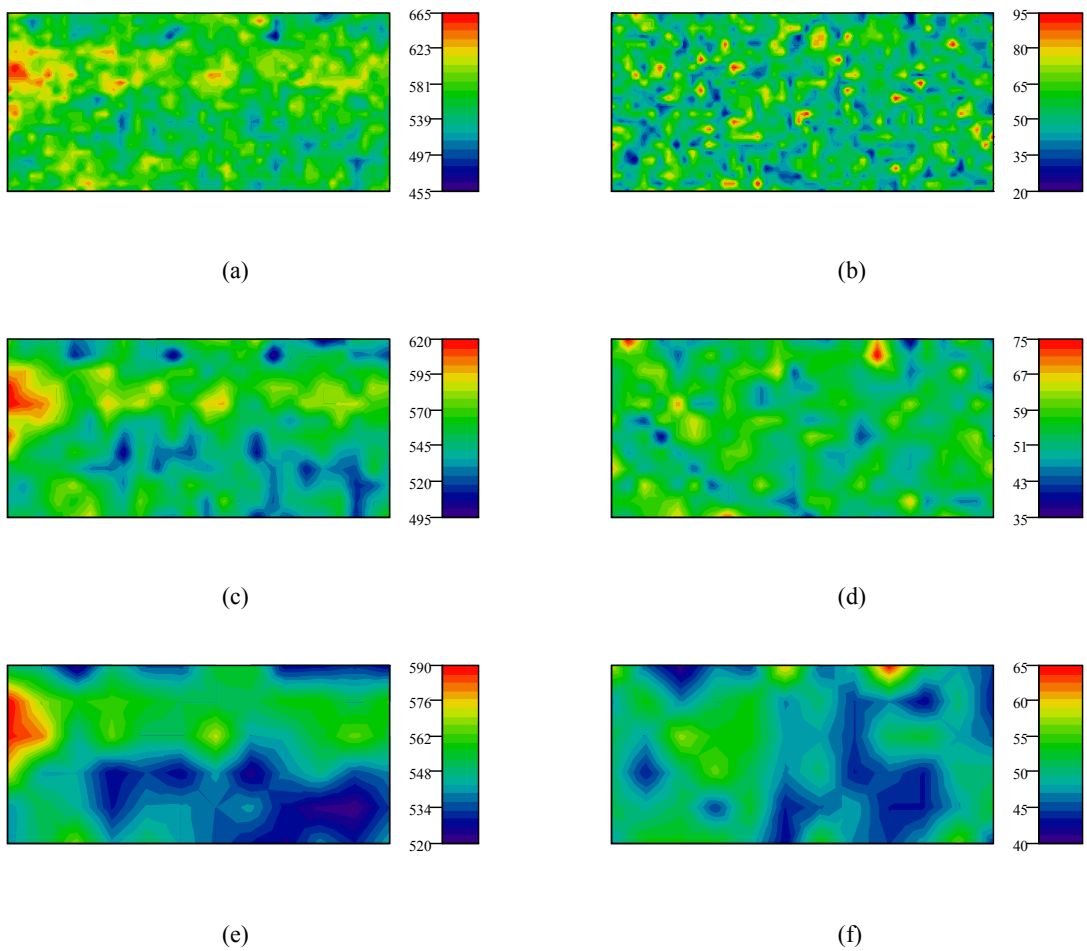

Figure C.27. *m3p3: (a) contour plot of density for windows size 50- by 50-mm, (b) contour plot of standard deviation for windows size 50- by 50-mm, (c) contour plot of density for windows size 100- by 100-mm, (d) contour plot of standard deviation for windows size 100- by 100-mm, (e) contour plot of density for windows size 200- by 200-mm, and (f) contour plot of standard deviation for windows size 200- by 200-mm.*

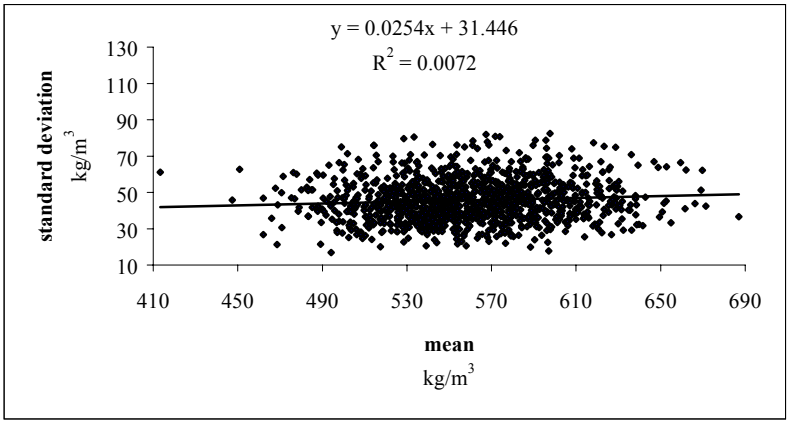

(a)

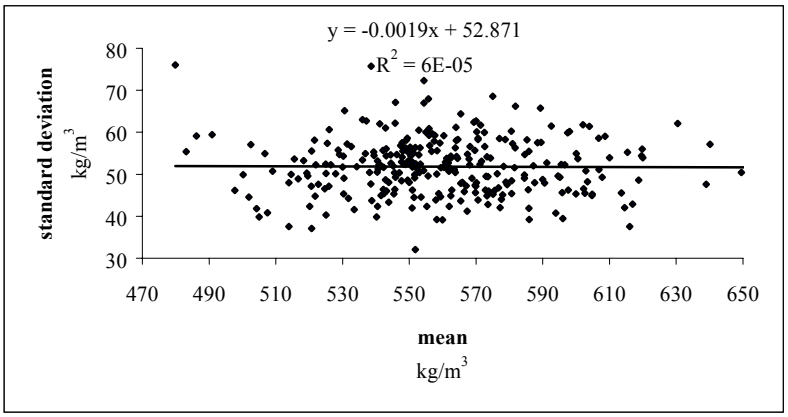

(b)

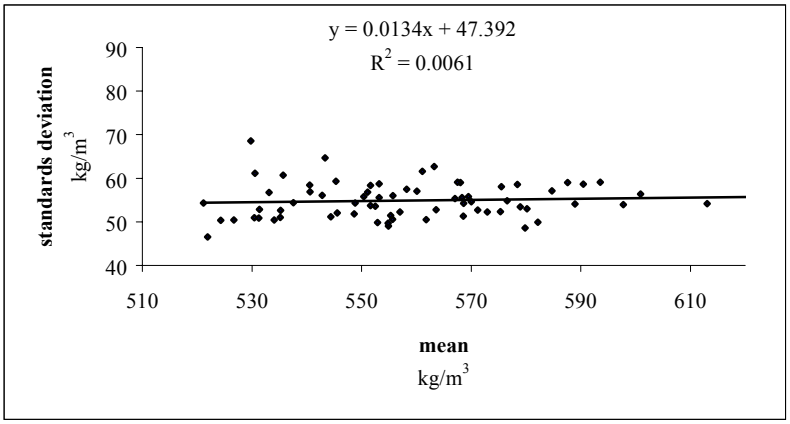

(c)

Figure C.28. *Proportional effect m3p3: (a) windows size 50- by 50-mm, (b) window size 100- by 100-mm, and (c) windows size 200- by 200-mm.*

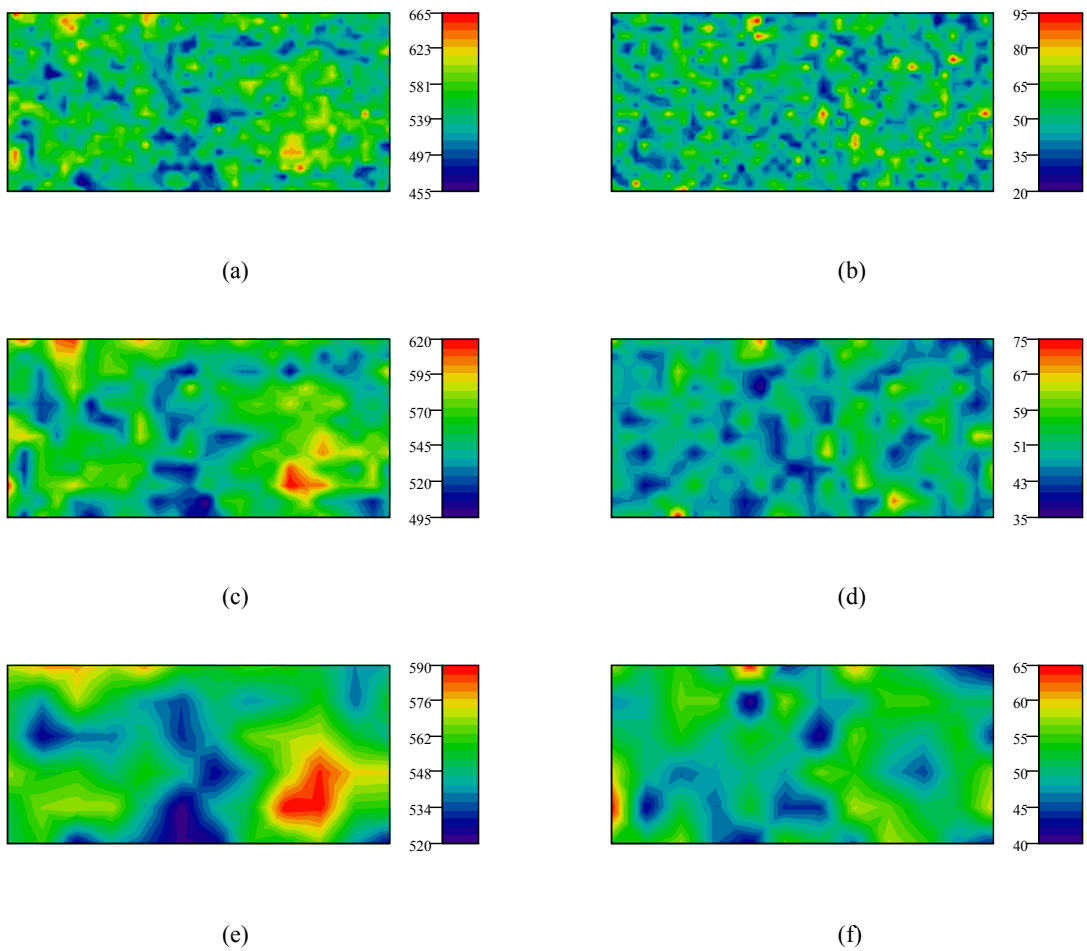

Figure C.29. *m3p4: (a) contour plot of density for windows size 50- by 50-mm, (b) contour plot of standard deviation for windows size 50- by 50-mm, (c) contour plot of density for windows size 100- by 100-mm, (d) contour plot of standard deviation for windows size 100- by 100-mm, (e) contour plot of density for windows size 200- by 200-mm, and (f) contour plot of standard deviation for windows size 200- by 200-mm.*

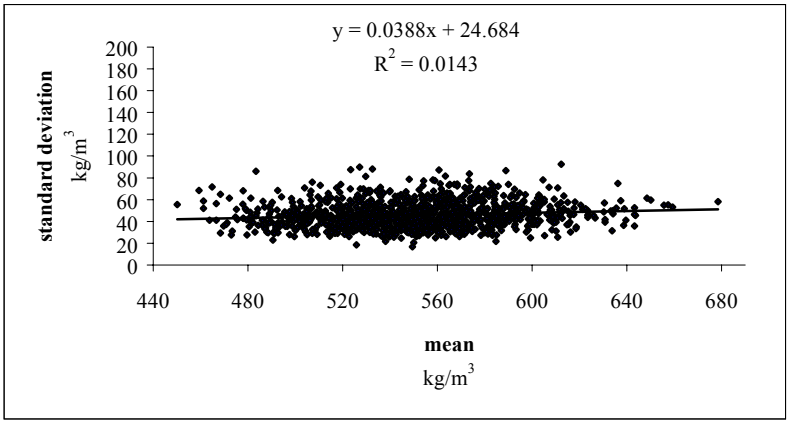

(a)

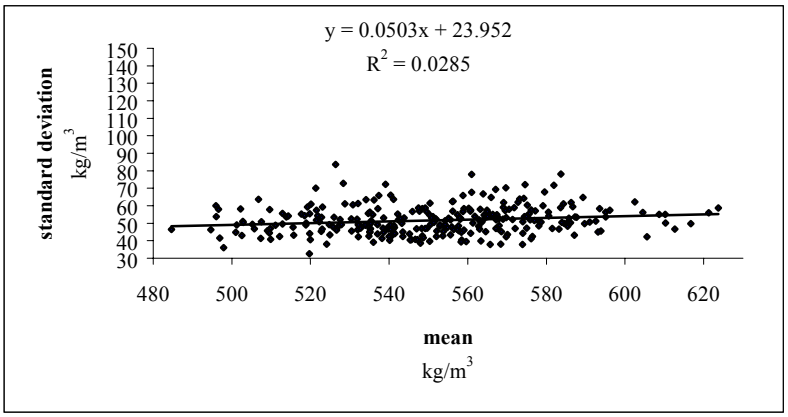

(b)

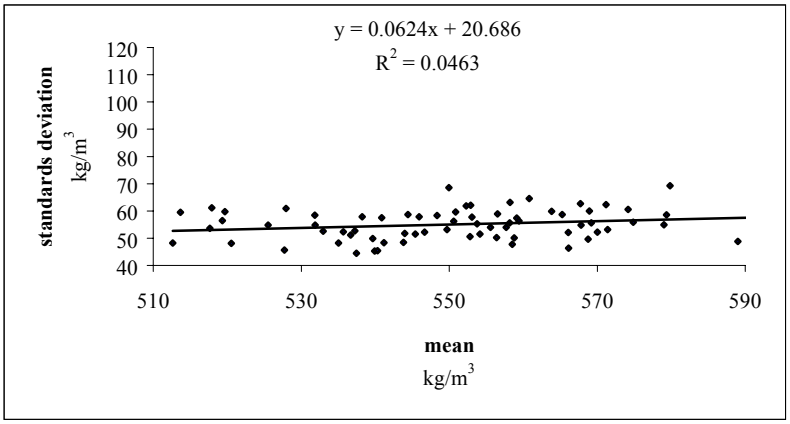

(c)

Figure C.30. *Proportional effect m3p4: (a) windows size 50- by 50-mm, (b) window size 100- by 100-mm, and (c) windows size 200- by 200-mm.*

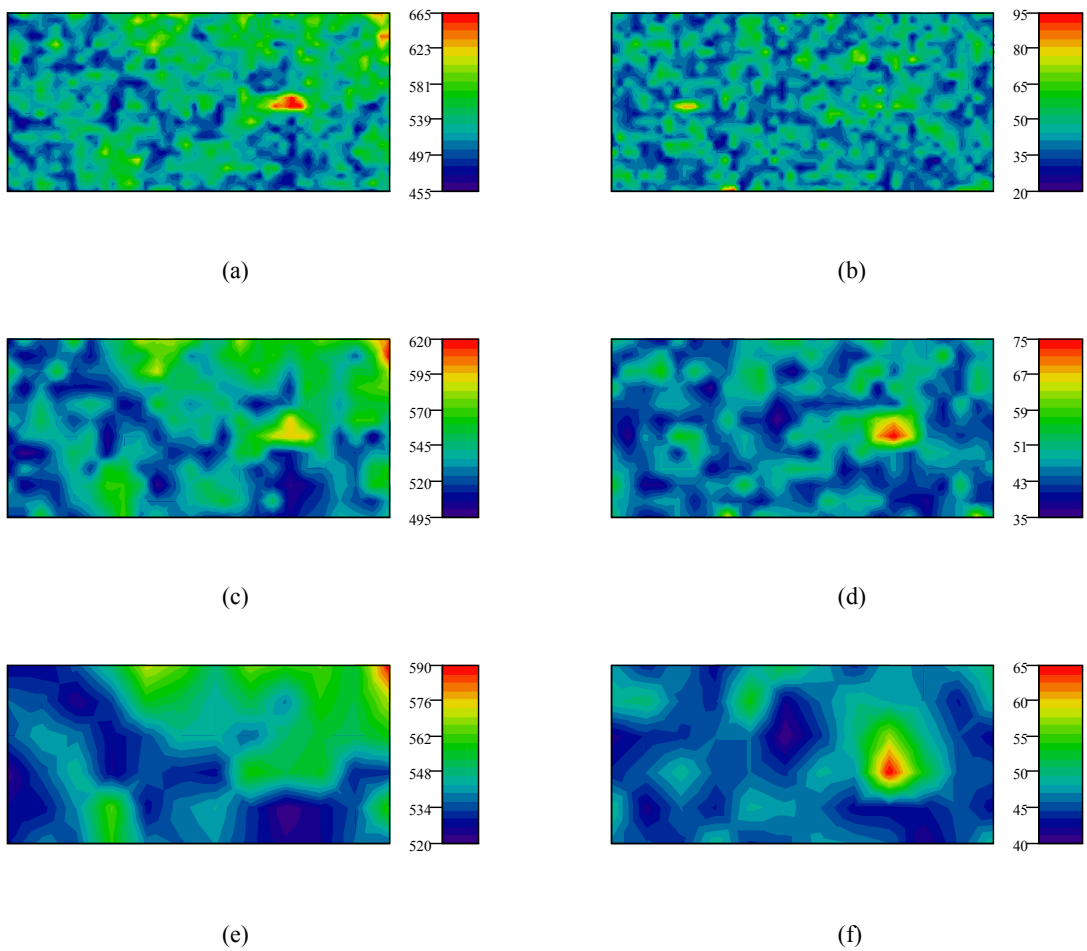

Figure C.31. *m3p5: (a) contour plot of density for windows size 50- by 50-mm, (b) contour plot of standard deviation for windows size 50- by 50-mm, (c) contour plot of density for windows size 100- by 100-mm, (d) contour plot of standard deviation for windows size 100- by 100-mm, (e) contour plot of density for windows size 200- by 200-mm, and (f) contour plot of standard deviation for windows size 200- by 200-mm.*

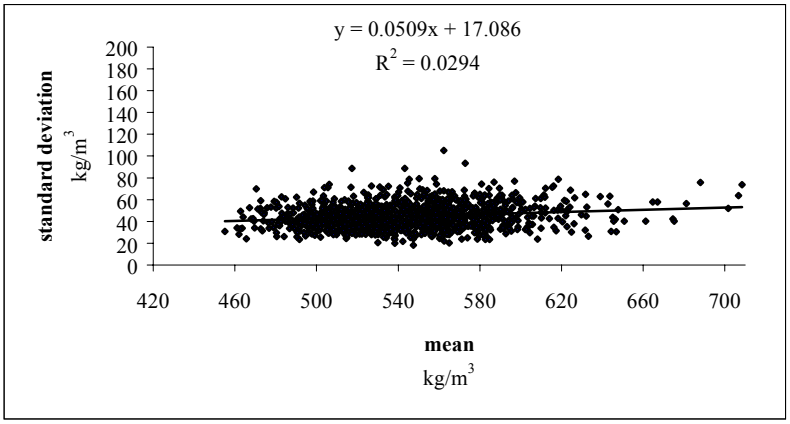

(a)

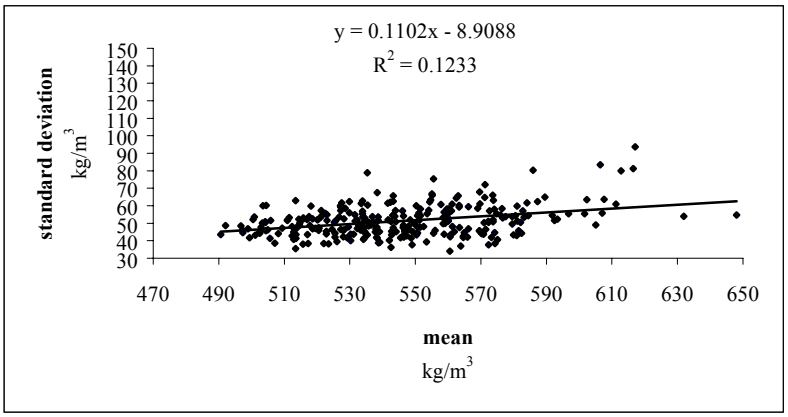

(b)

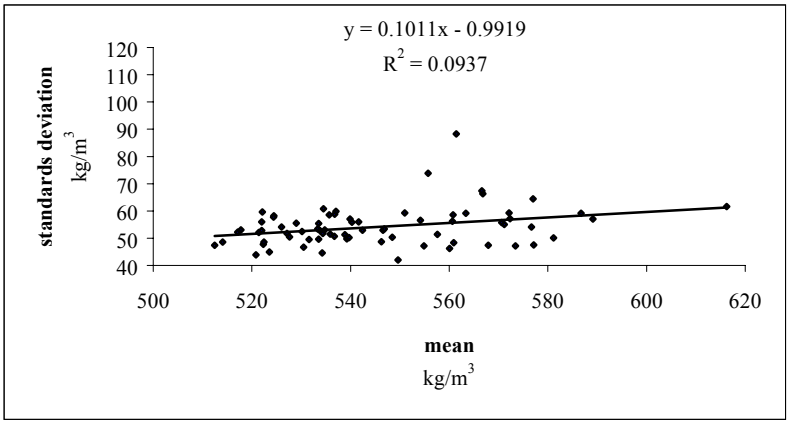

(c)

Figure C.32. *Proportional effect m3p5: (a) windows size 50- by 50-mm, (b) window size 100- by 100-mm, and (c) windows size 200- by 200-mm.*

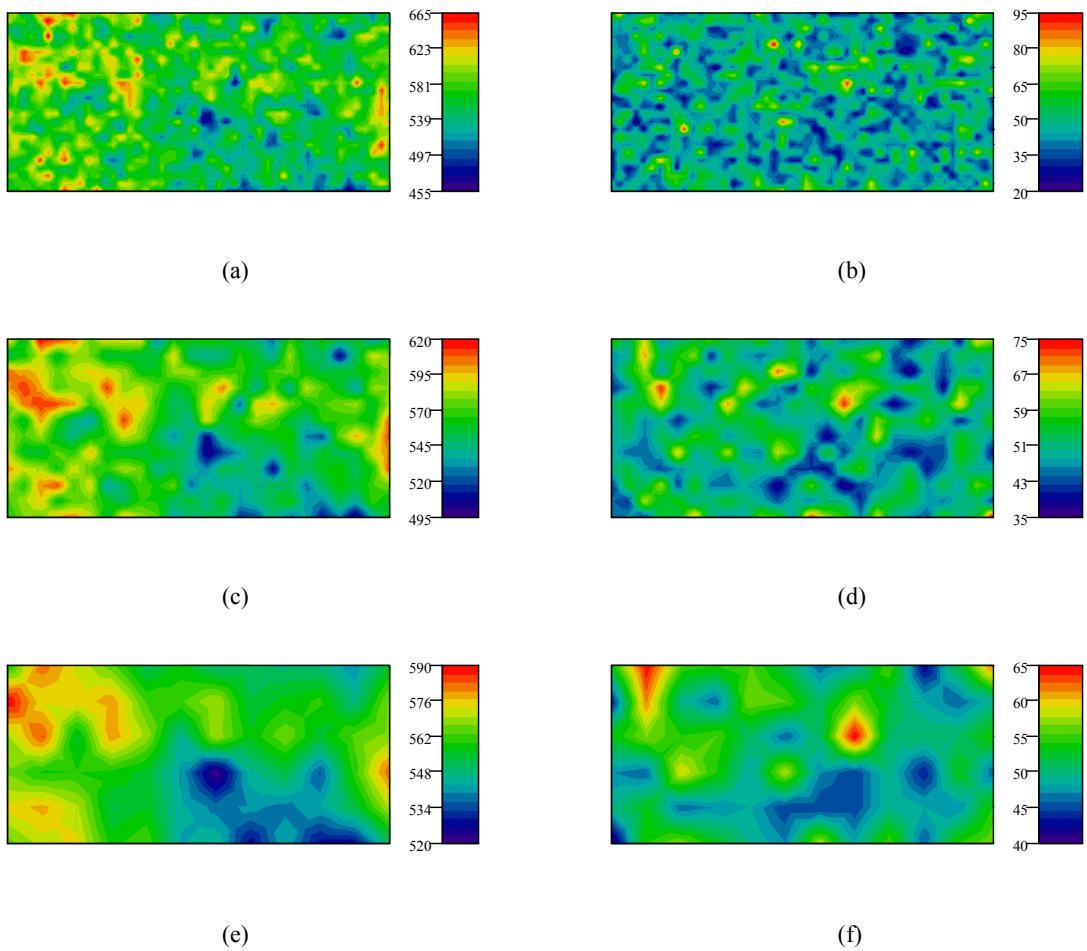

Figure C.33. *m3p6: (a) contour plot of density for windows size 50- by 50-mm, (b) contour plot of standard deviation for windows size 50- by 50-mm, (c) contour plot of density for windows size 100- by 100-mm, (d) contour plot of standard deviation for windows size 100- by 100-mm, (e) contour plot of density for windows size 200- by 200-mm, and (f) contour plot of standard deviation for windows size 200- by 200-mm.*

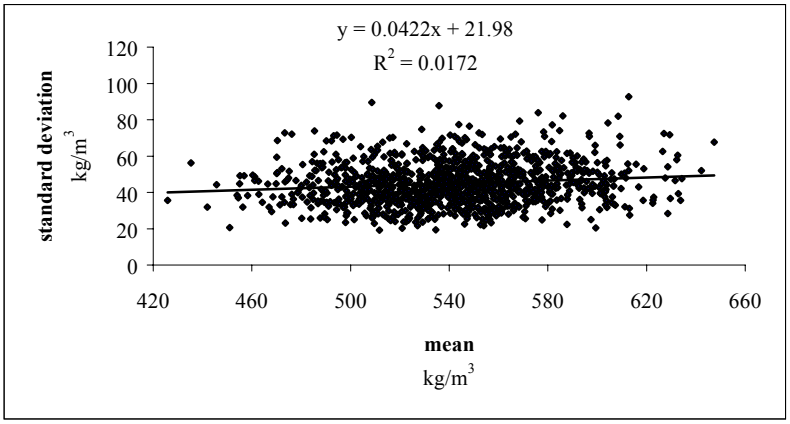

(a)

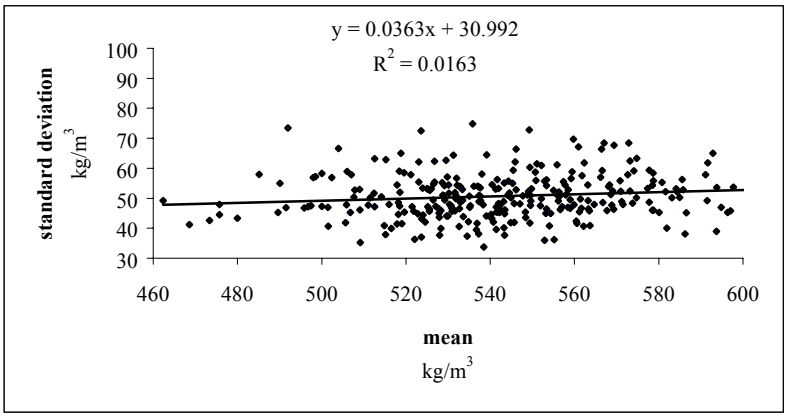

(b)

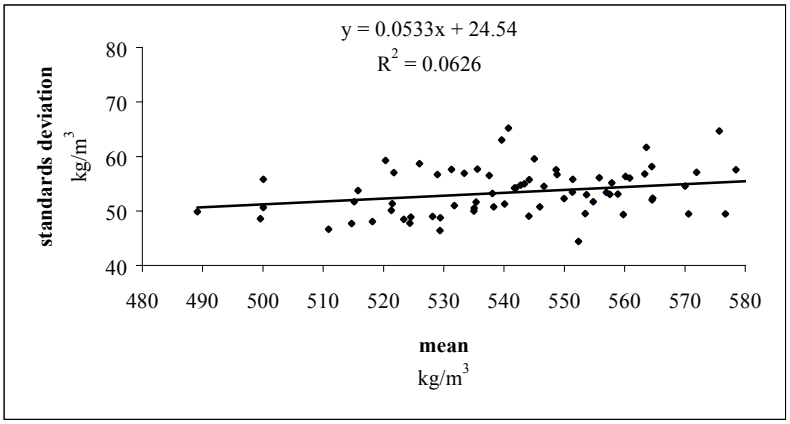

(c)

Figure C.34. *Proportional effect m3p6: (a) windows size 50- by 50-mm, (b) window size 100- by 100-mm, and (c) windows size 200- by 200-mm.*

Appendix D

Variogram and Correlogram

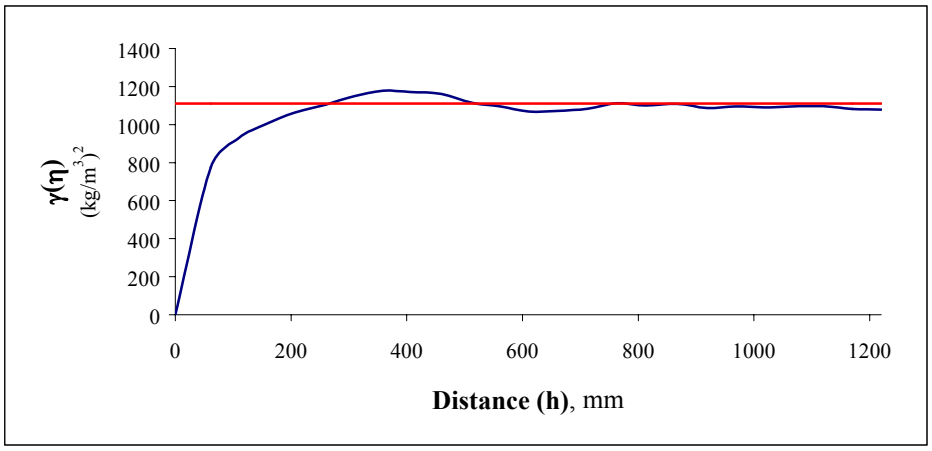

(a)

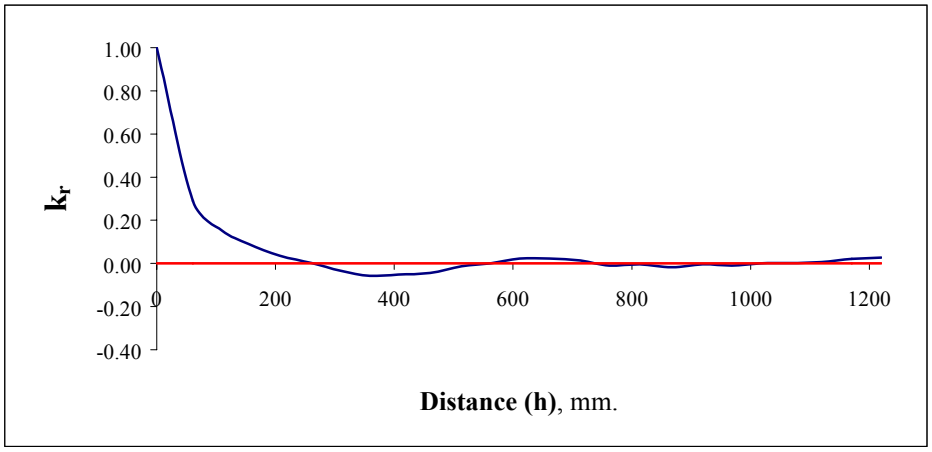

(b)

Figure D.1. *Panel m1p1: (a) omniderectional variogram, and (b) omnidirectional correlogram.*

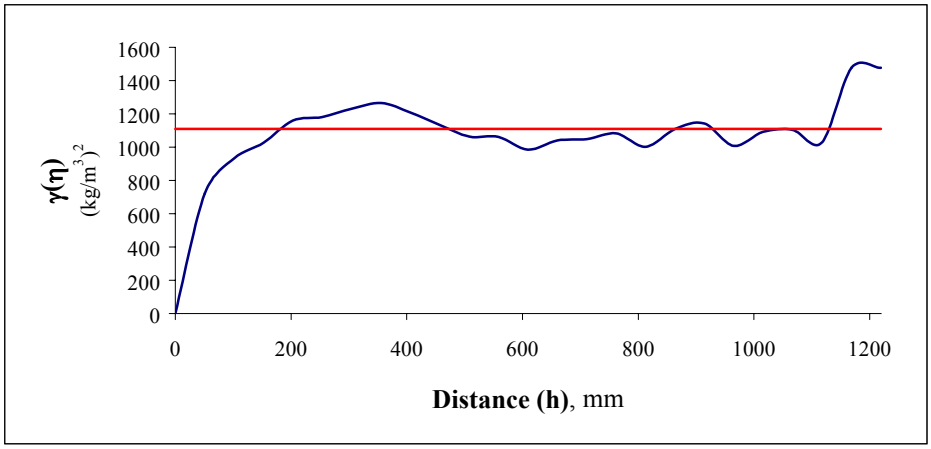

(a)

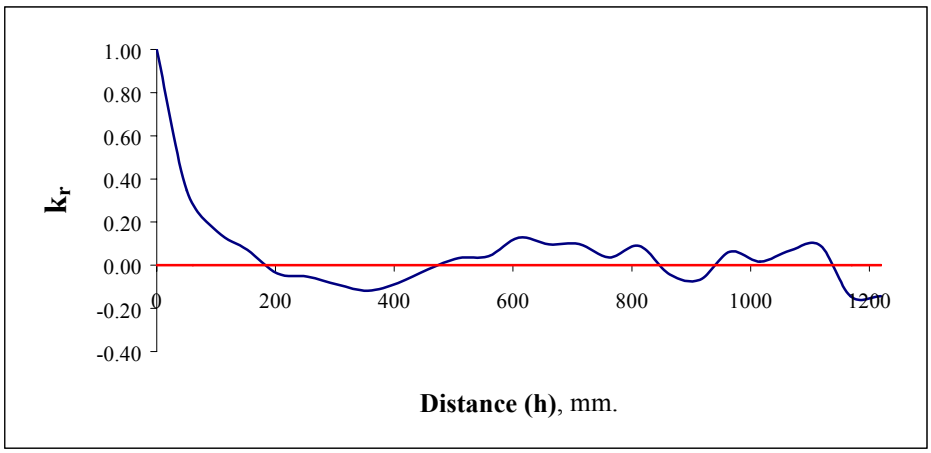

(b)

Figure D.2. *Panel m1p1: (a) transversal variogram, and (b) transversal correlogram.*

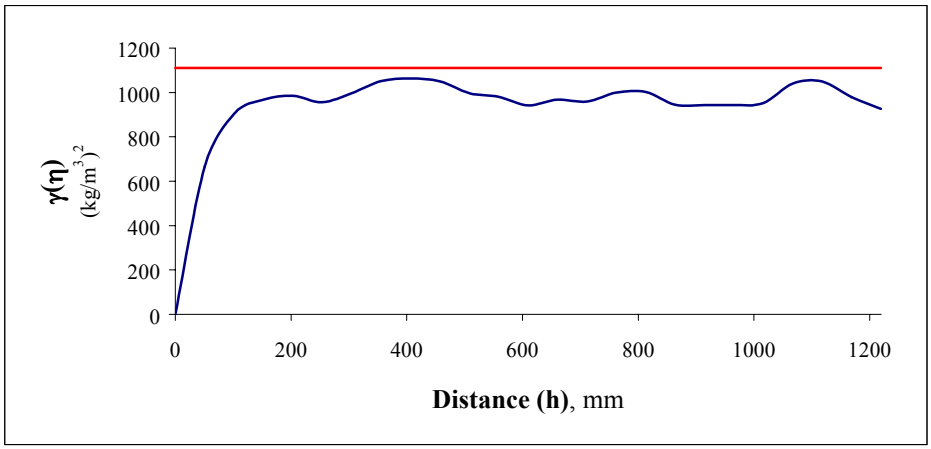

(a)

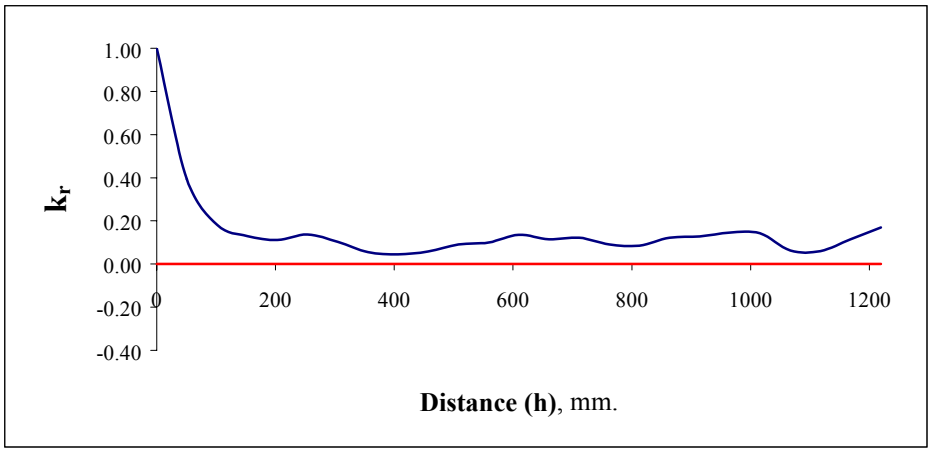

(b)

Figure D.3. *Panel m1p1: (a) longitudinal variogram, and (b) longitudinal correlogram.*

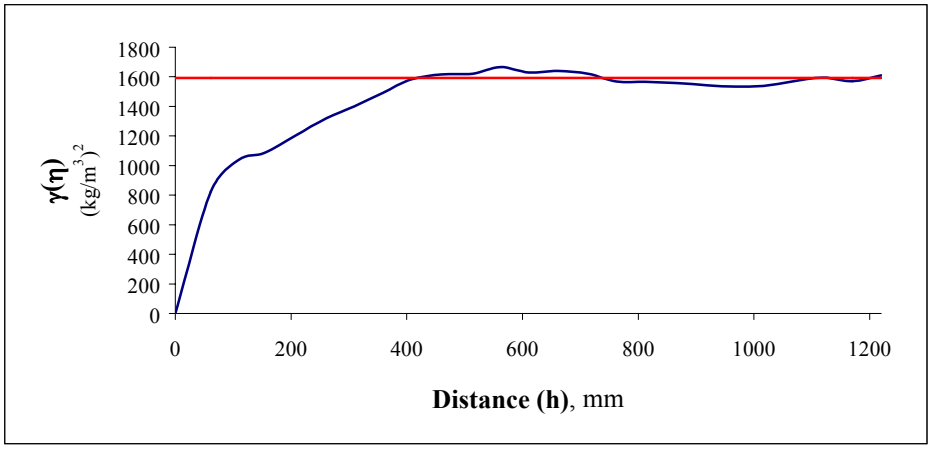

(a)

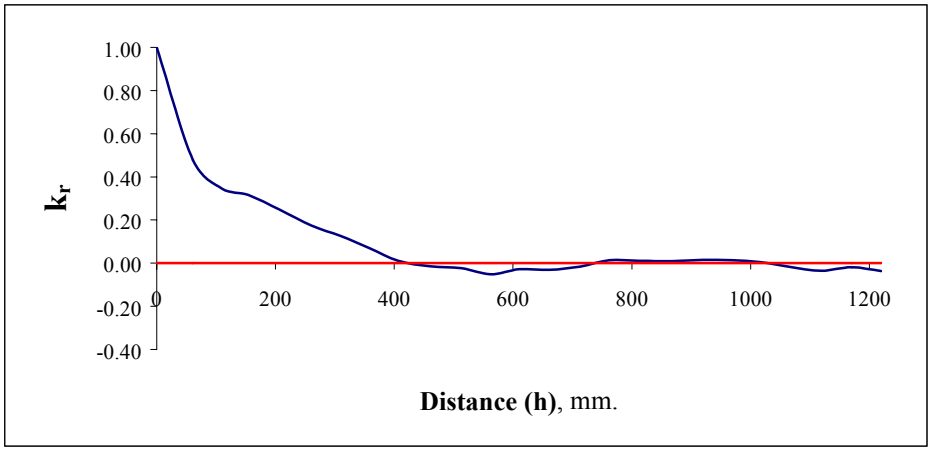

(b)

Figure D.4. *Panel m1p2: (a) omniderectional variogram, and (b) omnidirectional correlogram.*

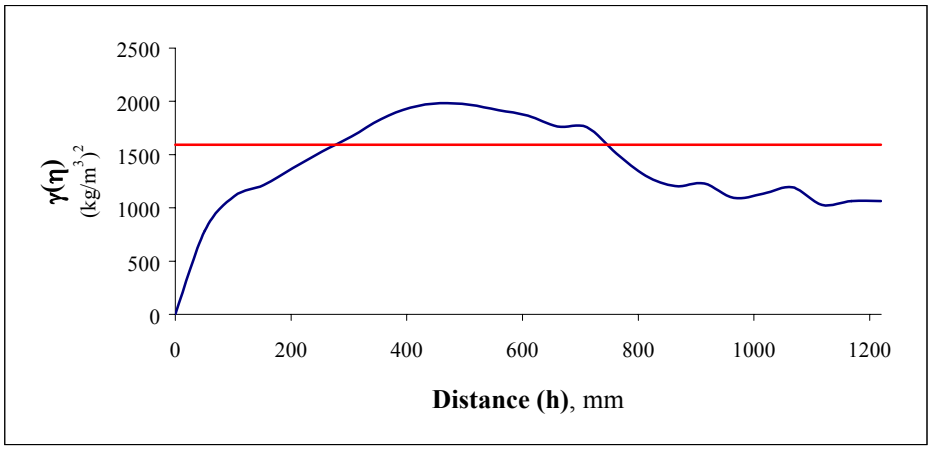

(a)

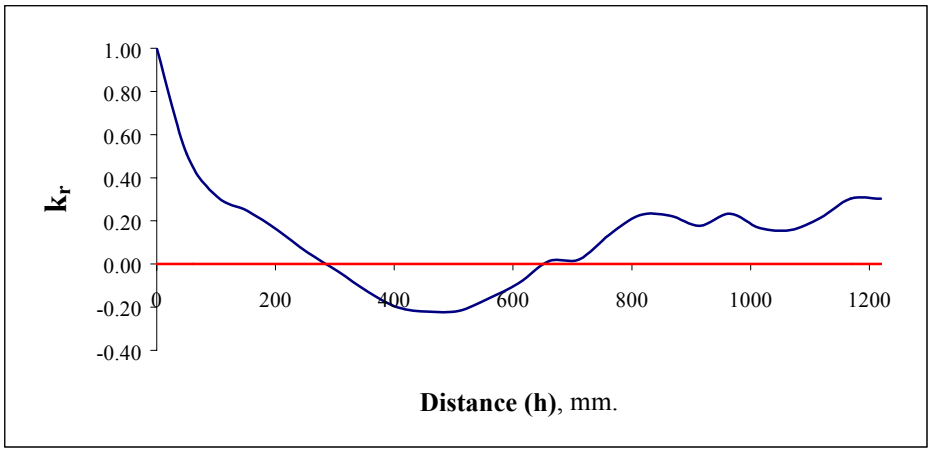

(b)

Figure D.5. *Panel m1p2: (a) transversal variogram, and (b) transversal correlogram.*

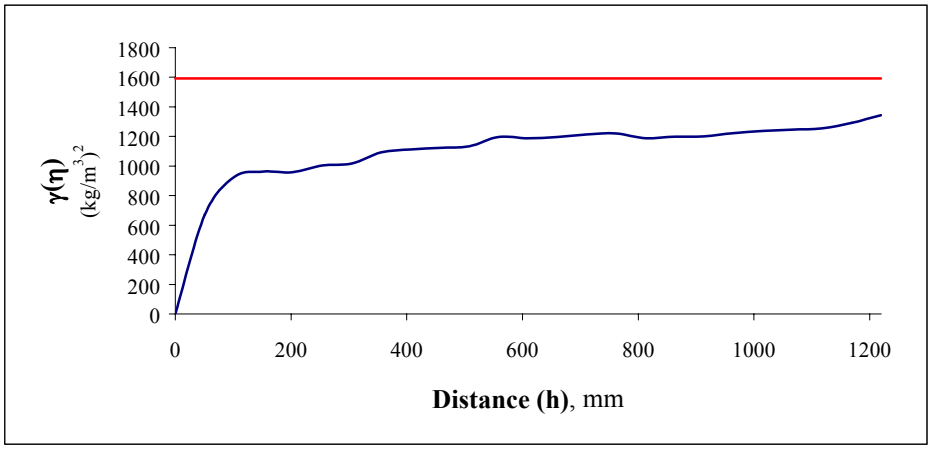

(a)

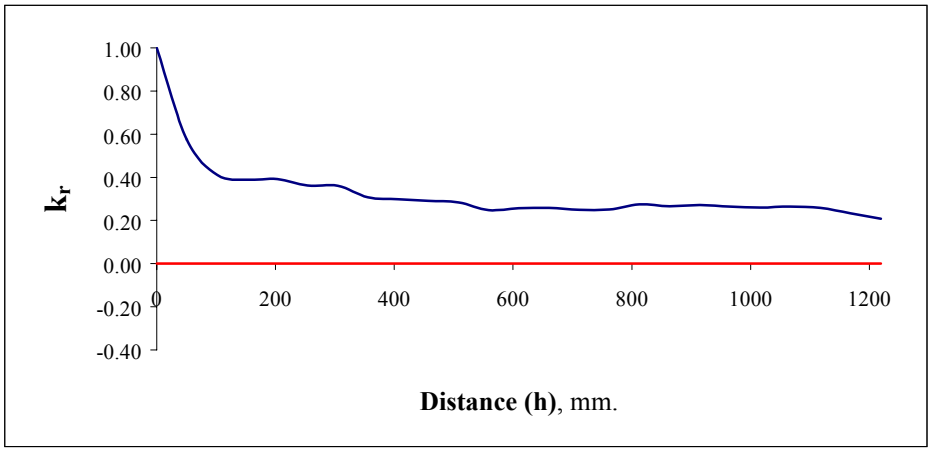

(b)

Figure D.6. *Panel m1p2: (a) longitudinal variogram, and (b) longitudinal correlogram.*

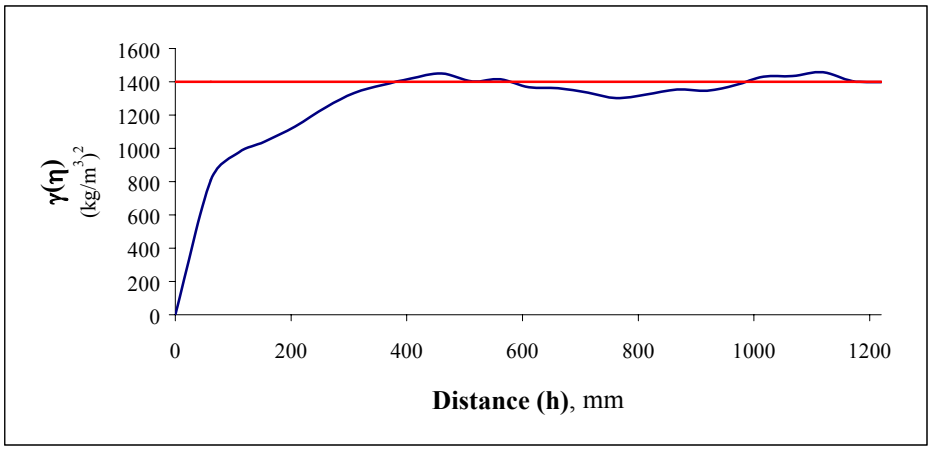

(a)

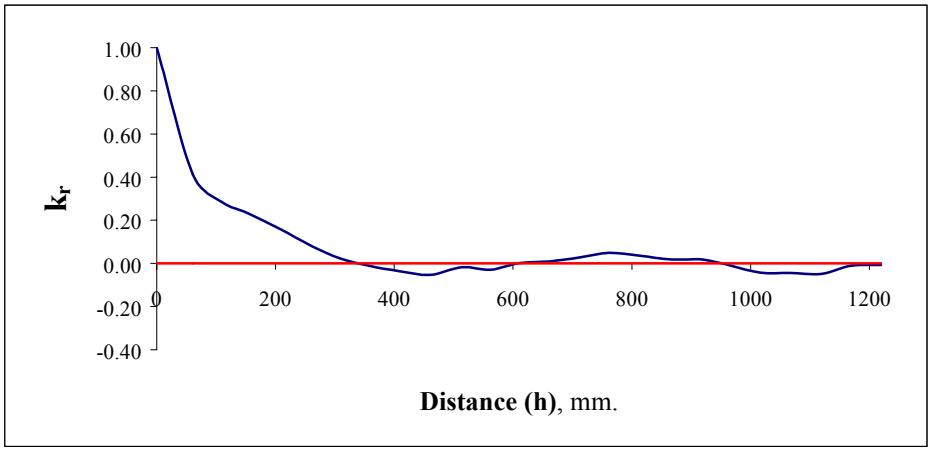

(b)

Figure D.7. *Panel m1p4: (a) omniderectional variogram, and (b) omnidirectional correlogram.*

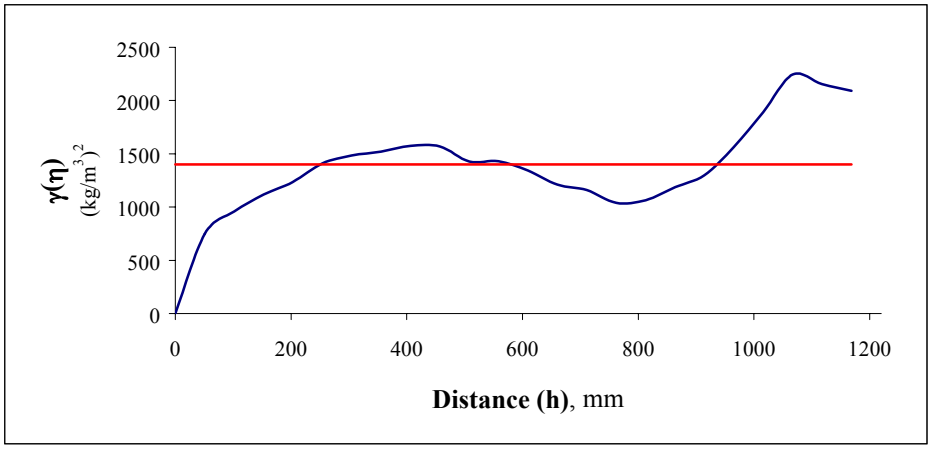

(a)

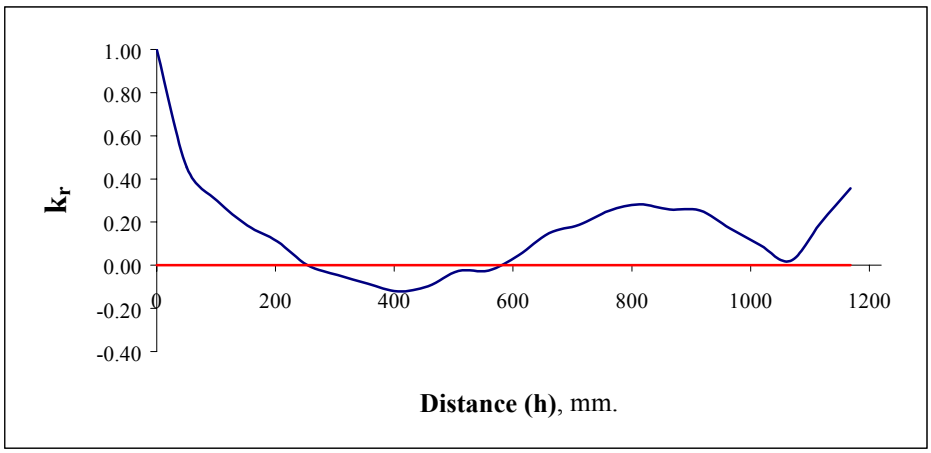

(b)

Figure D.8. *Panel m1p4: (a) transversal variogram, and (b) transversal correlogram.*

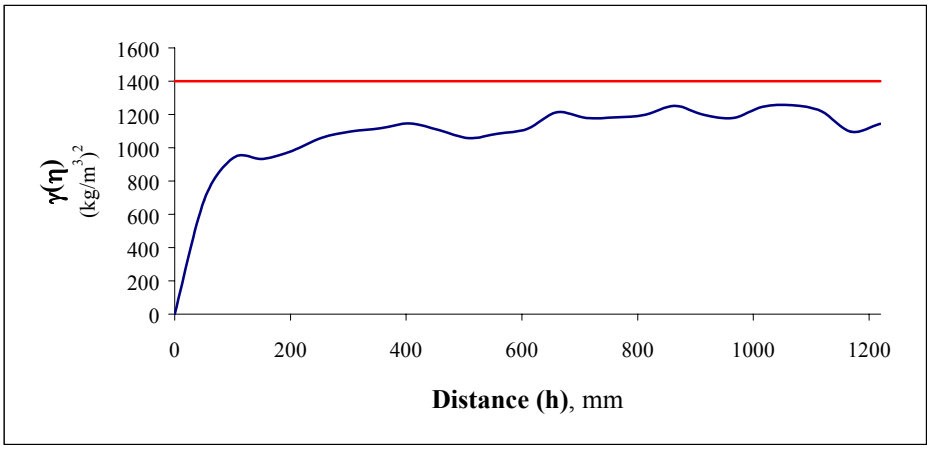

(a)

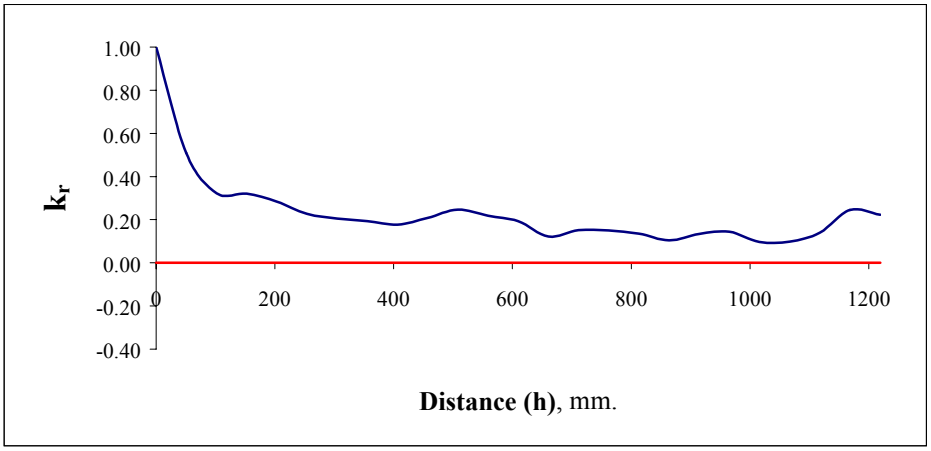

(b)

Figure D.9. *Panel m1p4: (a) longitudinal variogram, and (b) longitudinal correlogram.*

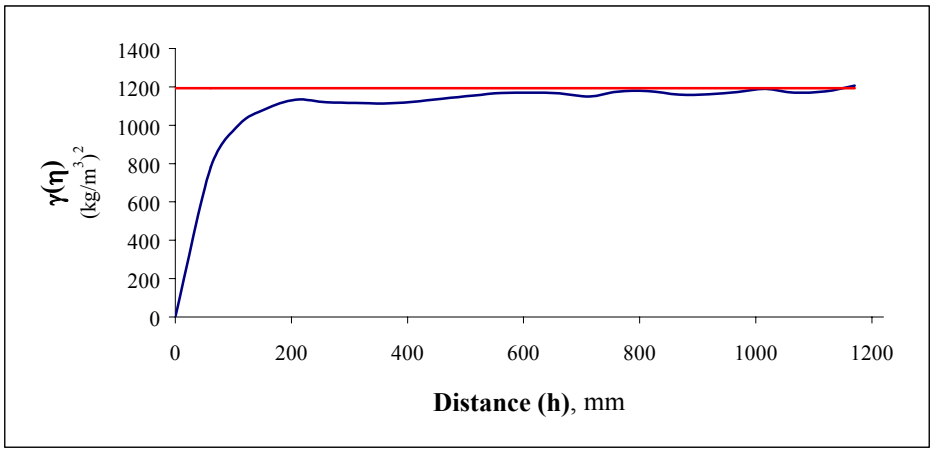

(a)

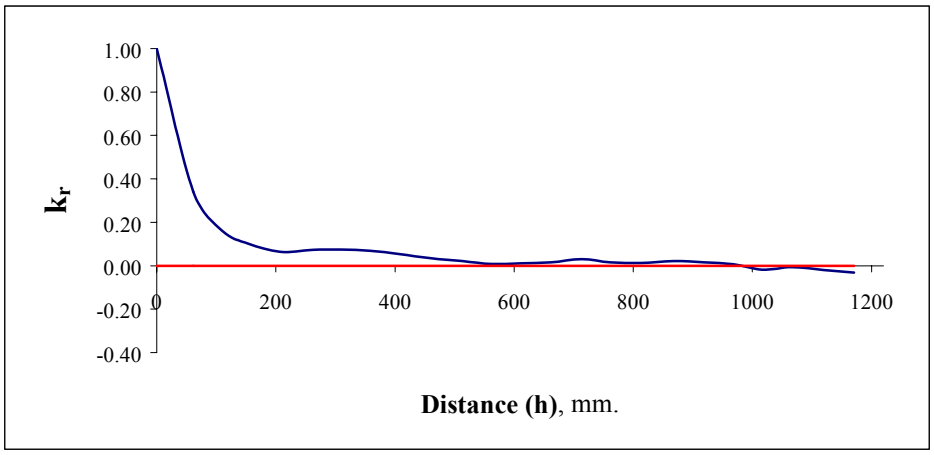

(b)

Figure D.10. *Panel m1p5: (a) omniderectional variogram, and (b) omnidirectional correlogram.*

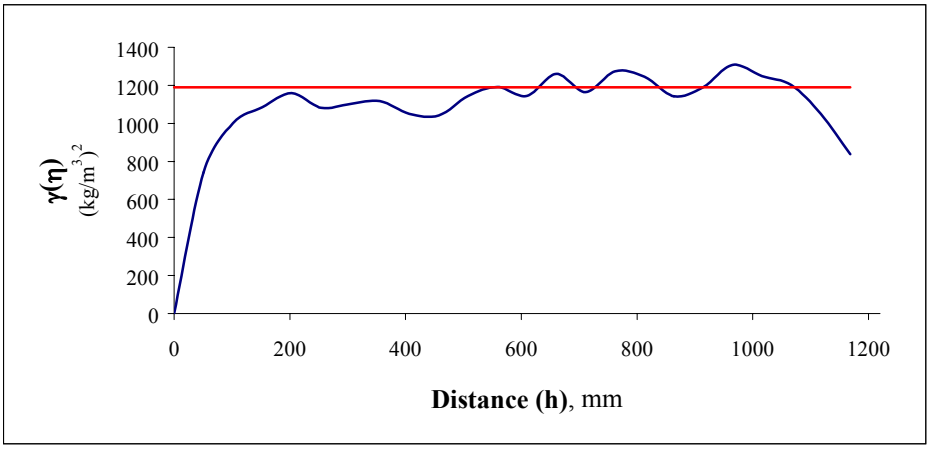

(a)

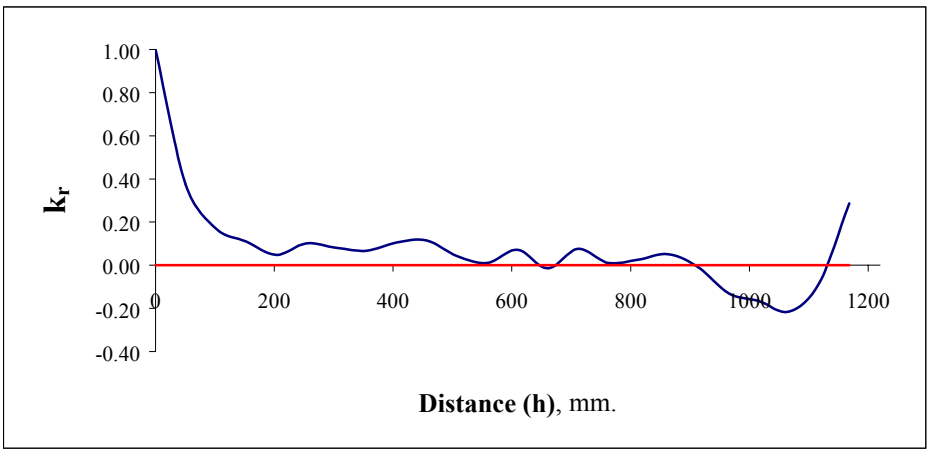

(b)

Figure D.11. *Panel m1p5: (a) transversal variogram, and (b) transversal correlogram.*

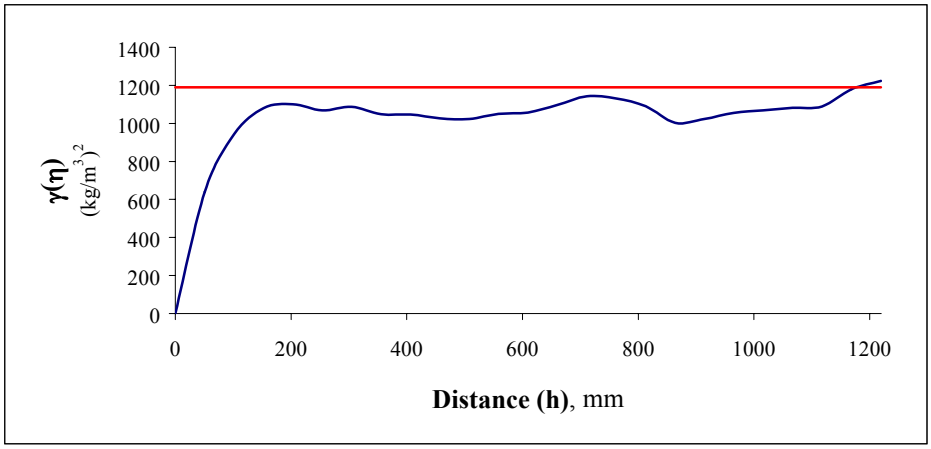

(a)

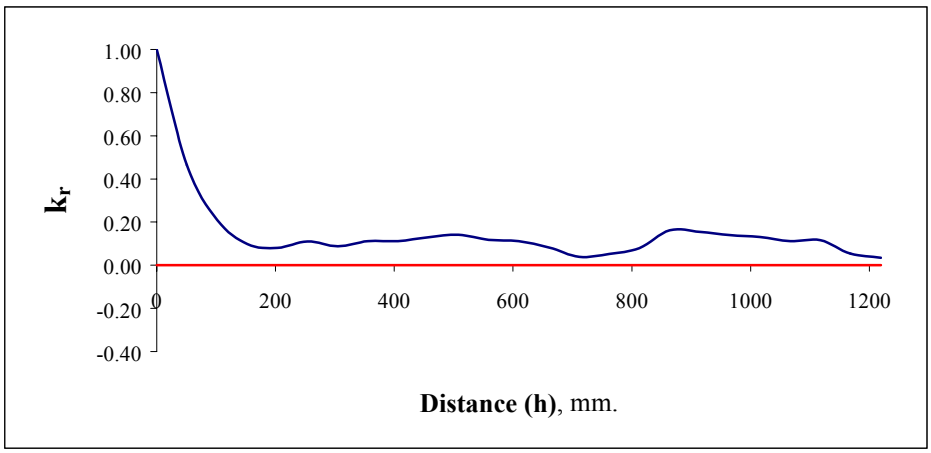

(b)

Figure D.12. *Panel m1p5: (a) longitudinal variogram, and (b) longitudinal correlogram.*

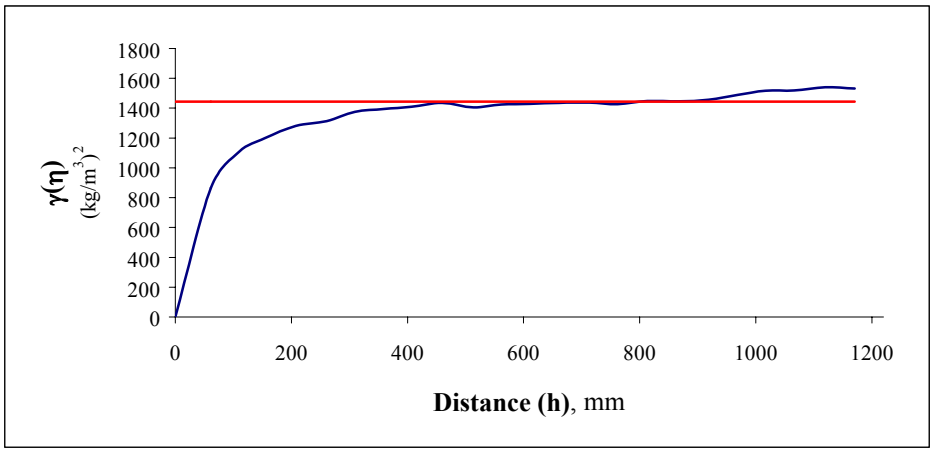

(a)

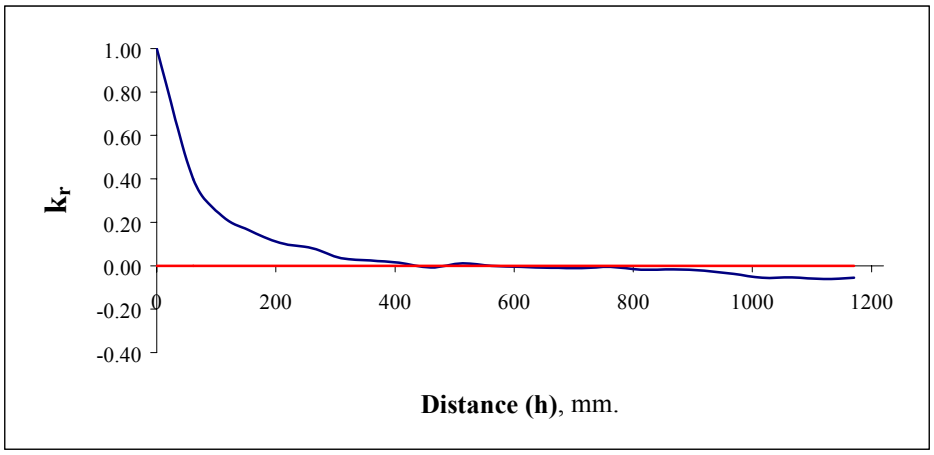

(b)

Figure D.13. *Panel m1p6: (a) omniderectional variogram, and (b) omnidirectional correlogram.*

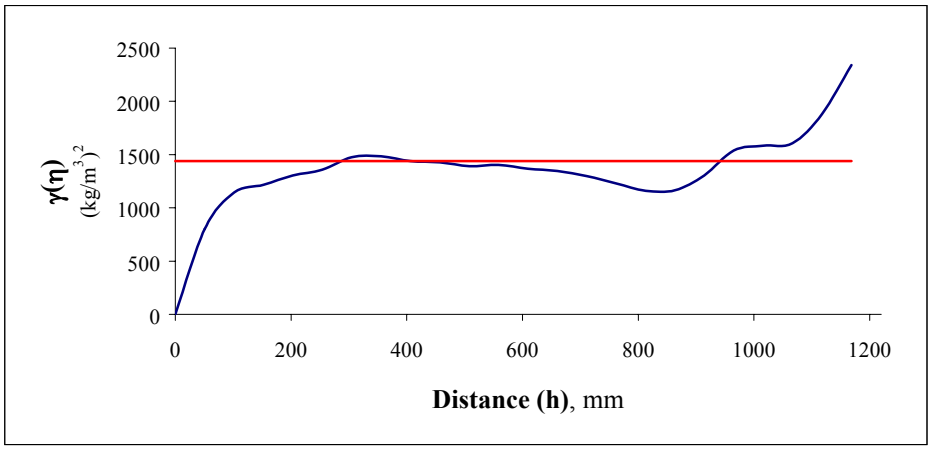

(a)

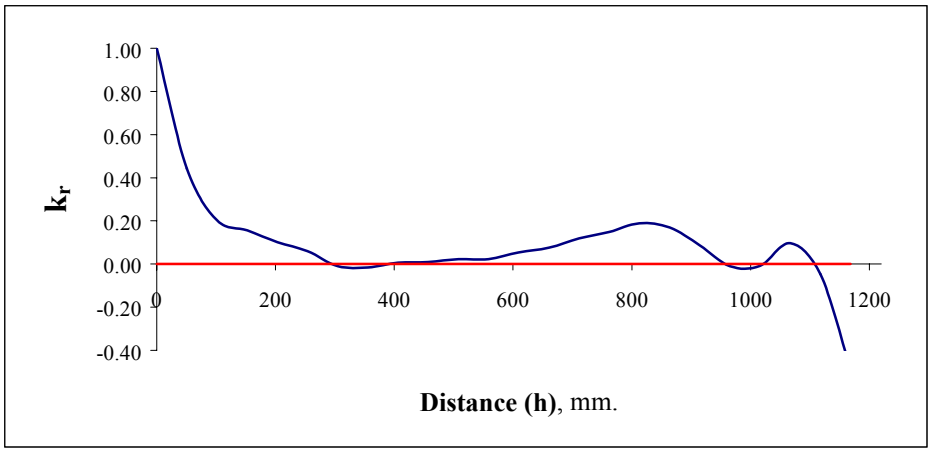

(b)

Figure D.14. *Panel m1p6: (a) transversal variogram, and (b) transversal correlogram.*

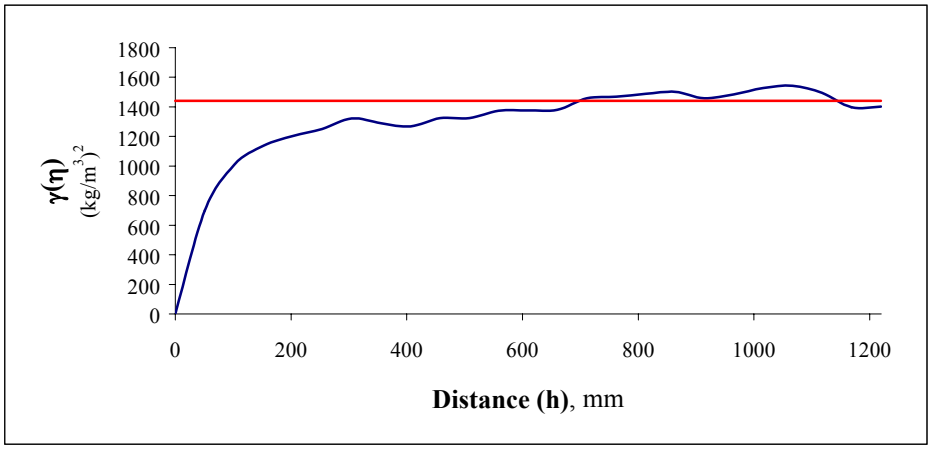

(a)

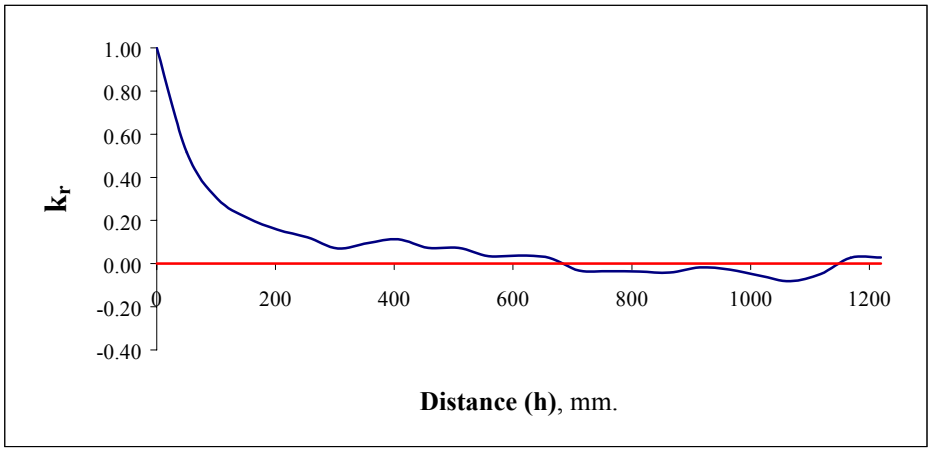

(b)

Figure D.15. *Panel m1p6: (a) longitudinal variogram, and (b) longitudinal correlogram.*

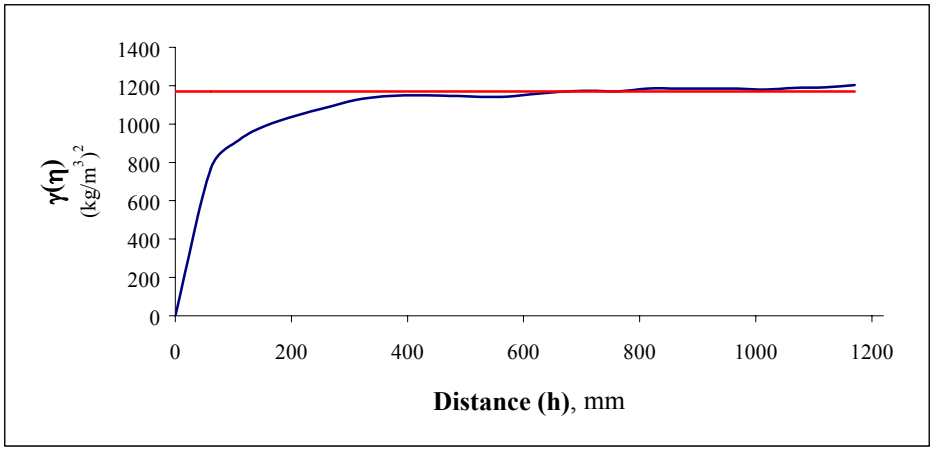

(a)

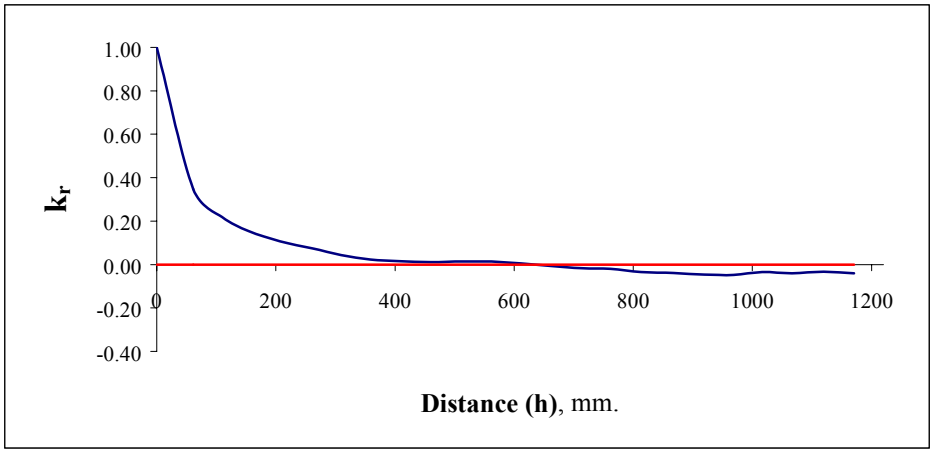

(b)

Figure D.16. *Panel m2p1: (a) omniderectional variogram, and (b) omnidirectional correlogram.*

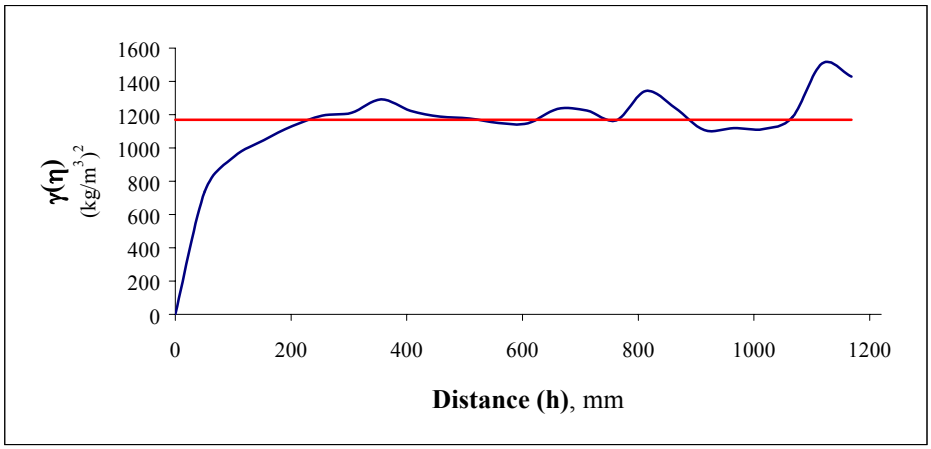

(a)

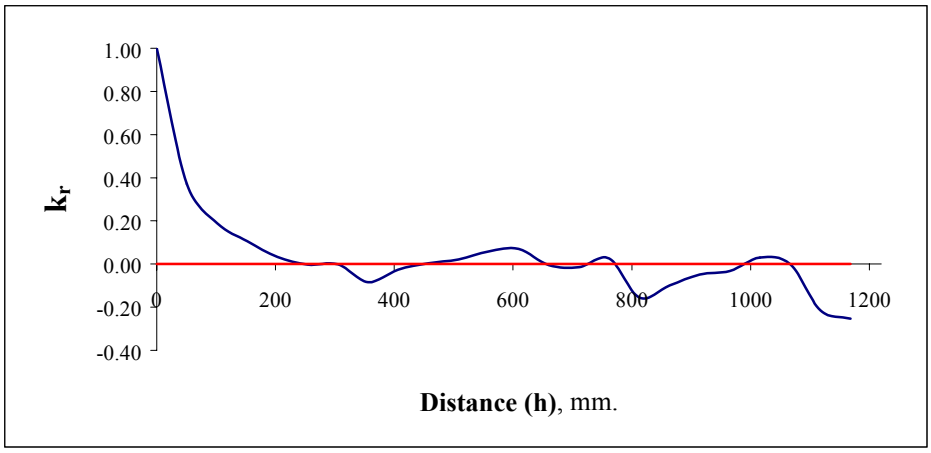

(b)

Figure D.17. *Panel m2p1: (a) transversal variogram, and (b) transversal correlogram.*

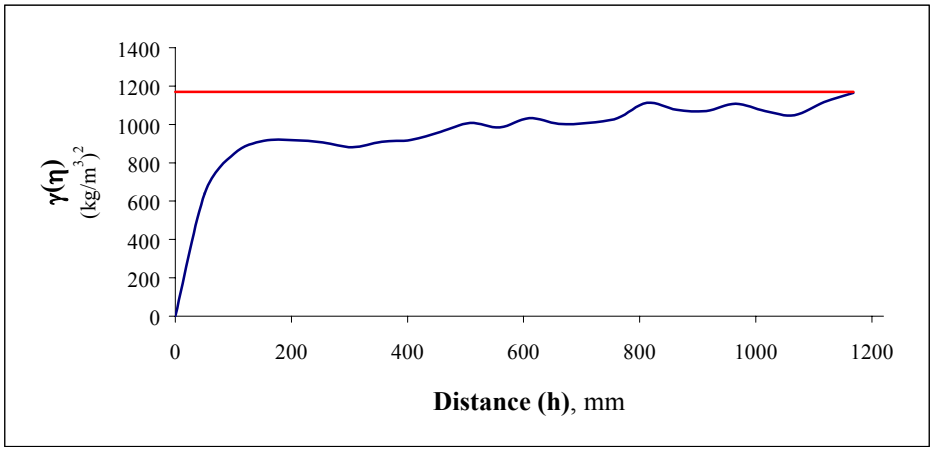

(a)

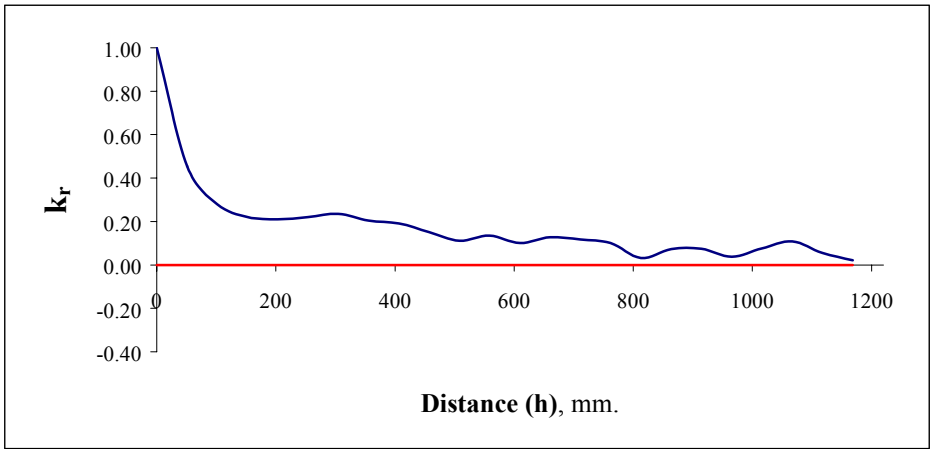

(b)

Figure D.18. *Panel m2p1: (a) longitudinal variogram, and (b) longitudinal correlogram.*

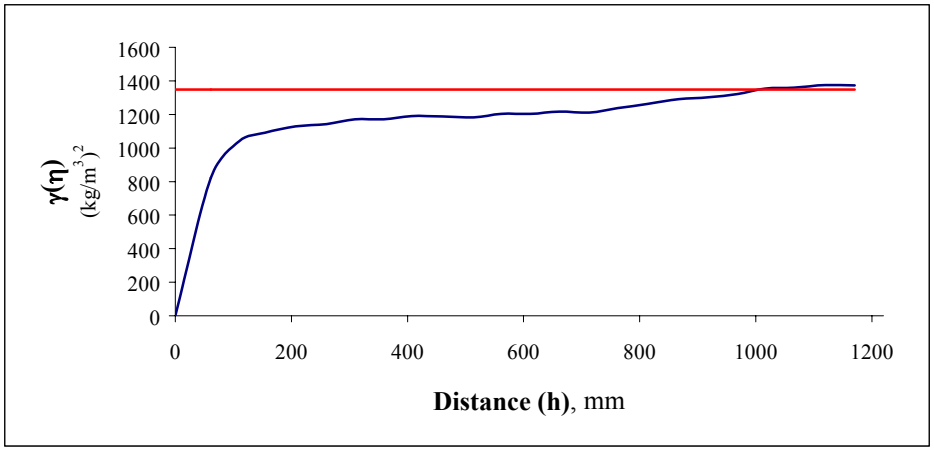

(a)

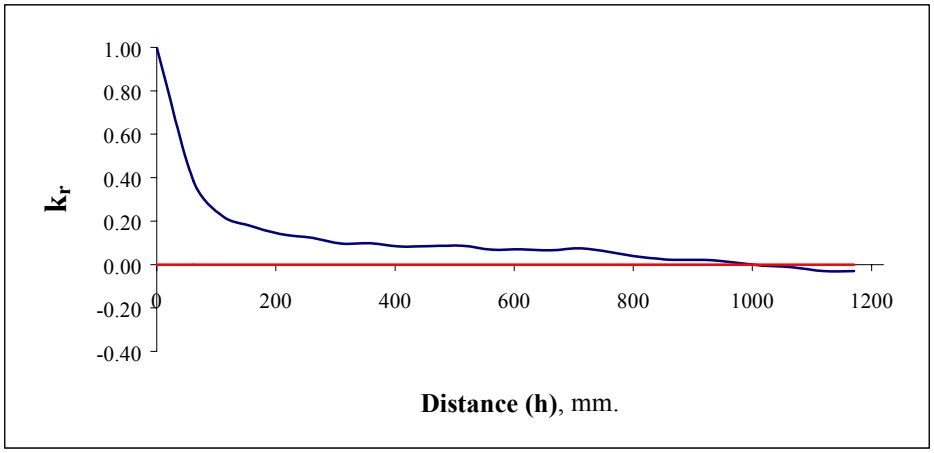

(b)

Figure D.19. *Panel m2p2: (a) omniderectional variogram, and (b) omnidirectional correlogram.*

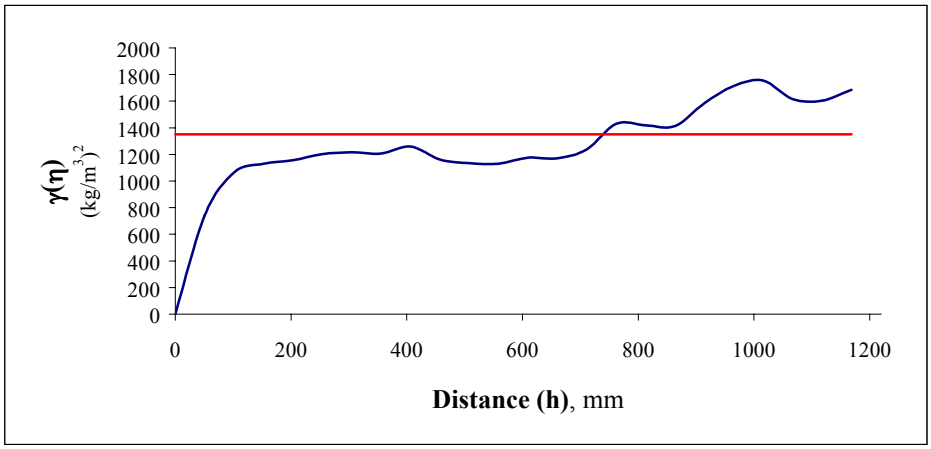

(a)

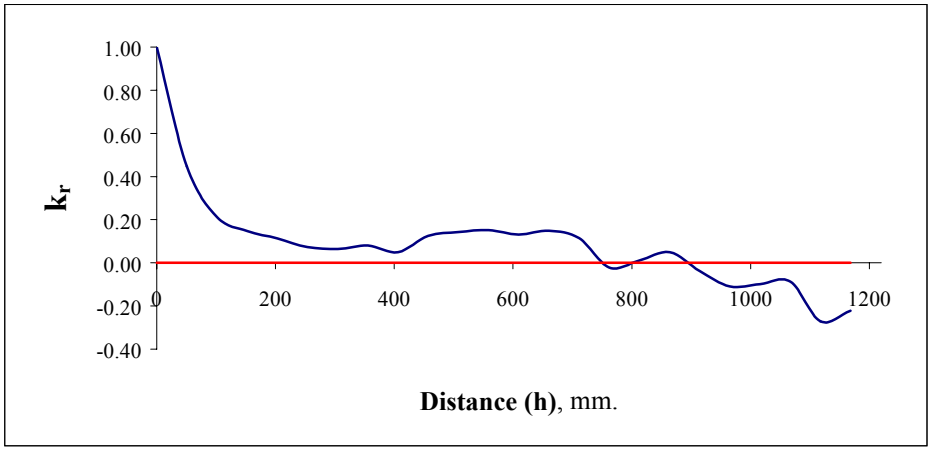

(b)

Figure D.20. *Panel m2p2: (a) transversal variogram, and (b) transversal correlogram.*

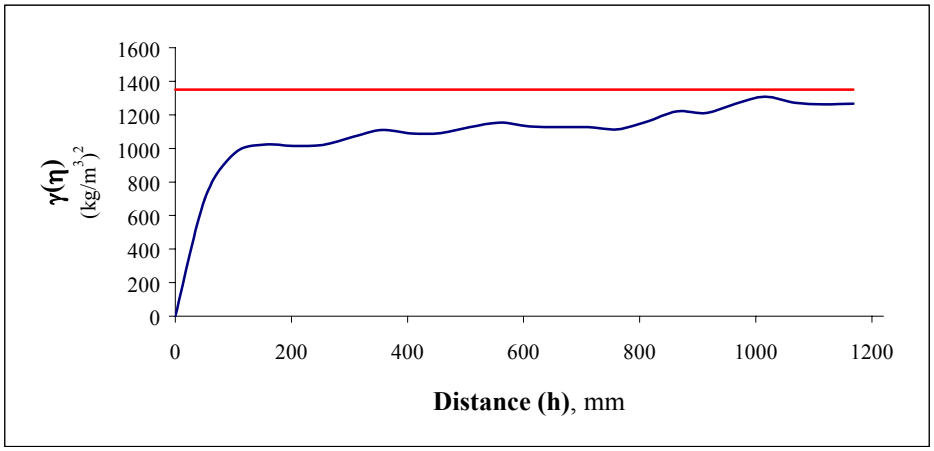

(a)

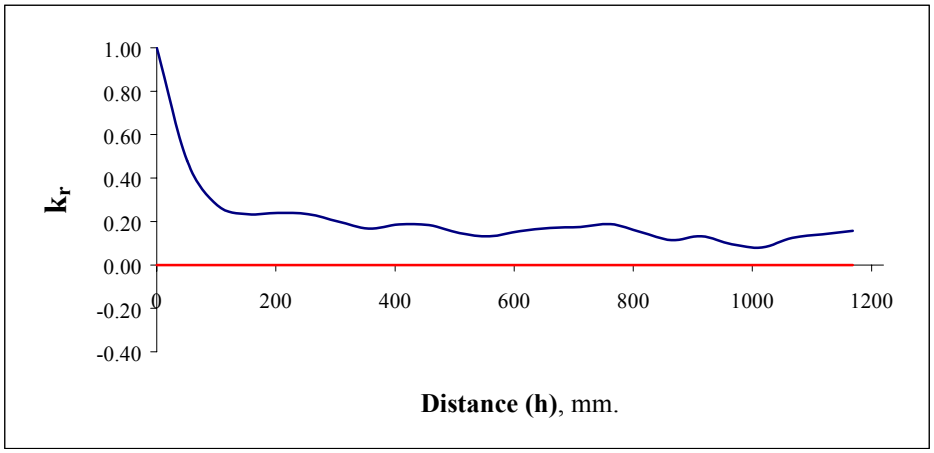

(b)

Figure D.21. *Panel m2p2: (a) longitudinal variogram, and (b) longitudinal correlogram.*

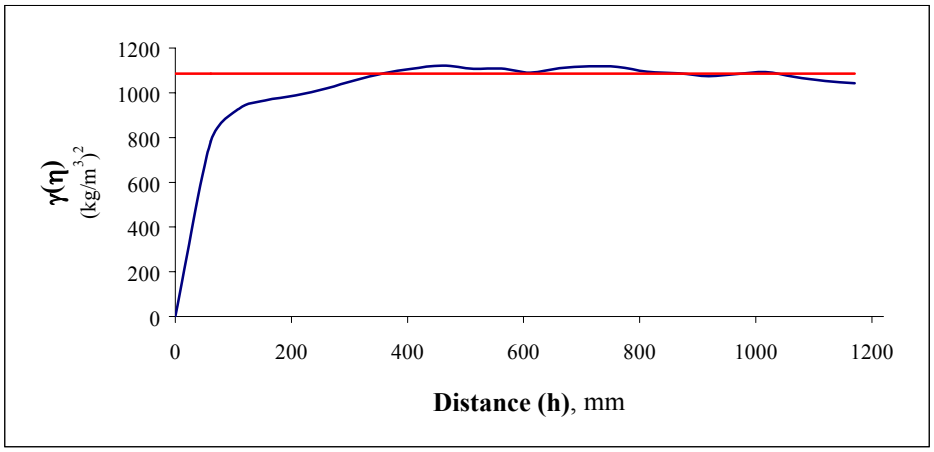

(a)

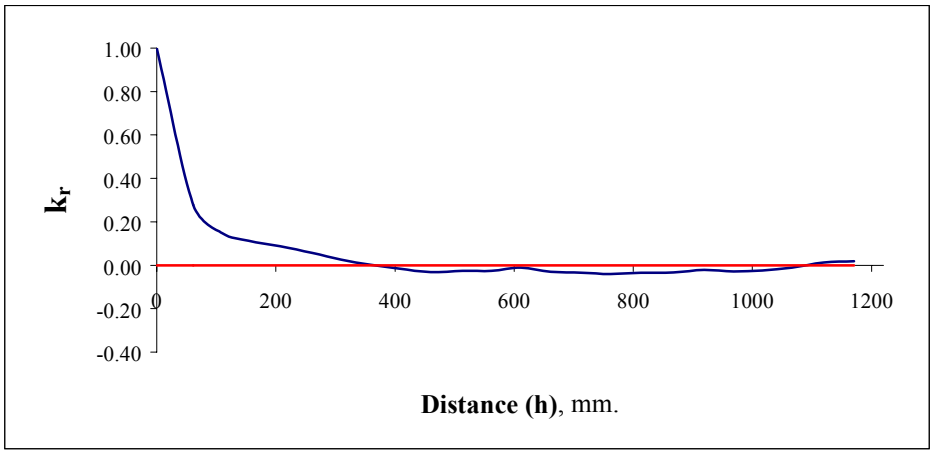

(b)

Figure D.22. *Panel m2p3: (a) omniderectional variogram, and (b) omnidirectional correlogram.*

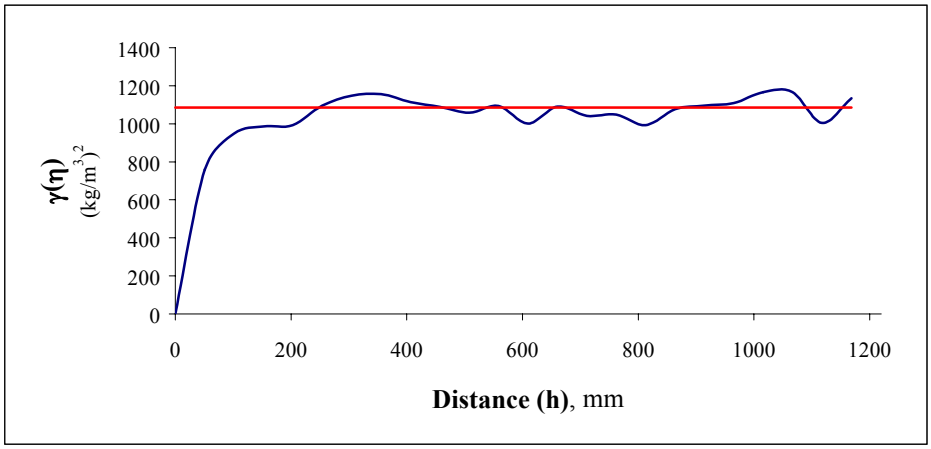

(a)

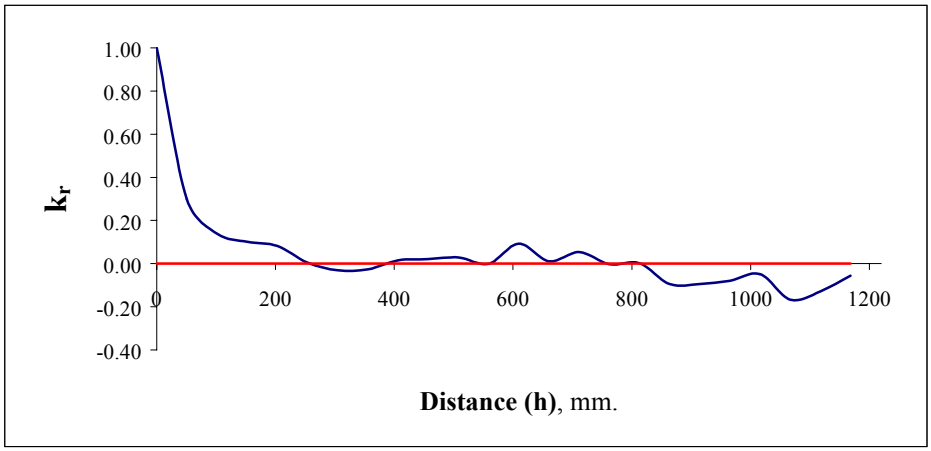

(b)

Figure D.23. *Panel m2p3: (a) transversal variogram, and (b) transversal correlogram.*

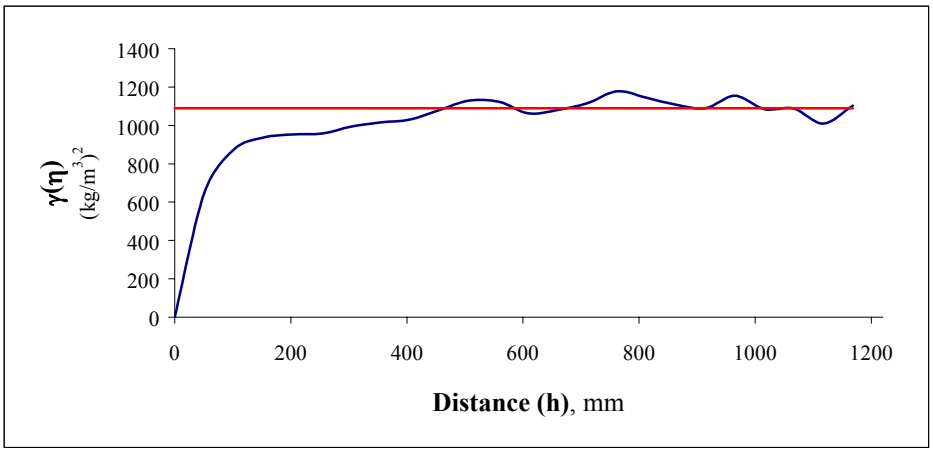

(a)

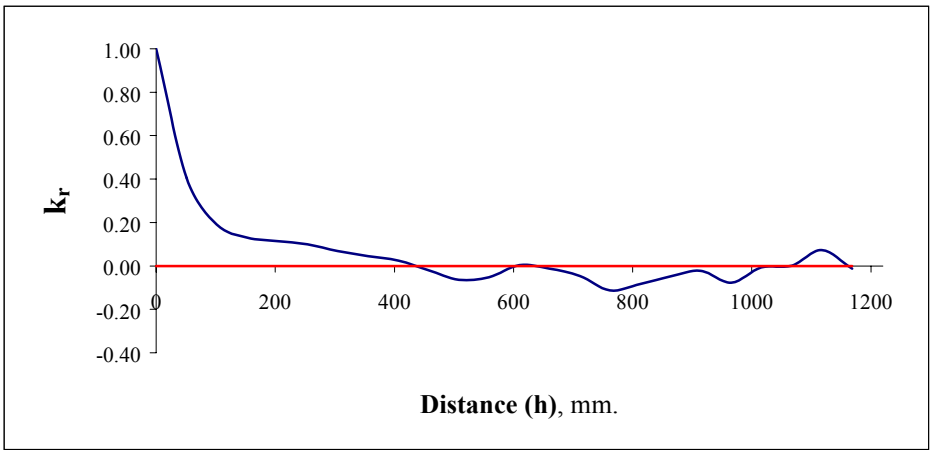

(b)

Figure D.24. *Panel m2p3: (a) longitudinal variogram, and (b) longitudinal correlogram.*

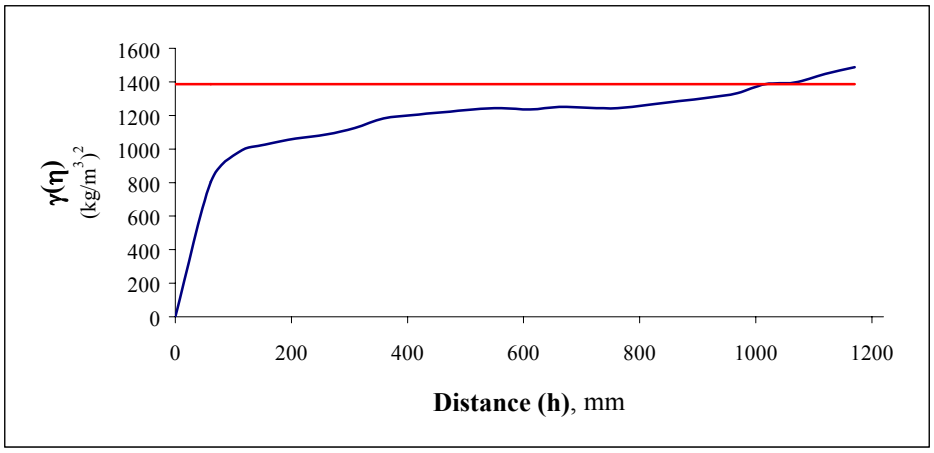

(a)

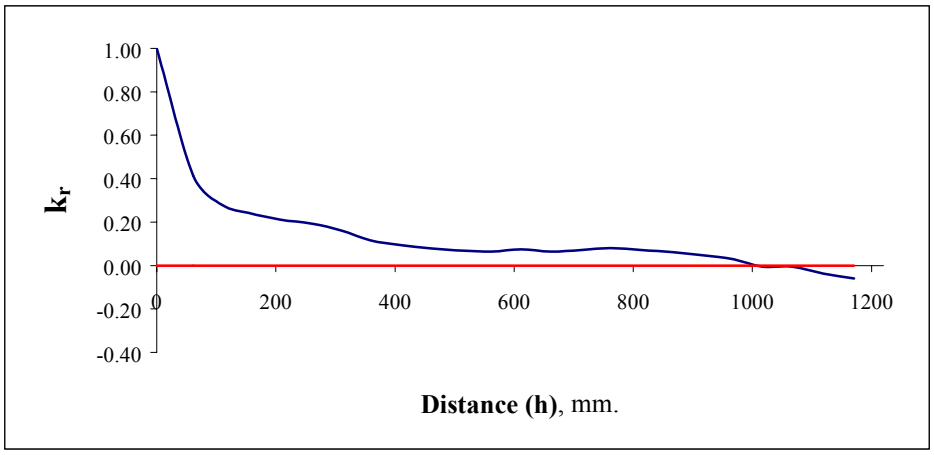

(b)

Figure D.25. *Panel m2p4: (a) omniderectional variogram, and (b) omnidirectional correlogram.*

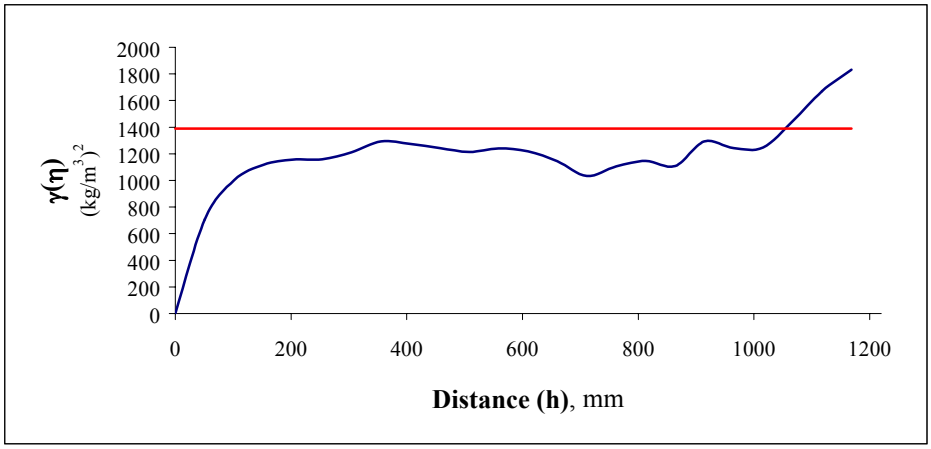

(a)

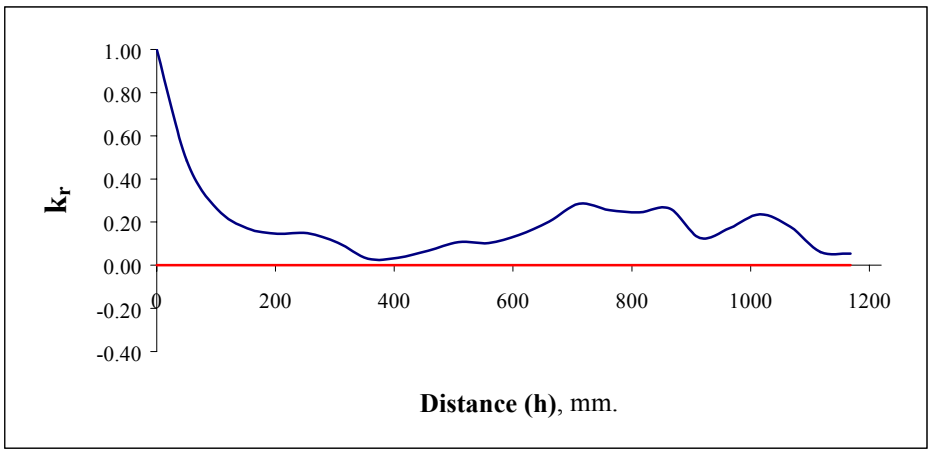

(b)

Figure D.26. *Panel m2p4: (a) transversal variogram, and (b) transversal correlogram.*

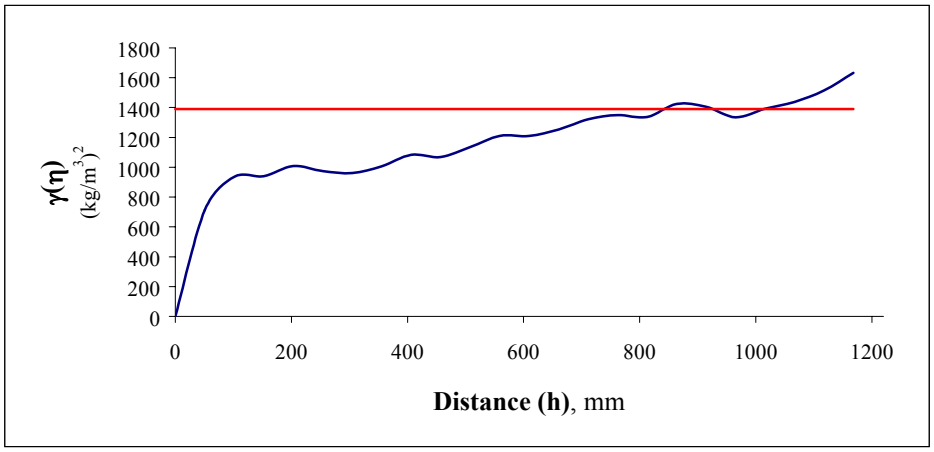

(a)

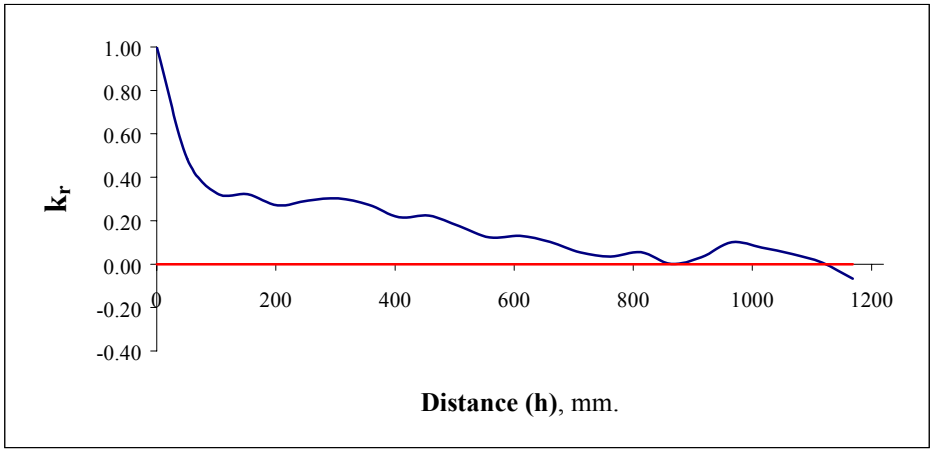

(b)

Figure D.27. *Panel m2p4: (a) longitudinal variogram, and (b) longitudinal correlogram.*

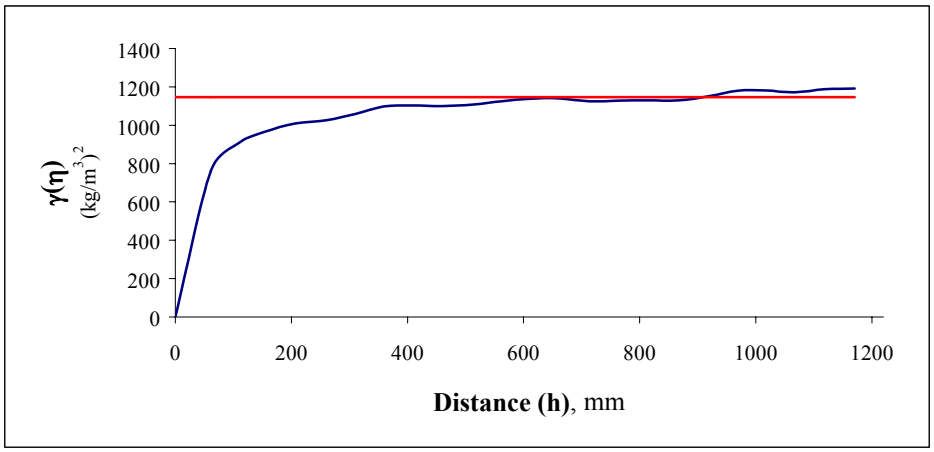

(a)

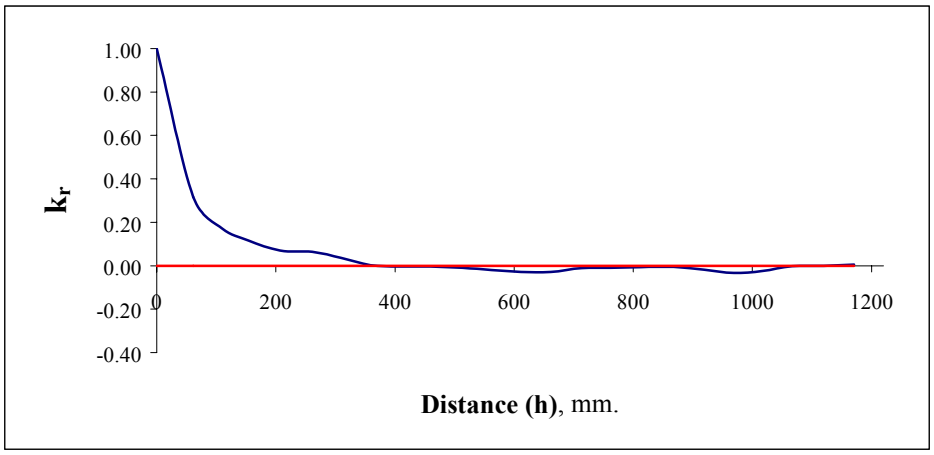

(b)

Figure D.28. *Panel m2p5: (a) omniderectional variogram, and (b) omnidirectional correlogram.*

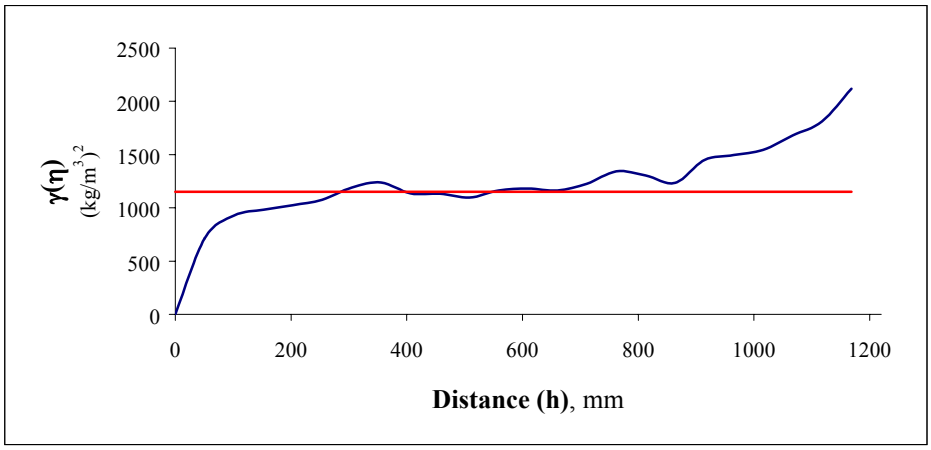

(a)

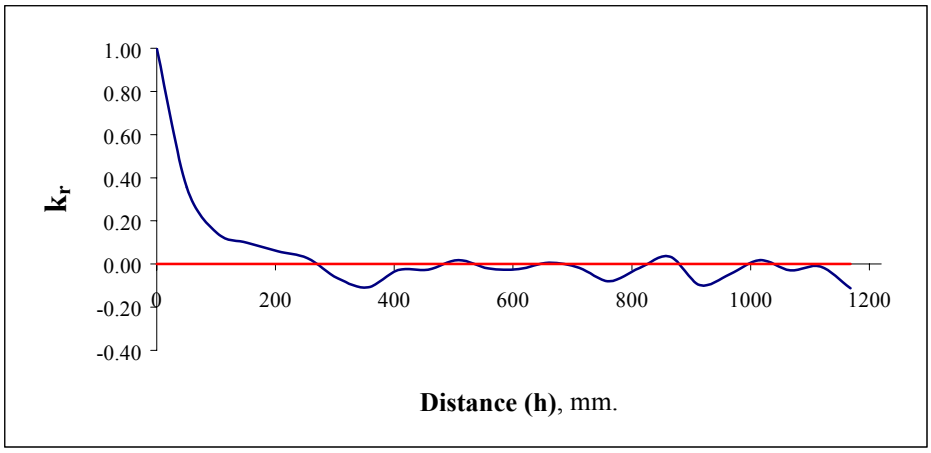

(b)

Figure D.29. *Panel m2p5: (a) transversal variogram, and (b) transversal correlogram.*

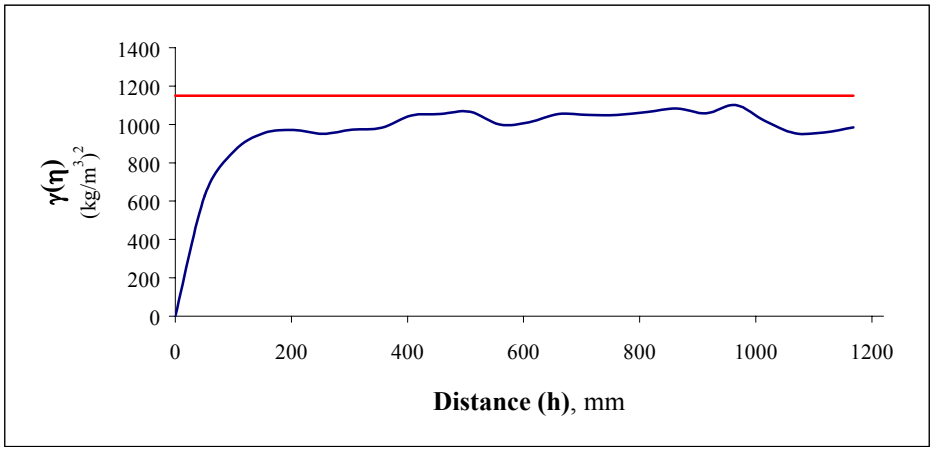

(a)

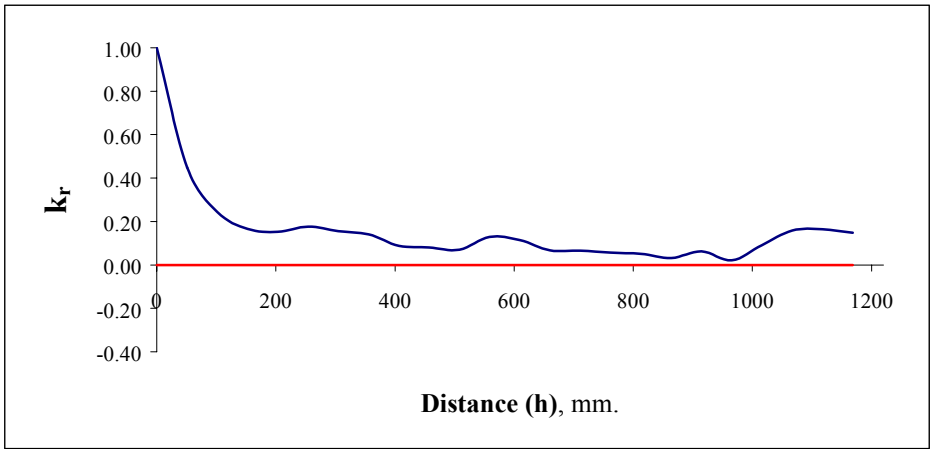

(b)

Figure D.30. *Panel m2p5: (a) longitudinal variogram, and (b) longitudinal correlogram.*

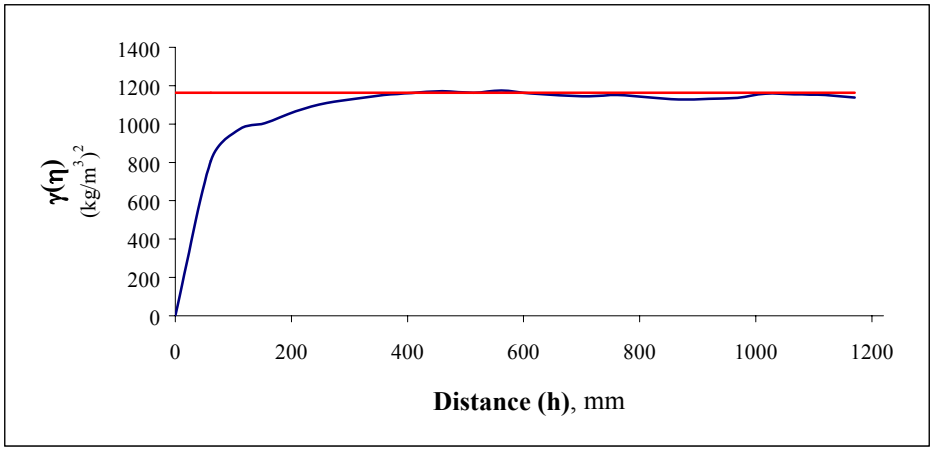

(a)

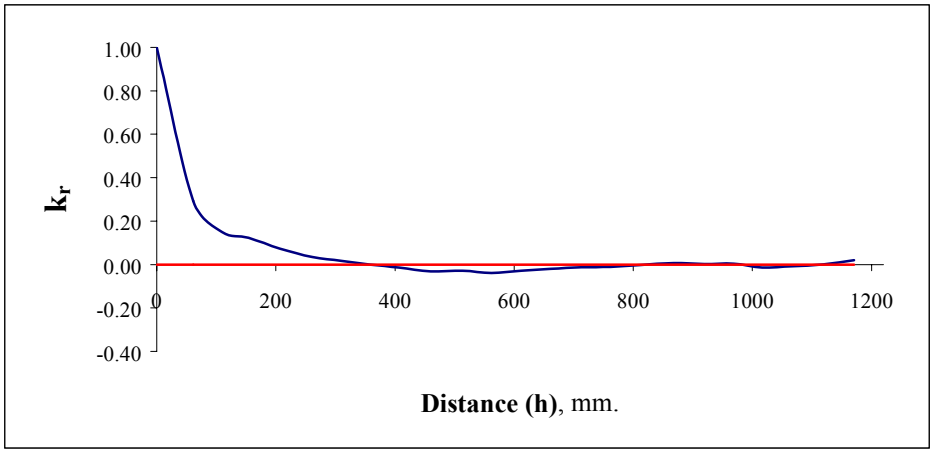

(b)

Figure D.31. *Panel m2p6: (a) omniderectional variogram, and (b) omnidirectional correlogram.*

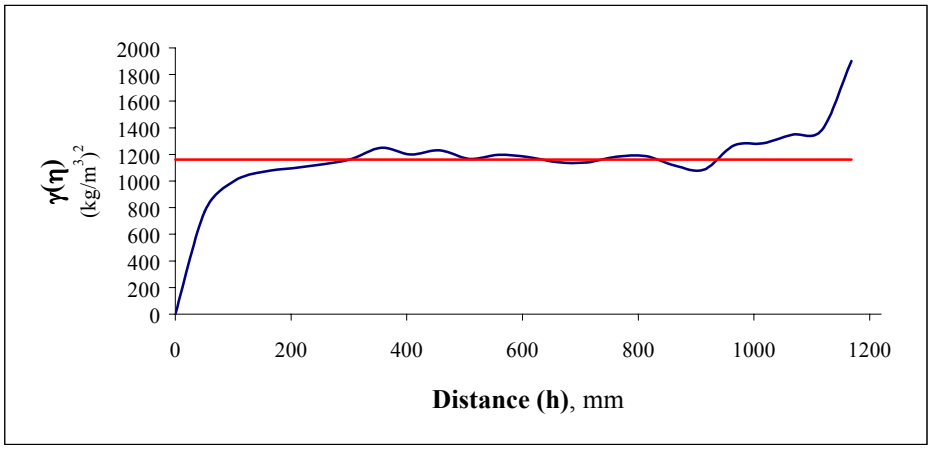

(a)

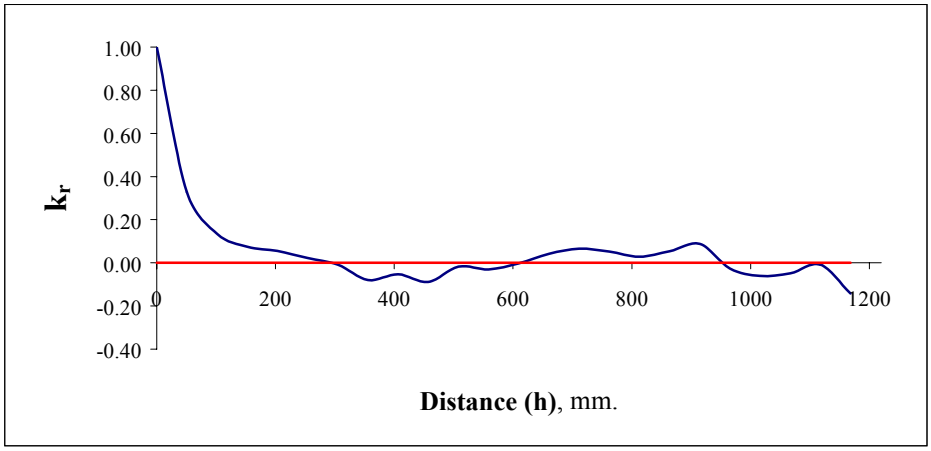

(b)

Figure D.32. *Panel m2p6: (a) transversal variogram, and (b) transversal correlogram.*

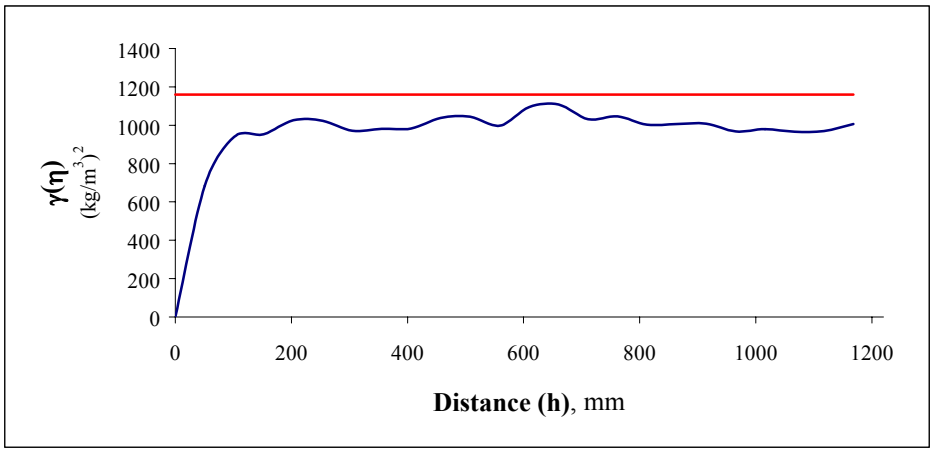
1400
1200
1000
800
600
400
200
0
γ(η)
(kg/m3)2
0
200
400
600
800
1000
1200
Distance (h), mm

(a)

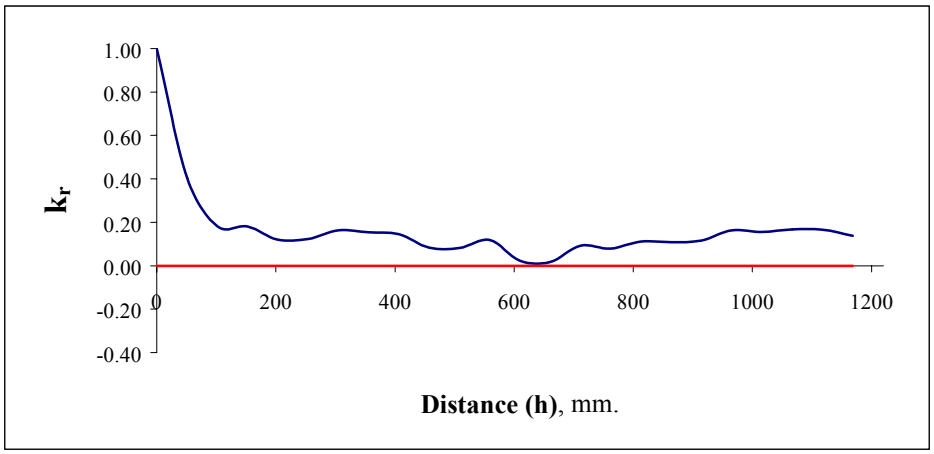
1.00
0.80
0.60
0.40
0.20
0.00
-0.20
-0.40
kr
0
200
400
600
800
1000
1200
Distance (h), mm.

(b)

Figure D.33. *Panel m2p6: (a) longitudinal variogram, and (b) longitudinal correlogram.*

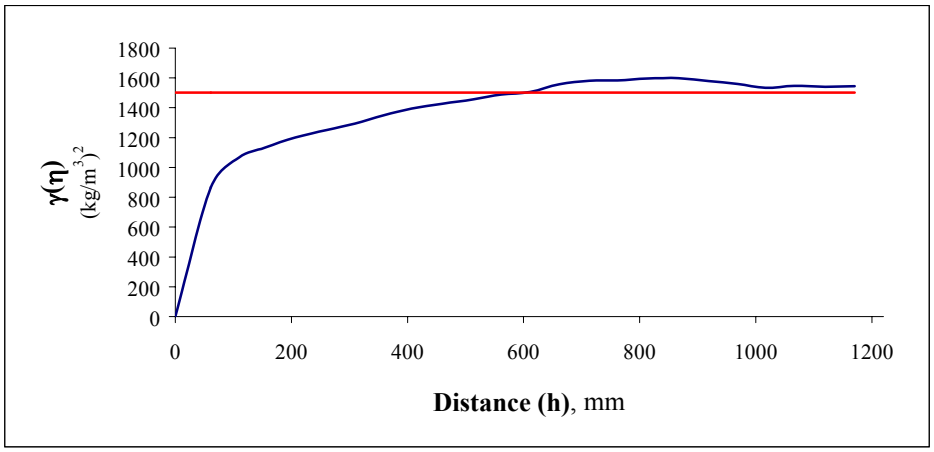

(a)

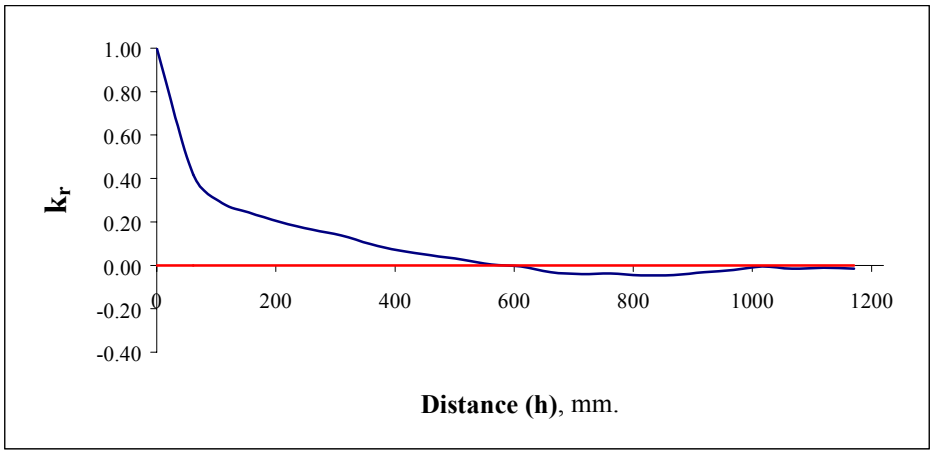

(b)

Figure D.34. *Panel m3p1: (a) omniderectional variogram, and (b) omnidirectional correlogram.*

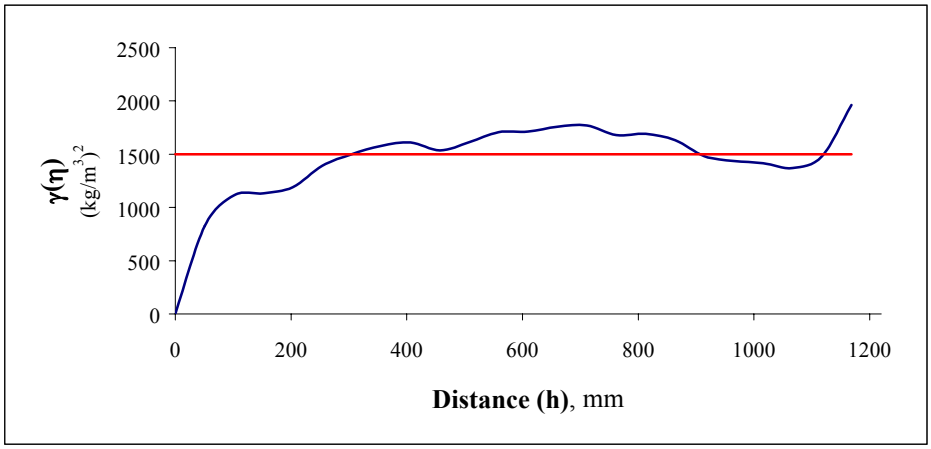
2500
2000
1500
1000
500
0
γ(η)
(kg/m3)2
0
200
400
600
800
1000
1200
Distance (h), mm

(a)

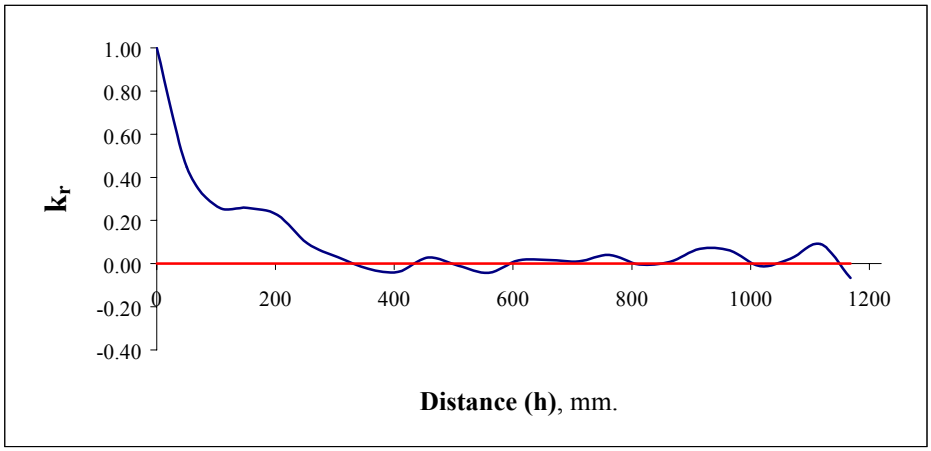
1.00
0.80
0.60
0.40
0.20
0.00
-0.20
-0.40
kr
0
200
400
600
800
1000
1200
Distance (h), mm.

(b)

Figure D.35. *Panel m3p1: (a) transversal variogram, and (b) transversal correlogram.*

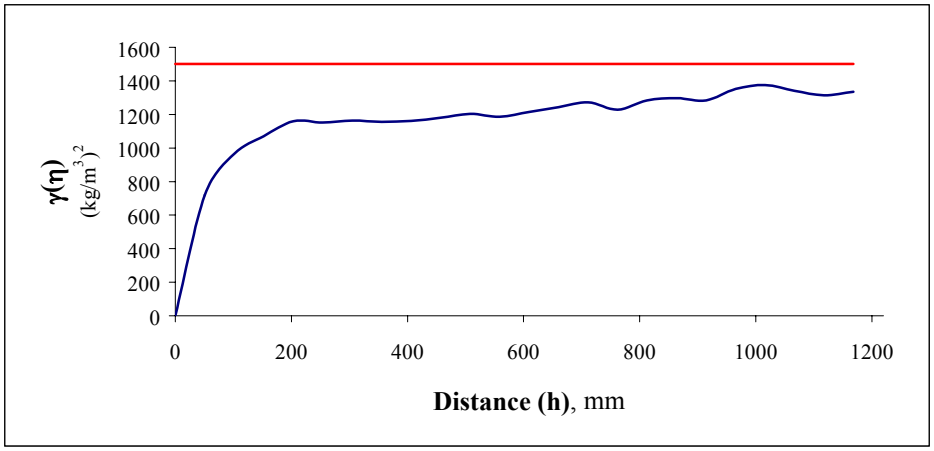

(a)

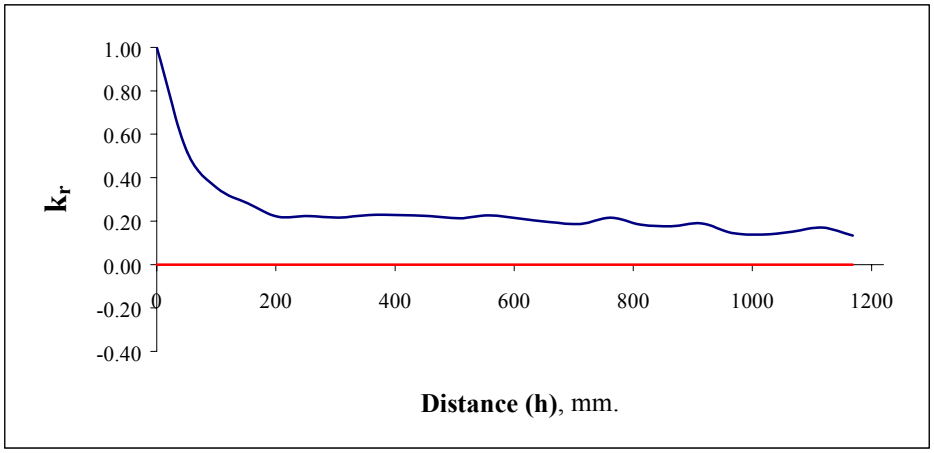

(b)

Figure D.36. *Panel m3p1: (a) longitudinal variogram, and (b) longitudinal correlogram.*

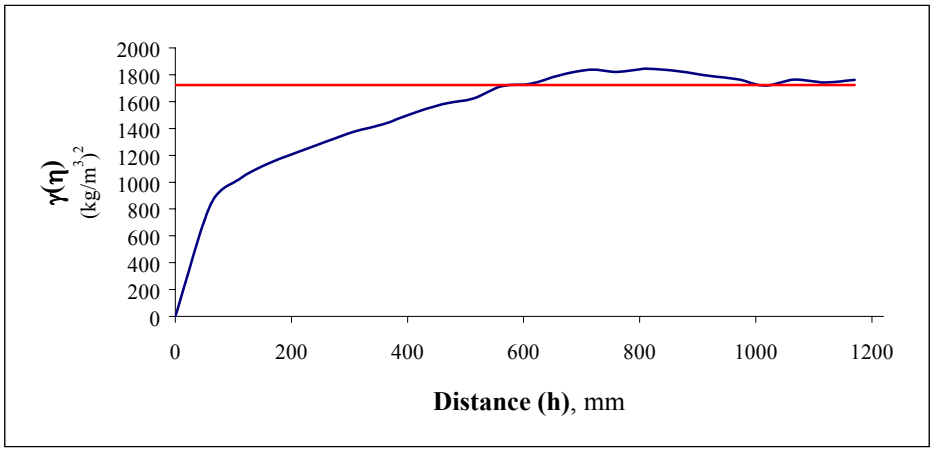

(a)

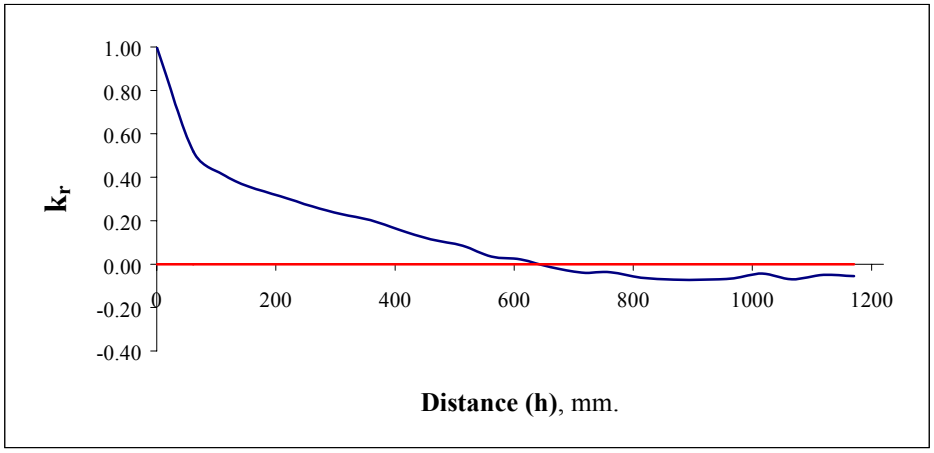

(b)

Figure D.37. *Panel m3p2: (a) omniderectional variogram, and (b) omnidirectional correlogram.*

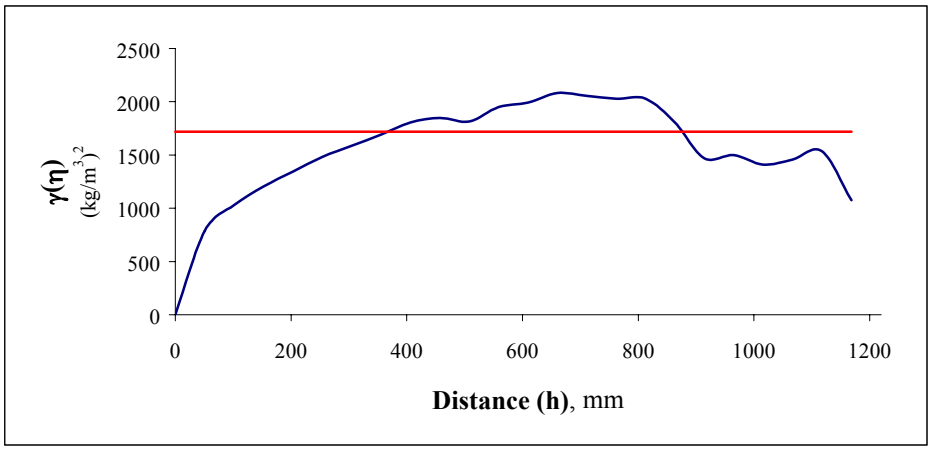
2500
2000
1500
1000
500
0
γ(η)
(kg/m3)2
0
200
400
600
800
1000
1200
Distance (h), mm

(a)

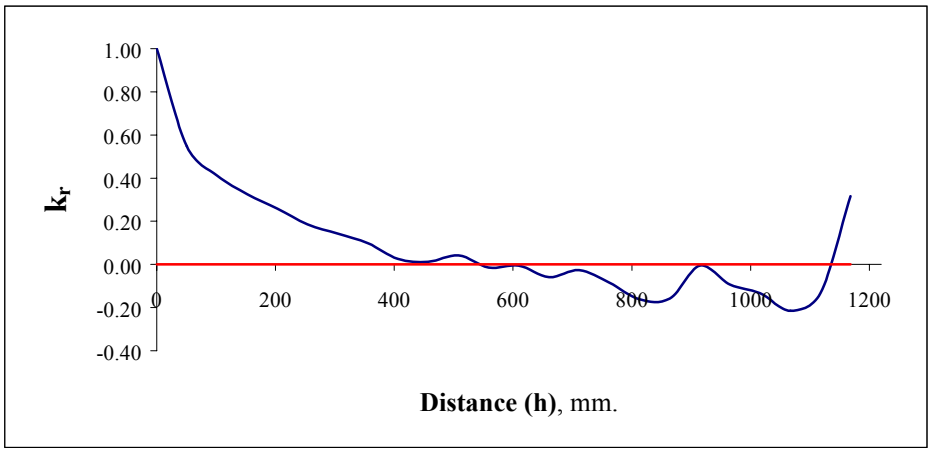
1.00
0.80
0.60
0.40
0.20
0.00
-0.20
-0.40
kr
0
200
400
600
800
1000
1200
Distance (h), mm.

(b)

Figure D.38. *Panel m3p2: (a) transversal variogram, and (b) transversal correlogram.*

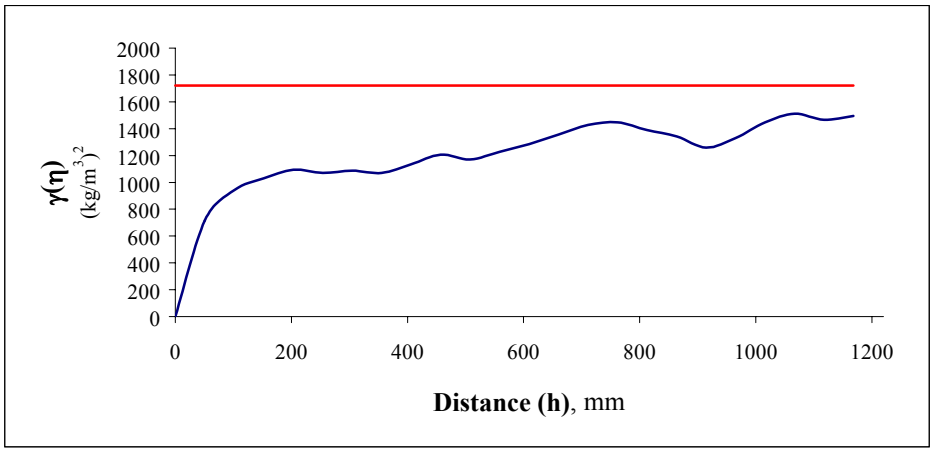

(a)

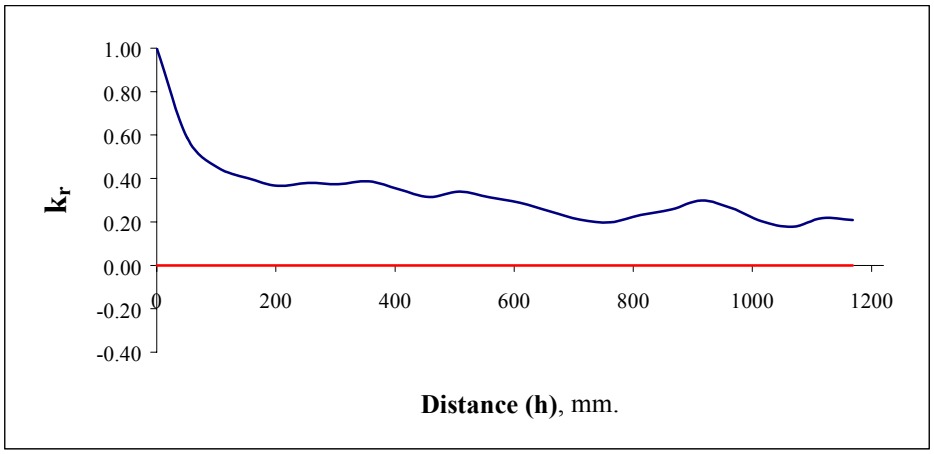

(b)

Figure D.39. *Panel m3p2: (a) longitudinal variogram, and (b) longitudinal correlogram.*

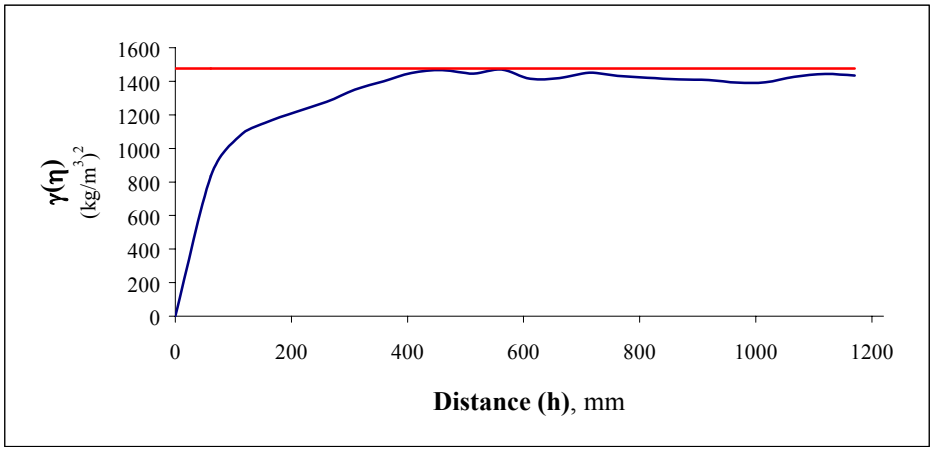

(a)

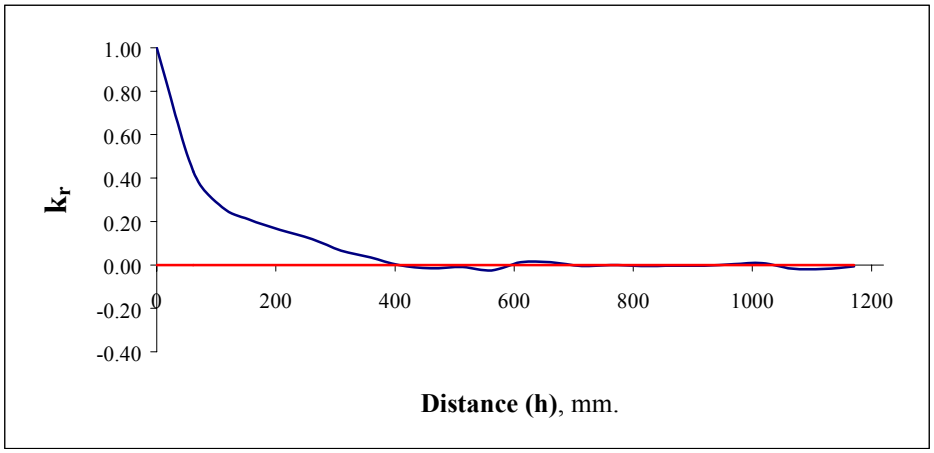

(b)

Figure D.40. *Panel m3p3: (a) omniderectional variogram, and (b) omnidirectional correlogram.*

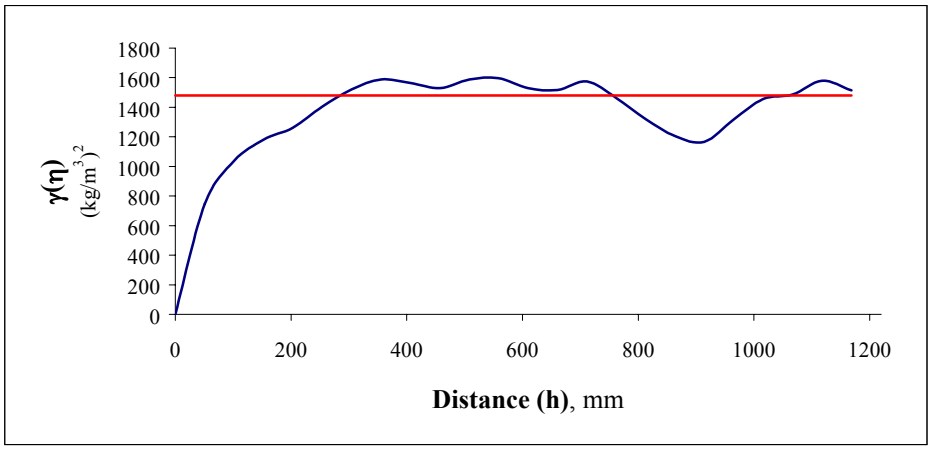

(a)

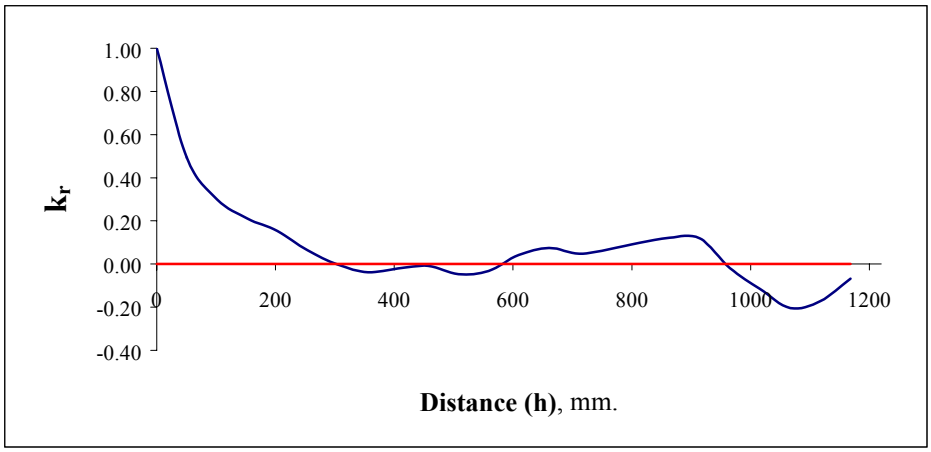

(b)

Figure D.41. *Panel m3p3: (a) transversal variogram, and (b) transversal correlogram.*

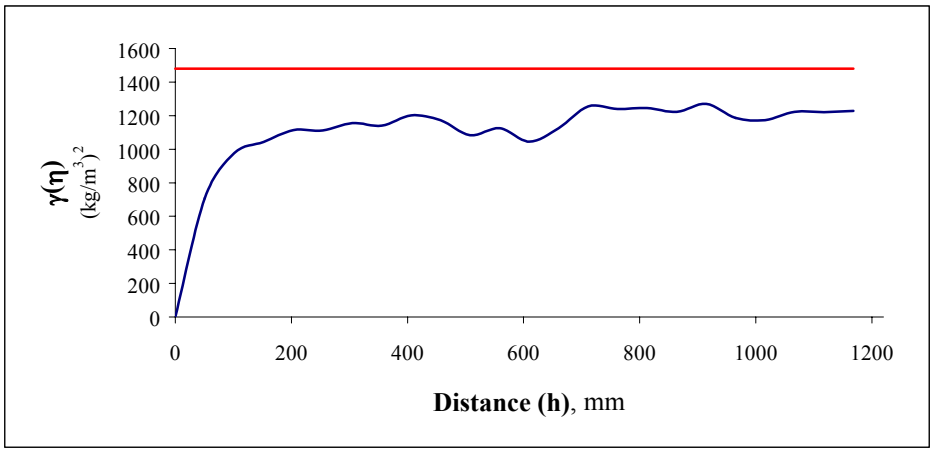

(a)

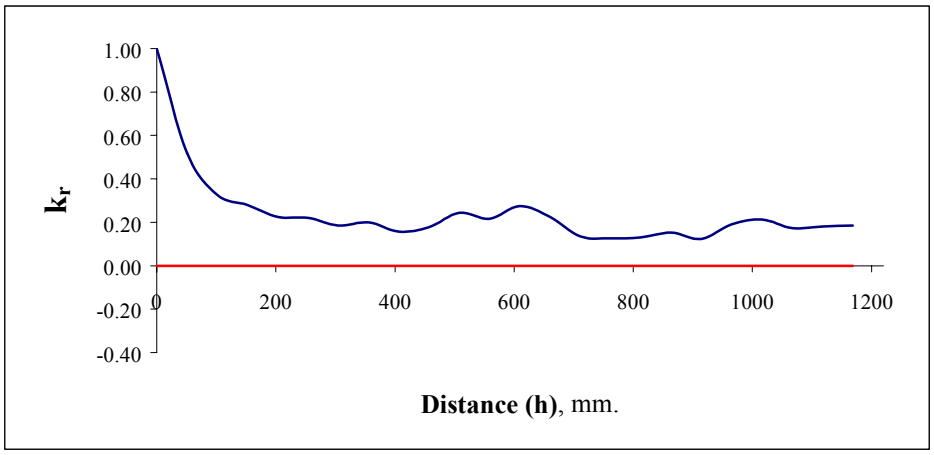

(b)

Figure D.42. *Panel m3p3: (a) Longitudinal Variogram, and (b) Longitudinal correlogram.*

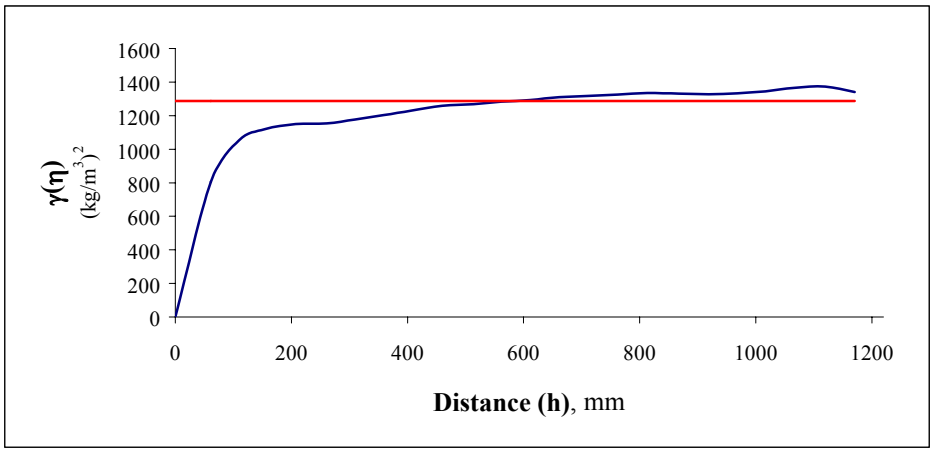

(a)

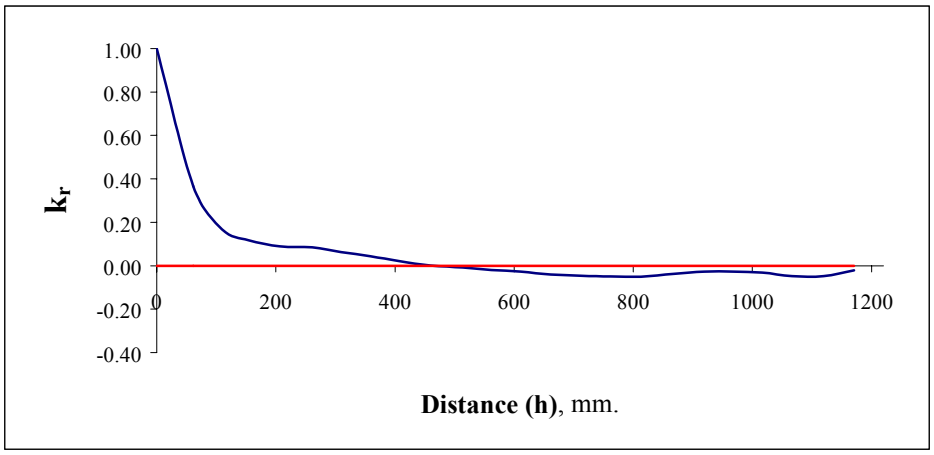

(b)

Figure D.43. *Panel m3p4: (a) omniderectional variogram, and (b) omnidirectional correlogram.*

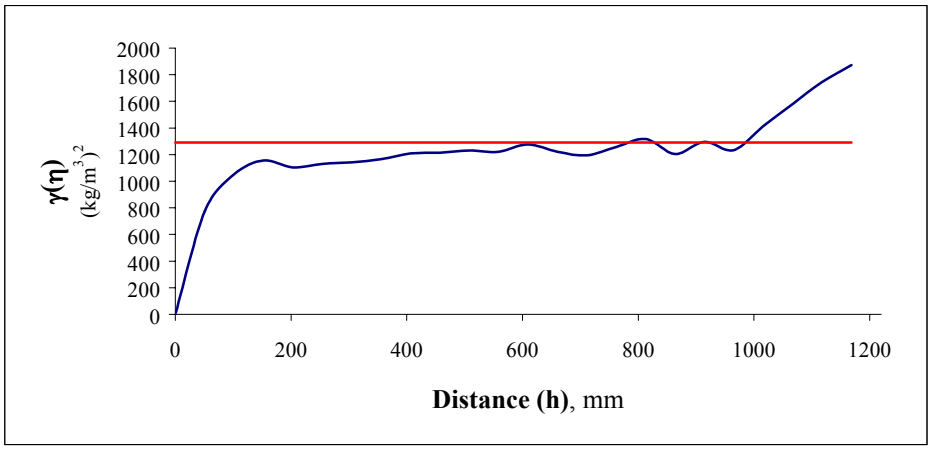

(a)

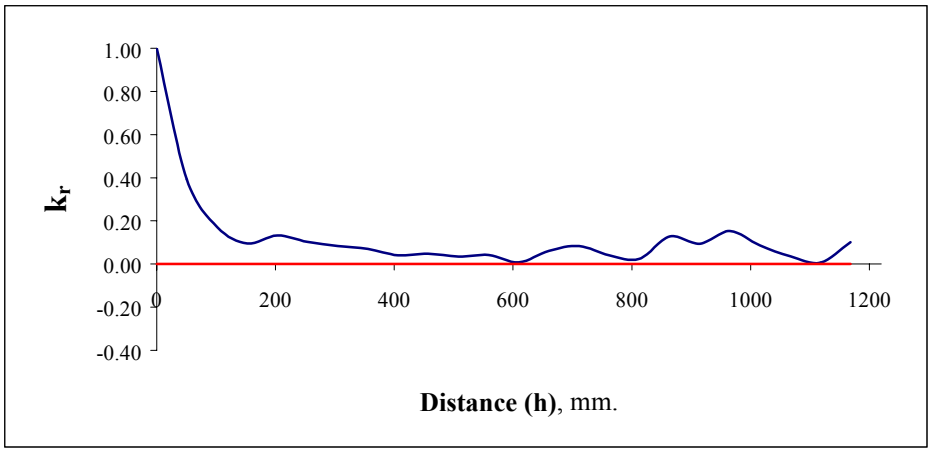

(b)

Figure D.44. *Panel m3p4: (a) transversal variogram, and (b) transversal correlogram.*

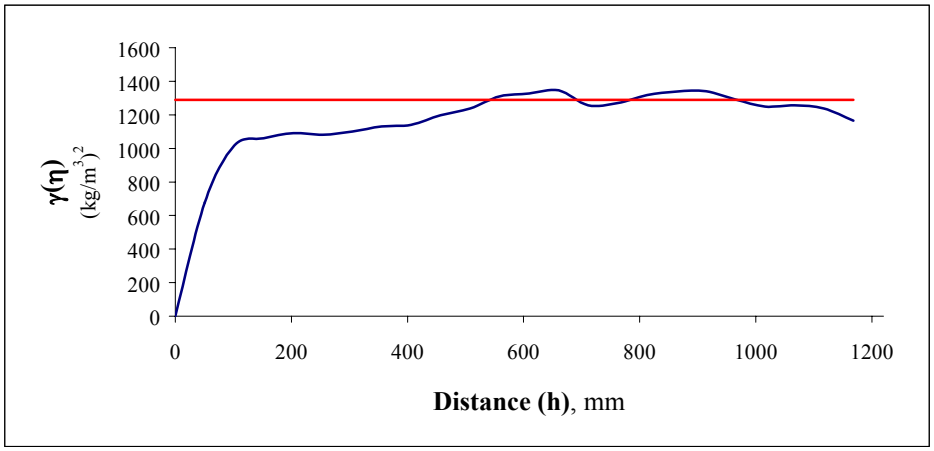

(a)

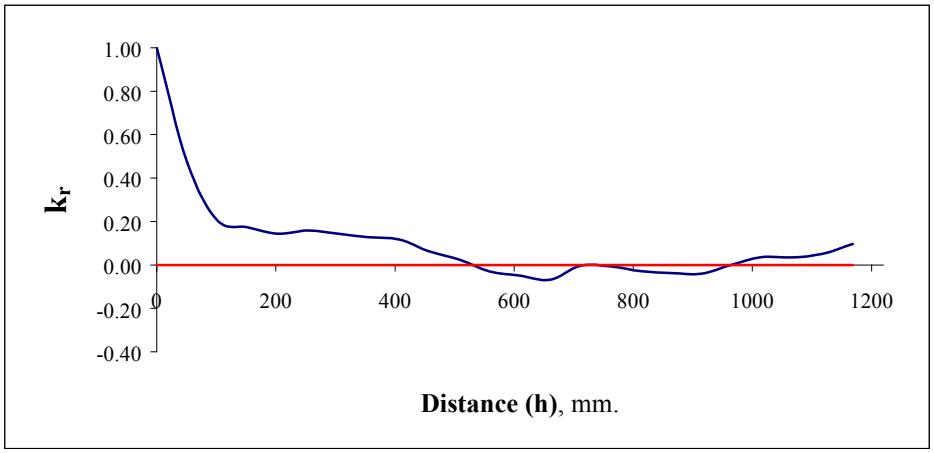

(b)

Figure D.45. *Panel m3p4: (a) longitudinal variogram, and (b) longitudinal correlogram.*

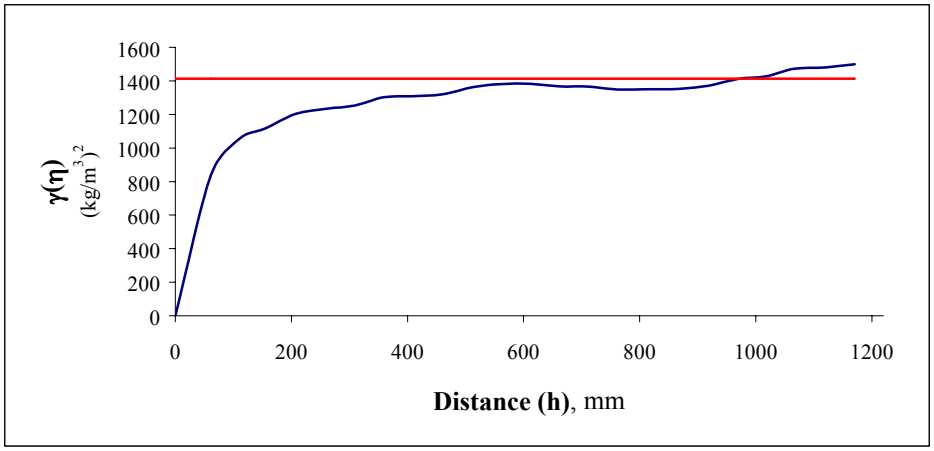

(a)

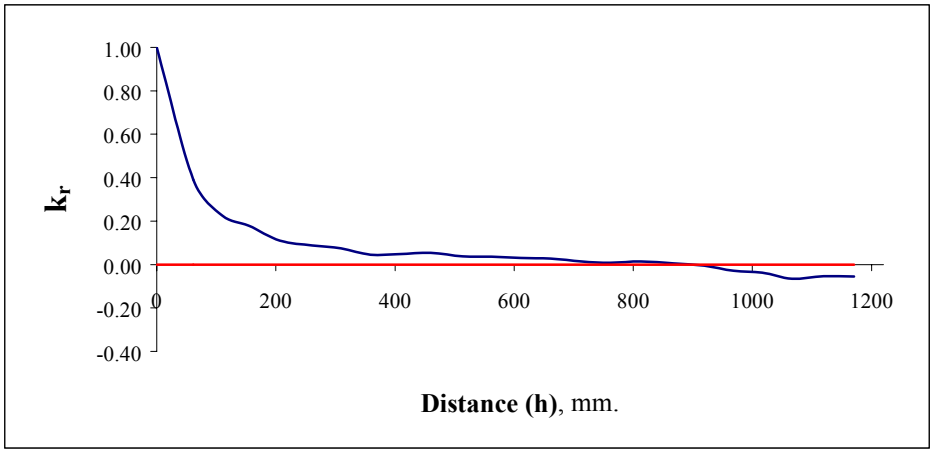

(b)

Figure D.46. *Panel m3p5: (a) omniderectional variogram, and (b) omnidirectional correlogram.*

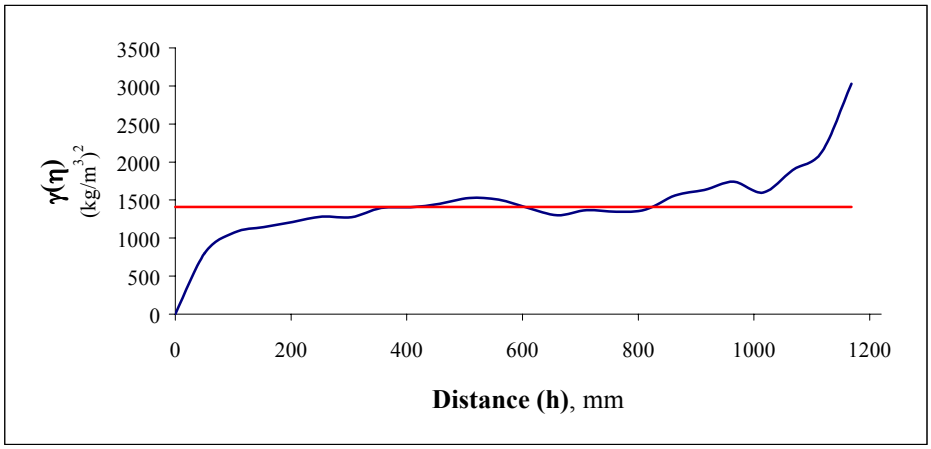

(a)

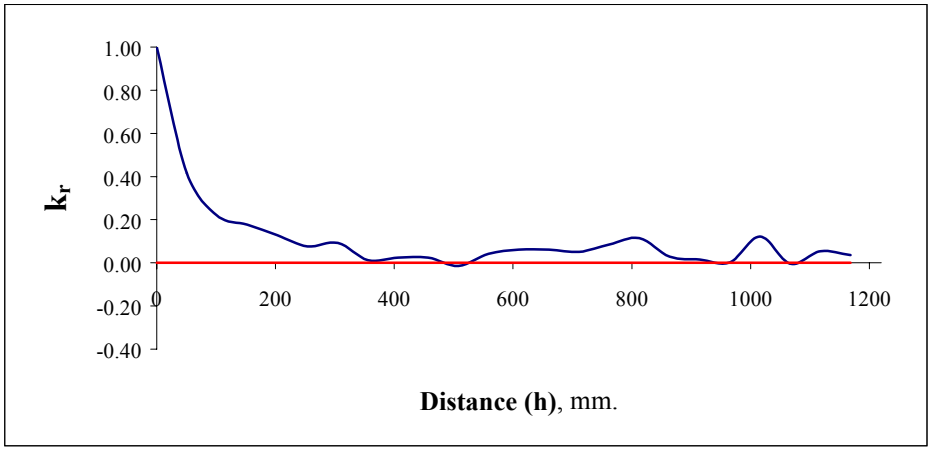

(b)

Figure D.47. *Panel m3p5: (a) transversal variogram, and (b) transversal correlogram.*

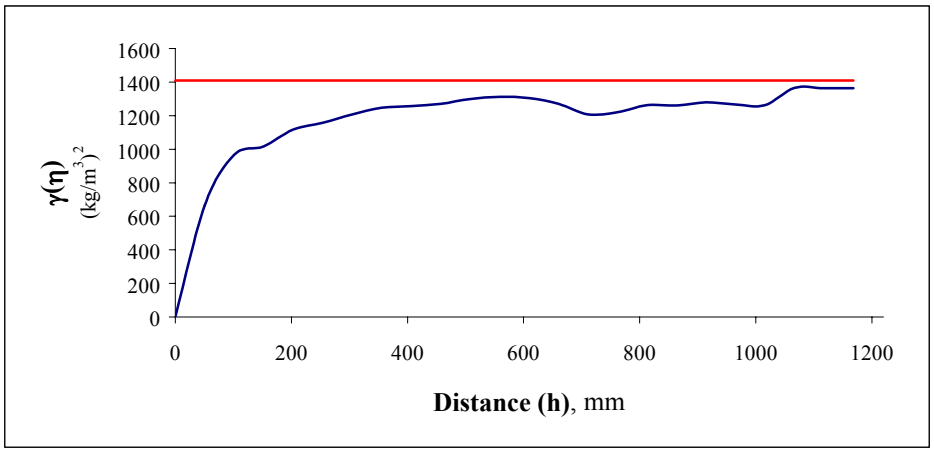

(a)

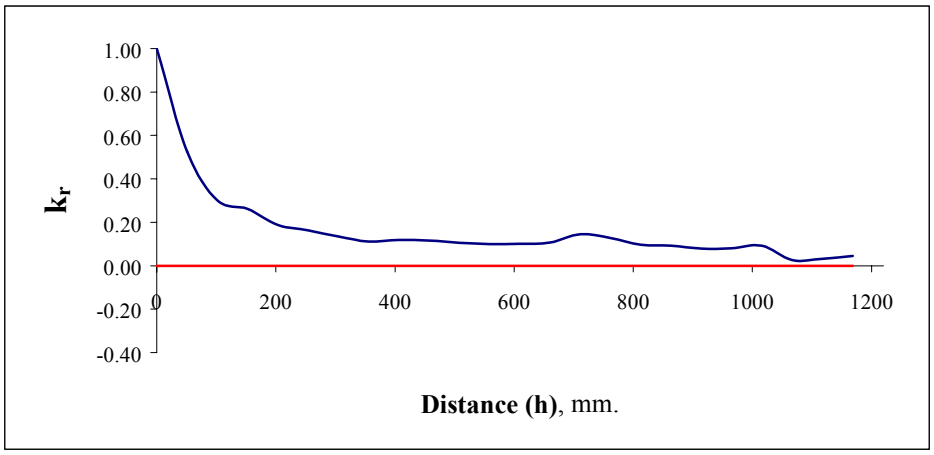

(b)

Figure D.48. *Panel m3p5: (a) longitudinal variogram, and (b) longitudinal correlogram.*

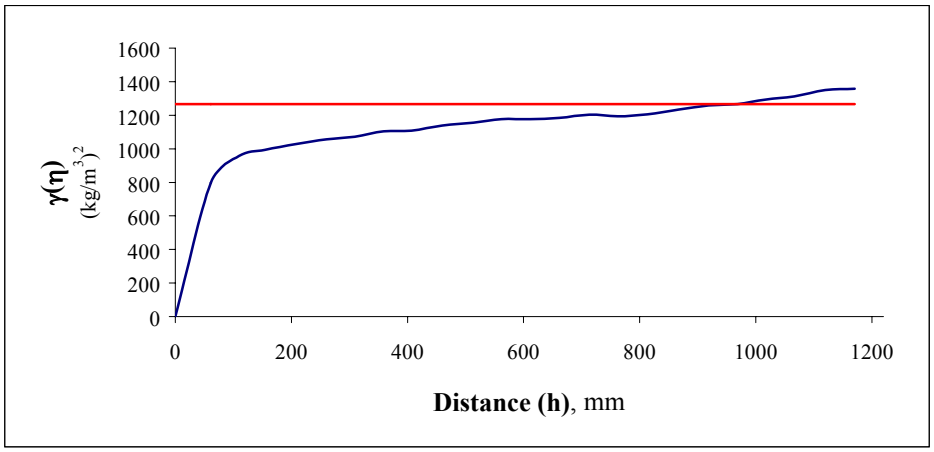

(a)

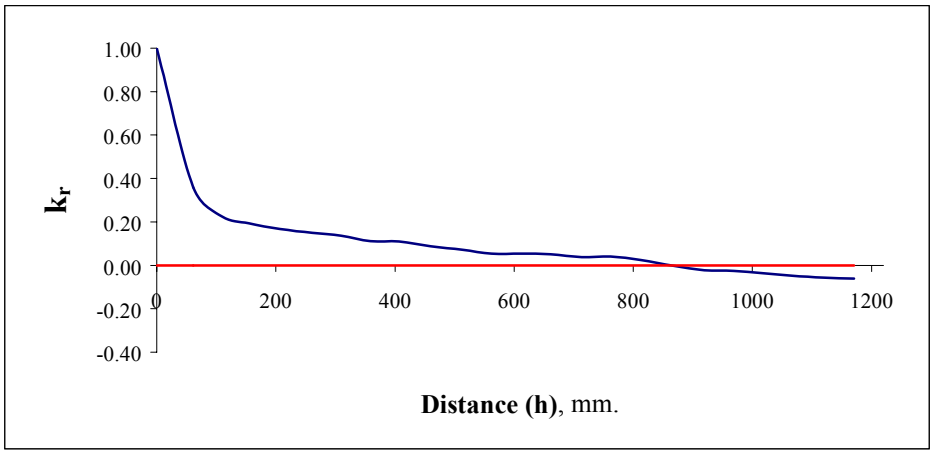

(b)

Figure D.49. *Panel m3p6: (a) omniderectional variogram, and (b) omnidirectional correlogram.*

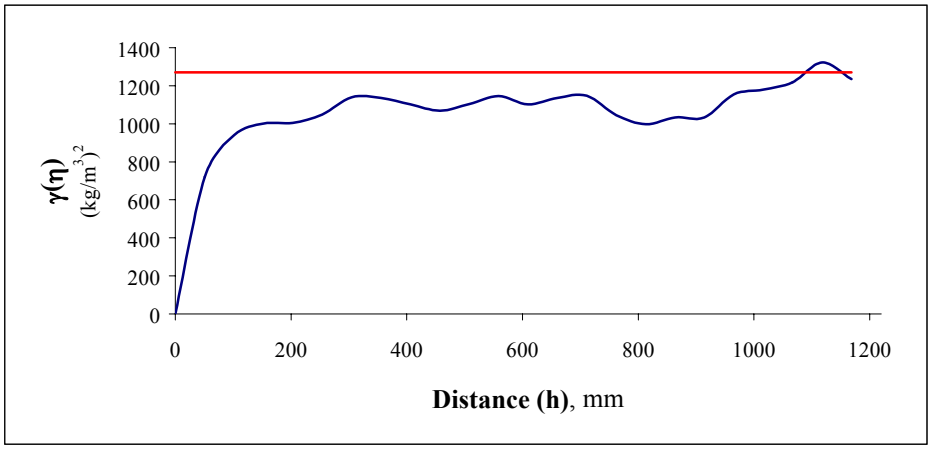

(a)

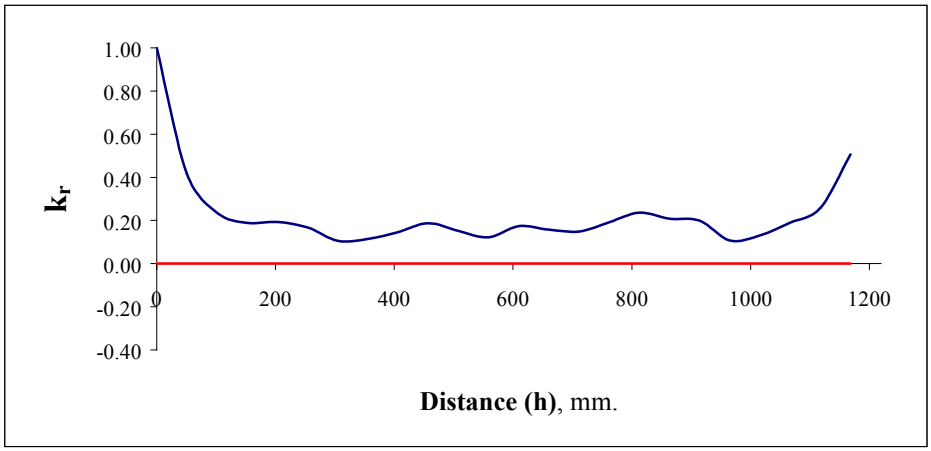

(b)

Figure D.50. *Panel m3p6: (a) transversal variogram, and (b) transversal correlogram.*

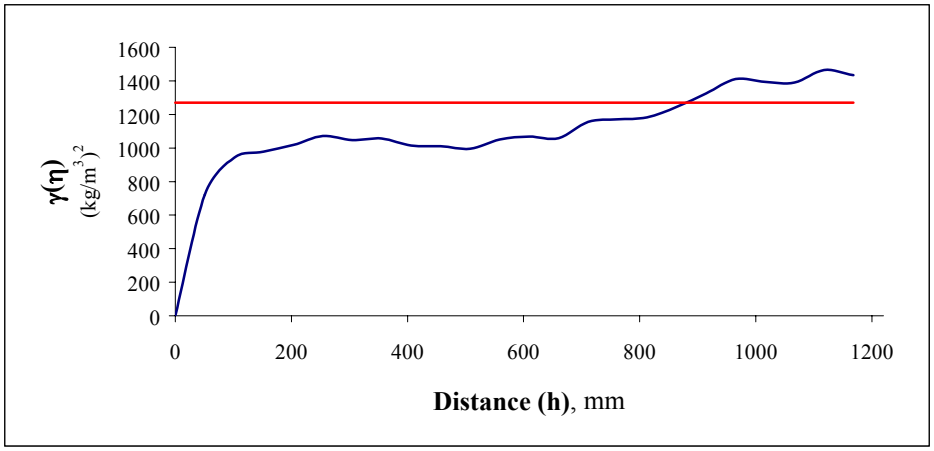

(a)

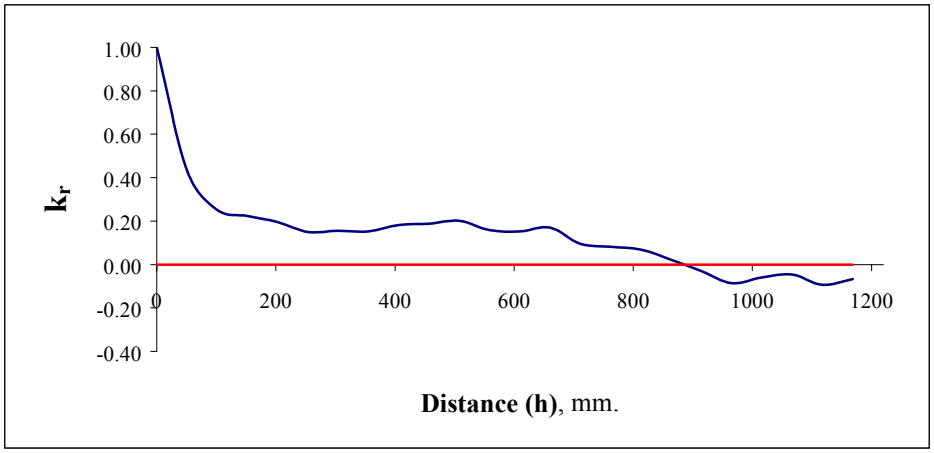

(b)

Figure D.51. *Panel m3p6: (a) longitudinal variogram, and (b) longitudinal correlogram.*

Appendix E

Fast Fourier Transform

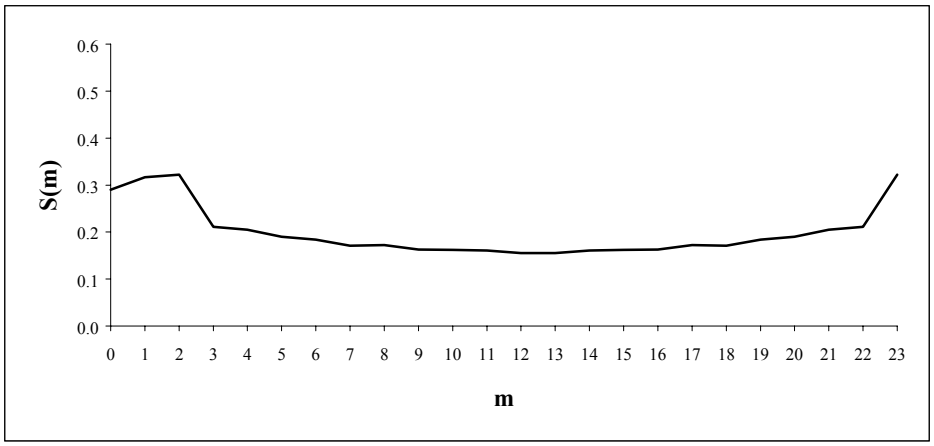

(a)

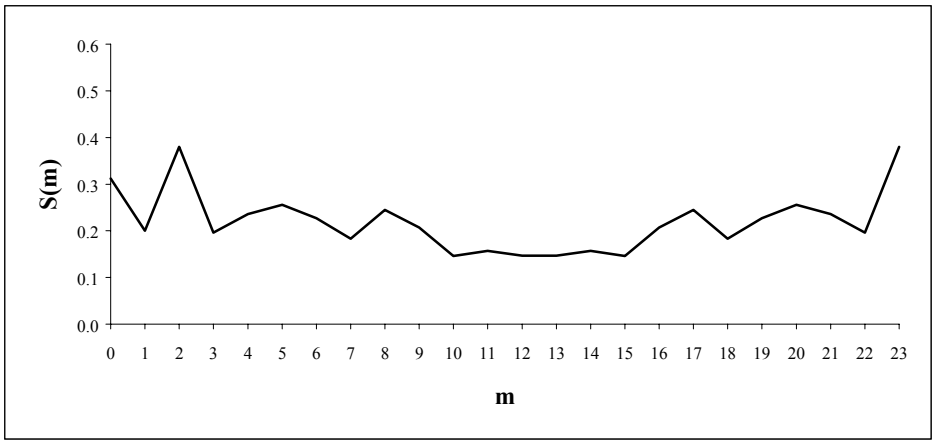

(b)

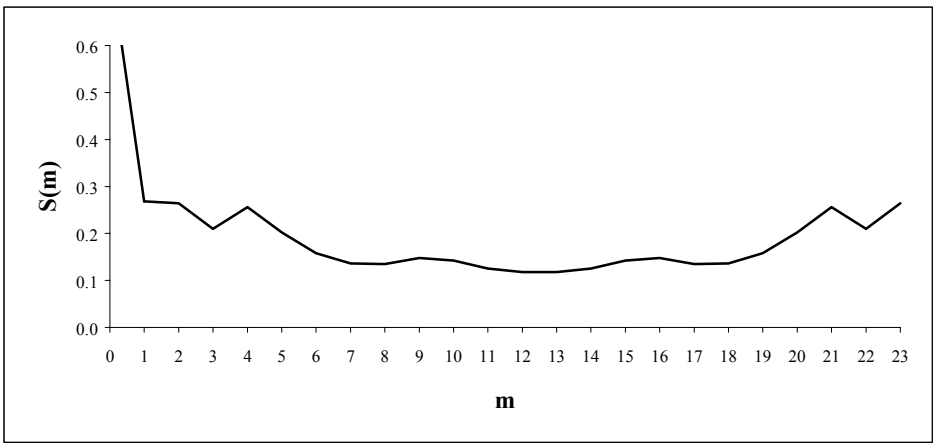

(c)

FigureE.1. *Fast Fourier transform m1p1: (a) omnicorrelogram, (b) transverse correlogram, and (c) longitudinal correlogram.*

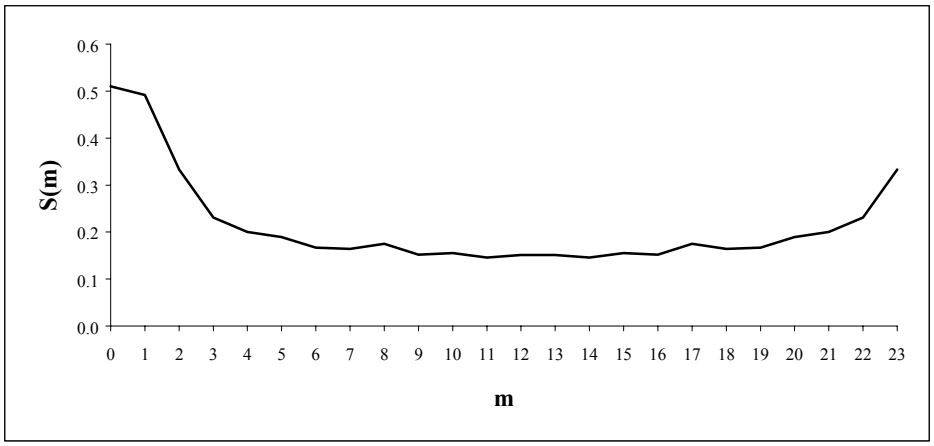

(a)

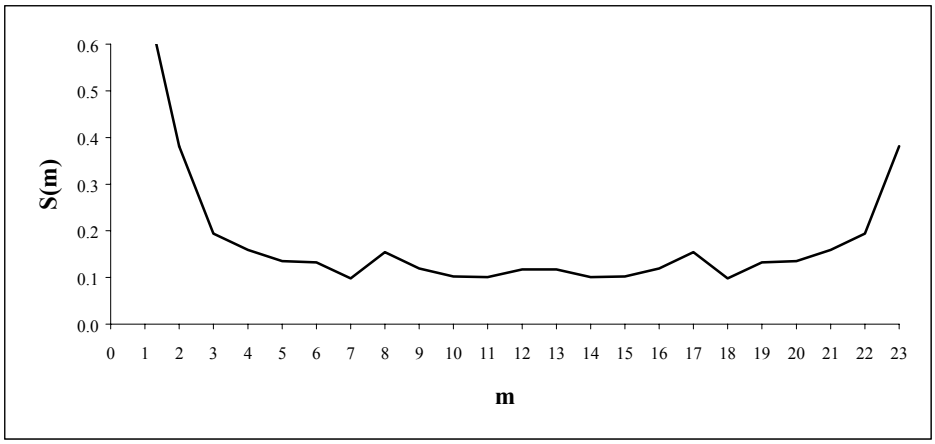

(b)

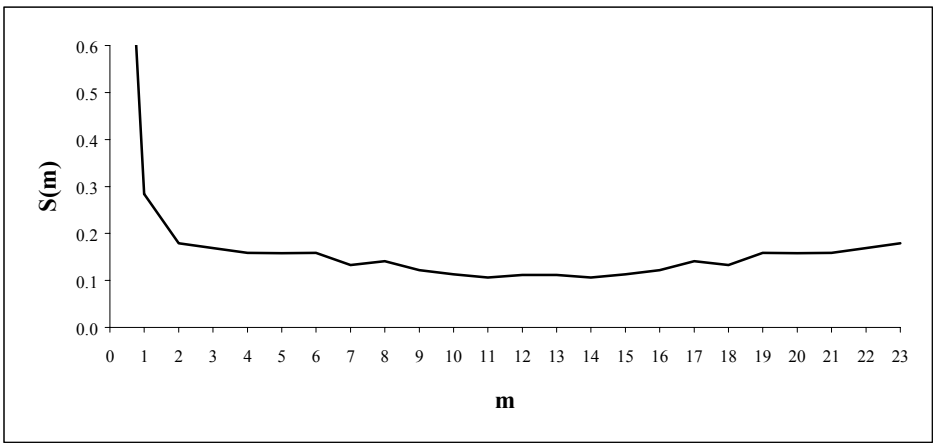

(c)

Figure E.2. *Fast fourier transform m1p2: (a) omnicorrelogram, (b) transverse correlogram, and (c) longitudinal correlogram.*

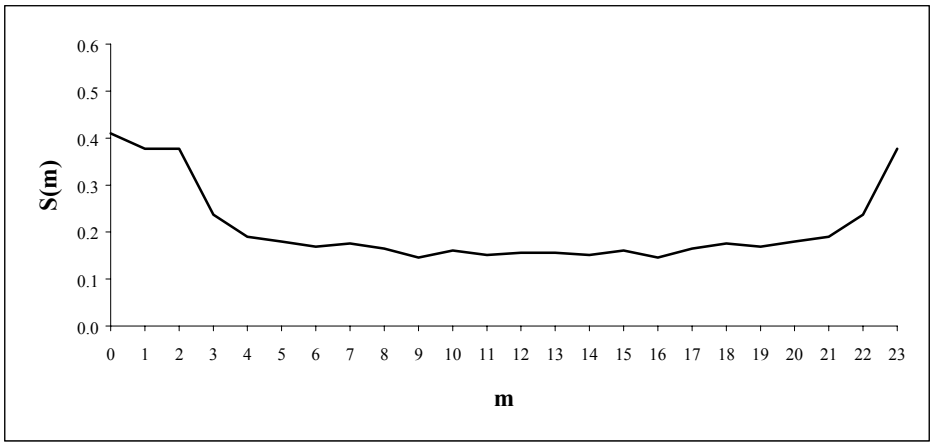

(a)

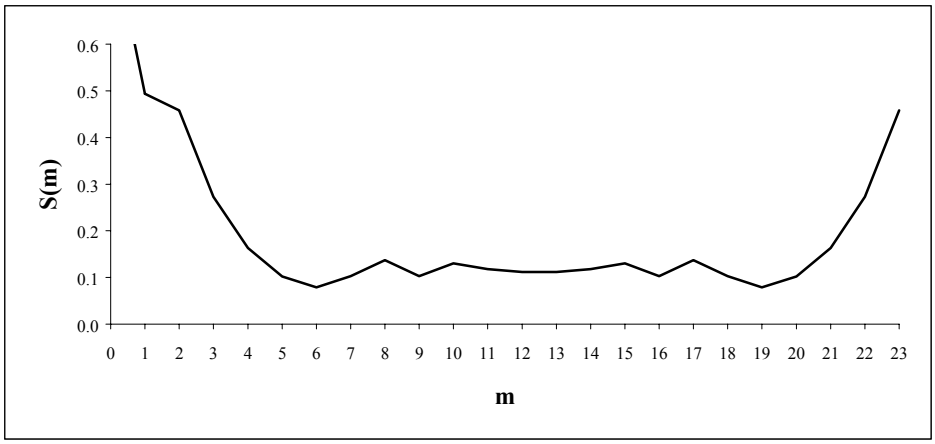

(b)

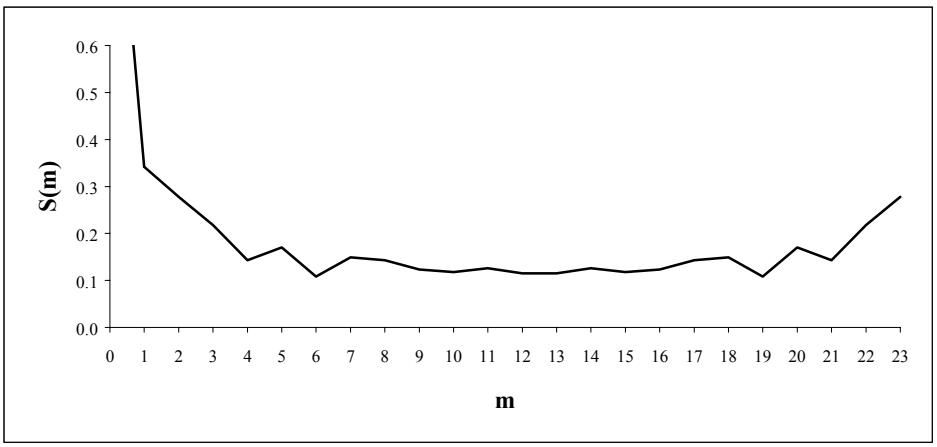

(c)

Figure E.3. *Fast Fourier transform m1p4: (a) omnicorrelogram, (b) transverse correlogram, and (c) longitudinal correlogram.*

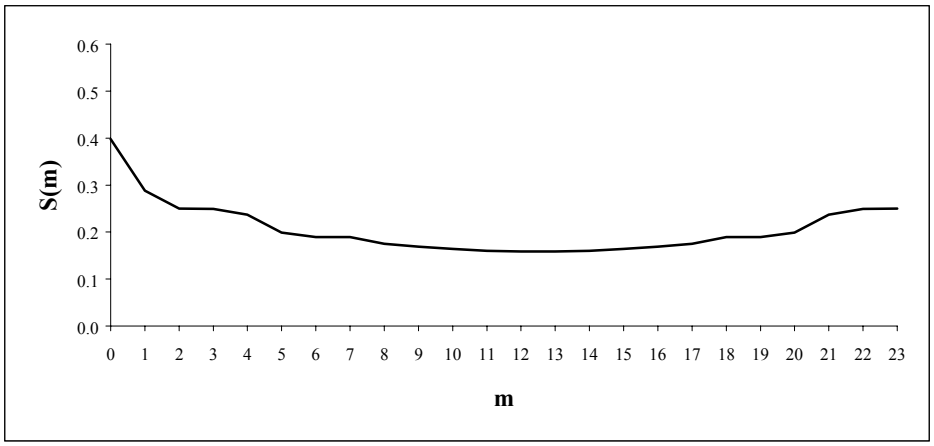

(a)

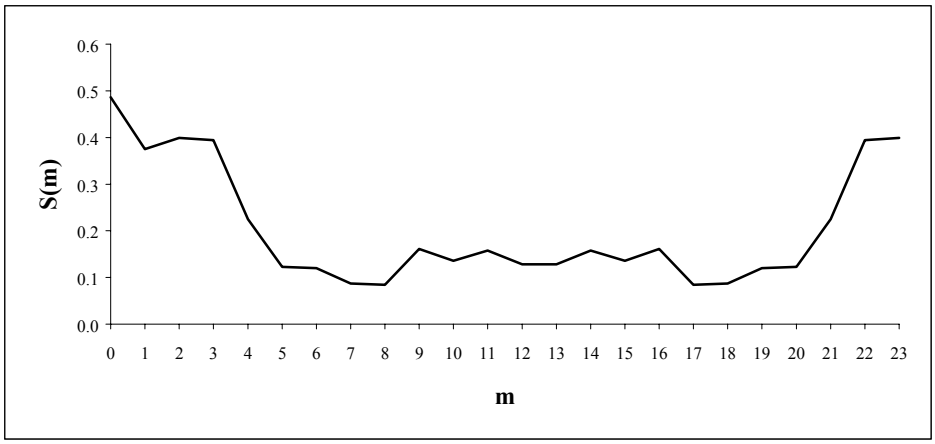

(b)

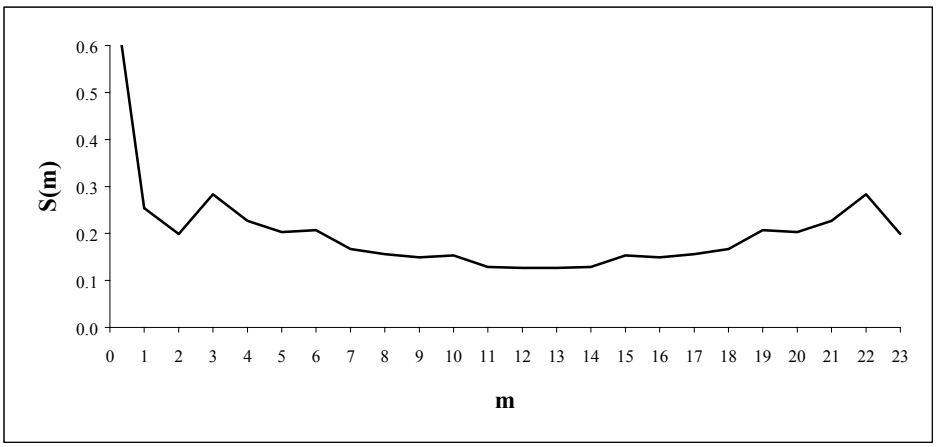

(c)

FigureE.4. *Fast Fourier transform m1p5: (a) omnicorrelogram, (b) transverse correlogram, and (c) longitudinal correlogram.*

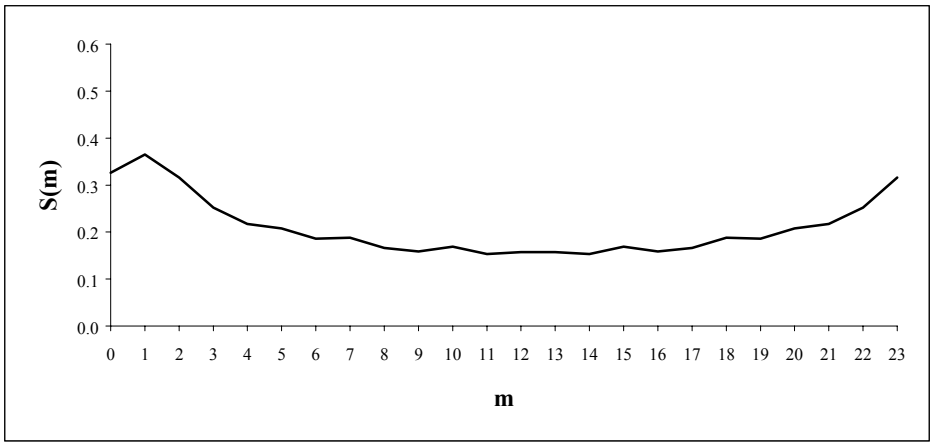

(a)

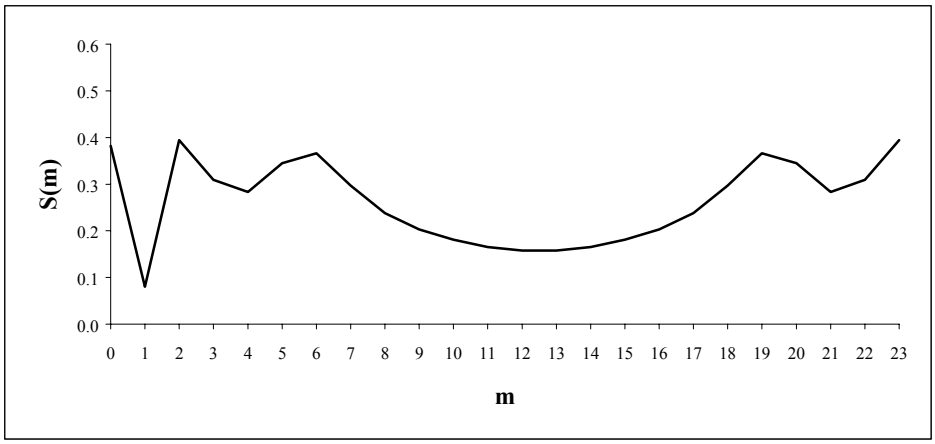

(b)

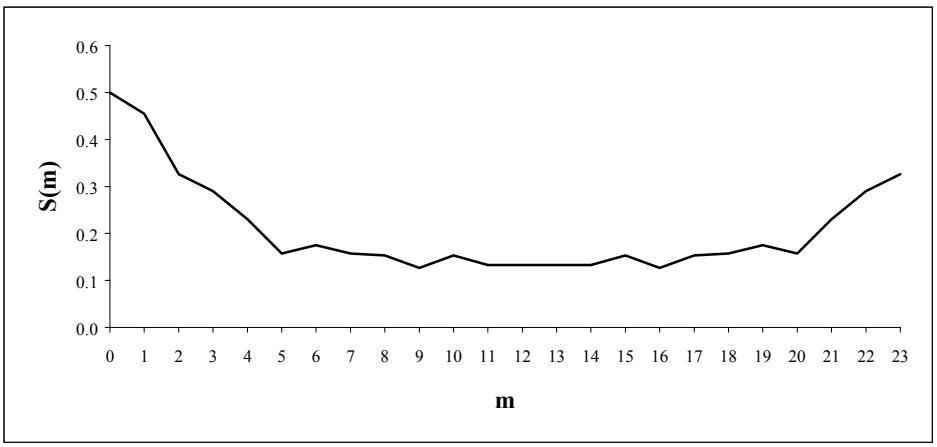

(c)

Figure E.5. *Fast Fourier transform m1p5: (a) omnicorrelogram, (b) transverse correlogram, and (c) longitudinal correlogram.*

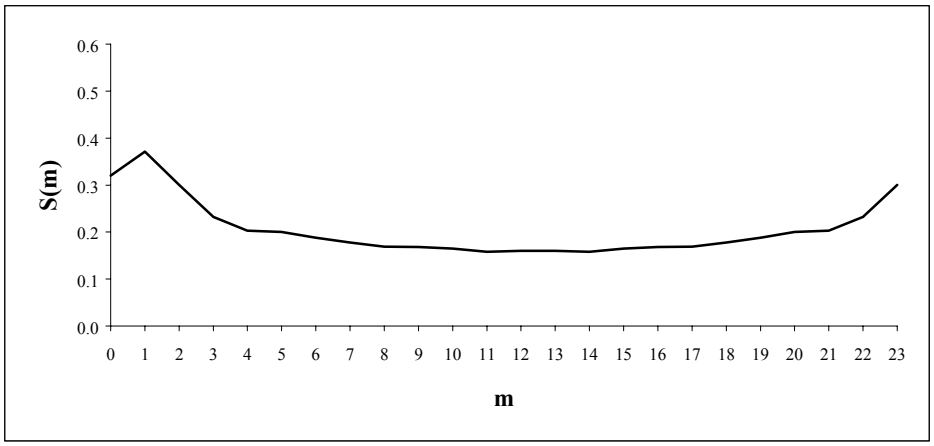

(a)

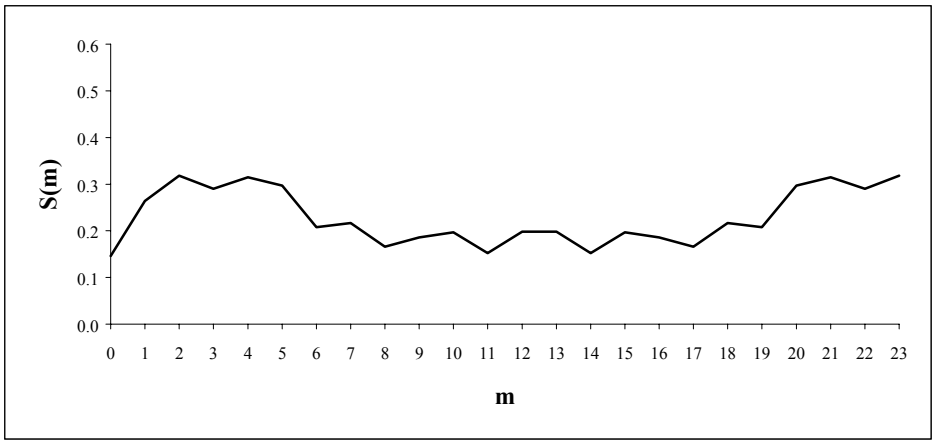

(b)

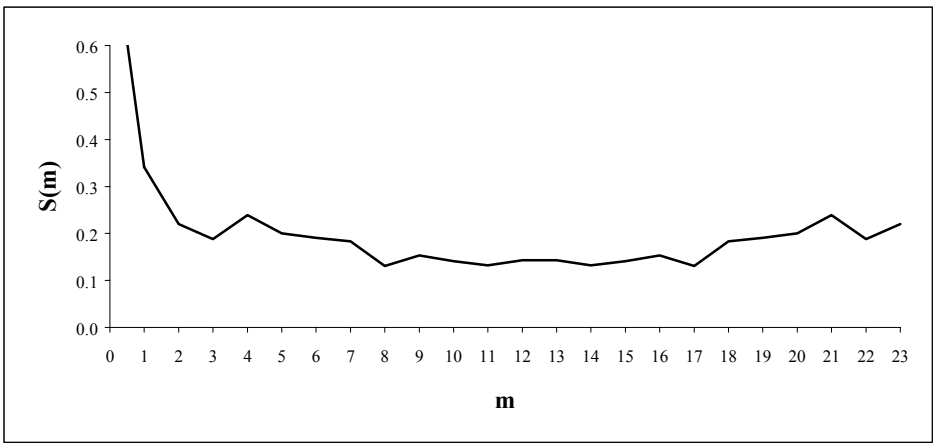

(c)

Figure E.6. *Fast Fourier transform m2p1: (a) omnicorrelogram, (b) transverse correlogram, and (c) longitudinal correlogram.*

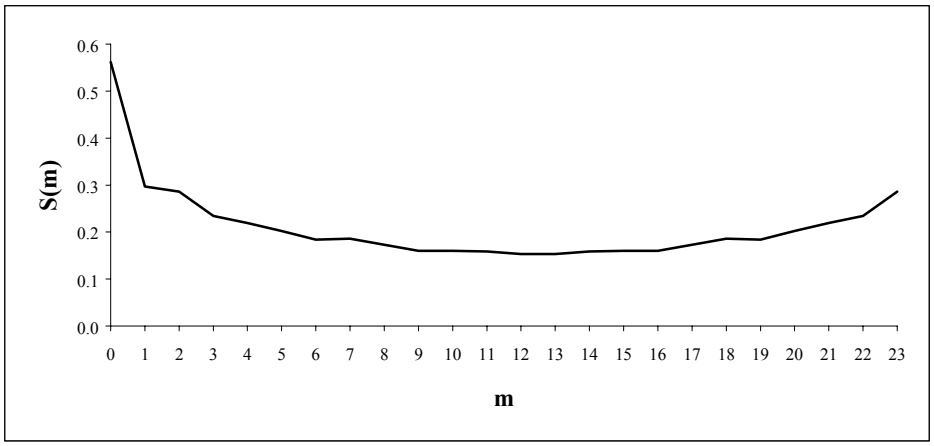

(a)

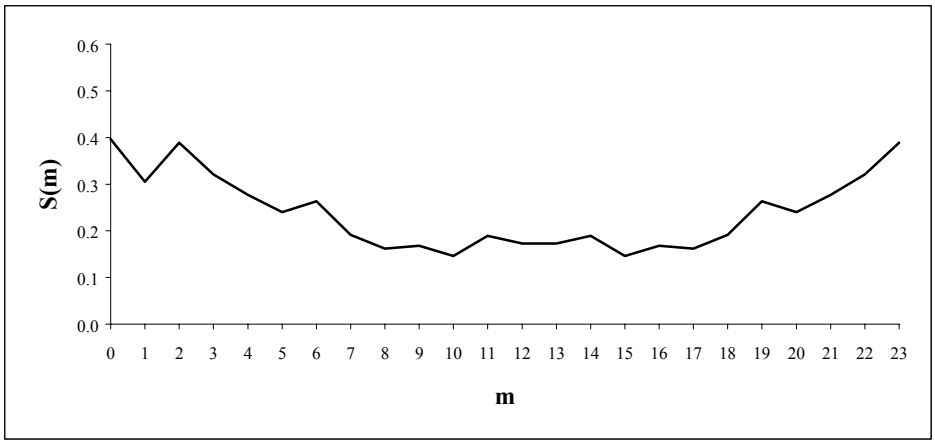

(b)

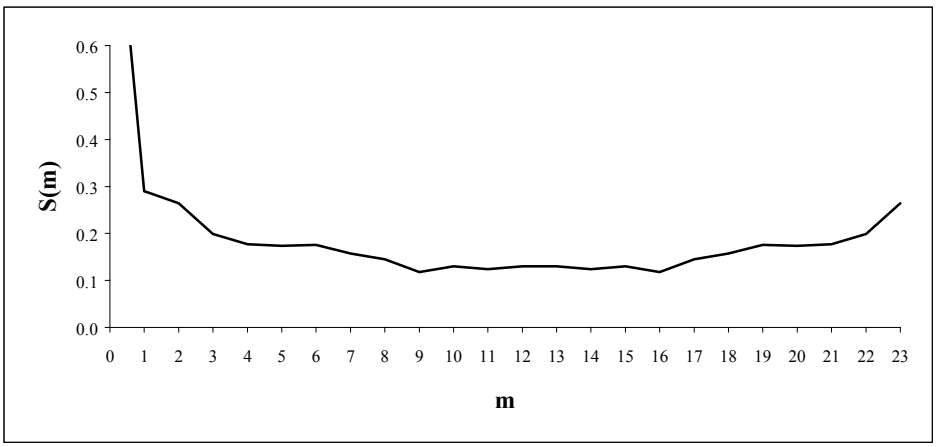

(c)

Figure E.7. *Fast Fourier transform m2p2: (a) omnicorrelogram, (b) transverse correlogram, and (c) longitudinal correlogram.*

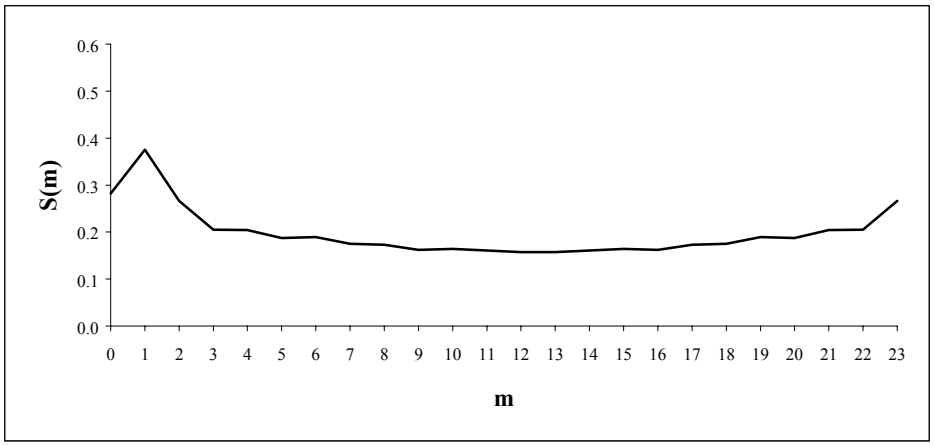

(a)

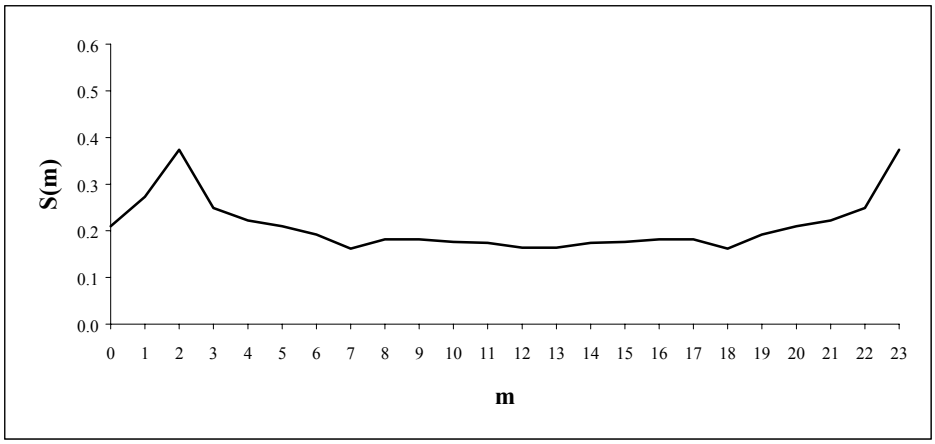

(b)

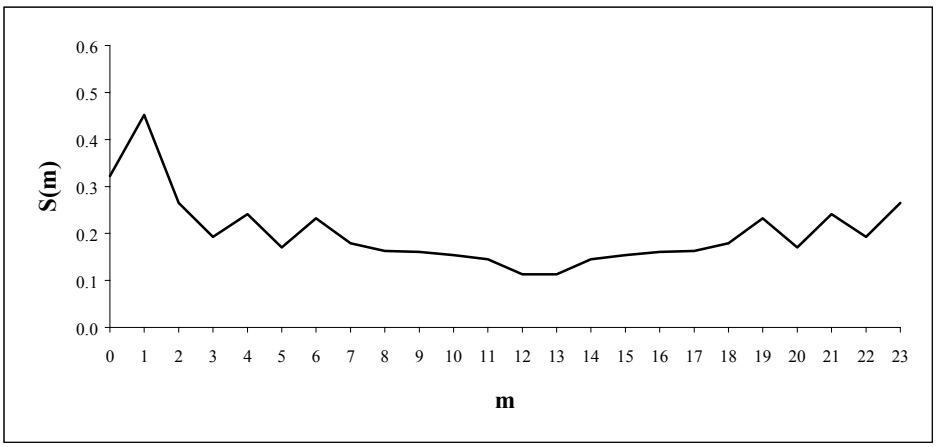

(c)

Figure E.8. *Fast Fourier transform m2p3: (a) omnicorrelogram, (b) transverse correlogram, and (c) longitudinal correlogram.*

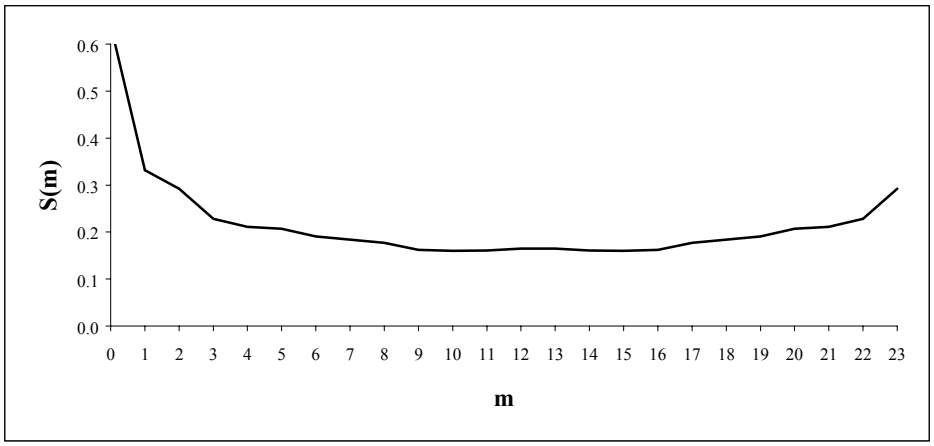

(a)

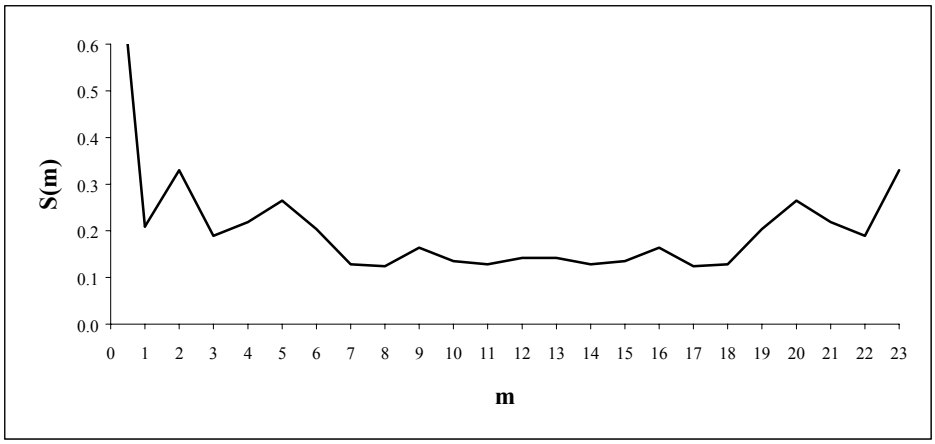

(b)

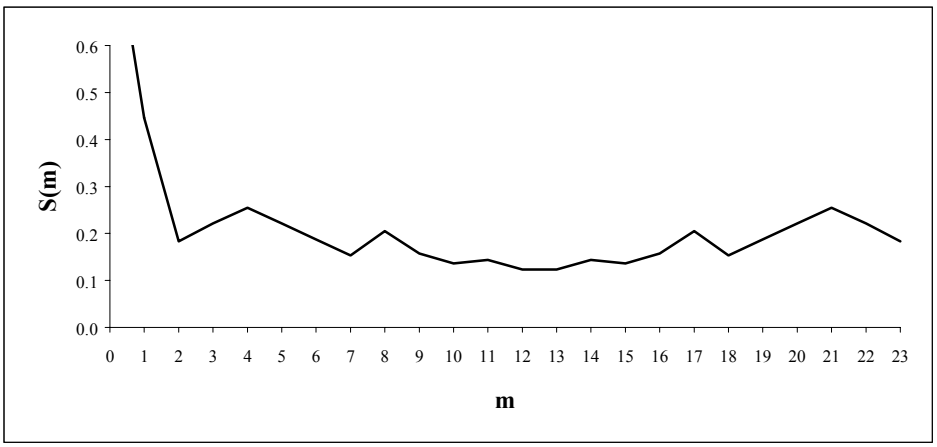

(c)

Figure E.9. *Fast Fourier transform m2p4: (a) omnicorrelogram, (b) transverse correlogram, and (c) longitudinal correlogram.*

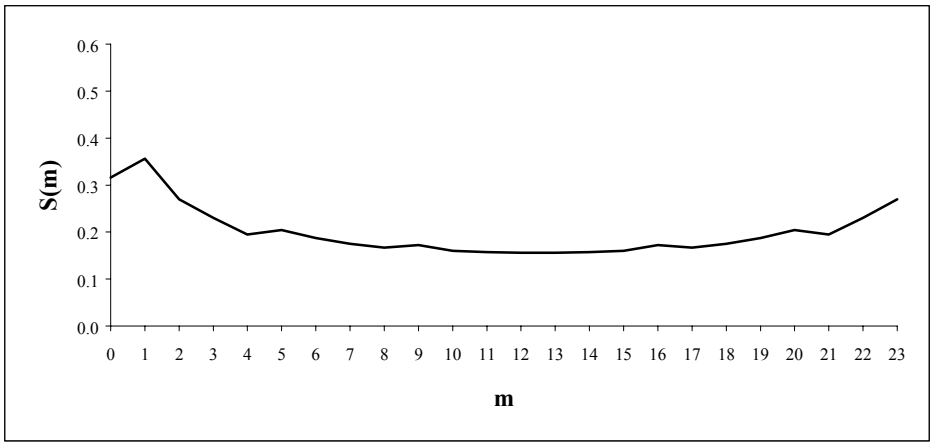

(a)

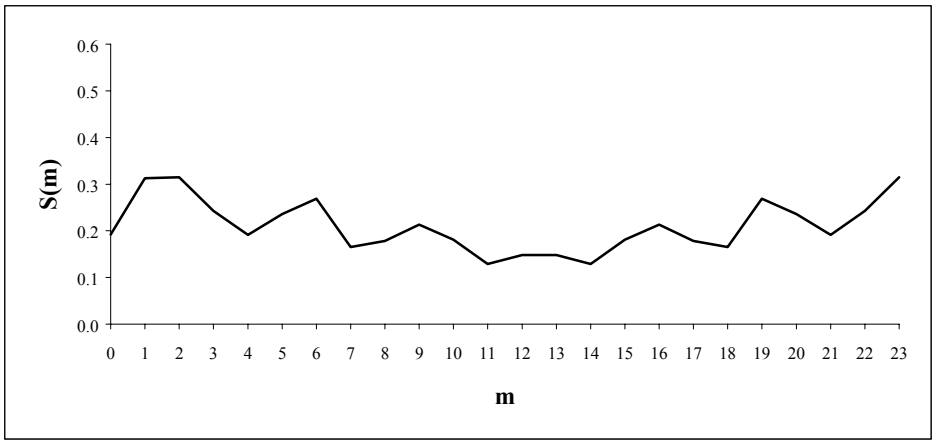

(b)

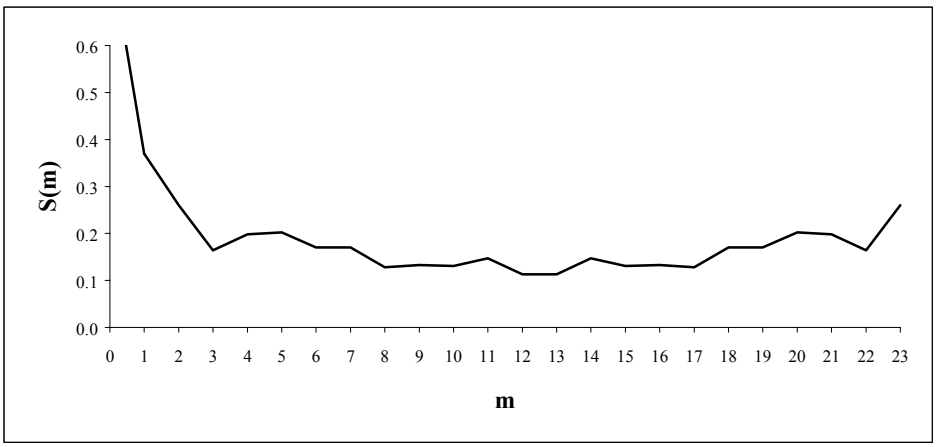

(c)

Figure E.10. *fast fourier transform m2p5: (a) omnicorrelogram, (b) transverse correlogram, and (c) longitudinal correlogram.*

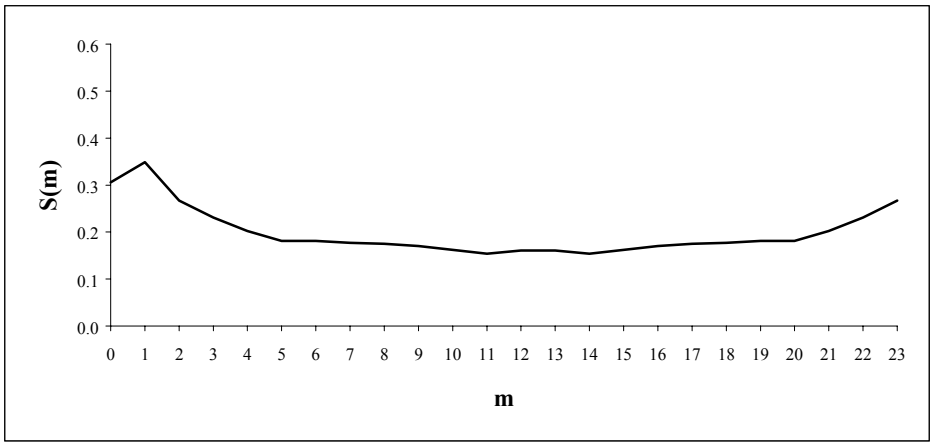

(a)

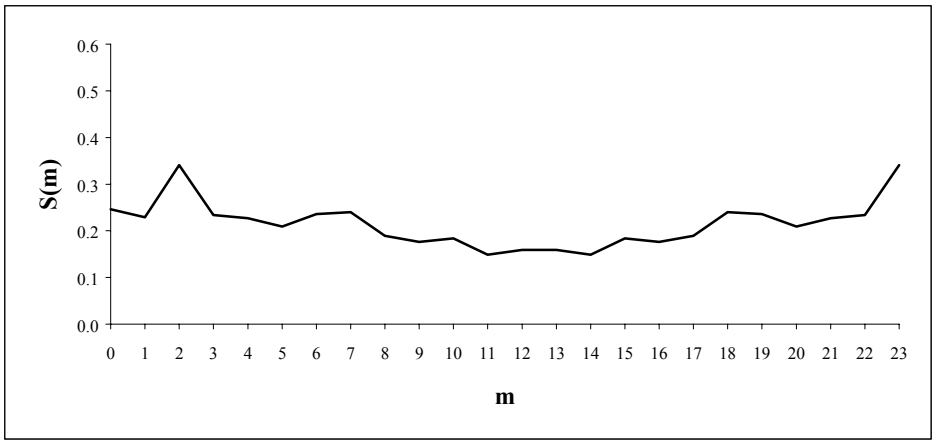

(b)

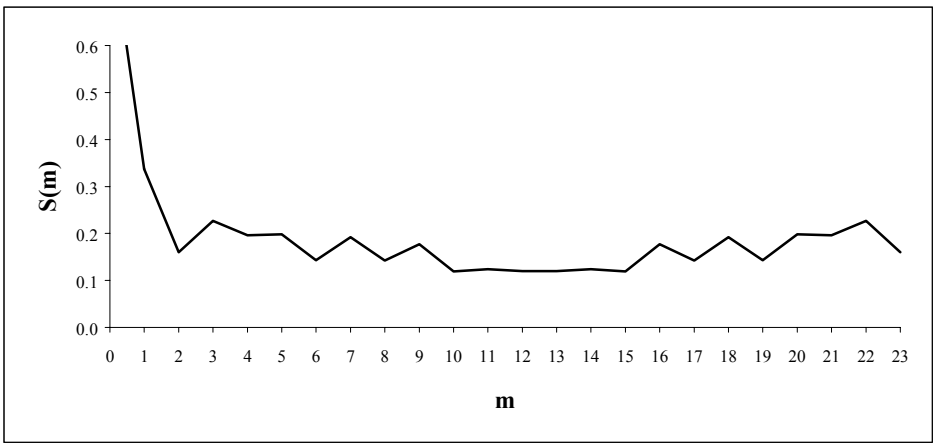

(c)

Figure E.11. *Fast Fourier transform m2p6: (a) omnicorrelogram, (b) transverse correlogram, and (c) longitudinal correlogram.*

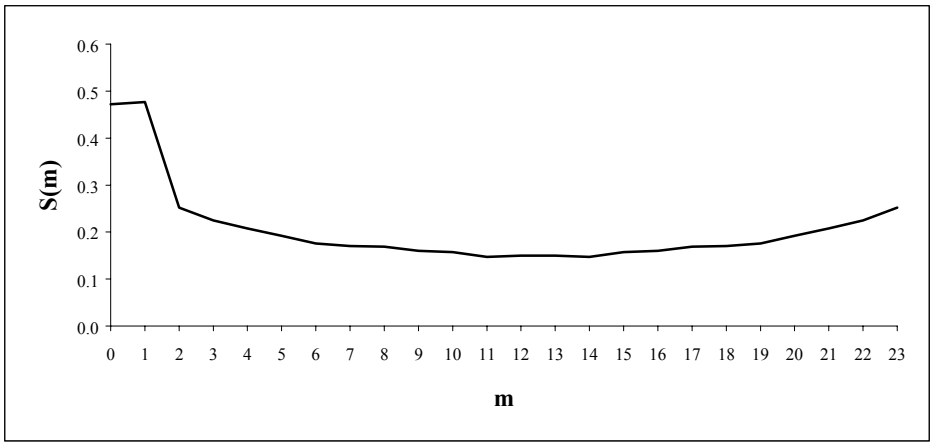

(a)

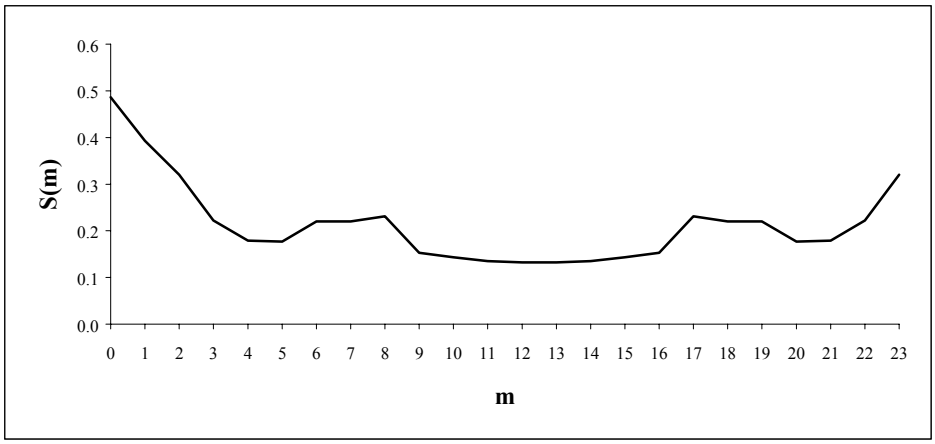

(b)

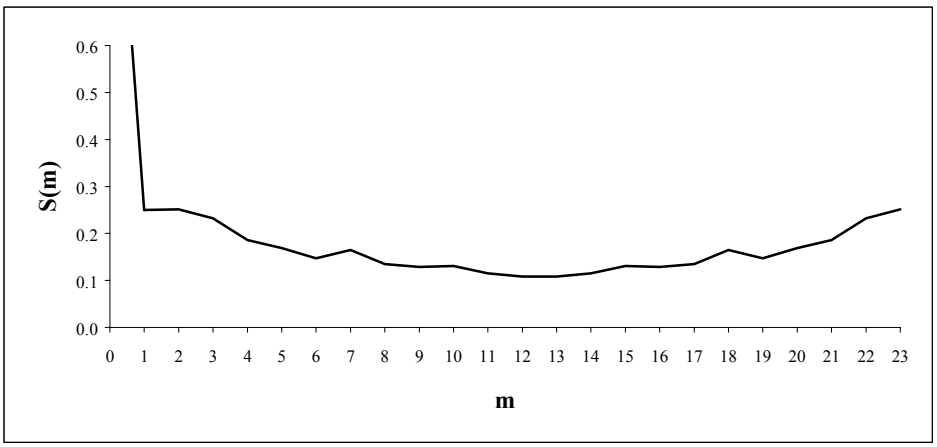

(c)

Figure E.12. *Fast Fourier transform m3p1: (a) omnicorrelogram, (b) transverse correlogram, and (c) longitudinal correlogram.*

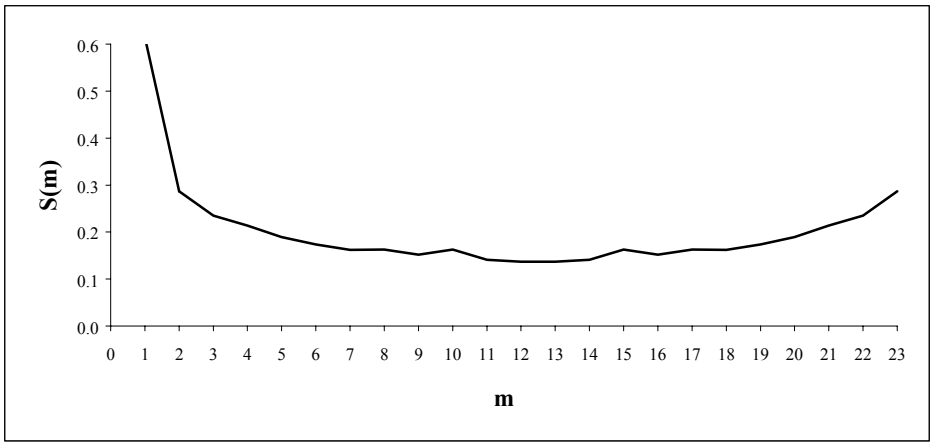

(a)

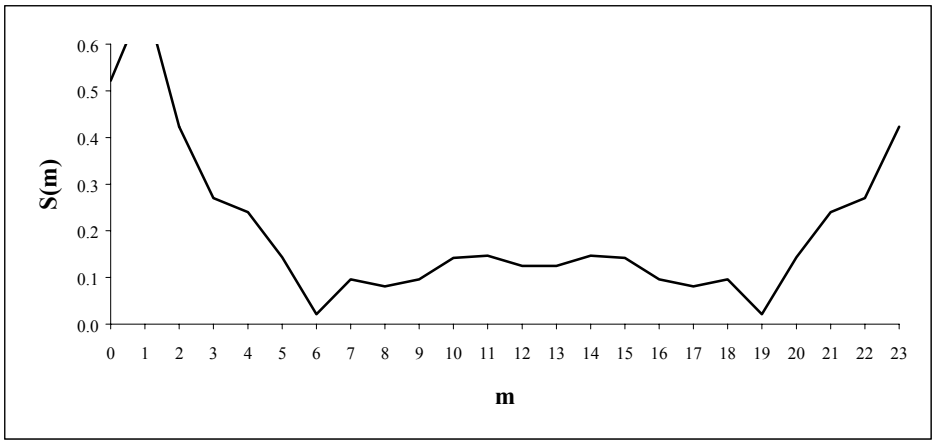

(b)

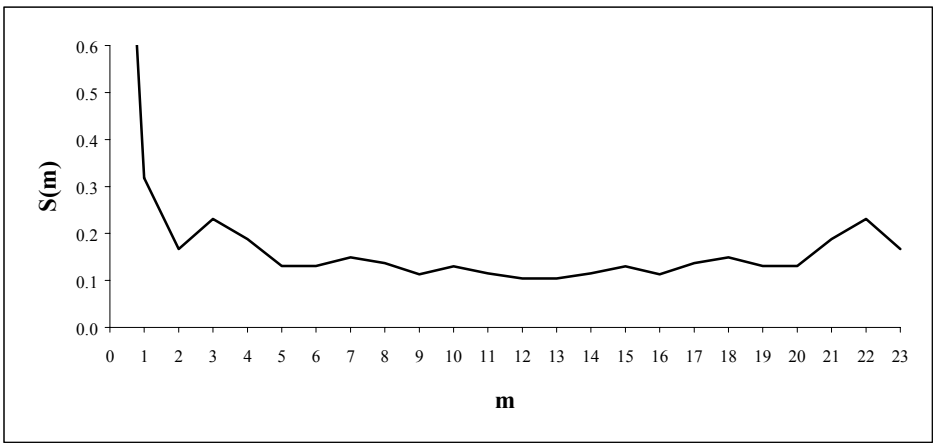

(c)

Figure E.13. *Fast fourier transform m3p2: (a) omnicorrelogram, (b) transverse correlogram, and (c) longitudinal correlogram.*

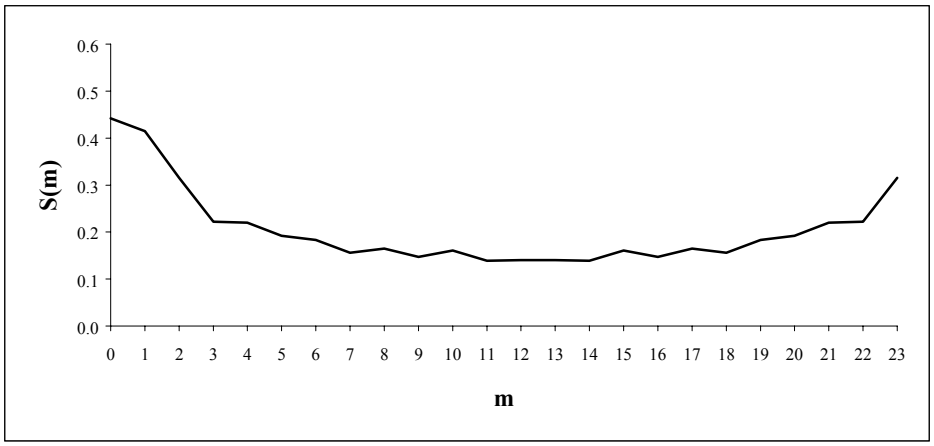

(a)

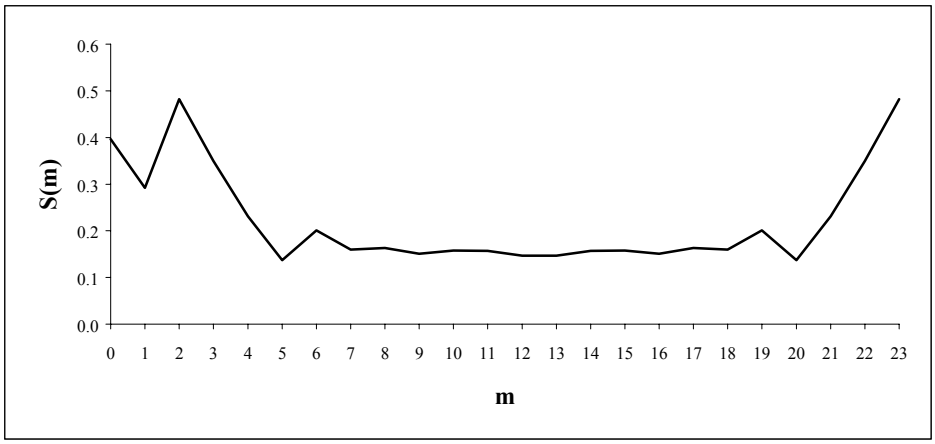

(b)

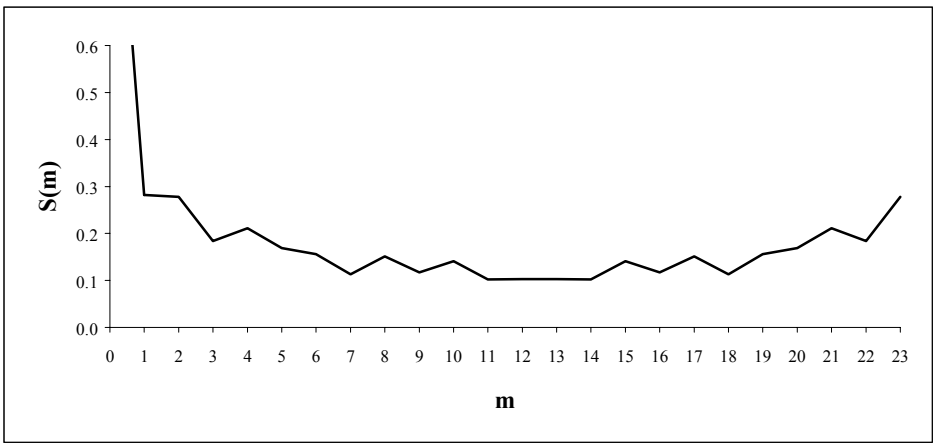

(c)

Figure E.14. *Fast Fourier transform m3p3: (a) omnicorrelogram, (b) transverse correlogram, and (c) longitudinal correlogram.*

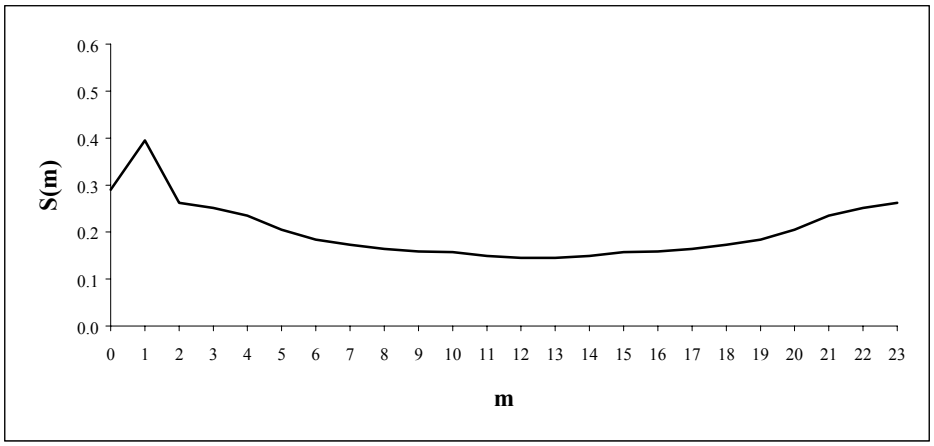

(a)

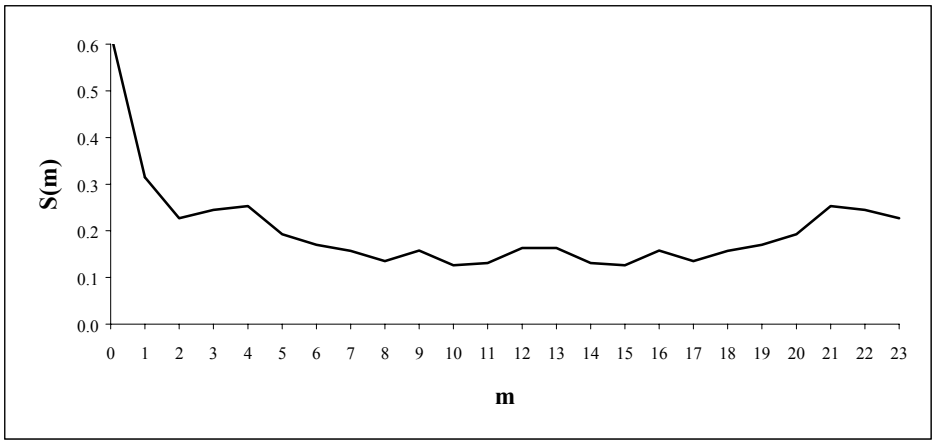

(b)

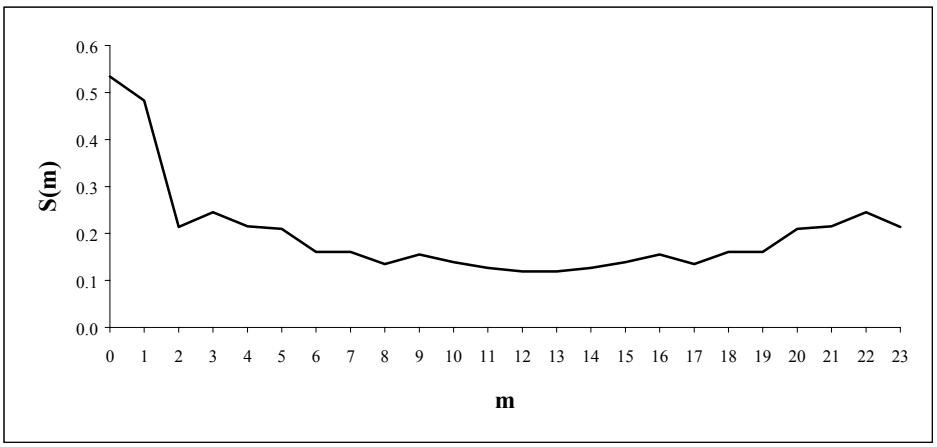

(c)

Figure E.15. *Fast Fourier transform m3p4: (a) omnicorrelogram, (b) transverse correlogram, and (c) longitudinal correlogram.*

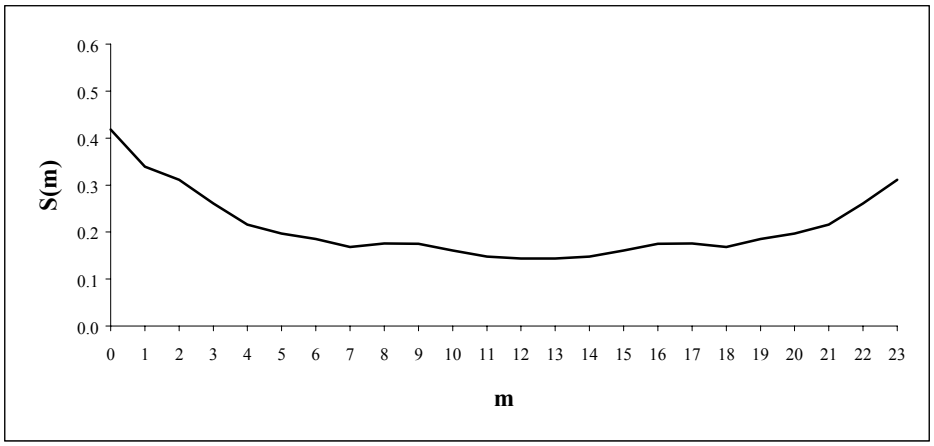

(a)

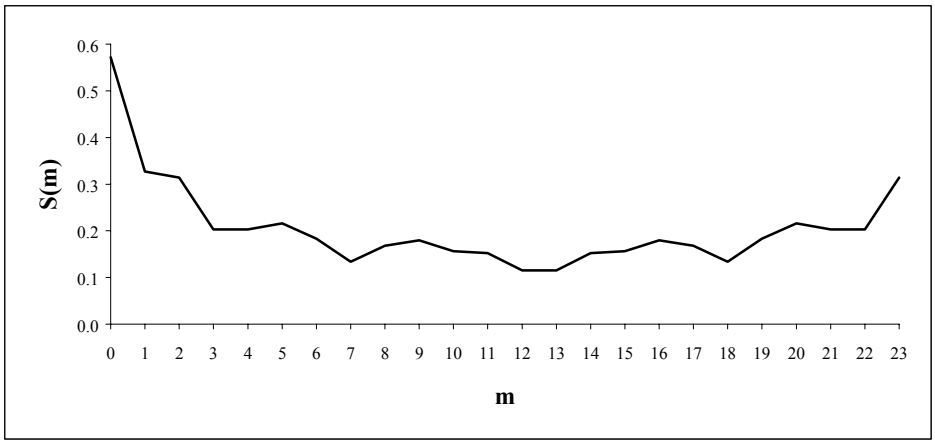

(b)

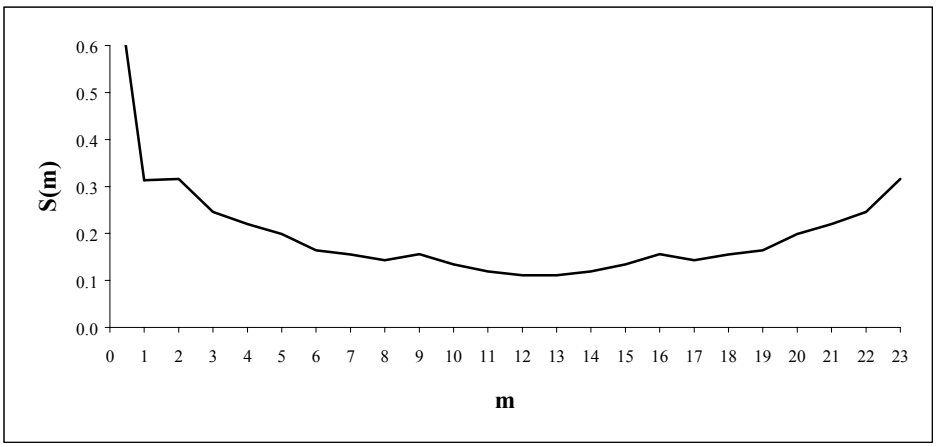

(c)

Figure E.16. *Fast Fourier transform m3p5: (a) omnicorrelogram, (b) transverse correlogram, and (c) longitudinal correlogram.*

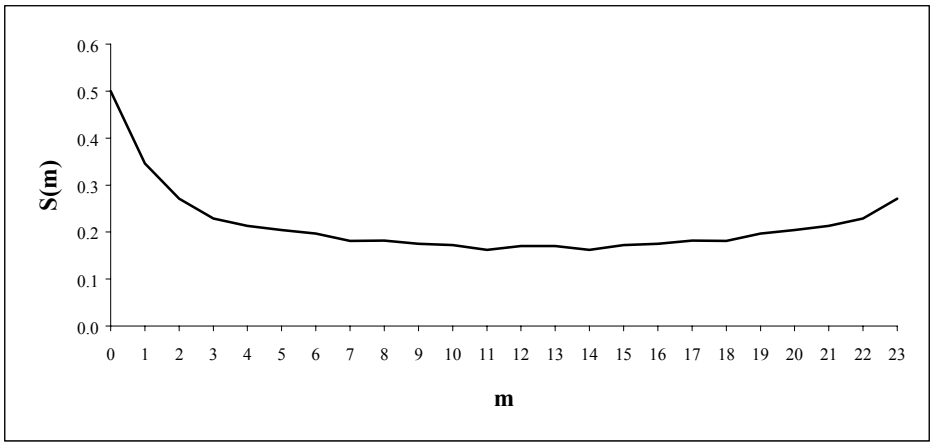

(a)

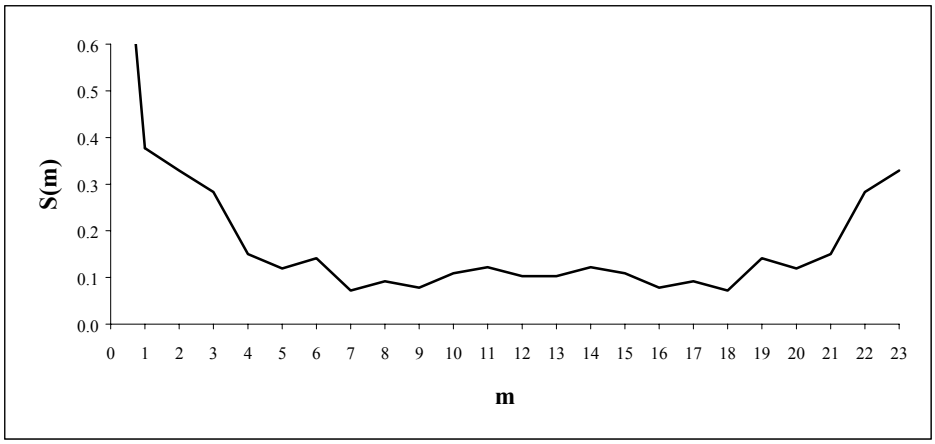

(b)

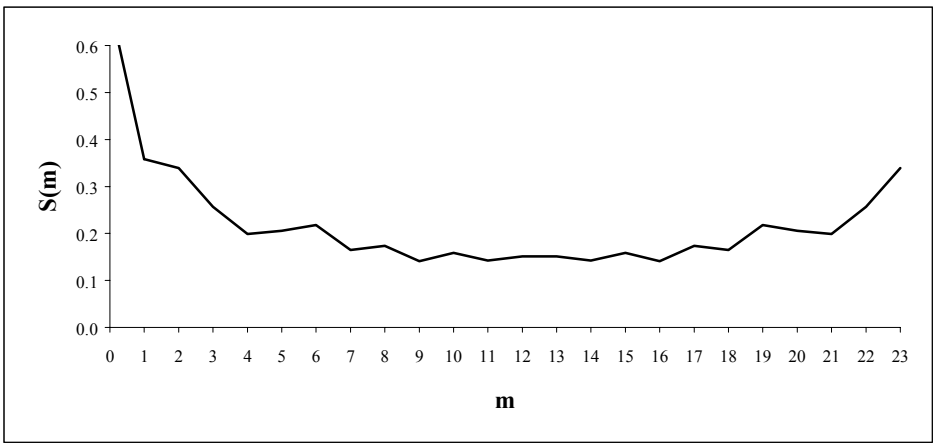

(c)

Figure E.17. *Fast Fourier transform m3p6: (a) omnicorrelogram, (b) transverse correlogram, and (c) longitudinal correlogram.*

Appendix F

Density Results Areas

Specimen	d1 kg/m³	d2 kg/m³	d3 kg/m³	d4 kg/m³	d5 kg/m³	d6 kg/m³	d7 kg/m³	d8 kg/m³	d9 kg/m³	d10 kg/m³	d11 kg/m³	dG kg/m³	deflection mm
m1p1	551	554	559	562	569	577	578	580	584	587	585	561	2.15
m1p2	641	638	613	604	598	596	595	597	600	602	602	596	2.00
m1p3	557	558	553	557	556	552	550	552	557	562	564	562	2.29
m1p4	584	583	566	562	565	567	566	563	561	561	562	573	2.20
m1p5	492	489	489	494	504	515	522	528	533	539	543	557	2.51
m1p6	527	525	531	536	541	544	544	543	544	548	549	551	2.43
m2p1	573	577	580	574	576	576	576	579	584	585	587	572	2.13
m2p2	632	623	613	615	617	614	611	604	606	606	602	576	1.84
m2p3	581	582	583	582	583	583	581	582	581	583	582	571	2.18
m2p4	578	579	580	588	587	585	581	579	576	576	576	574	2.22
m2p5	530	533	531	535	536	534	533	533	535	536	536	564	2.42
m2p6	587	590	600	599	592	591	592	590	589	584	578	561	2.27
m3p1	607	611	607	601	603	602	598	593	593	592	588	581	2.03
m3p2	517	517	527	536	537	536	534	536	538	544	546	569	2.46
m3p3	591	593	603	602	601	607	611	614	614	611	607	575	1.87
m3p4	534	535	537	530	528	527	526	526	524	524	527	551	2.46
m3p5	540	540	532	541	549	549	545	543	544	543	540	543	2.40
m3p6	539	540	546	553	564	571	574	575	574	573	573	557	2.13

Table F.1. *Density data values for different sizes and maximum deflection.*

Specimen	d1 kg/m³	d2 kg/m³	d3 kg/m³	d4 kg/m³	d5 kg/m³	d6 kg/m³	d7 kg/m³	d8 kg/m³	d9 kg/m³	d10 kg/m³	d11 kg/m³	dG kg/m³	u. load kN
m1p1	546	546	539	554	559	562	569	577	578	580	584	561	2.80
m1p2	653	653	655	638	613	604	598	596	595	597	600	596	3.56
m1p3	505	505	537	558	553	557	556	552	550	552	557	562	2.80
m1p4	577	577	582	583	566	562	565	567	566	563	561	573	3.11
m1p5	492	492	504	489	489	494	504	515	522	528	533	557	2.62
m1p6	531	531	531	525	531	536	541	544	544	543	544	551	2.48
m2p1	584	584	578	577	580	574	576	576	576	579	584	572	3.30
m2p2	659	659	650	623	613	615	617	614	611	604	606	576	3.94
m2p3	647	647	596	582	583	582	583	583	581	582	581	571	3.17
m2p4	588	588	588	579	580	588	587	585	581	579	576	574	2.91
m2p5	578	578	535	533	531	535	536	534	533	533	535	564	2.51
m2p6	523	523	562	590	600	599	592	591	592	590	589	561	3.49
m3p1	586	586	592	611	607	601	603	602	598	593	593	581	3.23
m3p2	527	527	530	517	527	536	537	536	534	536	538	569	2.70
m3p3	580	580	594	593	603	602	601	607	611	614	614	575	3.48
m3p4	499	499	526	535	537	530	528	527	526	526	524	551	3.02
m3p5	537	537	547	540	532	541	549	549	545	543	544	543	2.93
m3p6	547	547	532	540	546	553	564	571	574	575	574	557	3.32

Table F.2. *Density data values for different sizes and ultimate load.*

Appendix G

Relationship plots between Density and Mechanical Properties

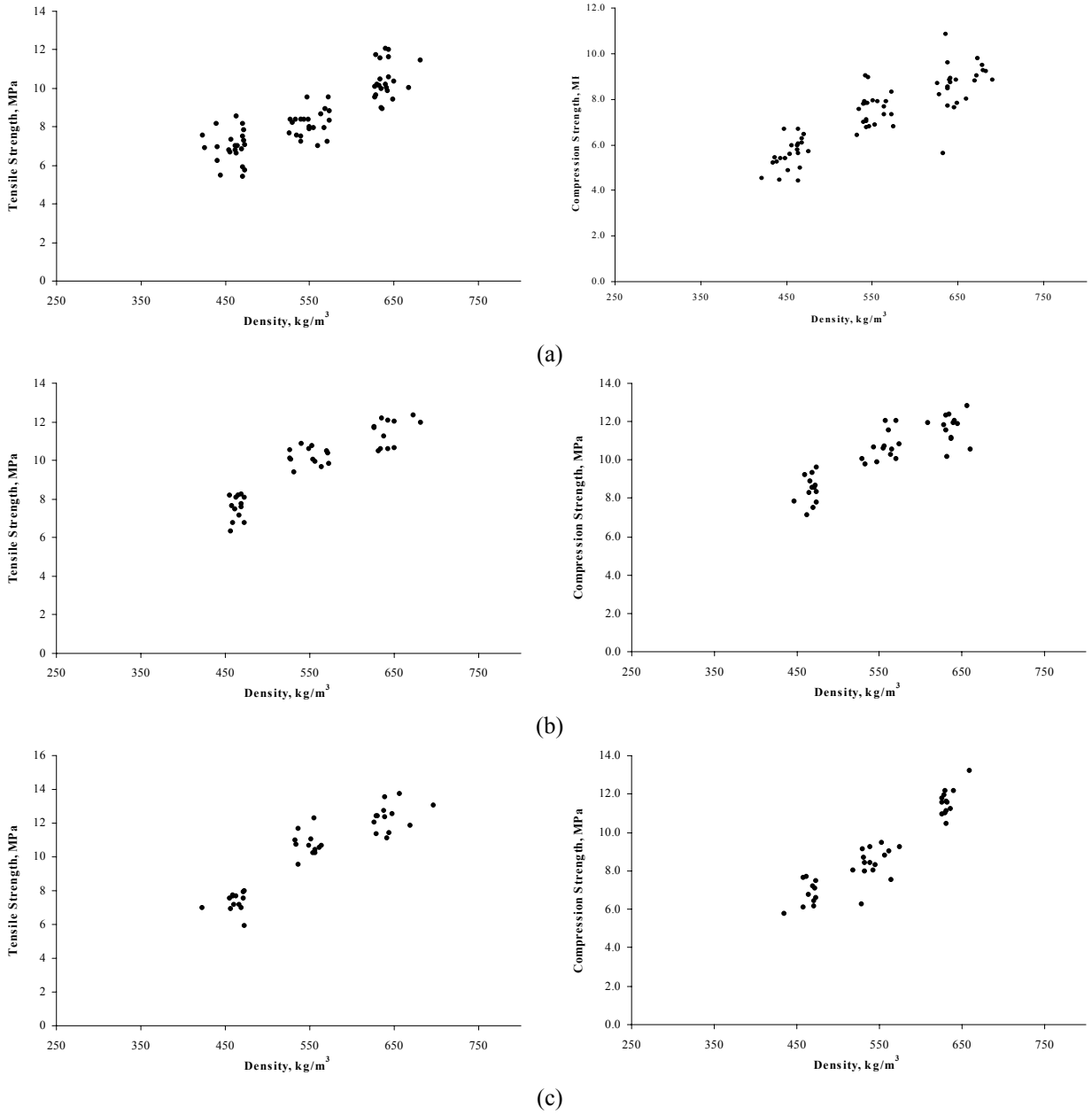

Figure G.1. *Tensile and compression strength vs. density at different sizes at the central part: (a) 12.7- by 12.7-mm, (b) 25.4- by 25.4-mm, and (c) 50.8- by 50.8-mm.*

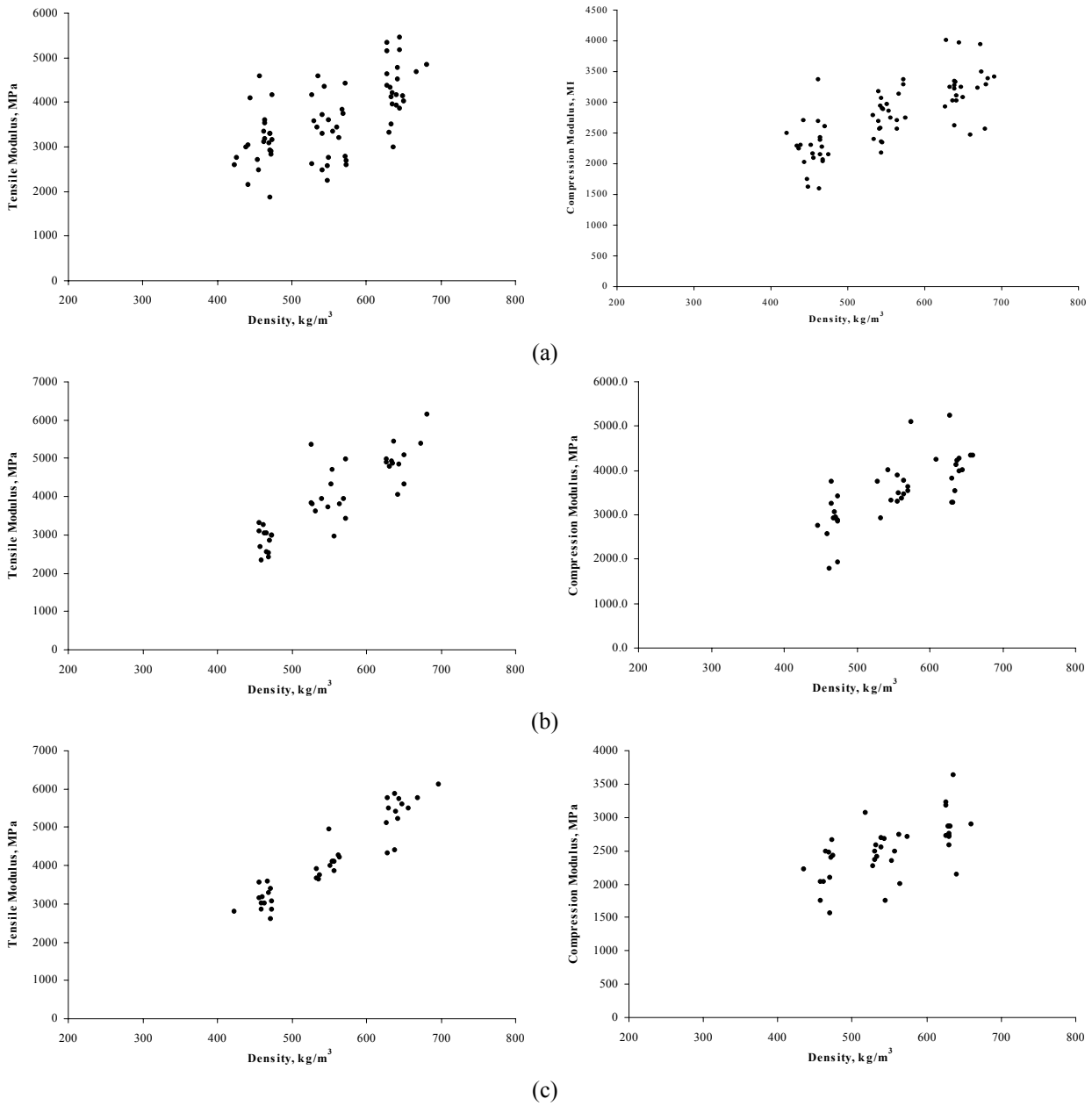

Figure G.2. *Tensile and compression modulus vs. density at different sizes at the central part (extensometer of 12.7 mm gauge-length): (a) 12.7- by 12.7-mm, (b) 25.4- by 25.4-mm, and (c) 50.8- by 50.8-mm.*

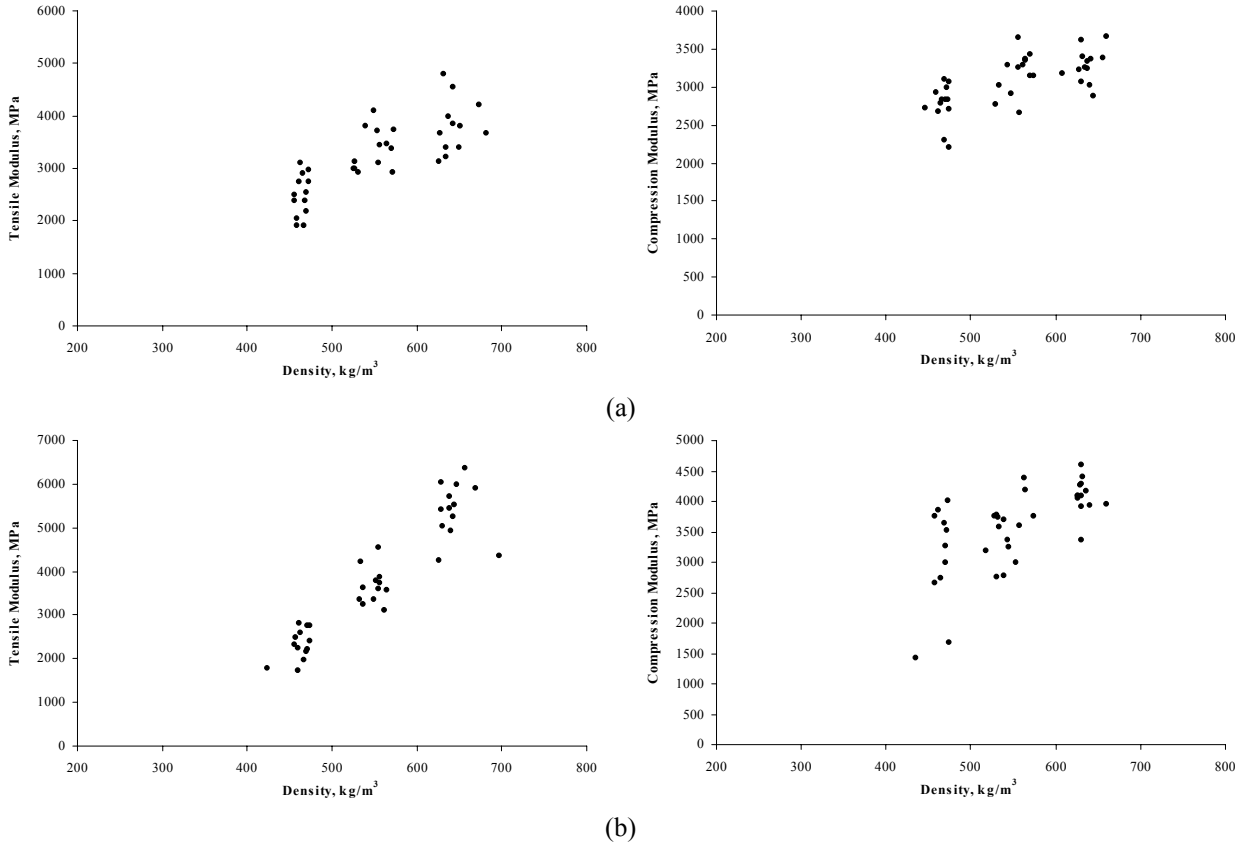

Figure G.3. *Tensile and compression modulus vs. density at different sizes at the central part (extensometer of 25.4 mm gauge-length): (a) 25.4- by 25.4-mm and (b) 50.8- by 50.8-mm.*

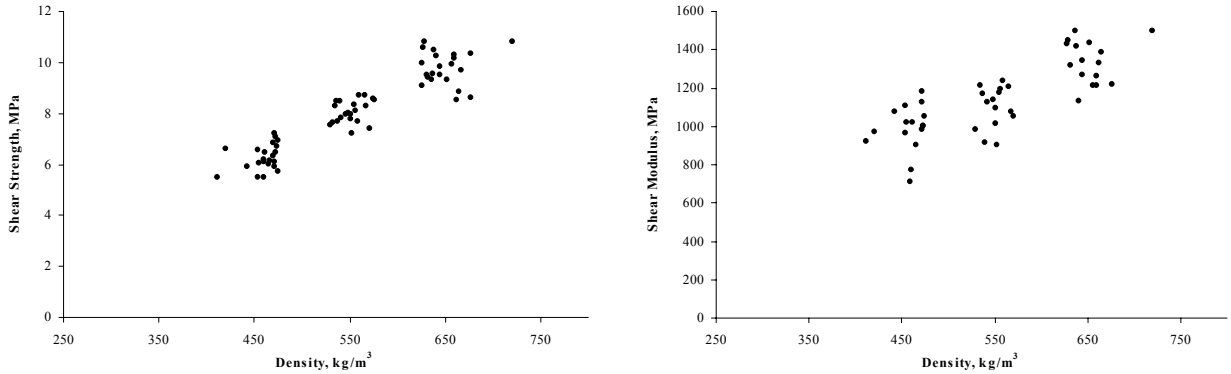

Figure G.4. *Shear strength and shear modulus vs. density.*

Appendix H

Testing Results

Tensile test,
Compression test,
And
Shear test

Tensile test results

Test label	Density kg/m^3	E MPa	σ_t MPa	Test label	Density kg/m^3	E MPa	σ_t MPa	Test label	Density kg/m^3	E MPa	σ_t MPa
T-0.5/450-1	473	4178	5.8	T-0.5/550-1	547	2240	9.6	T-0.5/650-1	640	3937	10.2
T-0.5/450-2	462	3343	7.0	T-0.5/550-2	549	3607	7.9	T-0.5/650-2	628	4378	11.8
T-0.5/450-4	455	2480	6.7	T-0.5/550-3	533	3440	8.4	T-0.5/650-4	633	4116	10.5
T-0.5/450-5	470	3315	8.2	T-0.5/550-4	543	4350	8.4	T-0.5/650-5	632	4337	10.2
T-0.5/450-6	439	3008	8.2	T-0.5/550-5	527	4162	8.4	T-0.5/650-6	636	2997	9.0
T-0.5/450-7	454	2727	6.8	T-0.5/550-6	548	2578	8.4	T-0.5/650-7	628	5346	9.7
T-0.5/450-8	469	3104	6.9	T-0.5/550-7	526	2624	7.7	T-0.5/650-8	648	4153	9.4
T-0.5/450-9	470	1874	7.5	T-0.5/550-8	560	3444	7.0	T-0.5/650-9	644	5472	12.0
T-0.5/450-10	472	2833	7.8	T-0.5/550-9	535	4592	7.6	T-0.5/650-10	644	3863	10.6
T-0.5/450-11	472	2911	7.3	T-0.5/550-10	573	2684	8.8	T-0.5/650-12	627	5152	10.1
T-0.5/450-12	426	2757	6.9	T-0.5/550-11	540	3729	7.2	T-0.5/650-13	630	3327	10.2
T-0.5/450-13	444	4101	5.5	T-0.5/550-12	555	3349	8.0	T-0.5/650-14	627	4651	9.5
T-0.5/450-14	441	3038	7.0	T-0.5/550-13	568	3751	8.9	T-0.5/650-15	640	4160	12.1
T-0.5/450-15	441	2156	6.3	T-0.5/550-14	540	2478	7.5	T-0.5/650-16	644	5170	11.7
T-0.5/450-16	463	3194	6.7	T-0.5/550-15	572	2791	9.5	T-0.5/650-17	634	4213	10.0
T-0.5/450-17	462	3127	6.8	T-0.5/550-16	573	2606	8.3	T-0.5/650-18	650	4020	10.4
T-0.5/450-18	464	3607	7.0	T-0.5/550-17	571	4432	7.3	T-0.5/650-19	634	3959	9.0
T-0.5/450-20	473	3156	7.1	T-0.5/550-18	549	2774	8.0	T-0.5/650-21	681	4845	11.5
T-0.5/450-21	457	4597	7.4	T-0.5/550-20	563	3218	8.7	T-0.5/650-22	633	3521	11.6
T-0.5/450-22	471	2922	5.9	T-0.5/550-21	567	3852	8.0	T-0.5/650-23	642	4771	9.9
T-0.5/450-23	423	2604	7.6	T-0.5/550-22	530	3593	8.2	T-0.5/650-24	667	4699	10.0
T-0.5/450-24	463	3536	8.6	T-0.5/550-23	540	3309	8.4	T-0.5/650-25	641	4532	10.0
T-0.5/450-25	470	3310	5.4								

Table H.1. *Tensile test results for specimen size 12.7- by 215.9-mm*

Test label	d kg/m^3	$E_{0.5}$ MPa	$E_{1.0}$ MPa	σ_t MPa	Test label	d kg/m^3	$E_{0.5}$ MPa	$E_{1.0}$ MPa	σ_t MPa	Test label	d kg/m^3	$E_{0.5}$ MPa	$E_{1.0}$ MPa	σ_t MPa
T-1.0/450-1	468	2538	2398	8.2	T-1.0/550-2	549	3737	4100	10.6	T-1.0/650-1	681	6146	3674	12.0
T-1.0/450-2	473	3003	2757	6.8	T-1.0/550-3	564	3808	3481	9.7	T-1.0/650-3	626	4894	3134	11.7
T-1.0/450-3	472	2997	2967	8.1	T-1.0/550-4	526	5362	2997	10.6	T-1.0/650-4	626	4986	3672	11.7
T-1.0/450-4	463	3046	3113	8.1	T-1.0/550-5	531	3635	2933	9.4	T-1.0/650-5	642	4059	4552	12.1
T-1.0/450-5	458	2331	2045	6.8	T-1.0/550-6	527	3822	2996	10.1	T-1.0/650-7	631	4794	4795	10.5
T-1.0/450-6	469	2432	2540	7.7	T-1.0/550-7	570	3951	3383	10.5	T-1.0/650-8	634	4882	3406	12.2
T-1.0/450-7	465	2566	2906	8.2	T-1.0/550-8	572	4993	3745	9.8	T-1.0/650-9	650	4338	3396	10.7
T-1.0/450-8	456	3331	2390	6.3	T-1.0/550-9	556	2973	3445	10.0	T-1.0/650-10	633	4941	3216	10.6
T-1.0/450-10	458	2700	1911	7.6	T-1.0/550-10	553	4325	3729	10.8	T-1.0/650-11	643	4836	3867	10.6
T-1.0/450-11	466	3051	1927	7.2	T-1.0/550-12	571	3420	2923	10.4	T-1.0/650-12	650	5081	3819	12.0
T-1.0/450-12	461	3275	2747	7.5	T-1.0/550-13	526	3848	3132	10.1	T-1.0/650-13	637	5443	4004	11.3
T-1.0/450-13	455	3095	2494	8.2	T-1.0/550-14	540	3961	3803	10.9	T-1.0/650-14	673	5395	4221	12.3
T-1.0/450-15	469	2868	2178	7.6	T-1.0/550-15	554	4703	3119	10.0					

Table H.2. *Tensile test results for specimen size 25.4- by 228.6-mm*

Test label	d kg/m^3	$E_{0.5}$ MPa	$E_{1.0}$ MPa	σ_t MPa	Test label	d kg/m^3	$E_{0.5}$ MPa	$E_{1.0}$ MPa	σ_t MPa	Test label	d kg/m^3	$E_{0.5}$ MPa	$E_{1.0}$ MPa	σ_t MPa
T-2.0/450-2	459	2849	2255	7.7	T-2.0/550-2	549	4964	3351	10.7	T-2.0/650-1	628	4323	6043	12.4
T-2.0/450-3	423	2813	1792	7.0	T-2.0/550-3	555	4121	4571	12.3	T-2.0/650-2	697	6131	4376	13.1
T-2.0/450-4	473	3076	2764	5.9	T-2.0/550-6	562	4266	3128	10.6	T-2.0/650-3	642	5219	5262	11.1
T-2.0/450-5	471	3413	2232	7.6	T-2.0/550-7	552	3995	3791	11.1	T-2.0/650-4	638	5883	5463	12.4
T-2.0/450-6	455	3574	2332	7.6	T-2.0/550-8	532	3686	3377	11.0	T-2.0/650-5	669	5761	5909	11.9
T-2.0/450-7	463	3015	2616	7.7	T-2.0/550-9	556	4118	3731	10.4	T-2.0/650-6	637	4422	5731	12.7
T-2.0/450-8	473	2867	2420	8.0	T-2.0/550-10	554	4109	3617	10.2	T-2.0/650-7	639	5411	4950	13.6
T-2.0/450-9	456	3163	2508	6.9	T-2.0/550-11	564	4225	3571	10.7	T-2.0/650-8	630	5500	5060	12.4
T-2.0/450-10	459	3011	1742	7.7	T-2.0/550-12	537	3770	3265	9.6	T-2.0/650-9	644	5759	5521	11.4
T-2.0/450-11	466	3587	1974	7.2	T-2.0/550-13	536	3647	3631	11.7	T-2.0/650-11	628	5769	5436	11.3
T-2.0/450-13	469	3289	2177	7.0	T-2.0/550-14	556	3868	3869	10.2	T-2.0/650-12	626	5126	4271	12.0
T-2.0/450-14	471	2615	2770	7.9	T-2.0/550-15	533	3932	4221	10.8	T-2.0/650-13	647	5608	5989	12.6
T-2.0/450-15	460	3175	2813	7.2						T-2.0/650-14	656	5503	6385	13.7

Table H.3. *Tensile test results for specimen size 50.8- by 254.0-mm*

Compression test results

Test label	Density kg/m^3	E MPa	σ_t MPa	Test label	Density kg/m^3	E MPa	σ_t MPa	Test label	Density kg/m^3	E MPa	σ_t MPa
C-0.5/450-1	470	2612	6.5	C-0.5/550-4	575	2746	6.8	C-0.5/650-1	672	3945	9.1
C-0.5/450-2	463	1592	6.1	C-0.5/550-5	544	2349	7.9	C-0.5/650-2	638	3217	9.6
C-0.5/450-3	468	2069	6.1	C-0.5/550-6	553	2866	6.9	C-0.5/650-4	649	3078	7.8
C-0.5/450-4	448	1620	5.4	C-0.5/550-7	542	2946	9.0	C-0.5/650-5	638	3345	7.7
C-0.5/450-5	434	2295	5.2	C-0.5/550-8	532	2787	6.4	C-0.5/650-6	626	2936	8.7
C-0.5/450-6	454	2162	5.6	C-0.5/550-9	543	3072	6.8	C-0.5/650-7	669	3231	8.8
C-0.5/450-7	438	2300	5.3	C-0.5/550-10	534	2402	7.6	C-0.5/650-8	682	3395	9.2
C-0.5/450-8	456	2102	6.0	C-0.5/550-11	564	2571	7.7	C-0.5/650-9	632	3253	5.6
C-0.5/450-9	475	2147	5.7	C-0.5/550-12	540	2697	7.8	C-0.5/650-10	679	3298	9.3
C-0.5/450-10	462	3369	6.0	C-0.5/550-13	564	2710	7.3	C-0.5/650-11	659	2469	8.0
C-0.5/450-11	447	1752	6.7	C-0.5/550-14	551	2976	8.0	C-0.5/650-12	673	3506	9.8
C-0.5/450-12	464	2437	4.4	C-0.5/550-15	542	2589	7.8	C-0.5/650-13	628	4012	8.2
C-0.5/450-13	466	2271	5.0	C-0.5/550-16	541	2570	7.9	C-0.5/650-14	647	3249	8.9
C-0.5/450-14	464	2146	5.7	C-0.5/550-17	572	3288	7.3	C-0.5/650-16	690	3423	8.8
C-0.5/450-15	421	2499	4.6	C-0.5/550-18	546	2892	6.8	C-0.5/650-17	641	3023	8.9
C-0.5/450-17	452	2305	4.9	C-0.5/550-19	540	3185	7.0	C-0.5/650-18	678	2565	9.5
C-0.5/450-18	442	2708	4.5	C-0.5/550-20	543	2360	7.1	C-0.5/650-19	645	3971	7.7
C-0.5/450-19	468	2041	6.3	C-0.5/550-21	566	3137	7.9	C-0.5/650-20	638	3277	8.6
C-0.5/450-20	443	2027	5.4	C-0.5/550-22	543	2178	7.0	C-0.5/650-21	636	3029	10.9
C-0.5/450-21	436	2248	5.5	C-0.5/550-23	572	3372	8.3	C-0.5/650-22	638	2625	8.5
C-0.5/450-22	462	2696	5.8	C-0.5/550-24	556	2751	7.9	C-0.5/650-23	641	3110	8.8
C-0.5/450-23	464	2395	6.7	C-0.5/550-25	545	2896	9.0	C-0.5/650-24	640	3327	8.9

Table H.4. *Compression test results for specimen size 12.7- by 63.5-mm*

Test label	d kg/m^3	$E_{0.5}$ MPa	$E_{1.0}$ MPa	σ_t MPa	Test label	d kg/m^3	$E_{0.5}$ MPa	$E_{1.0}$ MPa	σ_t MPa	Test label	d kg/m^3	$E_{0.5}$ MPa	$E_{1.0}$ MPa	σ_t MPa
C-1.0/450-1	471	2924	3003	8.6	C-1.0/550-1	573	5091	3154	10.8	C-1.0/650-1	630	3824	3075	11.6
C-1.0/450-4	468	2931	2309	8.6	C-1.0/550-2	529	3764	2779	10.1	C-1.0/650-2	659	4343	3666	10.6
C-1.0/450-5	469	3077	3108	9.4	C-1.0/550-3	564	3468	3363	10.3	C-1.0/650-3	641	4001	3377	12.0
C-1.0/450-6	462	1785	2675	7.1	C-1.0/550-4	557	3501	2659	12.0	C-1.0/650-4	636	4138	3337	11.2
C-1.0/450-7	465	3269	2837	8.9	C-1.0/550-5	570	3550	3431	12.1	C-1.0/650-5	632	3291	3401	10.2
C-1.0/450-8	474	1942	2218	7.8	C-1.0/550-6	555	3888	3651	10.7	C-1.0/650-6	640	4281	3034	11.9
C-1.0/450-9	470	2950	2844	7.5	C-1.0/550-7	564	3781	3377	10.5	C-1.0/650-7	627	5237	3235	11.8
C-1.0/450-10	474	2856	3072	9.6	C-1.0/550-9	555	3315	3257	10.6	C-1.0/650-8	644	4006	2882	11.9
C-1.0/450-11	459	2576	2926	9.3	C-1.0/550-10	569	3640	3146	10.0	C-1.0/650-9	608	4241	3183	12.0
C-1.0/450-12	474	2889	2715	8.3	C-1.0/550-11	533	2922	3032	9.8	C-1.0/650-10	656	4350	3388	12.8
C-1.0/450-13	473	3423	2843	8.7	C-1.0/550-12	561	3369	3294	11.6	C-1.0/650-11	637	4219	3254	11.1
C-1.0/450-14	464	3760	2796	8.3	C-1.0/550-14	543	4017	3300	10.7	C-1.0/650-12	630	3277	3623	12.3
C-1.0/450-15	446	2754	2728	7.8	C-1.0/550-15	546	3319	2924	9.9	C-1.0/650-13	634	3549	3265	12.4

Table H.5. *Compression test results for specimen size 25.4- by 76.2-mm*

Test label	d kg/m^3	$E_{0.5}$ MPa	$E_{1.0}$ MPa	σ_t MPa	Test label	d kg/m^3	$E_{0.5}$ MPa	$E_{1.0}$ MPa	σ_t MPa	Test label	d kg/m^3	$E_{0.5}$ MPa	$E_{1.0}$ MPa	σ_t MPa
C-2.0/450-1	528	2267	3763	6.3	C-2.0/550-1	530	2362	2774	9.2	C-2.0/650-1	628	2878	4280	12.0
C-2.0/450-2	457	1760	2673	6.1	C-2.0/550-2	543	2686	3379	8.0	C-2.0/650-2	631	2873	4419	11.6
C-2.0/450-3	461	2038	3872	7.7	C-2.0/550-3	532	2583	3744	8.4	C-2.0/650-3	626	3228	4061	11.8
C-2.0/450-4	518	3072	3204	8.1	C-2.0/550-4	539	2556	2776	9.3	C-2.0/650-4	625	3189	4108	11.6
C-2.0/450-6	435	2233	1422	5.8	C-2.0/550-5	553	2355	2996	9.5	C-2.0/650-5	630	2590	3372	11.0
C-2.0/450-7	457	2035	3765	7.7	C-2.0/550-7	557	2501	3599	8.8	C-2.0/650-6	630	2767	4291	11.6
C-2.0/450-8	472	2399	3527	7.1	C-2.0/550-8	574	2710	3760	9.3	C-2.0/650-7	626	2735	4102	11.0
C-2.0/450-9	473	2438	1681	6.6	C-2.0/550-9	545	1753	3262	8.3	C-2.0/650-8	640	2157	3935	12.2
C-2.0/450-10	470	1570	2991	6.2	C-2.0/550-10	538	2704	3707	8.4	C-2.0/650-10	636	3635	4175	11.3
C-2.0/450-11	473	2668	4024	7.5	C-2.0/550-11	564	2011	4187	7.5	C-2.0/650-11	629	2732	3914	12.2
C-2.0/450-12	470	2098	3270	6.4	C-2.0/550-12	533	2417	3592	8.0	C-2.0/650-12	630	2867	4598	10.4
C-2.0/450-13	464	2498	2746	6.8	C-2.0/550-13	562	2738	4386	9.0	C-2.0/650-13	659	2900	3958	13.3
C-2.0/450-14	469	2483	3643	7.2	C-2.0/550-15	530	2501	3792	8.7	C-2.0/650-14	631	2721	4095	11.1

Table H.6. *Compression test results for specimen size 50.8- by 76.2-mm*

Shear test results

Test label	d kg/m^3	G MPa	τ MPa	Test label	d kg/m^3	G MPa	τ MPa	Test label	d kg/m^3	G MPa	τ MPa
S-450-1	474	1055	6.9	**S-550-1**	539	920	8.5	**S-650-1**	651	1436	9.4
S-450-2	473	1006	6.7	**S-550-2**	552	908	7.2	**S-650-2**	659	1262	10.3
S-450-3	472	1004	7.1	**S-550-3**	536	1170	8.5	**S-650-4**	659	1213	10.2
S-450-4	459	716	6.2	**S-550-4**	567	1078	8.3	**S-650-5**	676	1222	8.6
S-450-5	470	621	6.9	**S-550-7**	570	1055	7.4	**S-650-7**	631	1319	9.5
S-450-6	455	1021	6.1	**S-550-8**	548	1138	8.0	**S-650-8**	628	1454	10.8
S-450-7	471	986	5.9	**S-550-9**	575	1250	8.5	**S-650-9**	638	1419	10.5
S-450-8	461	1024	6.5	**S-550-10**	556	1194	8.1	**S-650-10**	636	1501	9.6
S-450-9	466	640	6.2	**S-550-11**	565	1211	8.7	**S-650-11**	677	849	10.4
S-450-10	471	1129	7.2	**S-550-13**	550	1097	7.8	**S-650-12**	627	1431	10.6
S-450-11	471	1185	6.1	**S-550-14**	534	1218	8.3	**S-650-13**	720	1503	10.8
S-450-12	469	1546	6.4	**S-550-15**	554	1178	8.4	**S-650-14**	640	1137	10.3
S-450-13	420	973	6.6	**S-550-16**	559	739	8.7	**S-650-15**	626	986	9.1
S-450-14	453	1109	6.6	**S-550-17**	558	1242	7.7	**S-650-16**	666	1780	9.7
S-450-15	459	1761	5.5	**S-550-18**	546	1274	8.0	**S-650-17**	664	1392	8.9
S-450-16	474	651	5.7	**S-550-19**	529	984	7.6	**S-650-18**	644	1347	9.5
S-450-17	465	906	6.0	**S-550-20**	532	899	7.6	**S-650-19**	635	1078	9.3
S-450-18	460	777	6.1	**S-550-21**	550	1014	8.0	**S-650-20**	662	1335	8.5
S-450-19	442	1076	5.9	**S-550-22**	537	1804	7.7	**S-650-21**	626	1964	10.0
S-450-20	472	1321	6.5	**S-550-23**	574	849	8.6	**S-650-22**	644	1269	9.8
S-450-22	453	966	5.5	**S-550-24**	541	1128	7.8	**S-650-23**	632	1584	9.4
S-450-24	411	927	5.5					**S-650-24**	656	1215	9.9

Table H.7. *Shear test results for specimen size 19.05- by 76.2-mm*

Appendix I

Scatter Plots and Regression Curves

Tensile properties, Compression properties, and Shear properties
versus
Density

Tensile Properties

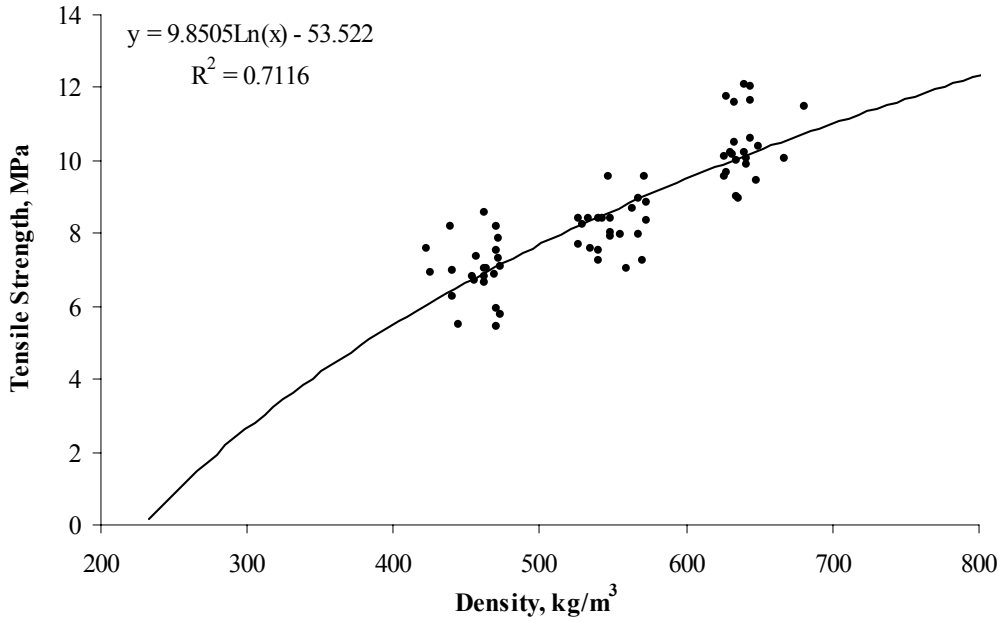

Figure I.1. *Tensile strength vs. density for specimen size 12.7- by 215.9-mm*

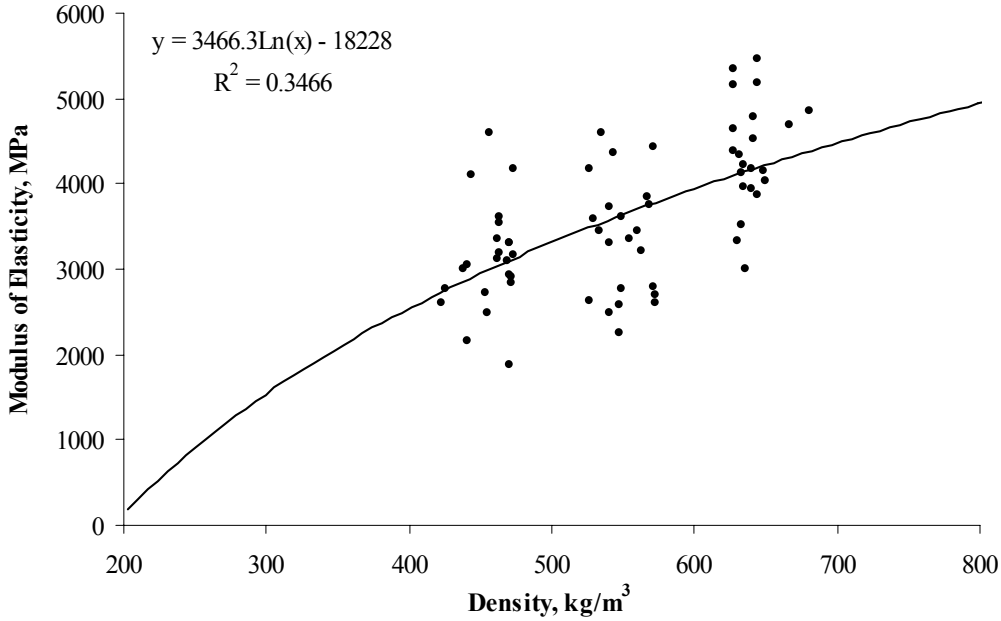

Figure I.2. *Tensile modulus of elasticity parralel to Surface (extonsometers of 12.7 mm gauge-length) vs. density for specimen size 12.7- by 215.9-mm.*

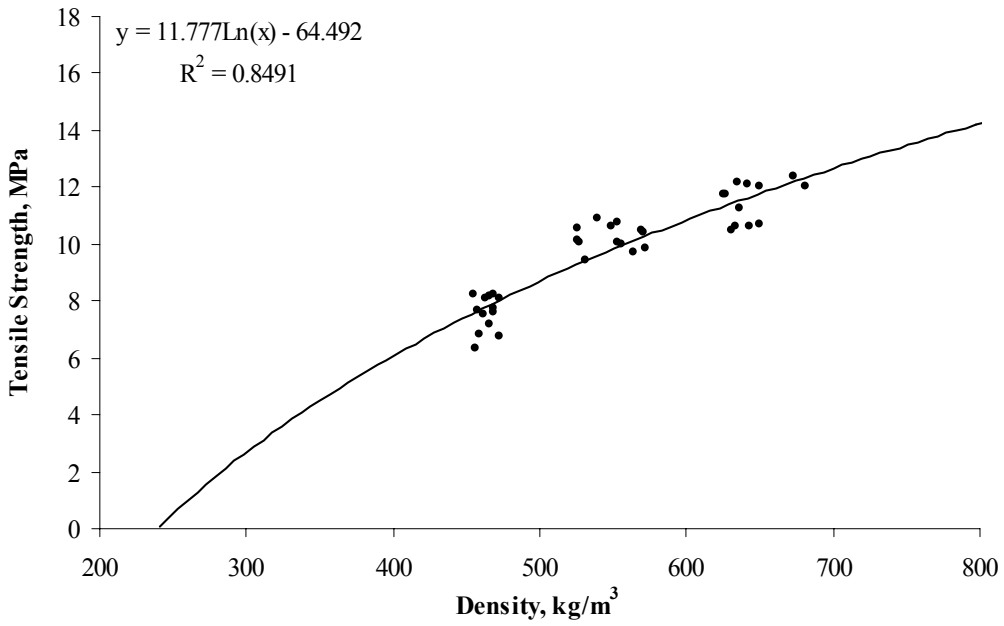

Figure I.3. *Tensile strength vs. density for specimen size 25.4- by 228.6-mm*

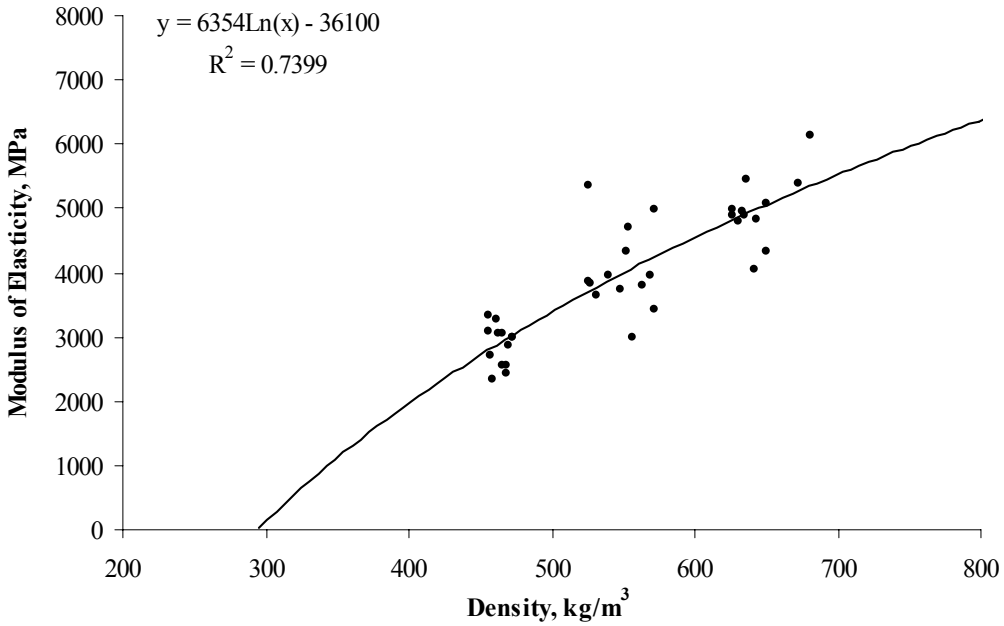

Figure I.4. *Tensile modulus of elasticity parralel to Surface (extonsometers of 12.7 mm gauge-length) vs. density for specimen size 25.4- by 228.6-mm.*

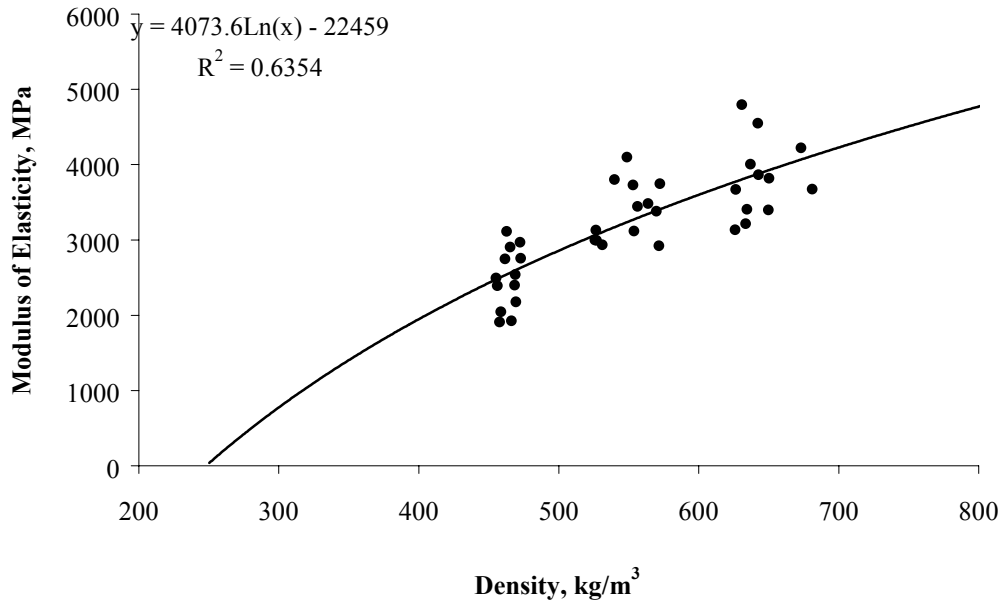

Figure I.5. *Tensile modulus of elasticity parralel to Surface (extonsometers of 25.4 mm gauge-length) vs. density for specimen size 25.4- by 228.6-mm.*

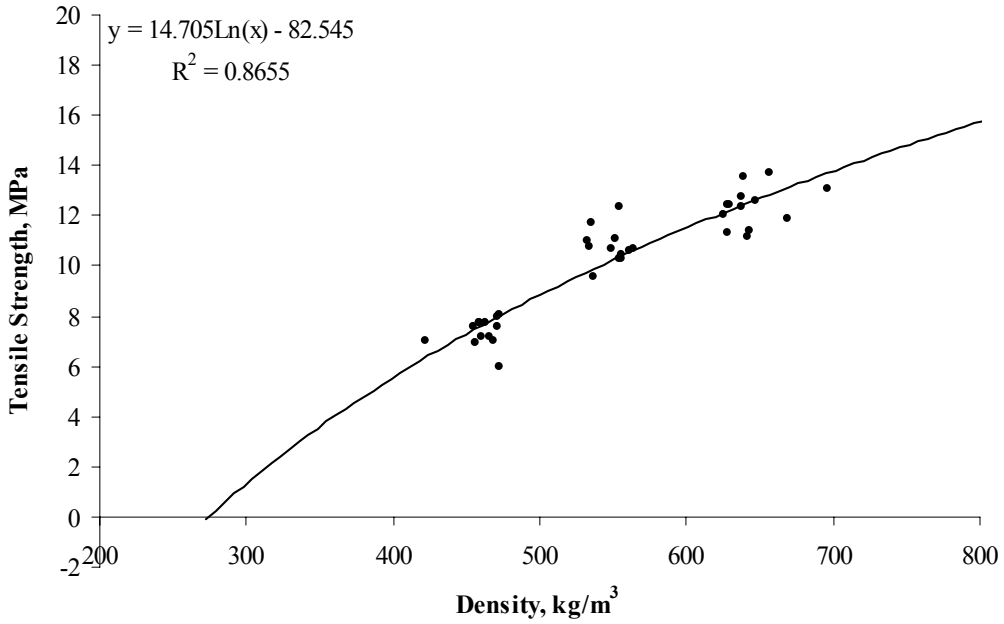

Figure I.6. *Tensile strength vs. density for specimen size 50.8- by 254.0-mm*

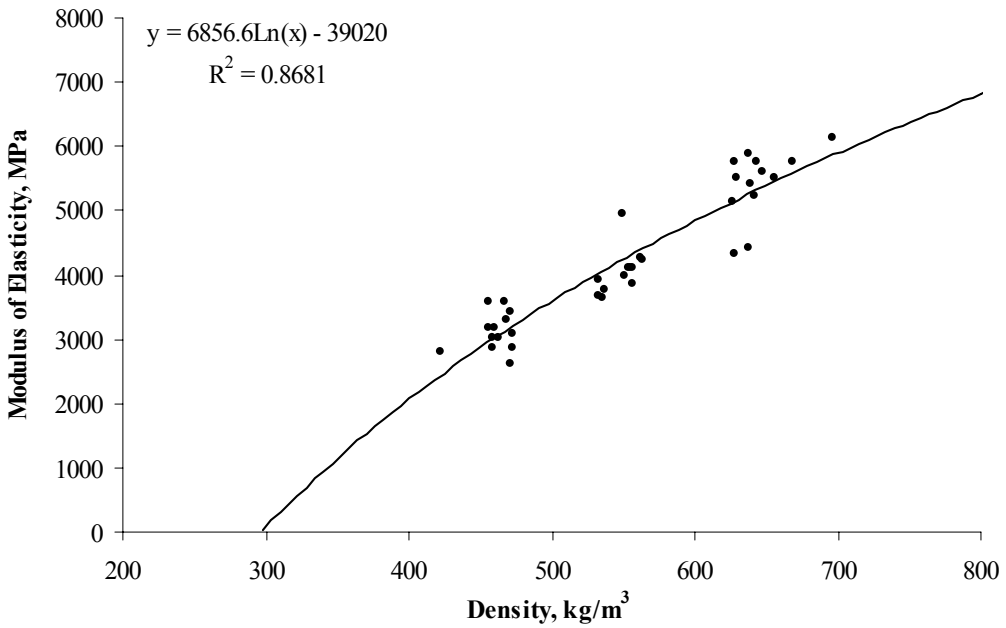

Figure I.7. *Tensile modulus of elasticity parralel to Surface (extonsometers of 12.7 mm gauge-length) vs. density for specimen size 50.8- by 254.0-mm.*

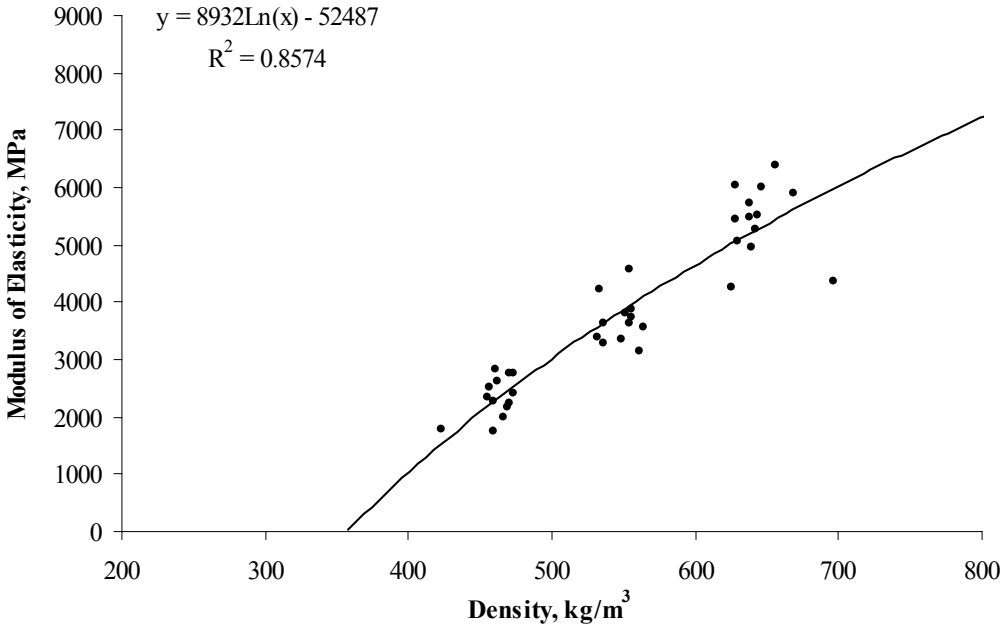

Figure I.8. *Tensile modulus of elasticity parralel to Surface (extonsometers of 25.4 mm gauge-length) vs. density for specimen size 50.8- by 254.0-mm.*

Compression Properties

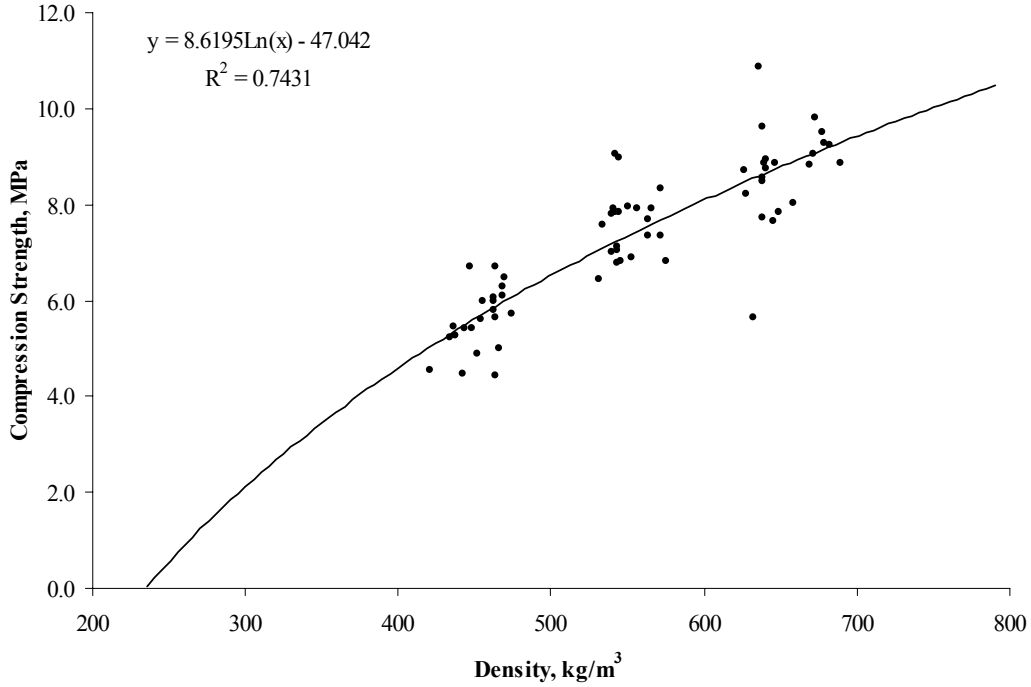

Figure I.9. *Compression strength vs. density for specimen size 12.7- by 63.5-mm*

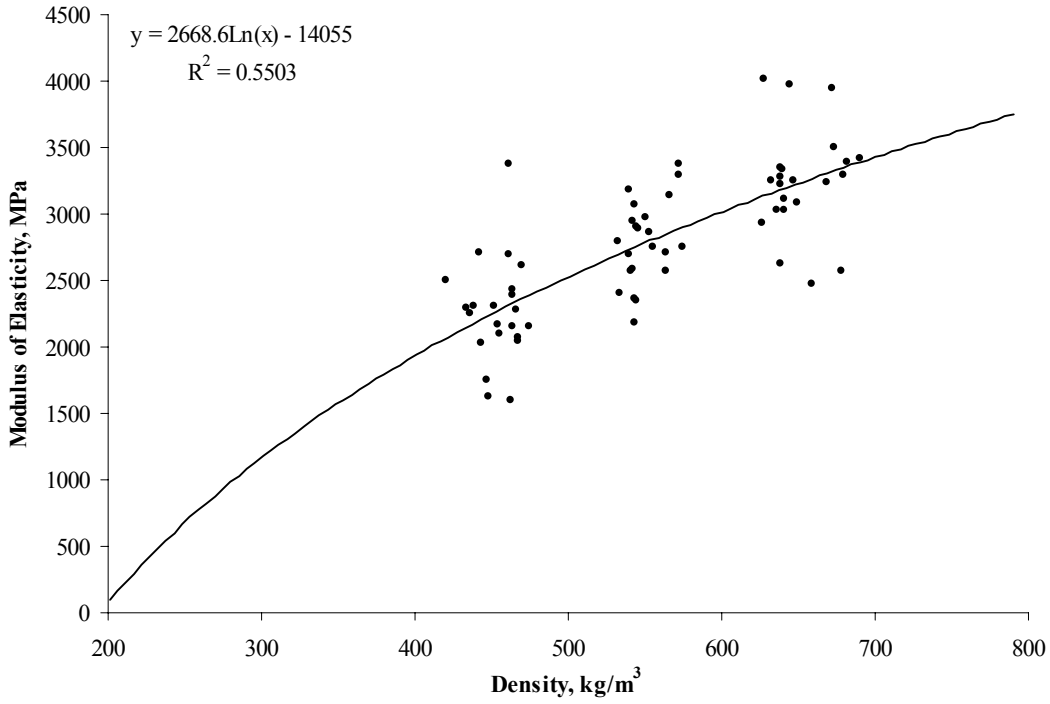

Figure I.10. *Compression modulus of elasticity parralel to Surface (extonsometers of 12.7 mm gauge-length) vs. density for specimen size 12.7- by 63.5-mm.*

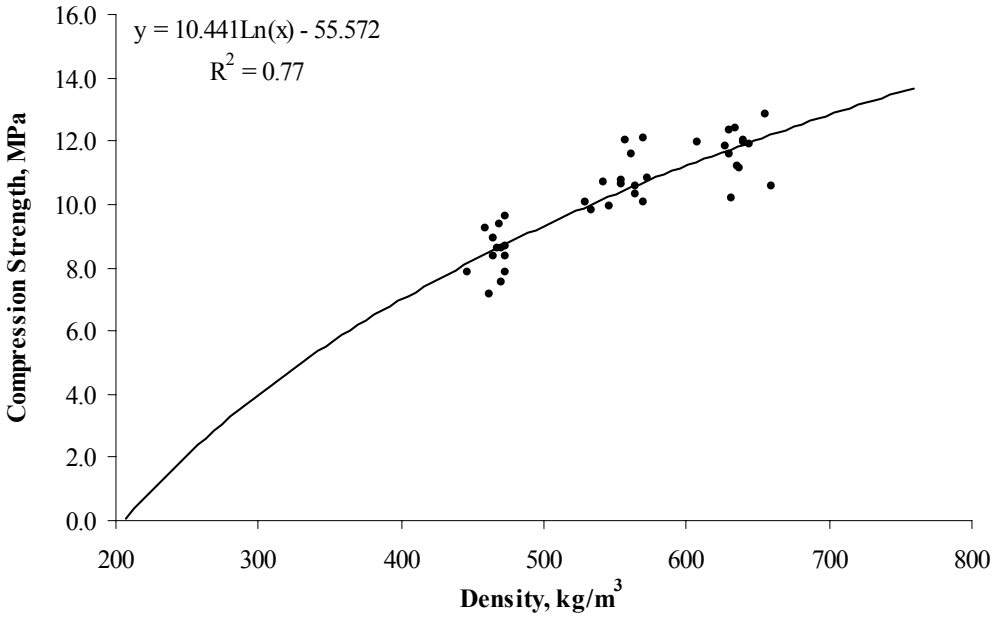

Figure I.11. *Compression strength vs. density for specimen size 25.4- by 76.2-mm*

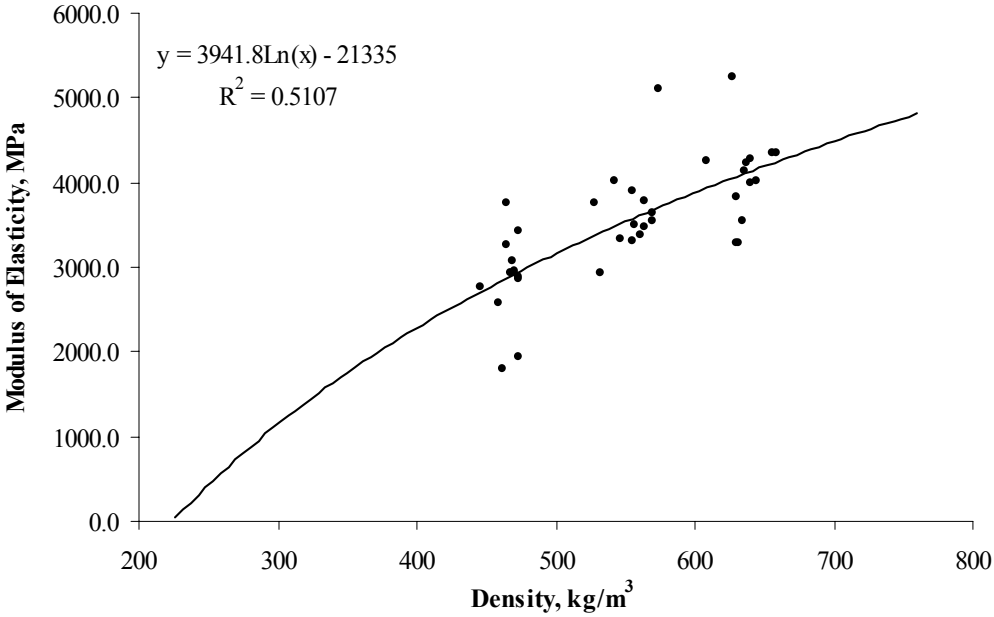

Figure I.12. *Compression modulus of elasticity parralel to Surface (extonsometers of 12.7 mm gauge-length) vs. density for specimen size 25.4- by 76.2-mm.*

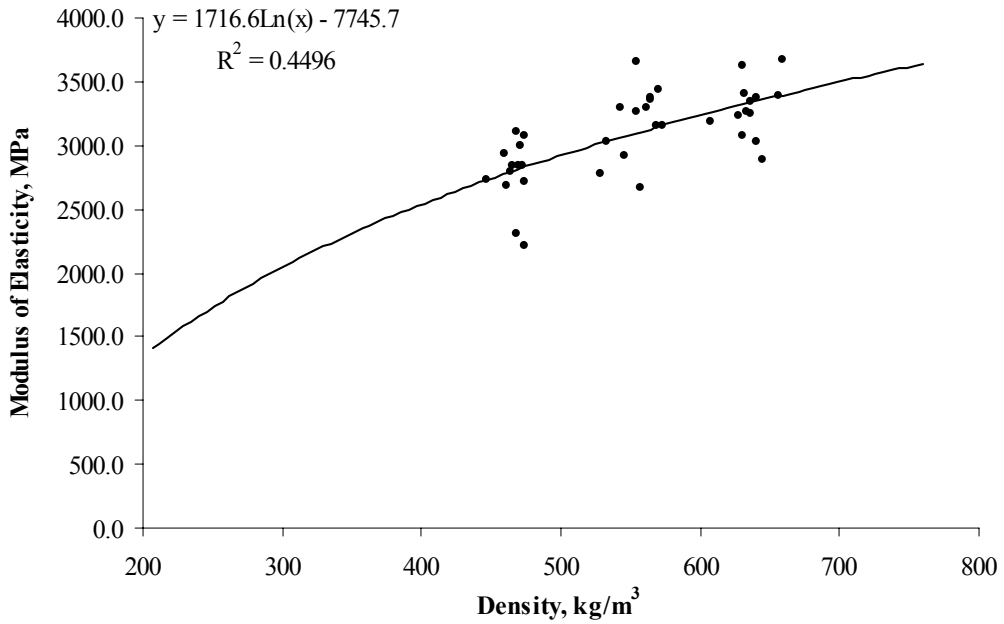

Figure I.13. *Compression modulus of elasticity parralel to Surface (extonsometers of 25.4 mm gauge-length) vs. density for specimen size 25.4- by 76.2-mm.*

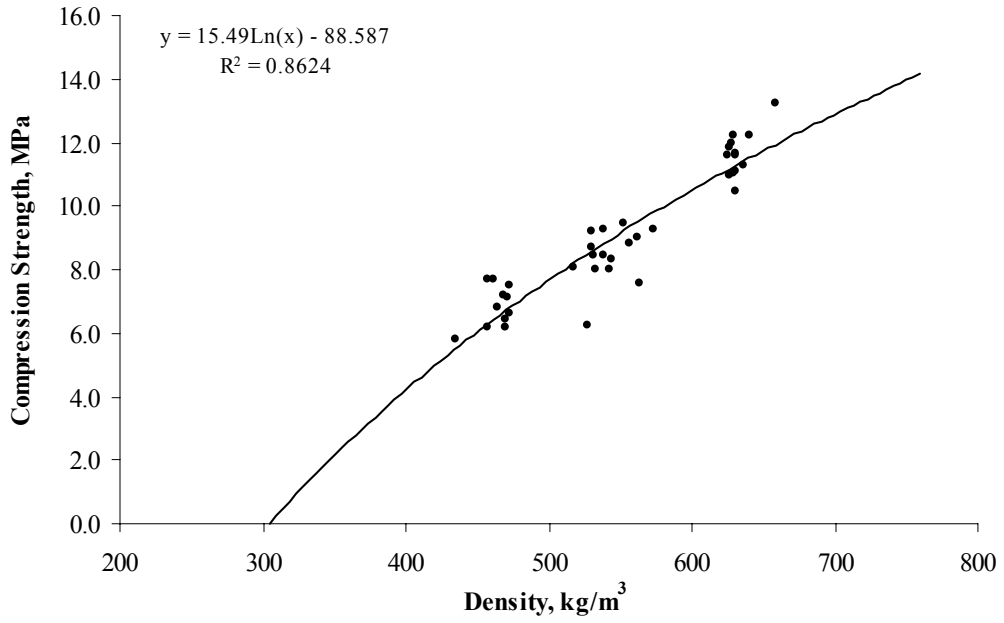

Figure I.14. *Compression strength vs. density for specimen size 50.8- by 76.2-mm*

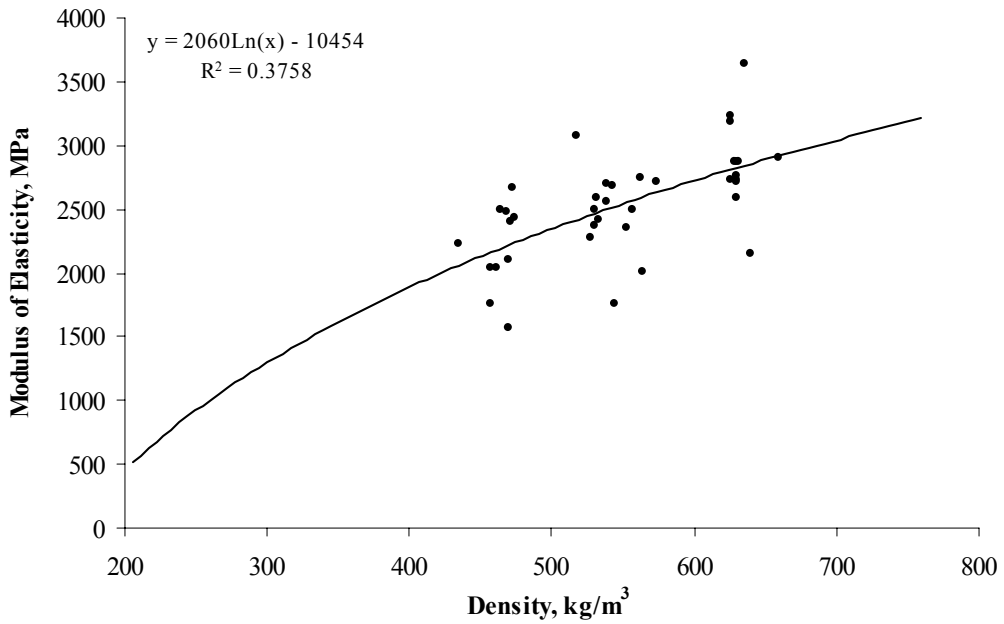

Figure I.15. *Compression modulus of elasticity paralel to Surface (extensometers of 12.7 mm gauge-length) vs. density for specimen size 50.8- by 76.2-mm.*

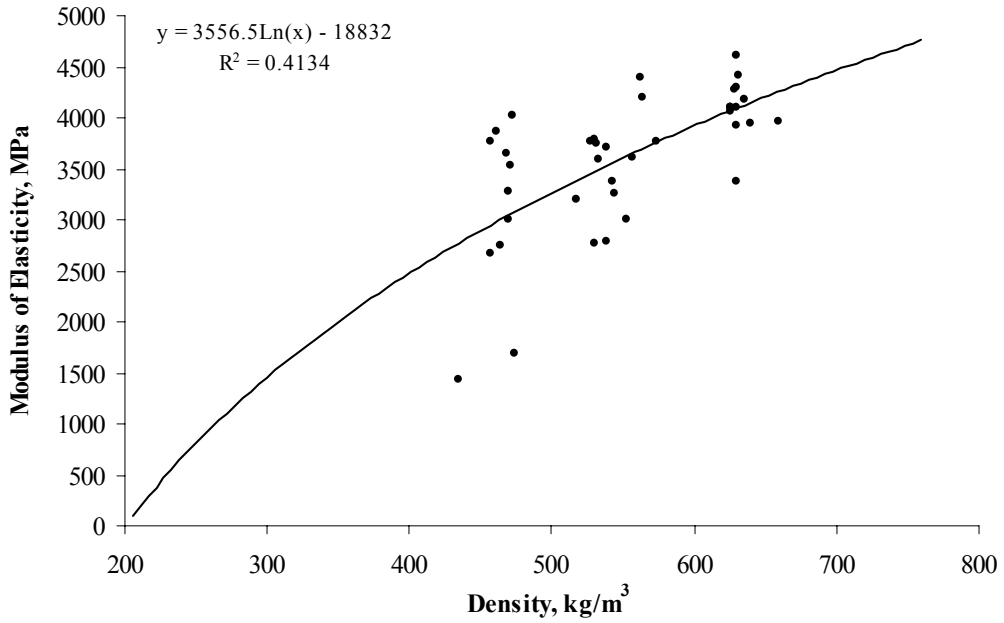

Figure I.16. *Compression modulus of elasticity parralel to Surface (extonsometers of 25.4 mm gauge-length) vs. density for specimen size 50.8- by 76.2-mm.*

Shear Properties

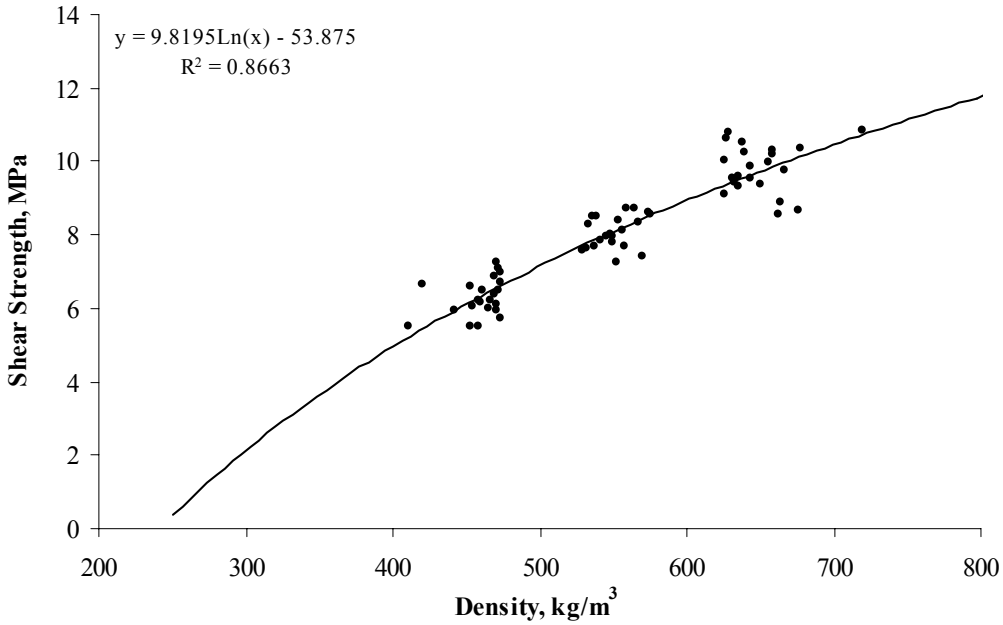

Figure I.17. *Shear strength vs. density*

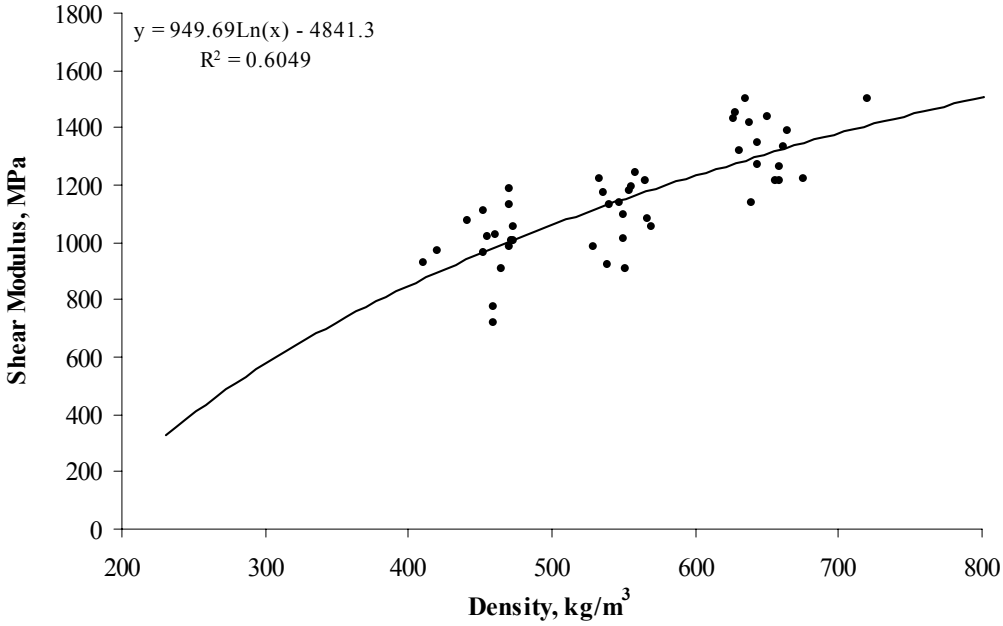

Figure I.18. *Shear modulus vs. density*